

AQUAPORIN IN CANCER CELL MIGRATION: DISCOVERY OF NEW PHARMACOLOGICAL BLOCKERS AND A NOVEL LITHIUM SENSOR

A thesis submitted for the
degree of Doctor of Philosophy

Jinxin Pei, B.Sc. (Hons.)



THE UNIVERSITY
of **ADELAIDE**

Adelaide Medical School
The University of Adelaide
South Australia

June 2017

Table of Contents

DECLARATION	7
ACKNOWLEDGMENTS	9
CHAPTER 1 REVIEW: AQUAPORINS AS PHARMACEUTICAL TARGETS	10
Contextual statement	11
Statement of Authorship	13
1.1 Overview of aquaporin channel functions in brain fluid homeostasis and cell migration	20
1.1.1 AQP4 in cerebral edema	20
1.1.2 AQP1 in cell migration	24
1.2 Small molecule drug discovery for aquaporin channels	26
1.2.1 Modulators of water channel activity	26
1.2.2 Regulation of AQP1 ion channel activity	28
1.3 Translational promise of pharmacological modulators of aquaporin channels in brain edema, cancer and other disorders	29
1.3.1 Targeting AQP4 channels in brain edema	30
1.3.2 Differential regulation of expression of AQP channel types in cancer cells	31
1.3.2 Targeting AQP1 channels in cell migration and metastasis	34
1.4 New avenues for aquaporin drug discovery from traditional and alternative medicines	35

References	39
Figure Legends	59
Figures and Tables	60
CHAPTER 2 – AQUAPORIN-1 ION CHANNELS IN CANCER CELL MIGRATION: DISCOVERY OF NEW PHARMACOLOGICAL BLOCKERS.	64
Contextual statement	65
Statement of Authorship	67
2.1 Abstract	71
2.2 Introduction	72
2.3 Material and Methods	75
2.4 Results	80
2.4 Discussion	84
2.4 References	88
2.4 Figure Legends	94
2.4 Figures and Tables	96
CHAPTER 3 – THE DISCOVERY OF NOVEL PHYTOCHEMICALS THAT SLOW CANCER CELL MIGRATION	103
Contextual statement	104
Statement of Authorship	106

3.1 Abstract	110
3.2 Introduction	111
3.3 Material and Methods	114
3.4 Results	121
3.5 Discussion	127
3.6 References	134
3.7 Table	142
3.8 Figure Legends	144
3.9 Figures	149

CHAPTER 4 – DISCOVERY OF A NOVEL LITHIUM SENSOR FOR THE REAL-TIME ANALYSIS OF ION CONDUCTANCE IN AQP1 **155**

Contextual statement	156
Statement of Authorship	158
4.1 Abstract	161
4.2 Introduction	162
4.3 Results and Discussion	163
4.4 Conclusion	170
4.5 Methods	173
4.6 References	177
4.7 Figure Legends	180
4.8 Figures	184

Conclusion	189
Appendix	202
Papers in published journal format	203

Declaration and Published Works

This work contains no material which has been accepted for the award of any other degree or diploma in any university or other tertiary institution to Jinxin Pei and, to the best of my knowledge and belief, contains no material previously published or written by another person, except where due reference has been made in the text.

I give consent to this copy of my thesis when deposited in the University Library, being made available for loan and photocopying, subject to the provisions of the Copyright Act 1968.

The author acknowledges that copyright of published works contained within this thesis (as listed below*) resides with the copyright holder(s) of those works.

I also give permission for the digital version of my thesis to be made available on the web, via the University's digital research repository, the Library catalogue, the Australasian Digital Theses Program (ADTP) and also through web search engines, unless permission has been granted by the University to restrict access for a period of time.

.....
Jinxin Pei

.....
Date

*Work in this thesis has appeared in the following publications:

Pei JV, Ameliorate JL, Kourghi M, De Ieso ML, and Yool AJ (2016) Drug discovery and therapeutic targets for pharmacological modulators of aquaporin channels, in *Aquaporins in Health and Disease: New Molecular Targets For Drug Discovery* (Soveral G, Casinin A, and Nielsen S, eds) pp 275–297, CRC Press, Oxfordshire, United Kingdom.

Kourghi M[§], **Pei JV[§]**, De Ieso ML, Flynn G, and Yool AJ (2016) Bumetanide derivatives AqB007 and AqB011 selectively block the aquaporin-1 ion channel conductance and slow cancer cell migration. *Mol Pharmacol* 89:133–140 ([§] co-first authors)

Pei, J.V, Kourghi M, De Ieso ML, Campbell EM, Doward HS, Hardingham JE, and Yool AJ (2016) Differential Inhibition of Water and Ion Channel Activities of Mammalian Aquaporin-1 by Two Structurally Related Bacopaside Compounds Derived from the Medicinal Plant *Bacopa monnieri*. *Mol Pharmacol* **90**, 496-507.

Acknowledgements

I would like to thank Professor Andrea Yool for her guidance and supervision throughout my PhD. I am especially thankful for the time and energy she has put into revising and guiding me on writing scientific papers and this thesis. I am also grateful for the freedom she has given me to pursue my own ideas. I would like to also thank my co-supervisor Professor David O'Carroll for his guidance and supervision in many aspects of my study. Thank you to Dr. Ewan Campbell for mentoring me during the early stage of my PhD, and to Dr. Sabrina Heng for her valuable help during the later stage of my PhD.

Many thanks to all the past and present members of the Yool group for providing assistance in every aspect of my PhD, especially: to Mr. Mohammad Kourghi for conducting electrophysiology experiments for my research, Mr. Michael De Ieso for conducting western blot experiments for my research.

I would like to thank Adelaide Microscopy for providing access to imaging equipment for my study and enormous help from Dr. Agatha Labridis for all my microscope training and troubleshooting.

And last, but most importantly, to my family: my mother and father, my wife Michelle and my dear daughter Kimberley—Thank you for your enormous support, encouragement and love. Without you, I would not have been able to achieve all these.

**CHAPTER 1 REVIEW:
AQUAPORINS AS
PHARMACEUTICAL TARGETS**

CONTEXTUAL STATEMENT

Drug discovery and therapeutic targets for pharmacological modulators of aquaporin channels

AIM: To review the association between aquaporins (AQPs) and various diseases and to review the potential of AQPs as therapeutic targets.

Hypothesis: Modulators of AQP channels are promising pharmaceutical targets for drug development treating brain edema, cancer and other disorders.

Conclusions:

1. AQP4 channels subserve water movement during cerebral edema formation; AQP4 pharmacological agents will be advantageous for interventions in brain fluid disorders particularly if administered with an understanding of the dynamic mechanisms of aquaporin channel regulation.
2. Various types of AQPs are upregulated in cancer cells suggesting AQPs are ideal candidates as pharmaceutical targets.
3. AQP1 contributes to cell migration and angiogenesis and facilitates tumour growth and metastasis through mechanisms that remain to be defined. Pharmacological modulation of AQP1 could be a pivotal adjunct to existing cancer therapies, improving the prognosis for cancer patients by slowing cancer angiogenesis and metastases.
4. In addition to the heavy metals (mercury, silver and gold) previously characterized as AQP1 water channel blockers, the first small molecule modulators discovered for both AQP1 and AQP4 were AqB013 which is an antagonist of water channel activity, AqF026 which is a water channel agonist.

Other new antagonists have since been described by research groups around the world.

5. Both AQP1 and AQP4 are highly functional water channels, but only the expression of AQP1 enables rapid cell movement in certain classes of cells. One important difference is that AQP1 but not AQP4 can function as a gated monovalent cation channel. The loop D region in AQP1 is essential for AQP1 function as an ion channel.
6. The small molecule agent AqB011 and Cd⁺ ions selectively block the AQP1 ionic conductance, but not water channel activity.
7. New avenues for aquaporin drug discovery can be found from traditional and alternative medicines. Few candidate species have been selected after meta-analysis of literature. The species are: *Polyporus umbellatus*, *Poria cocos*, and *Bacopa monnieri*.

Statement of Authorship

Title of Paper	Drug discovery and therapeutic targets for pharmacological modulators of aquaporin channels
Publication Status	<input checked="" type="checkbox"/> Published <input type="checkbox"/> Accepted for Publication <input type="checkbox"/> Submitted for Publication <input type="checkbox"/> Unpublished and Unsubmitted work written in manuscript style
Publication Details	Pei JV, Ameliorate JL, Kourghi M, De Ieso ML, and Yool AJ (2016) Drug discovery and therapeutic targets for pharmacological modulators of aquaporin channels, in Aquaporins in Health and Disease: New Molecular Targets For Drug Discovery (Soveral G, Casinin A, and Nielsen S, eds) pp 275–297, CRC Press, Oxfordshire, United Kingdom.

Principal Author

Name of Principal Author (Candidate)	Jinxin Pei			
Contribution to the Paper	Wrote the manuscript.			
Overall percentage (%)	60%			
Certification:	This paper reports on original research I conducted during the period of my Higher Degree by Research candidature and is not subject to any obligations or contractual agreements with a third party that would constrain its inclusion in this thesis. I am the primary author of this paper.			
Signature	<table border="1" style="width: 100%;"> <tr> <td style="width: 60%;"></td> <td style="width: 15%;">Date</td> <td style="width: 25%;">23/5/17</td> </tr> </table>		Date	23/5/17
	Date	23/5/17		

Co-Author Contributions

By signing the Statement of Authorship, each author certifies that:

- i. the candidate's stated contribution to the publication is accurate (as detailed above);
- ii. permission is granted for the candidate to include the publication in the thesis; and
- iii. the sum of all co-author contributions is equal to 100% less the candidate's stated contribution.

Name of Co-Author	Joshua L Ameliorate			
Contribution to the Paper	Wrote the manuscript.			
Signature	<table border="1" style="width: 100%;"> <tr> <td style="width: 60%;"></td> <td style="width: 15%;">Date</td> <td style="width: 25%;">28 / 05 / 17</td> </tr> </table>		Date	28 / 05 / 17
	Date	28 / 05 / 17		

Name of Co-Author	Mohamad Kourghi			
Contribution to the Paper	Wrote the manuscript.			
Signature	<table border="1" style="width: 100%;"> <tr> <td style="width: 60%;"></td> <td style="width: 15%;">Date</td> <td style="width: 25%;">23 / 05 / 2017</td> </tr> </table>		Date	23 / 05 / 2017
	Date	23 / 05 / 2017		

Name of Co-Author	Michael L. De Ieso
Contribution to the Paper	Wrote the manuscript.
Signature	
	Date 22/05/17

Name of Co-Author	Andrea J. Yool
Contribution to the Paper	Wrote the manuscript.
Signature	
	Date 22 May 2017

PUBLISHED MANUSCRIPT

**Drug discovery and therapeutic targets for pharmacological
modulators of aquaporin channels**

Jinxin V Pei ^{1,2}, Joshua L Burton ^{1,2,3}, Mohamad Kourghi ¹, Michael L De Ieso ¹, and
Andrea J Yool ^{1,2,3}

⁽¹⁾ School of Medical Sciences; ⁽²⁾ The Institute for Photonics and Advanced Sensing;
and

⁽³⁾ The Adelaide Centre for Neuroscience Research. University of Adelaide, SA
Australia

Ch 16 in *“Aquaporins in health and disease: New molecular targets for drug
discovery”*

G Soveral, S Nielsen and A Casini, eds. CRC Press

Corresponding author:

Prof Andrea J Yool

University of Adelaide

Medical School South, Level 4, Frome Road

Adelaide SA 5005 AUSTRALIA

phone +61 8 8313 3359

email: andrea.yool@adelaide.edu.au

Table of Contents

1 Overview of aquaporin channel functions in brain fluid homeostasis and cell migration

- 1.1 AQP4 in cerebral edema
- 1.2 AQP1 in cell migration

2 Small molecule drug discovery for aquaporin channels

- 2.1 Modulators of water channel activity
- 2.2 Regulation of AQP1 ion channel activity

3 Translational promise of pharmacological modulators of aquaporin channels in brain edema, cancer and other disorders

- 3.1 Targeting AQP4 channels in brain edema
- 3.2 Differential regulation of expression of AQP channel types in cancer cells
- 3.3 Targeting AQP1 channels in cell migration and metastasis

4 New avenues for aquaporin drug discovery from traditional and alternative medicines

Abstract

Fluid homeostasis in the body is well known to be regulated by ion channels and transporters, but equally important are the co-expressed classes of aquaporin water channels that facilitate transmembrane water movement. The field of aquaporin pharmacology is expanding rapidly with the new identification of small molecule drug-like agents with distinctive properties in aquaporin modulation, allowing exploration of potential therapeutic applications in brain edema, cancer and other disorders. Pharmacological agents could modulate AQPs by direct occlusion of the water pore itself, by acting at distinct sites that confer other channel properties, or by altering levels of protein expression or membrane targeting. Expanding the pharmacological portfolio will benefit basic research and promote new therapeutic strategies in many conditions involving aquaporins in the symptoms or disease processes. Exploring herbal alternative medicines as sources of pharmacological agents for aquaporins is likely to have a substantial impact on the field of aquaporin research, which has keenly awaited the development of chemical interventions as a platform for therapeutic approaches. Recent work is providing an enhanced understanding of the molecular mechanisms of action of traditional herbal medicines as novel sources of aquaporin modulators.

Aquaporins (AQPs) found throughout the kingdoms of life (Zardoya, 2005) are channel proteins which facilitate water and small solute movement across plasma membranes based on chemical, osmotic and hydrostatic gradients (Hachez and Chaumont, 2010; Ishibashi et al., 2011; Madeira et al., 2014). The existence of water channels in red blood cells and barrier membranes and their hallmark sensitivity to block by mercury (Benga et al., 1986; Macey, 1984; Macey et al., 1972; Naccache and Sha'afi, 1974) were deduced before AQP1 cDNA was cloned and characterized in the early 1990s (Preston and Agre, 1991; Preston et al., 1992). Progress since has defined thirteen mammalian subtypes of AQPs, their relative protein abundance, tissue-specific distributions, and expression levels under various conditions. AQP crystal structures have provided insights into the homotetrameric channel structure, and the location of the water pores within each of the four subunits (Ishibashi et al., 2009; Jensen et al., 2003; Sui et al., 2001). AQP1 is a tetrameric channel with water pores located within each of the four individual subunits (Fu et al., 2000; Sui et al., 2001). Review articles have emphasized the compelling need for development of AQP modulators as candidate treatments for a variety of disorders (Castle, 2005; Frigeri et al., 2007; Huber et al., 2012; Jeyaseelan et al., 2006). However, prior to 2009, the discovery of AQP pharmacological agents had not progressed substantially beyond mercuric compounds, which lacked translational potential due to toxicity, and agents that affected multiple targets and lacked potency. Recent advances have shown that drug-like lead compounds are emerging, complementing work that has investigated the functional roles of aquaporins by overexpression or targeted genetic knockdown and deletion.

1 Overview of aquaporin channel functions in brain fluid homeostasis and cell migration

Fluid homeostasis in the body is regulated by partnerships of ion channels and transporters with co-expressed classes of aquaporin channels (Conde et al., 2010; Fischbarg, 2010). The thirteen classes of mammalian aquaporin water channels (AQPs 0 to 12) are expressed in tissue-specific patterns in the body, and are essential in regulating the movement of fluid across barrier membranes, and contributing to control of cell volume, production of cerebral spinal fluid, edema formation and recovery, mediating renal function, and more (Ishibashi, 2009; Nielsen et al., 2007). Under pathological conditions, dysfunctions in the control of fluid movement create serious problems. The physiological importance of AQP channels and their compelling potential value as therapeutic targets have motivated researchers to work toward defining a pharmacological panel of chemical modulators for AQPs. A comprehensive pharmacological portfolio for all classes of aquaporins will provide an array of new therapeutic opportunities that will continue to expand as new roles for aquaporin channels are uncovered. Two major areas of current interest in aquaporin-based mechanisms of disease are brain swelling after injury or stroke, and the migration of cancer cells in the process of metastasis.

1.1 AQP4 in cerebral edema

An area of intense interest for new therapies directed at AQPs is aimed at reducing brain swelling after acute traumatic injury or stroke (Mack and Wolburg, 2013; Yool et al., 2009). Cerebral edema and increased intracranial pressure are life-threatening sequelae of severe brain injuries, associated with a poor prognosis as evidenced by a mortality rate near 60 to 80% (Feickert et al., 1999; Hacke et al., 1996). Traumatic

brain injury affects an estimated 10 million people annually; according to the World Health Organization, it will be the major cause of death and disability by the year 2020 (Hyder et al., 2007). Nearly one-third of hospitalized traumatic brain injury patients die from injuries that are secondary to the initial trauma, including neuroinflammation, excitotoxicity, brain edema, and intracranial hypertension (Miller et al., 1992). Traumatic brain injury reduces life expectancy and compromises quality of life (Schiehser et al., 2014) with increased incidences of seizures, sleep disorders, neurodegenerative disease, neuroendocrine dysregulation, psychiatric problems, and non-neurological disorders that can persist years after the injury event (Masel and DeWitt, 2010). The burden of mortality and morbidity makes traumatic brain injury a pressing public health and medical concern, but there is currently no targeted pharmacological treatment for reducing the secondary damage (Park et al., 2008).

Cerebral ischemia following severe traumatic brain injury involves a combination of cytotoxic and vasogenic events (Hossmann, 1994; Papadopoulos et al., 2004; Shi et al., 2012; Tourdias et al., 2011). Brain edema commonly occurs when cerebral blood flow drops beneath 10ml/100g/min, and essential ionic pump activity is impaired. During the first 5 h of ischemia, blood brain barrier integrity can be maintained without substantial brain swelling (Betz et al., 1989), but upon reperfusion, a rise in brain water content can occur in conjunction with an elevation in intracranial pressure depending on the extent of ischemia, and the delay until cerebral blood flow is restored (Avery et al., 1984). Conventional treatments focus on reducing edema and intracranial pressure using hyperventilation, mannitol, diuretics, corticosteroids or barbiturates (Manno et al., 1999; Winter et al., 2005). Decompressive craniectomy involves the surgical removal of part of the skull, creating a space for the swollen brain tissue to expand. This surgical method improves survival, but doesn't fully address pathological

outcomes as many patients are left moderately or severely disabled (Fischer et al., 2011; Vahedi et al., 2007).

Work in animal models relies on optimizing the reliability and reproducibility of the injury event. The middle cerebral artery occlusion model in rodents has been a standard method for testing experimental therapeutic agents, but is difficult in part because of unexplained variability in infarct volumes. When analyzed with computed tomography cerebral blood volume maps, variability was found to result from unintended occlusion of a second artery (the anterior choroidal artery) in a subset of animals, causing expanded infarct areas (McLeod et al., 2013). Brain computed tomography perfusion imaging provides a powerful tool for improving the experimental method by fully defining the arteries affected by occlusion, and accurately identifying the infarct core and penumbra domains (McLeod et al., 2011).

The concept of edema as being the primary cause of increased intracranial pressure has been challenged; small ischemic strokes in rats resulted in minimal amounts of edema but were associated with a substantial elevation in intracranial pressure at 24 h, which was effectively countered by application of hypothermia soon after the stroke event. Mechanisms in addition to cerebral edema alone must be considered as important drivers of intracranial pressure elevation (Murtha et al., 2014a; Murtha et al., 2014b). Assessing the regulated contributions of transporters and channels including AQP1 and AQP4 might offer insight into possible molecular mechanisms generating the distinct outcomes.

AQP4 is the predominant water channel in the brain, localized to the blood-brain barrier, ependymal cells lining the ventricles, subependymal astrocytes and the glia limitans (Amiry-Moghaddam and Ottersen, 2003; Nagelhus and Ottersen, 2013; Xiao and Hu, 2014) for their involvement in water movement both in and out of the brain

(Mack and Wolburg, 2013). Studies in AQP4-deficient mouse models showing partial protection from water intoxication and edema after stroke (Manley et al., 2000; Papadopoulos and Verkman, 2008) support the idea that ligand modulators of AQP4 could revolutionize clinical treatment of brain edema. To date, progress in the field has been limited by the lack of availability of pharmacologic modulators of the AQP channels. Identification of agonists and antagonists of AQP4 remains an important goal in the field of cerebral edema research. AQP4 channels subserve water movement during cerebral edema formation (Jullienne and Badaut, 2013; Manley et al., 2000), highlighting them as an attractive therapeutic target for non-surgical management of cerebral edema (Yool, 2007a; Yool et al., 2009).

Alterations in levels of AQP expression in response to cerebral fluid imbalance can offer clues for understanding the functional roles of water channels, assuming the goal is to restore homeostasis. In experimental models of cerebral ischemia, expression levels of AQP4 were reduced in the initial period post-injury, and significantly increased thereafter (Taniguchi et al., 2000; Yamamoto et al., 2001). Regulation of AQP4 expression appears to correlate with levels of the transcription factor HIF-1 α (hypoxia-inducible factor 1-alpha) (Kaur et al., 2006). Early after traumatic brain injury (5h), levels of HIF-1 α were low and increased to peak at 24-48 h post-injury (Ding et al., 2009; Higashida et al., 2011). Inhibition of HIF-1 α correlated with decreased AQP4 and attenuated swelling post-injury (Shenaq et al., 2012). The temporal pattern of AQP4 regulation suggests that downregulation of channels early after injury could be a protective response to limit the influx of fluid into the brain, whereas delayed upregulation might serve to enable fluid export and the restore fluid homeostasis. However, altered gene expression responses are not spatially uniform. A reduction in AQP4 expression occurred in astrocytes within the ischemic core while an elevation

in AQP4 expression was seen in glial endfeet in the surrounding penumbra, in a middle cerebral artery occlusion model (Frydenlund et al., 2006). Spatially selective regulation of AQP4 might limit water influx into the ischemic core without preventing the amelioration of vasogenic edema in the penumbra. The loss of AQP4 was not linked to a decrease in the astrocyte marker, glial fibrillary acidic protein, GFAP (Friedman et al., 2009), indicating that decreased AQP4 expression was not an indirect effect of glial cell loss in the injured domain.

AQP4 water channels are dynamically regulated components of brain fluid homeostasis, being mobilized or deactivated as needed to reduce damage arising from shifts or disturbances in cerebral fluid homeostasis. The temporal and spatial patterns of AQP4 regulation are contingent upon the extent and duration of injury and stage of pathology. AQP pharmacological agents will be advantageous for intervention brain fluid disorders particularly if administered with an understanding of the dynamic mechanisms of aquaporin channel regulation.

1.2 AQP1 in cell migration

Cell migration is essential in development, repair, regeneration, and immune protection in multicellular organisms. In 1937, the neuroanatomist Ramon y Cajal pondered: "What mysterious forces stimulate the migrations of cells...?" (Kater and Letourneau, 1985). Currently it is thought that branched assemblies of actin filaments, actively polymerising at the leading edge, generate the primary force which pushes out thin ruffled membrane extensions known as lamellipodia (Le Clairche and Carlier, 2008). Parallel arrays of actin are stalled by small loads on the order of 1 pN (Footer et al., 2007), but branched actin networks with many points of contact can generate nN of force per μm^2 , on the scale needed for movement through viscous extracellular

environments (Marcy et al., 2004; Parekh et al., 2005). Cell adhesions at the leading edge hold the new position while the trailing edge detaches, and the cell resets for the next push forward.

Aquaporins found in all the kingdoms of life facilitate fluxes of water and small solutes across membranes (King et al., 2004). In diverse motile cells from amoeba to human, specific AQPs are localized in lamellipodial leading edges. When these cells are made AQP-deficient (for example by genetic knock-out or RNA-interference techniques), cell migration is greatly impaired. Reintroduction of AQP restores rates of movement, but interestingly, the effects of different AQPs are not interchangeable (McCoy and Sontheimer, 2007).

Of the 13 known mammalian classes of AQPs, the three often associated with migration thus far are AQPs 1, 3 and 5. In the "World Cell Race" event held at the American Society for Cell Biology meeting in 2011, cell lines were submitted by teams around the world; the winner was a bone marrow stem cell which covered the 400 μm track at a speed of at 5.2 $\mu\text{m}/\text{min}$. Bone marrow stem cells express lamellipodial AQP1 that is required for migration (Meng et al., 2014). The need for AQPs in migration extends to life forms other than mammals. The amoeba *Dictyostelium discoideum* migrates in a chemotactic response to external cAMP signals, and expresses an AQP orthologous to human AQP1 (48% amino acid sequence similarity) which is localized in lamellipodia (von Bulow et al., 2012). If *D. discoideum* had been in the competition, it might have taken the honors, moving at up to 11 $\mu\text{m}/\text{min}$ in response to cAMP chemotactic stimuli (Van Duijn and Inouye, 1991). Other contenders could have included activated T-cells moving at >10 $\mu\text{m}/\text{min}$ (Katakai et al., 2013) which express AQPs 1, 3, and 5 (Moon et al., 2004); and fibroblasts moving at up to 9 $\mu\text{m}/\text{min}$ (Ware et al., 1998) which express AQP1 (Minami et al., 2001).

Even though AQP1 and AQP4 are both highly functional water channels, the expression of AQP1 enables rapid cell movement, whereas expression of AQP4 does not. One important difference is that AQP1 but not AQP4 can function as a gated monovalent cation channel (Anthony et al., 2000; Yool and Campbell, 2012). AQP1 ion channel activity has been replicated in other laboratories (Saparov et al., 2001; Zhang et al., 2007), but its physiological significance remains unknown. During migration, changes in cytoplasmic volume are required. Fluid flux is commonly thought of as a passive process in which water follows salt. Yet the observation that water channels cannot simply be swapped between cells suggests that other properties in addition to water channel function are needed. The pro-migratory effect of AQP1 and its orthologs appears to be a convergent target of evolution across phyla.

2 Small molecule drug discovery for aquaporin channels

Inhibitors of AQPs have long been heralded as important goal in the field. A database of structurally diverse compounds will be of substantial value in expanding our understanding of drug structure-activity relationships and molecular sites of action for aquaporin pharmacological modulators. Pharmacological agents could modulate AQPs by direct occlusion of the water pore itself, by acting at distinct sites that confer other channel properties, or by altering levels of protein expression or membrane targeting.

2.1 Modulators of water channel activity

Regulatory domains in aquaporins can control membrane localization, interaction with proteins to create signaling complexes and scaffolds, and gated permeation of small solutes other than water through AQPs (Cowan et al., 2000; Yool, 2007a; Yool,

2007b). Much of the work to date has focused on agents that act to occlude the water pore. The existence of water channels in cell membranes and their hallmark sensitivity to block by mercury were deduced before the first AQP1 cDNA was cloned (Preston and Agre, 1991; Preston et al., 1992). Finding non-mercurial AQP blockers has been essential for aquaporin drug discovery (**Table 1**). Silver and gold compounds were reported to block water channel activity of both plant and human aquaporins (Niemietz and Tyerman, 2002; Tyerman et al., 2002). Membrane-permeable derivatives of the loop diuretic drugs bumetanide and furosemide have proven useful as pharmacological antagonist AqB013 (Migliati et al., 2009) and agonist AqF026 (Yool et al., 2013) agents for AQP1 and AQP4 water channel activities. Characterized in vitro and in rodent models in vivo, these candidate AQP drugs appear to be effective and well tolerated. In a mouse model of peritoneal dialysis, the lack of effect of the agonist AqF026 in AQP1 knockout animals indicated specificity of action without appreciable off-target effects (Yool et al., 2013). Other groups also have investigated arylsulfonamides as AQP blockers (Gao et al., 2006; Huber et al., 2007; Ma et al., 2004; Seeliger et al., 2013). Acetazolamide (AZA) has been reported to inhibit AQP4 water permeability with an IC_{50} value of 0.9 μ M. *In silico* docking suggested an interaction between the sulfonamide group of AZA and both arginine 216 and glycine 209 (Huber et al., 2007). As compared to AQP4, AQP1 was less sensitive to AZA, with an IC_{50} value estimated at $5.5 \pm 0.5 \mu$ M (Seeliger et al., 2013).

2.2 Regulation of AQP1 ion channel activity

The passage of water and ions occurs through pharmacologically distinct pathways in AQP1 (Saparov et al., 2001; Yool et al., 2002). The cGMP-gated cation permeation pathway is thought to be in the central pore of the tetramer, based on molecular

dynamic simulations (Yu et al., 2006) and effects of site-directed mutations on altering ionic conductance properties (Campbell et al., 2012). Conduction of ions in AQP1 channels is inhibited by Cd^{2+} but not tetraethylammonium ion (TEA^+); whereas water transport which occurs through the individual pores located in each subunit is sensitive to TEA^+ , AqB013, AqF026, but not Cd^{2+} (Boassa et al., 2006; Brooks et al., 2000; Migliati et al., 2009; Yool et al., 2002; Yool et al., 2013). In silico docking identified possible extracellular binding by TEA^+ (Detmers et al., 2006), but indicated intracellular sites of action for the arylsulfonamides, supported by results of site-directed mutations and biological assays. AqB013 is thought to occlude the water pore at the internal vestibule whereas the AQP agonist, AqF026, appears to potentiate water channel activity by interacting with an intracellular gate (loop D) between the 4th and 5th transmembrane domains (Yool et al., 2013).

The loop D domain serves as a gate for AQP channel activity in mammalian AQP1 (Yu et al., 2006), AQP4 (Zelenina et al., 2002), amoeba AQP-B (von Bulow et al., 2012) and plant AQP (Tornroth-Horsefield et al., 2006). In AQP1, loop D domain is involved in the regulation of cation channel activity activated by cGMP (Yu et al., 2006). The loop D sequence is highly conserved across species in AQP1 channels from fish to mammals, yet mutations in this domain do not impact water channel activity, suggesting that loop D is essential for AQP1 functions other than water permeability. Mutations at specific loop D positions in AQP1 remove ion channel activity without impairing water channel activity (Yu et al., 2006). The retention of water channel functionality showed that the mutation did not interfere with expression, trafficking or assembly of AQP1 channel.

Other regulatory domains in AQP1 have been suggested in the carboxy-terminal domain. A putative cGMP-dependent modulatory domain with sequence similarity to

the cGMP-phosphodiesterase selectivity domain was identified in the AQP1 C-terminus (Boassa and Yool, 2002; Boassa and Yool, 2003). Mutations of conserved phosphodiesterase-like residues in this domain did not remove cGMP-dependent activation of AQP1, but reduced the efficacy of cGMP by right-shifting the dose-response curve. An EF-hand motif found in calcium binding proteins (Grabarek, 2006) has been proposed in the carboxyl terminal domain of AQP1 but its functional role has not yet been defined (Fotiadis et al., 2002). A tyrosine phosphorylation site in the carboxyl terminal serves a modulatory role in governing the availability of AQP1 to be gated as a cGMP-dependent cation channel (Campbell et al., 2012). A PDZ protein-protein ligand domain identified in AQP1 (Ile260 to Arg264) in the C terminus was shown to be important for targeting AQP1 into a membrane complex needed to maintain vestibular fluid balance in the inner ear (Cowan et al., 2000). Regulatory domains and transmembrane pore regions in AQPS are both attractive candidates for the development of drug agents.

3 Translational promise of pharmacological modulators of aquaporin channels in brain edema, cancer and other disorders

Pharmacological control of the direct fluid flow pathways between blood and brain could provide for invaluable therapeutic interventions in cerebral pathologies involving abnormal water fluxes such as stroke, hydrocephalus, and brain tumors. Aquaporin-4 is a logical choice as a molecular target for drug development (Papadopoulos and Verkman, 2007; Yool et al., 2009). It is abundantly expressed in the central nervous system near the blood-brain barrier at glial cell endfeet, and provides a major pathway for fluid homeostasis (Amiry-Moghaddam and Ottersen, 2003).

3.1 Targeting AQP4 channels in brain edema

Conventional approaches have relieved intracranial pressure with hyperventilation, hyperosmotic agents, diuretics and decompressive craniectomy (Diedler et al., 2009; Park et al., 2008; Werner and Engelhard, 2007), but are limited in effectiveness by treating symptoms rather than causes of edema. A major challenge has been the lack of interventions for controlling fluid movement in brain edema. Astrocytes have been proposed to have a bimodal contribution, with a positive role in fluid homeostasis and limiting brain injury, and a negative role in worsening the neuroinflammation, cerebral edema, and elevated intracranial pressure associated with secondary brain injury following neurotrauma (Laird et al., 2008).

Now with the characterization of novel AQP agonists and antagonists, it will be possible to investigate potential pharmacological treatments for cerebral edema (Yool et al., 2009) with an intriguing capacity for bimodal regulation of AQP water channel activity. For example, in a rat model of cerebral edema induced by diffuse traumatic brain injury, a single intravenous application of the AQP antagonist AqB013 within five hours post-injury dramatically reduced edema formation, and single administration of the AQP agonist AqF026 at 1 to 2 days post-injury accelerated the resolution of brain edema (Burton, Vink and Yool, 2015; MS submitted). Each modulator was beneficial alone; however, of interest was the observation that a sequential treatment of antagonist followed by agonist each at their optimal single timepoints provided a powerful combination that further enhanced protection of motor function, reduced brain swelling and decreased brain albumin content post-injury. Understanding the biphasic role of AQP4 in cerebral edema and the actions of aquaporin pharmacological modulators will be likely to open new avenues for development of therapeutic interventions after traumatic brain injury.

3.2 Differential regulation of expression of AQP channel types in cancer cells

Evidence emerging within the past decade is providing increasingly strong support for the role of selected classes of AQPs as important constituents in cancer cell biological mechanisms. Data show a strong positive correlation between AQP expression levels and tumor severity (Machida et al., 2011). Tumor cells selectively increase levels of expression of different specific types of AQPs; in some cases there is an increase in an AQP class normally expressed in the cell type (Saadoun et al., 2002a), but in other cancers the upregulated class of AQP is not found at appreciable levels in the original tissue (Moon et al., 2003). AQPs are linked with a variety of properties of cancer cells, such as tumor size expansion, edema, cell adhesion, migration, and proliferation, that enhance tumor growth and metastasis (Hu and Verkman, 2006; Saadoun et al., 2002a; Saadoun et al., 2002b).

For AQP1 and AQP5 channels, *de novo* expression has been observed in early stage colorectal carcinoma development, but is not detectable in normal colonic epithelium (Moon et al., 1997; Moon et al., 2003) for purposes that remain incompletely understood in the context of cancer progression. When transfected into melanoma and breast cancer cell lines, increased AQP1 expression was associated with an increase in both in vitro cell migration and in vivo metastasis (Hu and Verkman, 2006). When melanoma cells B16F10 were implanted subcutaneously, AQP1 null mice showed slower melanoma tumor growth and impaired tumor angiogenesis as compared with wild type mice (Saadoun et al., 2005).

AQP1 contributes to cell migration and angiogenesis and facilitates tumor growth and metastasis through mechanisms that remain to be defined. In its proposed activity as a dual water and ion channel (Yool and Weinstein, 2002), AQP1 could be one

mechanism used for enhancing migration rate in a subset of classes of aggressive cancers. Facilitation of cell migration appears to be achieved in other types of cells by colocalization of water-selective aquaporins in combination with ion transporters (Chai et al., 2013; Stroka et al., 2014).

AQP3 increased migration and proliferation of corneal epithelial cells in wild-type as compared with *Aqp1*-null mice, and was important in peritoneal fibrosis and wound healing (Ryu et al., 2012). In squamous skin cell carcinomas and bronchioloalveolar carcinomas, AQP3 upregulation influenced metastasis and proliferation (Hara-Chikuma and Verkman, 2008a; Machida et al., 2011). After si-RNA knockdown of AQP3 expression, weaker cell adhesion and impaired cell growth were observed (Kusayama et al., 2011). In non-small cell lung cancer, AQP3 knockdown suppressed tumor growth and reduced angiogenesis (Xia et al., 2014). In agreement, AQP3 null mice show reduced glycerol transport, and were more resistant to skin cancer formation (Hara-Chikuma and Verkman, 2008b).

AQP4 appears to assist with water balance in the tumor environment, and has been postulated to play a role in cell-cell adhesion, possibly via an extracellular helical domain in loop C that could interact with adjacent cells. Expression of AQP4 conferred adhesive properties in cells that lacked classic adhesion molecules, as shown by L-cell cluster formation in AQP4-positive cells but not control cells (Hiroaki et al., 2006); however other work has not confirmed the idea (Zhang and Verkman, 2008). More studies will be required to determine what factors influence a putative role of AQP4 in tumor cell adhesion. AQP4 can be phosphorylated by protein kinase C (PKC) at Ser-180. Phosphorylation level is inversely proportional to water permeability. Mutation of Ser-180 to alanine increased AQP4 water permeability by approximately two-fold (McCoy et al., 2010). In AQP4-transfected glioma D54MG cells, both AQP4 water

permeability and tumor cell migration were decreased when protein kinase C (PKC) was activated by phorbol ester treatment. It is postulated that cells with suppressed AQP4 activity have a compromised ability to adjust cell shape during migration (McCoy et al., 2010). In contrast, when D54MG cells were transfected with AQP1, neither of the properties of water channel activity or cell migration were affected by PKC modulators (McCoy et al., 2010).

AQP5 expression is increased in pancreatic, colon cancers and myelogenous leukemia cells (Machida et al., 2011; Woo et al., 2008). Proliferation of human ovarian cancer cells has also been correlated with AQP5 expression levels (Chae et al., 2008a). The involvement of AQP5 in cancer invasion has been demonstrated to depend on phosphorylation of Ser-156 located in the loop-D domain through a c-Src signaling pathway (Chae et al., 2008b). Deletion of AQP5 but not AQP1 nor AQP3 was correlated with decreased activation of the epithelial growth factor receptor signal cascade (EGFR/ERK/MAPK) which regulated cancer cell migration and proliferation (Zhang et al., 2010). Results from many studies now show that AQP3 and AQP5 contribute to processes of tumor proliferation, but the link from aquaporin function to the regulation of growth remains to be defined.

As depicted in **Figure 1**, AQP expression can be polarized in the lamellipodia of migrating cells, together with transporters such as the Na^+/H^+ , the $\text{Cl}^-/\text{HCO}_3^-$ exchanger or the $\text{Na}^+-\text{K}^+-\text{Cl}^-$ co-transporter. Localized ion fluxes are proposed to create a driving force for osmotic water fluxes, in parallel with the osmotic effects of actin polymerization and depolymerization, that could drive the membrane protrusions. This concept has been presented as an 'osmotic engine model' (Stroka et al., 2014) based on studies of AQP5 and Na^+/H^+ exchangers polarized to the leading edges in mouse S180 sarcoma cells migrating in a confined environment.

3.3 Targeting AQP1 channels in cell migration and metastasis

Tumor cell migration enables metastasis and tissue invasion, and is a major cause of death in patients with cancer (Bogenrieder and Herlyn, 2003). A review of literature shows that AQP1 expression is upregulated in a subset of aggressive cancers; whereas AQP1 deletion or downregulation impedes migration of AQP1-expressing cancer cells *in vitro* and reduces metastasis *in vivo* (Deb et al., 2012; Verkman et al., 2008; Yool et al., 2009). Wound-healing and transwell migration assays have demonstrated impaired migration of tumor cells lacking AQP1 as compared to wild type (Jiang, 2009; Jiang et al., 2009; Jiang and Jiang, 2010; Li et al., 2006). Cell migration rate in AQP1-knockdown cells can be rescued by adenovirus-mediated AQP1 expression. Similarly, transfection of AQP1 into tumor cells that lack endogenous AQP1 show accelerated cell migration rate *in vitro* as compared to control cells (Hu and Verkman, 2006; McCoy and Sontheimer, 2007).

Manipulation of tumor cell migration rate via AQP1 expression levels has been explored in rodent models *in vivo*. Increased AQP1 expression increased tumor cell extravasation, quantified by the numbers of fluorescently-tagged tumor cells which infiltrated mouse lung tissue after injection into tail vein (Hu and Verkman, 2006). In a mouse model that spontaneously developed well-differentiated, luminal-type breast adenomas with lung metastases, genetic deletion of AQP1 correlated with reductions in lung metastases, tumor mass, and tumor volume with abnormal microvascular anatomy and reduced vessel density as compared to wild type mice (Esteva-Font et al., 2014). AQP1 expression facilitated endothelial cell migration, and augmented tumor growth *in vivo* by the facilitation of angiogenesis (El Hindy et al., 2013; Nicchia et al., 2013). Impaired melanoma growth was observed in AQP1-null mice after

subcutaneous tumor cell implantation, and attributed to reduced aortic endothelial cell migration (Saadoun et al., 2005).

AQP1 is an attractive therapeutic target for controlling tumor growth and migration. Pharmacological modulation of AQP1 could be a pivotal adjunct to existing cancer therapies, improving the prognosis for cancer patients by slowing cancer angiogenesis and metastases.

4 New avenues for aquaporin drug discovery from traditional and alternative medicines

Complementary and alternative medicine practices provide an intriguing starting point in searches for novel pharmacological modulators for aquaporin channels, drawing on cultural insights of native botanical agents from Asian, indigenous Australian, American, Indian and other sources of cultural knowledge. Given the importance of aquaporins in human health and disease, AQP modulatory agents have a compelling potential to benefit research and health care globally. Scientific evidence is needed to understand the molecular mechanisms that underlay therapeutic actions of alternative medicines which have been used around the world from ancient times to treat fluid imbalance disorders and diseases (de Morais Lima et al., 2011; Karou et al., 2011; Kong et al., 2015; Nie et al., 2013). Possible agents for aquaporin channels might be present in native botanical agents used for treating conditions such as kidney and gastrointestinal disorders, swelling, brain edema, and inflammation, which in theory could be benefiting from altered AQP channel activity in mitigating the dysfunctions. Botanical compounds over many centuries have been an important source of useful drugs. As reviewed by Wachtel-Galor and Benzie (2011; CRC Press 'Herbal Medicines: Biomedical and Clinical Aspects'), about 25% of the drugs prescribed

worldwide are derived from plants, including morphine derived from poppy seeds (*Papaver somniferum*), digoxin from foxglove (*Digitalis lanata*), aspirin from willow bark, antimalarials such as quinine from Cinchona bark (*Cinchona officinalis*), and artemisinin derived from *Artemisia annua*. The potential value for translation into a novel pharmacology for AQP channels is immense. Expanding the pharmacological portfolio for aquaporins will not only benefit basic research but could also prompt strategies for therapeutic interventions in cancers, lung and cardiac edema, secretory and digestive dysfunctions, and other conditions involving tissues in which AQPs are expressed.

Two principal groups of phytochemicals of interest appear to be emerging from the data available thus far: (i) polysaccharides (glucans) extracted from aqueous fractions; and (ii) triterpenes (polyporosterones) extracted from organic fractions of medicinal plants. A meta-analysis of published data on extracts and isolated compounds from an edible mushroom *Polyporus umbellatus* show it acts as a diuretic, anti-cancer, immunostimulant and hepatoprotective agent (Zhao, 2013). An aqueous fraction of the Chinese medicinal fungus Fu Ling *Poria cocos* contains multiple saccharides, and has been reported to attenuate renal AQP2 expression at the transcription and translational levels (Lee et al., 2012b). Extracts of Fu Ling also act as a diuretic and suppress the growth and invasiveness of various tumor cell lines (Cheng et al., 2013; Ling et al., 2011; Zhao et al., 2012). Similar to *P. umbellatus*, various triterpenes have been extracted and identified from *P. cocos* (Rios, 2011). In a study of papilloma carcinogenesis, poricoic acid C was demonstrated to decrease the incidence to 27% as compared with 100% in the control group (Akihisa et al., 2007). A bioactive compound (ginsenoside Rg3) found in the ginseng root extract was shown to attenuate cell migration via inhibition of AQP1 expression in PC-3M prostate cancer cells *in vitro*,

and demonstrated the potential usefulness of pharmacological modulation of AQP1 in manipulating tumor cell migration (Pan et al., 2012).

Diverse classes of channels and transporters are modulated by curcumin (isolated from tumeric in the ginger family), including voltage-gated K⁺ and Ca²⁺ channels, the volume-regulated anion channel VRAC, the Ca²⁺ release-activated Ca²⁺ channel CRAC, AQP4 channels, glucose transporters, and others (Zhang et al., 2014). As compared with vehicle-injected rats, a lower level of AQP4 expression was observed in rats injected with 40 mg/kg curcumin. In the same experiment, a neuroprotective effect of curcumin was demonstrated in a rat model of hypoxic ischemic brain damage (Yu et al., 2012).

Bacopa (*Bacopa monnieri*), a water hyssop also known as Brahmi in traditional Indian medicine, has been used in complementary medicine remedies for centuries to improve memory and treat anxiety and depression (Russo and Borrelli, 2005). The main active components are triterpenes (bacosides, bacopasides and bacosaponins) (Russo and Borrelli, 2005). Some of the beneficial effects of Bacopa could potentially involve aquaporin channels; however, the diverse group of candidate targets of action remains to be investigated. Tumor size decreased when mice with subcutaneously implanted S180 sarcoma cells were treated with bacopa extracts (Peng et al., 2010). Bacopa confers neuroprotective effects after ischemic brain injury (Liu et al., 2013; Saraf et al., 2010), which might suggest testing for a possible link with AQP4, known to be a key contributor in pathological outcomes of brain injury (Kim et al., 2010; Lee et al., 2012a; Shin et al., 2011). Bacopa also has also been used for control of epilepsy (Shanmugasundaram et al., 1991), and some anti-epileptic drugs have been demonstrated inhibit AQP4 water permeability (Huber et al., 2009).

Plant derived polysaccharide and triterpenes compounds possess diverse pharmacological functions. A subset of them appear to have theoretical potential (based simply on the nature of their cellular and systemic effects *in vivo*), to regulate AQP levels of expression or function directly or indirectly. A sample of interesting phytochemical candidates and their structures are listed in **Table 2**. While still speculative at this point, the concept is worth further investigation. More research is needed focusing on phytochemicals as sources of candidate pharmacological agents for aquaporins. Intriguing connections between botanical medicinal agents and aquaporins remain to be investigated, but could be a valuable source of new lead compounds for broadening the field of aquaporin pharmacology, and better understanding the molecular mechanisms of action of alternative medicinal agents.

References

- Akihisa T, Nakamura Y, Tokuda H, Uchiyama E, Suzuki T, Kimura Y, Uchikura K and Nishino H (2007) Triterpene acids from *Poria cocos* and their anti-tumor-promoting effects. *Journal of natural products* **70**(6):948-953.
- Amiry-Moghaddam M and Ottersen OP (2003) The molecular basis of water transport in the brain. *Nature reviews Neuroscience* **4**(12):991-1001.
- Anthony TL, Brooks HL, Boassa D, Leonov S, Yanochko GM, Regan JW and Yool AJ (2000) Cloned human aquaporin-1 is a cyclic GMP-gated ion channel. *Mol Pharmacol* **57**(3):576-588.
- Avery S, Crockard HA and Russell RR (1984) Evolution and resolution of oedema following severe temporary cerebral ischaemia in the gerbil. *Journal of neurology, neurosurgery, and psychiatry* **47**(6):604-610.
- Benga G, Popescu O, Pop VI and Holmes RP (1986) p-(Chloromercuri)benzenesulfonate binding by membrane proteins and the inhibition of water transport in human erythrocytes. *Biochemistry* **25**(7):1535-1538.
- Betz AL, Iannotti F and Hoff JT (1989) Brain edema: a classification based on blood-brain barrier integrity. *Cerebrovascular and brain metabolism reviews* **1**(2):133-154.
- Boassa D, Stamer WD and Yool AJ (2006) Ion channel function of aquaporin-1 natively expressed in choroid plexus. *J Neurosci* **26**(30):7811-7819.
- Boassa D and Yool AJ (2002) A fascinating tail: cGMP activation of aquaporin-1 ion channels. *Trends Pharmacol Sci* **23**(12):558-562.

- Boassa D and Yool AJ (2003) Single amino acids in the carboxyl terminal domain of aquaporin-1 contribute to cGMP-dependent ion channel activation. *BMC Physiol* **3**:12.
- Bogenrieder T and Herlyn M (2003) Axis of evil: molecular mechanisms of cancer metastasis. *Oncogene* **22**(42):6524-6536.
- Brooks HL, Regan JW and Yool AJ (2000) Inhibition of aquaporin-1 water permeability by tetraethylammonium: involvement of the loop E pore region. *Mol Pharmacol* **57**(5):1021-1026.
- Campbell EM, Birdsell DN and Yool AJ (2012) The activity of human aquaporin 1 as a cGMP-gated cation channel is regulated by tyrosine phosphorylation in the carboxyl-terminal domain. *Mol Pharmacol* **81**(1):97-105.
- Castle NA (2005) Aquaporins as targets for drug discovery. *Drug Discov Today* **10**(7):485-493.
- Chae YK, Kang SK, Kim MS, Woo J, Lee J, Chang S, Kim DW, Kim M, Park S, Kim I, Keam B, Rhee J, Koo NH, Park G, Kim SH, Jang SE, Kweon IY, Sidransky D and Moon C (2008a) Human AQP5 plays a role in the progression of chronic myelogenous leukemia (CML). *PloS one* **3**(7):e2594.
- Chae YK, Woo J, Kim MJ, Kang SK, Kim MS, Lee J, Lee SK, Gong G, Kim YH, Soria JC, Jang SJ, Sidransky D and Moon C (2008b) Expression of aquaporin 5 (AQP5) promotes tumor invasion in human non small cell lung cancer. *PloS one* **3**(5):e2162.
- Chai RC, Jiang JH, Kwan Wong AY, Jiang F, Gao K, Vatcher G and Hoi Yu AC (2013) AQP5 is differentially regulated in astrocytes during metabolic and traumatic injuries. *Glia* **61**(10):1748-1765.

- Cheng S, Eliaz I, Lin J, Thyagarajan-Sahu A and Sliva D (2013) Triterpenes from *Poria cocos* suppress growth and invasiveness of pancreatic cancer cells through the downregulation of MMP-7. *International journal of oncology* **42**(6):1869-1874.
- Conde A, Dhalluin G, Chaumont F, Chaves M and Geros H (2010) Transporters, channels, or simple diffusion? Dogmas, atypical roles and complexity in transport systems. *Int J Biochem Cell Biol* **42**(6):857-868.
- Cowan CA, Yokoyama N, Bianchi LM, Henkemeyer M and Fritzsche B (2000) EphB2 guides axons at the midline and is necessary for normal vestibular function. *Neuron* **26**(2):417-430.
- de Morais Lima GR, de Albuquerque Montenegro C, de Almeida CL, de Athayde-Filho PF, Barbosa-Filho JM and Batista LM (2011) Database survey of anti-inflammatory plants in South America: a review. *Int J Mol Sci* **12**(4):2692-2749.
- Deb P, Pal S, Dutta V, Boruah D, Chandran VM and Bhatnagar HS (2012) Correlation of expression pattern of aquaporin-1 in primary central nervous system tumors with tumor type, grade, proliferation, microvessel density, contrast-enhancement and perilesional edema. *J Cancer Res Ther* **8**(4):571-577.
- Detmers FJ, de Groot BL, Muller EM, Hinton A, Konings IB, Sze M, Flitsch SL, Grubmuller H and Deen PM (2006) Quaternary ammonium compounds as water channel blockers. Specificity, potency, and site of action. *J Biol Chem* **281**(20):14207-14214.
- Diedler J, Sykora M, Blatow M, Juttler E, Unterberg A and Hacke W (2009) Decompressive surgery for severe brain edema. *J Intensive Care Med* **24**(3):168-178.

- Ding JY, Kreipke CW, Speirs SL, Schafer P, Schafer S and Rafols JA (2009) Hypoxia-inducible factor-1alpha signaling in aquaporin upregulation after traumatic brain injury. *Neuroscience letters* **453**(1):68-72.
- El Hindy N, Bankfalvi A, Herring A, Adamzik M, Lambertz N, Zhu Y, Siffert W, Sure U and Sandalcioglu IE (2013) Correlation of aquaporin-1 water channel protein expression with tumor angiogenesis in human astrocytoma. *Anticancer research* **33**(2):609-613.
- Esteva-Font C, Jin B-J and Verkman A (2014) Aquaporin-1 gene deletion reduces breast tumor growth and lung metastasis in tumor-producing MMTV-PyVT mice. *FASEB J* **28**(3):1446-1453.
- Feickert HJ, Drommer S and Heyer R (1999) Severe head injury in children: impact of risk factors on outcome. *J Trauma* **47**(1):33-38.
- Fischbarg J (2010) Fluid transport across leaky epithelia: central role of the tight junction and supporting role of aquaporins. *Physiol Rev* **90**(4):1271-1290.
- Fischer U, Taussky P, Gralla J, Arnold M, Brekenfeld C, Reinert M, Meier N, Mono ML, Schroth G, Mattle HP and Nedeltchev K (2011) Decompressive craniectomy after intra-arterial thrombolysis: safety and outcome. *J Neurol Neurosurg Psychiatry* **82**(8):885-887.
- Footer MJ, Kerssemakers JW, Theriot JA and Dogterom M (2007) Direct measurement of force generation by actin filament polymerization using an optical trap. *Proc Natl Acad Sci U S A* **104**(7):2181-2186.
- Fotiadis D, Suda K, Tittmann P, Jenö P, Philippsen A, Müller DJ, Gross H and Engel A (2002) Identification and structure of a putative Ca²⁺-binding domain at the C terminus of AQP1. *J Mol Biol* **318**(5):1381-1394.

- Friedman B, Schachtrup C, Tasi PS, Shih AY, Akassoglou K, Kellinfield D and Lyden PD (2009) Acute vascular disruption and aquaporin 4 loss after stroke. *Stroke*(40):2182-2190.
- Frigeri A, Nicchia GP and Svelto M (2007) Aquaporins as targets for drug discovery. *Curr Pharm Des* **13**(23):2421-2427.
- Frydenlund DS, Bhardwaj A, Otsuka T, Mylonakou MN, Yasumura T, Davidson KG, Zeynalov E, Skare O, Laake P, Haug FM, Rash JE, Agre P, Ottersen OP and Amiry-Moghaddam M (2006) Temporary loss of perivascular aquaporin-4 in neocortex after transient middle cerebral artery occlusion in mice. *Proceedings of the National Academy of Sciences*(103):13532–13536.
- Fu D, Libson A, Miercke LJ, Weitzman C, Nollert P, Krucinski J and Stroud RM (2000) Structure of a glycerol-conducting channel and the basis for its selectivity. *Science* **290**(5491):481-486.
- Gao J, Wang X, Chang Y, Zhang J, Song Q, Yu H and Li X (2006) Acetazolamide inhibits osmotic water permeability by interaction with aquaporin-1. *Analytical biochemistry* **350**(2):165-170.
- Grabarek Z (2006) Structural basis for diversity of the EF-hand calcium-binding proteins. *J Mol Biol* **359**(3):509-525.
- Hachez C and Chaumont F (2010) Aquaporins: a family of highly regulated multifunctional channels. *Adv Exp Med Biol* **679**:1-17.
- Hacke W, Schwab S, Horn M, Spranger M, De Georgia M and von Kummer R (1996) 'Malignant' middle cerebral artery territory infarction: clinical course and prognostic signs. *Arch Neurol* **53**(4):309-315.

- Hara-Chikuma M and Verkman AS (2008a) Aquaporin-3 facilitates epidermal cell migration and proliferation during wound healing. *Journal of molecular medicine* **86**(2):221-231.
- Hara-Chikuma M and Verkman AS (2008b) Prevention of skin tumorigenesis and impairment of epidermal cell proliferation by targeted aquaporin-3 gene disruption. *Molecular and cellular biology* **28**(1):326-332.
- Higashida T, Kreipke CW, Rafols JA, Peng C, Schafer S, Schafer P, Ding JY, Dornbos D, 3rd, Li X, Guthikonda M, Rossi NF and Ding Y (2011) The role of hypoxia-inducible factor-1alpha, aquaporin-4, and matrix metalloproteinase-9 in blood-brain barrier disruption and brain edema after traumatic brain injury. *Journal of neurosurgery* **114**(1):92-101.
- Hiroaki Y, Tani K, Kamegawa A, Gyobu N, Nishikawa K, Suzuki H, Walz T, Sasaki S, Mitsuoka K, Kimura K, Mizoguchi A and Fujiyoshi Y (2006) Implications of the aquaporin-4 structure on array formation and cell adhesion. *Journal of molecular biology* **355**(4):628-639.
- Hossmann YA (1994) Viability thresholds and the penumbra of focal ischemia. *Annals of Neurology*(36):557-565.
- Hu J and Verkman AS (2006) Increased migration and metastatic potential of tumor cells expressing aquaporin water channels. *FASEB journal : official publication of the Federation of American Societies for Experimental Biology* **20**(11):1892-1894.
- Huber VJ, Tsujita M, Kwee IL and Nakada T (2009) Inhibition of aquaporin 4 by antiepileptic drugs. *Bioorganic & medicinal chemistry* **17**(1):418-424.
- Huber VJ, Tsujita M and Nakada T (2012) Aquaporins in drug discovery and pharmacotherapy. *Mol Aspects Med* **33**(5-6):691-703.

- Huber VJ, Tsujita M, Yamazaki M, Sakimura K and Nakada T (2007) Identification of arylsulfonamides as Aquaporin 4 inhibitors. *Bioorganic & medicinal chemistry letters* **17**(5):1270-1273.
- Ishibashi K (2009) New members of mammalian aquaporins: AQP10-AQP12. *Handb Exp Pharmacol*(190):251-262.
- Ishibashi K, Hara S and Kondo S (2009) Aquaporin water channels in mammals. *Clin Exp Nephrol* **13**(2):107-117.
- Ishibashi K, Kondo S, Hara S and Morishita Y (2011) The evolutionary aspects of aquaporin family. *Am J Physiol Regul Integr Comp Physiol* **300**(3):R566-576.
- Jensen MO, Tajkhorshid E and Schulten K (2003) Electrostatic tuning of permeation and selectivity in aquaporin water channels. *Biophys J* **85**(5):2884-2899.
- Jeyaseelan K, Sepramaniam S, Armugam A and Wintour EM (2006) Aquaporins: a promising target for drug development. *Expert Opin Ther Targets* **10**(6):889-909.
- Jiang Y (2009) Aquaporin-1 activity of plasma membrane affects HT20 colon cancer cell migration. *IUBMB Life* **61**(10):1001-1009.
- Jiang Y, Chen K, Zhang T and Luo X (2009) Down-Regulation of Aquaporin-1 in W489 Colon Cancer Cells Inhibits Cell Migration, in *Bioinformatics and Biomedical Engineering, 2009 ICBBE 2009 3rd International Conference on* pp 1-5, IEEE.
- Jiang Y and Jiang Z-B (2010) Aquaporin 1-expressing MCF-7 mammary carcinoma cells show enhanced migration in vitro. *Journal of Biomedical Science and Engineering* **3**(01):95.

- Jullienne A and Badaut J (2013) Molecular contributions to neurovascular unit dysfunctions after brain injuries: lessons for target-specific drug development. *Future Neurol* **8**(6):677-689.
- Karou SD, Tchacondo T, Ilboudo DP and Simpore J (2011) Sub-Saharan Rubiaceae: a review of their traditional uses, phytochemistry and biological activities. *Pak J Biol Sci* **14**(3):149-169.
- Katakai T, Habiro K and Kinashi T (2013) Dendritic cells regulate high-speed interstitial T cell migration in the lymph node via LFA-1/ICAM-1. *J Immunol* **191**(3):1188-1199.
- Kater S and Letourneau P (1985) *Biology of the Nerve Growth Cone*. Alan R Liss, New York.
- Kaur C, Sivakumar V, Zhang Y and Ling EA (2006) Hypoxia-induced astrocytic reaction and increased vascular permeability in the rat cerebellum. *Glia* **54**(8):826-839.
- Kim JH, Lee YW, Park KA, Lee WT and Lee JE (2010) Agmatine attenuates brain edema through reducing the expression of aquaporin-1 after cerebral ischemia. *Journal of cerebral blood flow and metabolism : official journal of the International Society of Cerebral Blood Flow and Metabolism* **30**(5):943-949.
- King LS, Kozono D and Agre P (2004) From structure to disease: the evolving tale of aquaporin biology. *Nat Rev Mol Cell Biol* **5**(9):687-698.
- Kong G, Zhao Y, Li GH, Chen BJ, Wang XN, Zhou HL, Lou HX, Ren DM and Shen T (2015) The genus *Litsea* in traditional Chinese medicine: An ethnomedical, phytochemical and pharmacological review. *J Ethnopharmacol* **164**:256-264.

- Kusayama M, Wada K, Nagata M, Ishimoto S, Takahashi H, Yoneda M, Nakajima A, Okura M, Kogo M and Kamisaki Y (2011) Critical role of aquaporin 3 on growth of human esophageal and oral squamous cell carcinoma. *Cancer science* **102**(6):1128-1136.
- Laird MD, Vender JR and Dhandapani KM (2008) Opposing roles for reactive astrocytes following traumatic brain injury. *Neurosignals* **16**(2-3):154-164.
- Le Clainche C and Carlier MF (2008) Regulation of actin assembly associated with protrusion and adhesion in cell migration. *Physiol Rev* **88**(2):489-513.
- Lee K, Jo IY, Park SH, Kim KS, Bae J, Park JW, Lee BJ, Choi HY and Bu Y (2012a) Defatted sesame seed extract reduces brain oedema by regulating aquaporin 4 expression in acute phase of transient focal cerebral ischaemia in rat. *Phytotherapy research : PTR* **26**(10):1521-1527.
- Lee SM, Lee YJ, Yoon JJ, Kang DG and Lee HS (2012b) Effect of *Poria cocos* on hypertonic stress-induced water channel expression and apoptosis in renal collecting duct cells. *Journal of ethnopharmacology* **141**(1):368-376.
- Li Y, Feng X, Yang H and Ma T (2006) Expression of aquaporin-1 in SMMC-7221 liver carcinoma cells promotes cell migration. *Chinese Science Bulletin* **51**(20):2466-2471.
- Ling H, Zhang Y, Ng KY and Chew EH (2011) Pachymic acid impairs breast cancer cell invasion by suppressing nuclear factor-kappaB-dependent matrix metalloproteinase-9 expression. *Breast cancer research and treatment* **126**(3):609-620.
- Liu X, Yue R, Zhang J, Shan L, Wang R and Zhang W (2013) Neuroprotective effects of bacopaside I in ischemic brain injury. *Restorative neurology and neuroscience* **31**(2):109-123.

- Ma B, Xiang Y, Mu SM, Li T, Yu HM and Li XJ (2004) Effects of acetazolamide and anordiol on osmotic water permeability in AQP1-cRNA injected *Xenopus* oocyte. *Acta pharmacologica Sinica* **25**(1):90-97.
- Macey R (1984) Transport of water and urea in red blood cells. *Am J Physiol Cell Physiol* **246**:C195-C203.
- Macey RI, Karan DM and Farmer RE (1972) Properties of water channels in human red cells. *Biomembranes* **3**:331-340.
- Machida Y, Ueda Y, Shimasaki M, Sato K, Sagawa M, Katsuda S and Sakuma T (2011) Relationship of aquaporin 1, 3, and 5 expression in lung cancer cells to cellular differentiation, invasive growth, and metastasis potential. *Human pathology* **42**(5):669-678.
- Mack AF and Wolburg H (2013) A novel look at astrocytes: aquaporins, ionic homeostasis, and the role of the microenvironment for regeneration in the CNS. *Neuroscientist* **19**(2):195-207.
- Madeira A, Moura TF and Soveral G (2014) Aquaglyceroporins: implications in adipose biology and obesity. *Cell Mol Life Sci.*
- Manley GT, Fujimura M, Ma T, Noshita N, Filiz F, Bollen AW, Chan P and Verkman AS (2000) Aquaporin-4 deletion in mice reduces brain edema after acute water intoxication and ischemic stroke. *Nat Med* **6**(2):159-163.
- Manno EM, Adams RE, Derdeyn CP, Powers WJ and Dringier MN (1999) The effects of mannitol on cerebral edema after large hemispheric cerebral infarct. *Neurology* **52**(3):583-587.
- Marcy Y, Prost J, Carlier MF and Sykes C (2004) Forces generated during actin-based propulsion: a direct measurement by micromanipulation. *Proc Natl Acad Sci U S A* **101**(16):5992-5997.

- McCoy E and Sontheimer H (2007) Expression and function of water channels (aquaporins) in migrating malignant astrocytes. *Glia* **55**(10):1034-1043.
- McCoy ES, Haas BR and Sontheimer H (2010) Water permeability through aquaporin-4 is regulated by protein kinase C and becomes rate-limiting for glioma invasion. *Neuroscience* **168**(4):971-981.
- McLeod DD, Beard DJ, Parsons MW, Levi CR, Calford MB and Spratt NJ (2013) Inadvertent occlusion of the anterior choroidal artery explains infarct variability in the middle cerebral artery thread occlusion stroke model. *PLoS One* **8**(9):e75779.
- McLeod DD, Parsons MW, Levi CR, Beutement S, Buxton D, Roworth B and Spratt NJ (2011) Establishing a rodent stroke perfusion computed tomography model. *Int J Stroke* **6**(4):284-289.
- Meng F, Rui Y, Xu L, Wan C, Jiang X and Li G (2014) Aqp1 Enhances Migration of Bone Marrow Mesenchymal Stem Cells Through Regulation of FAK and beta-Catenin. *Stem Cells Dev* **23**(1):66-75.
- Migliati E, Meurice N, DuBois P, Fang JS, Somasekharan S, Beckett E, Flynn G and Yool AJ (2009) Inhibition of aquaporin-1 and aquaporin-4 water permeability by a derivative of the loop diuretic bumetanide acting at an internal pore-occluding binding site. *Molecular pharmacology* **76**(1):105-112.
- Minami S, Kobayashi H, Yamashita A, Yanagita T, Uezono Y, Yokoo H, Shiraishi S, Saitoh T, Asada Y, Komune S and Wada A (2001) Selective expression of aquaporin 1, 4 and 5 in the rat middle ear. *Hear Res* **158**(1-2):51-56.
- Moon C, King LS and Agre P (1997) Aqp1 expression in erythroleukemia cells: genetic regulation of glucocorticoid and chemical induction. *The American journal of physiology* **273**(5 Pt 1):C1562-1570.

- Moon C, Rousseau R, Soria JC, Hoque MO, Lee J, Jang SJ, Trink B, Sidransky D and Mao L (2004) Aquaporin expression in human lymphocytes and dendritic cells. *Am J Hematol* **75**(3):128-133.
- Moon C, Soria JC, Jang SJ, Lee J, Obaidul Hoque M, Sibony M, Trink B, Chang YS, Sidransky D and Mao L (2003) Involvement of aquaporins in colorectal carcinogenesis. *Oncogene* **22**(43):6699-6703.
- Murtha LA, McLeod DD, McCann SK, Pepperall D, Chung S, Levi CR, Calford MB and Spratt NJ (2014a) Short-duration hypothermia after ischemic stroke prevents delayed intracranial pressure rise. *Int J Stroke* **9**(5):553-559.
- Murtha LA, McLeod DD, Pepperall D, McCann SK, Beard DJ, Tomkins AJ, Holmes WM, McCabe C, Macrae IM and Spratt NJ (2014b) Intracranial pressure elevation after ischemic stroke in rats: cerebral edema is not the only cause, and short-duration mild hypothermia is a highly effective preventive therapy. *J Cereb Blood Flow Metab.*
- Naccache P and Sha'afi RI (1974) Effect of PCMBs on water transfer across biological membranes. *J Cell Physiol* **83**(3):449-456.
- Nicchia GP, Stigliano C, Sparaneo A, Rossi A, Frigeri A and Svelto M (2013) Inhibition of aquaporin-1 dependent angiogenesis impairs tumour growth in a mouse model of melanoma. *Journal of molecular medicine (Berlin, Germany)* **91**(5):613-623.
- Nie Y, Dong X, He Y, Yuan T, Han T, Rahman K, Qin L and Zhang Q (2013) Medicinal plants of genus *Curculigo*: traditional uses and a phytochemical and ethnopharmacological review. *J Ethnopharmacol* **147**(3):547-563.
- Nielsen S, Kwon TH, Frokiaer J and Agre P (2007) Regulation and dysregulation of aquaporins in water balance disorders. *J Intern Med* **261**(1):53-64.

- Niemietz CM and Tyerman SD (2002) New potent inhibitors of aquaporins: silver and gold compounds inhibit aquaporins of plant and human origin. *FEBS letters* **531**(3):443-447.
- Pan XY, Guo H, Han J, Hao F, An Y, Xu Y, Xiaokaiti Y, Pan Y and Li XJ (2012) Ginsenoside Rg3 attenuates cell migration via inhibition of aquaporin 1 expression in PC-3M prostate cancer cells. *European journal of pharmacology* **683**(1-3):27-34.
- Papadopoulos MC, Manley GT, Krishna S and Verkman AS (2004) Aquaporin-4 facilitates reabsorption of excess fluid in vasogenic brain edema. *The Federation of American Societies for Experimental Biology Journal*(18):1291-1293.
- Papadopoulos MC and Verkman AS (2007) Aquaporin-4 and brain edema. *Pediatric nephrology* **22**(6):778-784.
- Parekh SH, Chaudhuri O, Theriot JA and Fletcher DA (2005) Loading history determines the velocity of actin-network growth. *Nat Cell Biol* **7**(12):1219-1223.
- Park E, Bell JD and Baker AJ (2008) Traumatic brain injury: can the consequences be stopped? *CMAJ* **178**(9):1163-1170.
- Peng L, Zhou Y, Kong de Y and Zhang WD (2010) Antitumor activities of dammarane triterpene saponins from *Bacopa monniera*. *Phytotherapy research : PTR* **24**(6):864-868.
- Preston GM and Agre P (1991) Isolation of the cDNA for erythrocyte integral membrane protein of 28 kilodaltons: member of an ancient channel family. *Proc Natl Acad Sci U S A* **88**(24):11110-11114.

- Preston GM, Carroll TP, Guggino WB and Agre P (1992) Appearance of water channels in *Xenopus* oocytes expressing red cell CHIP28 protein. *Science* **256**(5055):385-387.
- Rios JL (2011) Chemical constituents and pharmacological properties of *Poria cocos*. *Planta medica* **77**(7):681-691.
- Russo A and Borrelli F (2005) *Bacopa monniera*, a reputed nootropic plant: an overview. *Phytomedicine : international journal of phytotherapy and phytopharmacology* **12**(4):305-317.
- Ryu HM, Oh EJ, Park SH, Kim CD, Choi JY, Cho JH, Kim IS, Kwon TH, Chung HY, Yoo M and Kim YL (2012) Aquaporin 3 expression is up-regulated by TGF-beta1 in rat peritoneal mesothelial cells and plays a role in wound healing. *The American journal of pathology* **181**(6):2047-2057.
- Saadoun S, Papadopoulos MC, Davies DC, Bell BA and Krishna S (2002a) Increased aquaporin 1 water channel expression in human brain tumours. *British journal of cancer* **87**(6):621-623.
- Saadoun S, Papadopoulos MC, Davies DC, Krishna S and Bell BA (2002b) Aquaporin-4 expression is increased in oedematous human brain tumours. *Journal of neurology, neurosurgery, and psychiatry* **72**(2):262-265.
- Saadoun S, Papadopoulos MC, Hara-Chikuma M and Verkman AS (2005) Impairment of angiogenesis and cell migration by targeted aquaporin-1 gene disruption. *Nature* **434**(7034):786-792.
- Saparov SM, Kozono D, Rothe U, Agre P and Pohl P (2001) Water and ion permeation of aquaporin-1 in planar lipid bilayers. Major differences in structural determinants and stoichiometry. *J Biol Chem* **276**(34):31515-31520.

- Saraf MK, Prabhakar S and Anand A (2010) Neuroprotective effect of *Bacopa monniera* on ischemia induced brain injury. *Pharmacology, biochemistry, and behavior* **97**(2):192-197.
- Seeliger D, Zapater C, Krenc D, Haddoub R, Flitsch S, Beitz E, Cerda J and de Groot BL (2013) Discovery of novel human aquaporin-1 blockers. *ACS chemical biology* **8**(1):249-256.
- Shanmugasundaram ER, Akbar GK and Shanmugasundaram KR (1991) Brahmighritham, an Ayurvedic herbal formula for the control of epilepsy. *Journal of ethnopharmacology* **33**(3):269-276.
- Shenaq M, Kassem H, Peng C, Schafer S, Ding JY, Fredrickson V, Guthikonda M, Kreipke CW, Rafols JA and Ding Y (2012) Neuronal damage and functional deficits are ameliorated by inhibition of aquaporin and HIF1alpha after traumatic brain injury (TBI). *Journal of the neurological sciences* **323**(1-2):134-140.
- Shi W-Z, Qi L-L, Fang S-H, Lu Y-B, Zhang W-P and Wei E-Q (2012) Aggravated chronic brain injury after focal cerebral ischemia in aquaporin-4-deficient mice. *Neuroscience Letters* **520**(1):121-125.
- Shin JA, Choi JH, Choi YH and Park EM (2011) Conserved aquaporin 4 levels associated with reduction of brain edema are mediated by estrogen in the ischemic brain after experimental stroke. *Biochimica et biophysica acta* **1812**(9):1154-1163.
- Stroka KM, Jiang H, Chen SH, Tong Z, Wirtz D, Sun SX and Konstantopoulos K (2014) Water permeation drives tumor cell migration in confined microenvironments. *Cell* **157**(3):611-623.

- Sui H, Han BG, Lee JK, Walian P and Jap BK (2001) Structural basis of water-specific transport through the AQP1 water channel. *Nature* **414**(6866):872-878.
- Taniguchi M, Yamashita T, Kumura E, Tamatani M, Kobayashi A, Yokawa T, Maruno M, Kato A, Ohnishi T, Kohmura E, Tohyama M and Yoshimine T (2000) Induction of aquaporin-4 water channel mRNA after focal cerebral ischemia in rat. *Brain research Molecular brain research* **78**(1-2):131-137.
- Tornroth-Horsefield S, Wang Y, Hedfalk K, Johanson U, Karlsson M, Tajkhorshid E, Neutze R and Kjellbom P (2006) Structural mechanism of plant aquaporin gating. *Nature* **439**(7077):688-694.
- Tourdias T, Mori N, Dragonu I, Cassagno N, Boiziau C, Aussudre J, Brochet B, Moonen C, Petry KG and Dousset V (2011) Differential aquaporin 4 expression during edema build-up and resolution phases of brain inflammation. *Journal of neuroinflammation* **8**:143.
- Tyerman SD, Niemietz CM and Bramley H (2002) Plant aquaporins: multifunctional water and solute channels with expanding roles. *Plant Cell Environ* **25**(2):173-194.
- Vahedi K, Vicaut E, Mateo J, Kurtz A, Orabi M, Guichard JP, Boutron C, Couvreur G, Rouanet F, Touze E, Guillon B, Carpentier A, Yelnik A, George B, Payen D and Bousser MG (2007) Sequential-design, multicenter, randomized, controlled trial of early decompressive craniectomy in malignant middle cerebral artery infarction (DECIMAL Trial). *Stroke* **38**(9):2506-2517.
- Van Duijn B and Inouye K (1991) Regulation of movement speed by intracellular pH during *Dictyostelium discoideum* chemotaxis. *Proc Natl Acad Sci U S A* **88**(11):4951-4955.

- Verkman A, Hara-Chikuma M and Papadopoulos MC (2008) Aquaporins—new players in cancer biology. *Journal of Molecular Medicine* **86**(5):523-529.
- von Bulow J, Muller-Lucks A, Kai L, Bernhard F and Beitz E (2012) Functional characterization of a novel aquaporin from *Dictyostelium discoideum* amoebae implies a unique gating mechanism. *J Biol Chem* **287**(10):7487-7494.
- Ware MF, Wells A and Lauffenburger DA (1998) Epidermal growth factor alters fibroblast migration speed and directional persistence reciprocally and in a matrix-dependent manner. *J Cell Sci* **111** (Pt 16):2423-2432.
- Werner C and Engelhard K (2007) Pathophysiology of traumatic brain injury. *British journal of anaesthesia* **99**(1):4-9.
- Winter CD, Adamides AA, Lewis PM and Rosenfeld JV (2005) A review of the current management of severe traumatic brain injury. *Surgeon* **3**(5):329-337.
- Woo J, Lee J, Chae YK, Kim MS, Baek JH, Park JC, Park MJ, Smith IM, Trink B, Ratovitski E, Lee T, Park B, Jang SJ, Soria JC, Califano JA, Sidransky D and Moon C (2008) Overexpression of AQP5, a putative oncogene, promotes cell growth and transformation. *Cancer letters* **264**(1):54-62.
- Xia H, Ma YF, Yu CH, Li YJ, Tang J, Li JB, Zhao YN and Liu Y (2014) Aquaporin 3 knockdown suppresses tumour growth and angiogenesis in experimental non-small cell lung cancer. *Experimental physiology* **99**(7):974-984.
- Yamamoto N, Yoneda K, Asai K, Sobue K, Tada T, Fujita Y, Katsuya H, Fujita M, Aihara N, Mase M, Yamada K, Miura Y and Kato T (2001) Alterations in the expression of the AQP family in cultured rat astrocytes during hypoxia and reoxygenation. *Brain research Molecular brain research* **90**(1):26-38.

- Yool AJ (2007a) Aquaporins: multiple roles in the central nervous system. *Neuroscientist* **13**(5):470-485.
- Yool AJ (2007b) Functional domains of aquaporin-1: keys to physiology, and targets for drug discovery. *Curr Pharm Des* **13**(31):3212-3221.
- Yool AJ, Brokl OH, Pannabecker TL, Dantzer WH and Stamer WD (2002) Tetraethylammonium block of water flux in Aquaporin-1 channels expressed in kidney thin limbs of Henle's loop and a kidney-derived cell line. *BMC physiology* **2**:4.
- Yool AJ, Brown EA and Flynn GA (2009) Roles for novel pharmacological blockers of aquaporins in the treatment of brain oedema and cancer. *Clin Exp Pharmacol Physiol.*
- Yool AJ and Campbell EM (2012) Structure, function and translational relevance of aquaporin dual water and ion channels. *Mol Aspects Med*:in press.
- Yool AJ, Morelle J, Cnops Y, Verbavatz JM, Campbell EM, Beckett EA, Booker GW, Flynn G and Devuyst O (2013) AqF026 is a pharmacologic agonist of the water channel aquaporin-1. *Journal of the American Society of Nephrology : JASN* **24**(7):1045-1052.
- Yool AJ and Weinstein AM (2002) New roles for old holes: Ion channel function in aquaporin-1. *News Physiological Sciences* **17**:68-72.
- Yu J, Yool AJ, Schulten K and Tajkhorshid E (2006) Mechanism of gating and ion conductivity of a possible tetrameric pore in aquaporin-1. *Structure* **14**(9):1411-1423.
- Yu L, Yi J, Ye G, Zheng Y, Song Z, Yang Y, Song Y, Wang Z and Bao Q (2012) Effects of curcumin on levels of nitric oxide synthase and AQP-4 in a rat model of hypoxia-ischemic brain damage. *Brain research* **1475**:88-95.

- Zardoya R (2005) Phylogeny and evolution of the major intrinsic protein family. *Biol Cell* **97**(6):397-414.
- Zelenina M, Zelenin S, Bondar AA, Brismar H and Aperia A (2002) Water permeability of aquaporin-4 is decreased by protein kinase C and dopamine. *Am J Physiol Renal Physiol* **283**(2):F309-318.
- Zhang H and Verkman AS (2008) Evidence against involvement of aquaporin-4 in cell-cell adhesion. *Journal of molecular biology* **382**(5):1136-1143.
- Zhang W, Zitron E, Homme M, Kihm L, Morath C, Scherer D, Hegge S, Thomas D, Schmitt CP, Zeier M, Katus H, Karle C and Schwenger V (2007) Aquaporin-1 channel function is positively regulated by protein kinase C. *J Biol Chem* **282**(29):20933-20940.
- Zhang X, Chen Q, Wang Y, Peng W and Cai H (2014) Effects of curcumin on ion channels and transporters. *Front Physiol* **5**:94.
- Zhang Z, Chen Z, Song Y, Zhang P, Hu J and Bai C (2010) Expression of aquaporin 5 increases proliferation and metastasis potential of lung cancer. *The Journal of pathology* **221**(2):210-220.
- Zhao YY (2013) Traditional uses, phytochemistry, pharmacology, pharmacokinetics and quality control of *Polyporus umbellatus* (Pers.) Fries: a review. *J Ethnopharmacol* **149**(1):35-48.
- Zhao YY, Feng YL, Du X, Xi ZH, Cheng XL and Wei F (2012) Diuretic activity of the ethanol and aqueous extracts of the surface layer of *Poria cocos* in rat. *Journal of ethnopharmacology* **144**(3):775-778.

Figure legend

Figure 1. Schematic diagram of the colocalization of AQP channels with ion transporters, other channels and exchangers at the leading edge of a lamellipodium in a migrating cell.

TABLE 1 Summary of aquaporin pharmacological modulators and proposed interaction sites

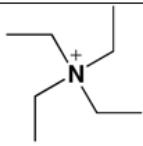
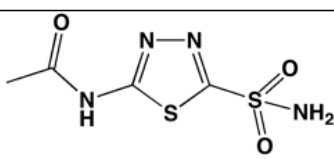
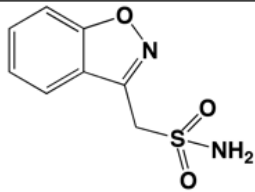
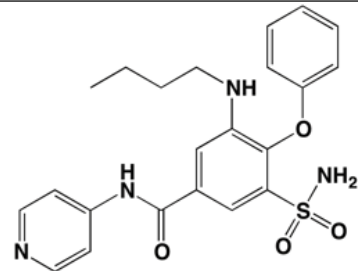
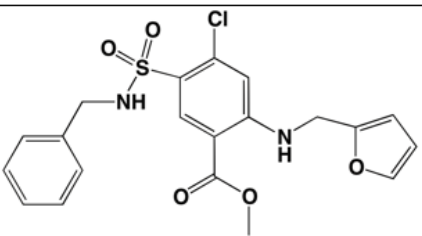
Name	Structure	Proposed binding site	Reference
Mercuric chloride HgCl ₂	Cl - Hg - Cl	Cys-189 in AQP1	(Preston et al., 1993)
Silver and gold compounds: AgNO ₃ , HAuCl ₄	$\text{Ag}^+ \left[\begin{array}{c} \text{O} \\ \\ \text{O}-\text{N}-\text{O} \\ \\ \text{O} \end{array} \right]^- \quad \text{H}^+ \left[\begin{array}{c} \text{Cl} \\ \\ \text{Cl}-\text{Au}-\text{Cl} \\ \\ \text{Cl} \end{array} \right]$	Cys-189 in AQP1	(Niemietz and Tyerman, 2002)
Tetraethylammonium ion (TEA ⁺)		Loop-E region	(Brooks et al., 2000; Yool et al., 2002)
Acetazolamide (AZA)		Arg-216 and Gly-209 in AQP4	(Huber et al., 2009; Huber et al., 2007)
Zonisamide		Possibly Arg-216 and Gly-209 in AQP4	(Huber et al., 2009)
AqB013		Intracellular vestibule of the water pore	(Migliati et al., 2009)
AqF026		Intracellular loop D domain	(Yool et al., 2013)

TABLE 2 Phytochemicals derived from medicinal plants traditionally used for treating potentially AQP-related diseases

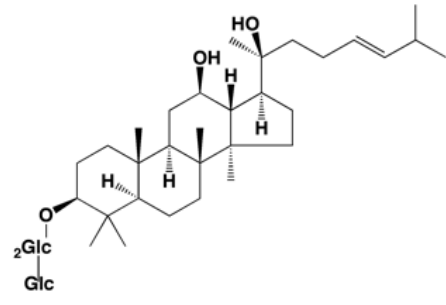
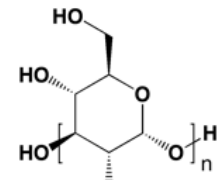
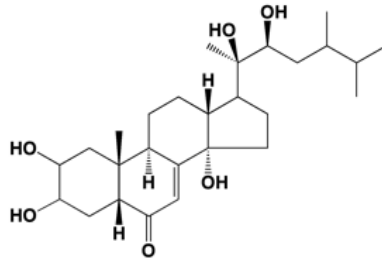
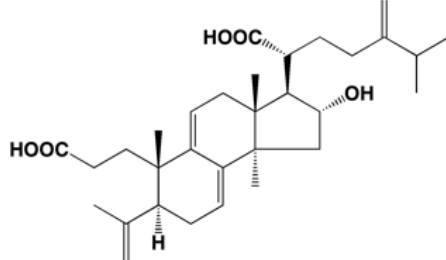
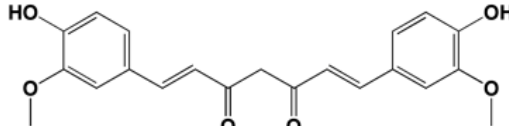
Plant source	Compound	Structure
<i>Panax ginseng</i>	Ginsenoside Rg3	
<i>Polyporus umbellatus</i>	(1→3)- α -D-glucan	
	Polyporusterone A	
<i>Poria cocos</i>	Poricoic acid A	
<i>Curcuma longa</i>	Curcumin	

Table 2, continued

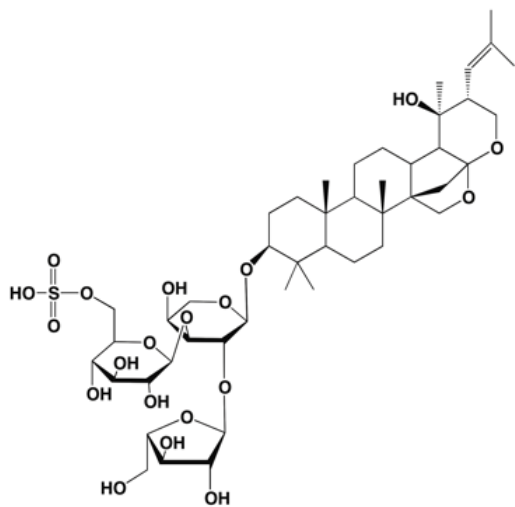
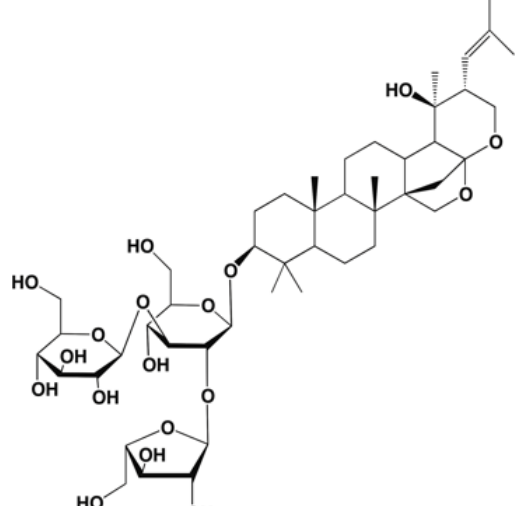
<p><i>Bacopa monnieri</i></p>	<p>Bacopaside I</p>	 <p>The chemical structure of Bacopaside I is a complex molecule consisting of a pentacyclic steroid nucleus. It features a methyl group at C-13, a methyl group at C-14, and a methyl group at C-15. The steroid core is linked via an ether bridge at C-3 to a chain of three sugar units: a glucose unit at C-3, a galactose unit at C-6, and a rhamnose unit at C-2. The glucose unit is substituted with a sulfate group at C-4. The rhamnose unit is substituted with a hydroxyl group at C-1. The galactose unit is substituted with a hydroxyl group at C-4. The steroid nucleus also has a hydroxyl group at C-20 and a methyl group at C-21. The C-17 position is substituted with a side chain consisting of a methyl group, a hydroxyl group, and a methyl group.</p>
	<p>Bacopaside II</p>	 <p>The chemical structure of Bacopaside II is a complex molecule consisting of a pentacyclic steroid nucleus. It features a methyl group at C-13, a methyl group at C-14, and a methyl group at C-15. The steroid core is linked via an ether bridge at C-3 to a chain of three sugar units: a glucose unit at C-3, a galactose unit at C-6, and a rhamnose unit at C-2. The glucose unit is substituted with a hydroxyl group at C-4. The rhamnose unit is substituted with a hydroxyl group at C-1. The galactose unit is substituted with a hydroxyl group at C-4. The steroid nucleus also has a hydroxyl group at C-20 and a methyl group at C-21. The C-17 position is substituted with a side chain consisting of a methyl group, a hydroxyl group, and a methyl group.</p>

Figure 1 (color)

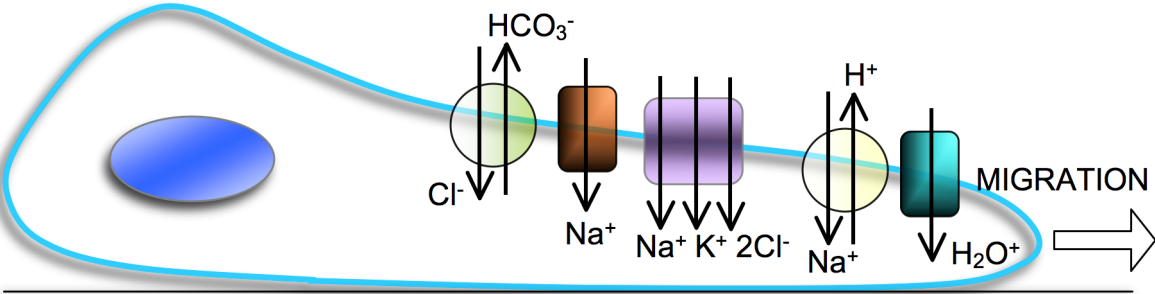
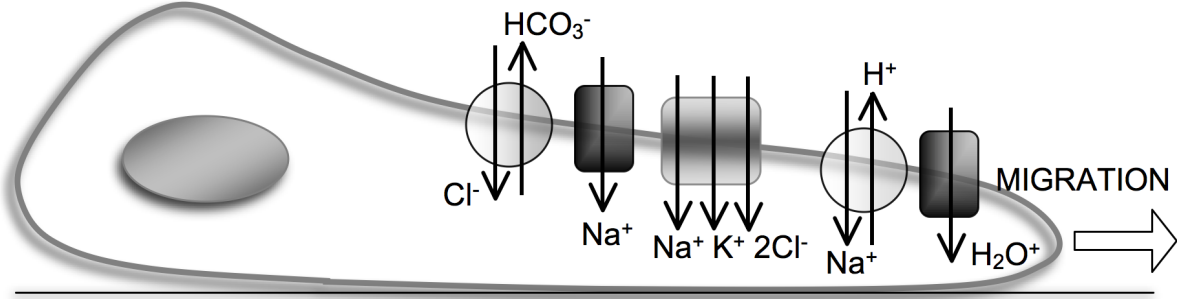


Figure 1 (grayscale)



**CHAPTER 2: AQUAPORIN-1 ION
CHANNELS IN CANCER CELL
MIGRATION: DISCOVERY OF NEW
PHARMACOLOGICAL BLOCKERS.**

CONTEXTUAL STATEMENT

Bumetanide derivatives AqB007 and AqB011 selectively block the Aquaporin-1 ion channel conductance and slow cancer cell migration.

AIM: To test various bumetanide derived chemicals (AqBs) for function as AQP1 modulators and to test their effects on cancer cell migration.

HYPOTHESIS: Various AqBs can block AQP1 ionic conductance and inhibit cancer cell migration with different efficacies that correlate with structural properties of the modulatory agents.

CONCLUSIONS:

1. Various structurally related bumetanide derivatives were tested for function as AQP1 ion channel antagonists. The order of potency for inhibition of the ionic conductance was AqB011 > AqB007 >> AqB006 ≥ AqB001.
2. The potency of inhibition matched with *in silico* modelling of the predicted order of energetically favoured binding. It was predicted that AqB011 interacts with poly-arginine region of loop D region.
3. Migration of human colon cancer (HT29) cells was assessed with a wound-closure assay in presence of a mitotic inhibitor. AqB011 and AqB007 significantly reduced migration rates of AQP1-positive HT29 cells without affecting viability.
4. Inhibition of the AQP1 ionic conductance could be a useful adjunct therapeutic approach for reducing metastasis in cancers that upregulate AQP1 expression.

COMMENTARY:

New AQP1 modulators presented in this chapter were the first agents demonstrated to act as selective AQP1 ion channel blockers. This chapter also provided the evidence for conclusions summarized in Chapter 1 on the role of the AQP1 ion conductance in cell migration. The significance of this work is the identification of the AQP1 ion channel as a key target for anti-cancer drug development, for the subset of aggressive cancer cells that rely on upregulation of AQP1 for rapid motility. Cancer cell migration in these lines was impaired by blocking the AQP1 ionic conductance.

Statement of Authorship

Title of Paper	Bumetanide derivatives AqB007 and AqB011 selectively block the aquaporin-1 ion channel conductance and slow cancer cell migration
Publication Status	<input type="checkbox"/> Published <input type="checkbox"/> Accepted for Publication <input type="checkbox"/> Submitted for Publication <input type="checkbox"/> Unpublished and Unsubmitted work written in manuscript style
Publication Details	Kourghi M, Pei JV, De Ieso ML, Flynn G, and Yool AJ (2016) Bumetanide derivatives AqB007 and AqB011 selectively block the aquaporin-1 ion channel conductance and slow cancer cell migration. Mol Pharmacol 89:133-140.

Principal Author

Name of Principal Author (Candidate)	Jinxin Pei and Mohamad Kourghi
Contribution to the Paper	Co-first authors, initiated and performed experiments, analysis on all samples, interpreted data, wrote the manuscript.
Overall percentage (%)	80%
Certification:	This paper reports on original research I conducted during the period of my Higher Degree by Research candidature and is not subject to any obligations or contractual agreements with a third party that would constrain its inclusion in this thesis. I am the primary author of this paper.
Signature	Date 23/5/17

Co-Author Contributions

By signing the Statement of Authorship, each author certifies that:

- i. the candidate's stated contribution to the publication is accurate (as detailed above);
- ii. permission is granted for the candidate to include the publication in the thesis; and
- iii. the sum of all co-author contributions is equal to 100% less the candidate's stated contribution.

Name of Co-Author	Michael L. De Ieso
Contribution to the Paper	Performed the experiment and wrote the manuscript.
Signature	Date 23/5/17

Name of Co-Author	Gary Flynn
Contribution to the Paper	Developed the new research tool.
Signature	Date 5/26/2017

Name of Co-Author	Andrea J. Yool		
Contribution to the Paper	Initiated the experiments and wrote the manuscript.		
Signature		Date	23 May 2017

Bumetanide derivatives AqB007 and AqB011 selectively block the Aquaporin-1 ion channel conductance and slow cancer cell migration.

Mohamad Kourghi, Jinxin V Pei, Michael L De Ieso, Gary Flynn, and Andrea J Yool

School of Medicine, University of Adelaide; Adelaide SA 5005 Australia (MK, JVP, MLDI, AJY)

Institute for Photonics and Advanced Sensing, University of Adelaide; Adelaide SA 5005 Australia (JVP, AJY)

Spacefill Enterprises LLC; Oro Valley, Arizona 85704 USA (GF)

Running title: Inhibition of AQP1 ion channels

Corresponding author: Prof Andrea Yool; Medical School South, level 4, Frome Rd, University of Adelaide, Adelaide SA 5005 Australia

andrea.yool@adelaide.edu.au ph: +61 8 8313 3359 fax: +61 8 8313 5384

Number of text pages: 28

Number of tables: 1

Number of figures: 6

Number of supplemental data files: 1

Numbers of words:

Abstract 246

Introduction 728

Discussion 845

Non-standard abbreviations: **AQP1** aquaporin-1; **AqB** aquaporin ligand bumetanide derivative (in numbered series)

Abstract

Aquaporins (AQPs) in the major intrinsic family of proteins mediate fluxes of water and other small solutes across cell membranes. AQP1 is a water channel, and under permissive conditions, a nonselective cation channel gated by cGMP. In addition to mediating fluid transport, AQP1 expression facilitates rapid cell migration in cell types including colon cancers and glioblastoma. Work here defines new pharmacological derivatives of bumetanide that selectively inhibit the ion channel but not the water channel activity of AQP1. Human AQP1 was analyzed in the *Xenopus laevis* oocyte expression system by two-electrode voltage clamp and optical osmotic swelling assays. AqB011 was the most potent blocker of the AQP1 ion conductance (IC_{50} 14 μ M) with no effect on water channel activity (at up to 200 μ M). The order of potency for inhibition of the ionic conductance was AqB011 > AqB007 >> AqB006 \geq AqB001. Migration of human colon cancer (HT29) cells was assessed with a wound-closure assay in presence of a mitotic inhibitor. AqB011 and AqB007 significantly reduced migration rates of AQP1-positive HT29 cells without affecting viability. The order of potency for AQP1 ion channel block matched the order for inhibition of cell migration, as well as *in silico* modeling of the predicted order of energetically favored binding. Docking models suggest that AqB011 and AqB007 interact with the intracellular loop D domain, a region involved in AQP channel gating. Inhibition of AQP1 ionic conductance could be a useful adjunct therapeutic approach for reducing metastasis in cancers that upregulate AQP1 expression.

Introduction

Osmotic water transport across biological membranes is facilitated by membrane proteins known as aquaporins (AQPs), found in all kingdoms of life (Campbell et al., 2008; Park and Saier, 1996; Reizer et al., 1993). To date, at least fifteen mammalian subfamilies have been identified, AQP0-AQP14 (Finn et al., 2014; Ishibashi, 2009). Aquaporin is organised as a tetramer of subunits, each comprising six transmembrane domains and five loops (A to E), and carrying a monomeric pore that allows the movement of water or other small solutes (Fu et al., 2000; Jung et al., 1994; Sui et al., 2001).

There is increasing recognition that certain classes of aggressive cancers depend on upregulation of AQP1 for fast migration and metastasis (Monzani et al., 2007). Though the precise mechanism for AQP1-enhanced motility remains unknown, both ion channels and water channels are essential in the cellular migration process (Schwab et al., 2007). AQP1 expression has been linked to metastasis and invasiveness of colon cancer cells (Jiang, 2009; Yoshida et al., 2013). In mammary and melanoma cancer cells, AQP1 facilitates tumor cell migration in vitro and metastasis in vivo (Hu and Verkman, 2006). Increased levels of AQP1 expression in astrocytoma correlate with clinical grade, serving as a diagnostic indicator of poor prognoses (El Hindy et al., 2013). AQP1-facilitated cell migration in glioma cannot be substituted by AQP4, indicating more than simple water channel function is involved in the migration-enhancing mechanism (McCoy and Sontheimer, 2007).

A subset of aquaporins have been shown to have ion channel function, including AQP0, AQP1, AQP6, plant nodulin, and *Drosophila* Big Brain (Yool and Campbell, 2012). In AQP1, multiple lines of evidence have shown the cGMP-dependent monovalent cation channel is located in the central pore at the four-fold axis of

symmetry, and is pharmacologically distinct from the monomeric water pores (Anthony et al., 2000; Boassa and Yool, 2003; Saparov et al., 2001; Yu et al., 2006; Zhang et al., 2007). The AQP1 ion channel has a unitary conductance of 150 pS in physiological saline, slow activation and deactivation kinetics, and is permeable to Na⁺, K⁺, and Cs⁺ but not divalent cations (Anthony et al., 2000; Yool et al., 1996). Loop D has been shown previously to be involved in cGMP-dependent gating of AQP1 ion channels (Yu et al., 2006). The low proportion of AQP1 water channels available to be gated as ion channels in reconstituted bilayers and heterologous expression systems has prompted uncertainty regarding the physiological relevance of the dual water and ion channel function in AQP1 (Saparov et al., 2001; Tsunoda et al., 2004). Further work has indicated that the availability of AQP1 ion channels to be activated by cGMP depends in part on tyrosine phosphorylation at the carboxyl terminal domain (Campbell et al., 2012).

Our characterization here of selective non-toxic pharmacological blockers of the AQP1 ion channel opens the first opportunity to define the functional roles of the AQP1 ion conductance. Prior to 2009, available AQP1 blockers were limited by low potency, lack of specificity, or toxicity. Mercury potently blocks AQP1 water permeability by covalent modification of a cysteine residue in loop E (Preston et al., 1993) but is highly toxic. Tetraethylammonium ion blocks the AQP1 water pore though not in all cell types (Brooks et al., 2000; Detmers et al., 2006; Sogaard and Zeuthen, 2008), and cadmium ion blocks the AQP1 ion channel (Boassa et al., 2006); but both lack selectivity for aquaporins. Effective compounds discovered recently include the arylsulfonamides AqB013 which blocks AQP1 and AQP4 water channel permeability (Migliati et al., 2009), and AqF026 which strongly potentiates AQP1 water channel activity (Yool et al., 2013). Other arylsulfonamides have been proposed as blockers of AQP4 channels

(Huber et al., 2009). A distinct class of agents acting on the external side of the membrane to block human AQP1 water flux has been identified as a source of candidate lead compounds for drug development (Seeliger et al., 2013).

Work here characterizes a novel set of AqB compounds (*Aq*: aquaporin ligand; *B*: bumetanide derivative) that differentially block the AQP1 ion channel without affecting water permeability. The most potent of these, AqB011, is a promising tool for dissecting the role of the AQP1 ion channel, while sparing osmotic water permeability. Understanding functional roles and regulation of AQP1 is essential for determining the full range of physiological roles it might serve, and its possible value as a therapeutic target in cancer metastasis.

Materials and Methods

Oocyte preparation and injection

The use of animals in this study has been carried out in accord with the Guide for the Care and Use of Laboratory Animals, licensed under the South Australian Animal Welfare Act 1985, with protocols approved by University of Adelaide Animal Ethics Committee. Unfertilized oocytes were harvested from anesthetized *Xenopus laevis* frogs and defolliculated by incubation in Type 1A collagenase (2 mg/ml) with trypsin inhibitor (0.3 mg/ml) in OR-2 saline (82 mM NaCl, 2.5 mM KCl, 1 mM MgCl₂, 5 mM HEPES; pH 7.3) at 16-18°C for 2-3 hours. Human Aquaporin-1 cDNA was provided by Prof P Agre (Preston et al., 1992; GenBank accession number NM_198098). AQP1 subcloned into a *X. laevis* β -globin plasmid was linearized with BamHI and transcribed in vitro (T3 mMessage mMachine; Ambion Inc., Austin TX USA), and cRNA was resuspended in sterile water. Prepared oocytes were injected with 50 nl of water (non-AQP1-expressing control oocytes), or 50 nl of water containing 1 ng of AQP1 cRNA, and incubated for 2 or more days at 16°C in ND96 saline (96 mM NaCl, 2 mM KCl, 1 mM MgCl₂, 1.8 mM CaCl₂, 5 mM HEPES, pH 7.3) to allow protein expression. Successful expression was confirmed by osmotic swelling assays. Batches of AQP1-expressing oocytes which lacked robust cGMP-activated conductance responses were further incubated overnight in ND96 saline with the tyrosine phosphatase inhibitor bisperoxovanadium (100 μ M; Santa Cruz Biotechnology, Dallas TX USA) as per published methods (Campbell et al., 2012). Chemicals were purchased from Sigma-Aldrich (St. Louis MO USA) unless otherwise specified.

AqB compounds: synthesis and preparation

The AqB compounds (custom-designed bumetanide derivatives) were synthesized by Dr G Flynn (Spacefill Enterprises LLC, Oro Valley AZ USA) as described in US-8,835,491-B2. To make AqB001, bumetanide was mixed with diazomethane (CH_2N_2) generated by reaction with Diazald® to create bumetanide methyl ester (MW 344.8; ClogP 2.10), which was dissolved in hot CHCl_3 , diluted with hexanes, and allowed to cool to provide the purified methyl ester as white flakes, whose mass and NMR spectra were consistent with the desired product. Reaction of bumetanide with 1.2 equivalents of 1,1'-carbonyldiimidazole (CDI) in ethyl acetate (EtOAc) under argon with heating afforded an intermediate imidazolide, which upon cooling formed a white solid that could be isolated by filtration and stored under argon for later use. Alternatively, the imidazolide solution could be reacted in situ with 2 equivalents of an amine to form the corresponding amides. In a typical reaction, the reaction mixture would be partitioned between water and ethyl acetate (EtOAc), the organic layer washed with brine, the solution filtered and concentrated, and the residue crystalized to form EtOAc/hexanes. AqB-006 (MW 413.9; ClogP 1.04) was prepared using morpholine as the amine; AqB007 (MW 470.0; ClogP 0.79) resulted from 2-(4-methylpiperazine-1-yl) ethylamine; and AqB011 (MW 434.9; ClogP 1.80) was prepared using 2-(morpholine-1-yl) ethylamine. The structures of all compounds were confirmed by high resolution mass spectrometry and NMR analysis. Chemicals were purchased from Sigma-Aldrich (St. Louis MO USA) unless otherwise specified.

Powdered compounds were dissolved in dimethyl sulfoxide (DMSO) to create 1000x stock solutions for each desired final dosage. An equal dilution of DMSO (0.1%) alone in saline was used as the vehicle control.

Quantitative Swelling Assay

For double-swelling assays, each oocyte served as its own control. Swelling rates were assayed first without drug treatment (S1), then oocytes incubated for 2 h in isotonic saline with or without the AqB compounds were reassessed in a second swelling assay (S2). Swelling rates in 50% hypotonic saline (isotonic Na saline diluted with an equal volume of water) were quantified by relative increases in oocyte cross-sectional area imaged by videomicroscopy (charge-coupled device camera; Cohu, San Diego, CA) at 0.5 frames per second for 30s using NIH ImageJ software. Rates were measured as slopes of linear regression fits of relative volume as a function of time using Prism (GraphPad Software Inc., San Diego CA USA).

Electrophysiology

For two-electrode voltage clamp, capillary glass electrodes (1–3 M Ω) were filled with 1 M KCl. Recordings were done in standard Na⁺ bath saline containing 100 mM NaCl, 2 mM KCl, 4.5 mM MgCl₂, and 5 mM HEPES, pH 7.3. cGMP was applied extracellularly at a final concentration of 10-20 μ M using the membrane-permeable cGMP analog [Rp]-8-[para-chlorophenylthio]-cGMP. Ionic conductance was monitored for at least 20 min after cGMP addition to allow development of maximal plateau responses. Conductance was determined by voltage step protocols from +60 to -110mV from a holding potential of -40 mV. Recordings were made with a GeneClamp amplifier and pClamp 9.0 software (Molecular Devices, Sunnyvale CA USA).

Circular Wound Closure Assay

The cancer cell lines used in this study were HT29 human colorectal adenocarcinoma cells (Chen et al., 1987) purchased from ATCC (HTB-38; American Type Culture Collection; Manassas VA USA) which strongly express endogenous AQP1; and SW480 human colorectal adenocarcinoma cells (CCL-228; from ATCC) which

express AQP5 but show little AQP1 expression. mRNA levels were evaluated by quantitative PCR and protein levels by western blot (H Dorward et al., MS in review). Confluent cultures of HT29 and SW480 cells were used in migration assays to measure effects of AqB treatments on rates of wound closure. Cells were plated in flat-bottom 96-well plates at 1.25×10^5 cells/well in DMEM media with 10% fetal bovine serum, and incubated at 37°C and 5% CO₂ for 12-18 hours to allow monolayer formation. Circular wounds were created by aspirating a central circle of cells with a p10 pipette. Wells were washed 2-3 times with phosphate-buffered saline to remove cell debris. Culture media (DMEM with 2% bovine calf serum) containing either vehicle or drug treatments in the presence of a mitotic inhibitor 5-fluoro-2'-deoxyuridine (100 ng/ml) were administered into the wells. Cultures were imaged at 0 and 24 h, and analysed using ImageJ software to calculate percent wound closure by the change in area:

$$((Area_0 - Area_{24})/Area_0) \times 100$$

Cytotoxicity Assay

Cell viability was quantified using the AlamarBlue cell viability assay (Molecular Probes, Eugene OR USA). Cells were plated at 10^4 cells/well in 96-well plates, and fluorescence signal levels were measured with a FLUOstar Optima microplate reader after 24 h incubation with concentrations of AqB011 from 1 to 80 μ M, to obtain quantitative measures of cell viability. Mercuric chloride (20 μ M) was used as a positive control for cytotoxicity.

Molecular Modelling

In silico modeling was conducted with methods reported previously (Yool et al., 2013). The crystal structure of human AQP1 was obtained from the Protein Data Bank (PDB ID: 1FQY). The tetrameric model (Supplemental Data) was generated in Pymol

(Version 1.7.4 Schrödinger, LLC) using coordinates provided in the pdb file. Renderings of the AqB ligands were generated in Chemdraw (Version 13.0, PerkinElmer), then converted into pdb format using the on-line SMILES translation tool (National Cancer Institute, US Dept Health and Human Services). Both AQP1 and ligand coordinates were prepared for docking using MGLtools (Version 1.5.4, Scripps Institute, San Diego CA USA). The docking was carried using Autodock Vina (Trott and Olson, 2010) with a docking grid covering the intracellular face of tetrameric pore.

Data Compilation and Statistics

Results compiled from replicate experiments are presented as box plots. The boxes represent 50% of the data, the error bars indicate the full range, and the horizontal bars are the median values. *n* values are in italics above the x-axis. Statistical differences were analyzed with one-way ANOVA and post-hoc Bonferroni tests and reported as ** $p < 0.0001$, * $p < 0.05$, and not significant (NS; $p > 0.05$).

Results

AQP1 ion channel inhibition by novel bumetanide derivatives

A set of four related compounds with structural modifications at the carboxylic acid moiety of bumetanide were tested for effects on the cGMP-activated ionic conductance in AQP1-expressing oocytes. Two-electrode voltage clamp recordings of AQP1-expressing oocytes (**Figure 1**) illustrate inhibition of the ionic conductance by extracellular application of AqB007 (200 μ M) and AqB011 (20 μ M), but no appreciable block of the AQP1 ion channel with 200 μ M AqB001 or AqB006. Initial recordings before cGMP application, and responses to the first application of cGMP recordings showed typical cGMP-dependent activation, as described previously (Anthony et al., 2000). Oocytes were then transferred into saline with the indicated agents for 2 hours, during which time the ionic conductances uniformly recovered to initial levels (**Figure 2**). In response to the second application of cGMP, oocytes treated with vehicle (DMSO), AqB001 or AqB006 showed increases in conductance comparable to the first response. However, the cGMP-activated conductance responses were inhibited after treatment with AqB007 or AqB011.

Trend plots (**Fig 2A**) show that the ionic conductance in AQP1-expressing oocytes was initially low, and was activated by the first bath application of membrane permeable cGMP. The ionic conductance then recovered to basal level during a 2h incubation without cGMP, and was tested for reactivation by a second application of cGMP after treatment with vehicle or AqB compounds. Recordings for oocytes incubated in saline without DMSO during the recovery period were comparable to those for the DMSO-treated group (not shown). Non-AQP1-expressing control oocytes showed no ionic conductance response to cGMP and no effect of the vehicle or drug treatments (**Fig 2B**).

Compiled data for the cGMP-activated ionic conductance values in AQP1-expressing oocytes are shown in the box plot (**Fig 3A**), and indicate the levels of block by 200 μ M AqB007 and 20 μ M AqB011 were statistically significant as compared with vehicle treated AQP1-expressing oocytes. Dose-response relationships (**Fig 3B**) yielded estimated IC_{50} values of 14 μ M for AqB011 and 170 μ M for AqB007.

AqB ion channel blockers have no effect on osmotic water permeability

Data for oocyte volumes standardized as a percentage of initial volume at time zero illustrate the mean swelling responses over 60 seconds after introduction of the oocytes into 50% hypotonic saline (**Fig 4A**). AQP1-expressing oocytes showed consistent osmotic swelling which was unaffected by treatment with vehicle (DMSO 0.1%) or AqB compounds at 200 μ M each. Non-AQP1-expressing control oocytes showed little osmotic water permeability.

To analyze possible effects of the AqB compounds on water channel activity, a double-swelling assay was used (**Fig 4B**). After the first swelling (S1) in hypotonic saline, oocytes were incubated in isotonic saline with or without the AqB compounds (200 μ M) for 2 h before assessing the second swelling response (S2). There were no significant differences between the first and second swelling rates in any of the treatment groups, confirming that the AqB ion channel agents did not affect AQP1 osmotic water permeability.

Molecular modelling of candidate intracellular binding sites

Putative binding sites on the AQP1 ion pore for AqB011 and AqB007 in the intracellular loop D domain can be suggested based on structural modelling and docking analyses (**Figure 5**). In silico modeling suggested the sites for the most favorable energies of

interaction for AqB007 and AqB011 were located at the intracellular face of the central pore (**Fig 5A**). Interestingly, the model predicted hydrogen bonding between the uniquely elongated moieties of the two effective AqB ligands and the initial pairs of arginine residues in the highly conserved loop D motifs from two adjacent subunits (**Fig 5B**); the same arginines (R159 and R160 in human AQP1) have been shown to be involved in AQP1 ion channel gating but not water channel activity in prior work (Yu et al., 2006). The more compact AqB006 docked weakly at a different position in the central vestibule (not shown). While in silico modeling does not define actual binding sites, it provides a testable hypothesis for future work, and offers intriguing support for the role of loop D in modulating AQP1 ion channel gating. The most favorable energy of interaction was calculated for AqB011 (at -9.2 kcal/mol). The next most favorable energy of interaction for AqB compounds with the AQP1 channel was for AqB007 (at -7.0 kcal/mol), followed by AqB006 (at -6.0 kcal/mol). This order of interaction strength for the AqB series matched their order of efficacy for inhibition of the AQP1 ion channel conductance (Figure 3).

Inhibition of AQP1 ion channel activity slows cancer cell migration

The effects of AqB006, AqB007 and AqB011 were tested in migration assays of human HT29 colon cancer cells (**Figure 6**) which natively express AQP1. Net migration rates were calculated from the percent closure of a circular wound area at 24 h (**Fig 6A**). Results showed that cancer cell migration was not impaired by AqB006, but was impaired significantly by AqB007 at 100 μ M, and AqB011 at 50 μ M and 100 μ M, as compared with vehicle-treated control HT29 cells (**Fig 6B**). AqB011 was more effective than AqB007 in blocking migration, consistent with relative efficacies of the agents as blockers of the ion channel conductance. In contrast, AqB011 at 100 μ M had no effect on the migration rate of SW480 colon cancer cells (**Fig. 6B**) which

express AQP5, but not AQP1, suggesting that the inhibitory effect of AqB011 appears to be selective for AQP1.

AqB compounds show low cytotoxicity

There was no significant difference in viability between vehicle-treated and untreated cells, and no effect of treatment with AqB011 for HT29 cells (**Table 1**). Cell viability was assessed with alamarBlue assays. The persistence of the fluorescent signal at 24 h confirmed there was no appreciable cytotoxic effect of AqB011 treatment on HT29 cells at concentrations up to 80 μ M. Mercuric chloride as a positive control caused significant cell death, measured as a decrease in fluorescence. AqB011 at doses used to block the AQP1 ionic conductance and cancer cell migration did not impact cell viability.

Discussion

The aim of this study was to search for selective small-molecule pharmacological agents capable of blocking the cGMP-activated cationic conductance in AQP1. Discovery of pharmacological modulators for AQP1 channels has been an important goal in the aquaporin field. AQP1 antagonist and agonist agents are expected to be useful for defining the complex roles of aquaporins in fundamental biological processes, as well as for characterizing AQP1 modulators as potential clinical agents in various conditions, such as cancer metastasis (Yool et al., 2009). AQP1 expression is upregulated in subtypes of aggressive cancer cells in which it facilitates cancer migration. Results here show that selective blockers of the AQP1 ion channel slow migration of human colon cancer cells in culture. Pharmacological inhibition of AQP1 is predicted to have a protective effect in reducing metastasis in cancer, but remains to be demonstrated *in vivo*.

Using bumetanide as a starting scaffold, we created an array of novel synthetic derivatives. Based on pilot data indicating a small inhibitory effect of AqB050 on the AQP1 ion channel at high doses (unpublished observations), we investigated a series of structurally related derivatives AqB006, AqB007, and AqB011, as well as a simple methylated version of bumetanide AqB001, to test for possible inhibitors of the AQP1 ionic conductance. Our findings demonstrated that AqB007 and AqB011 are effective inhibitors of the central ion pore of AQP1, with estimated IC_{50} values of 170 and 14 μ M, respectively. Both AqB007 and AqB011 showed dose-dependent inhibition of the central ion pore, whereas the intrasubunit water pores were unaffected, enabling the first dissection of physiological roles of the distinct channel functions. Measuring fluorescence signal intensity with the alumarBlue cell viability assay showed that AqB011 was not cytotoxic at doses that produced maximal ion channel inhibition.

The inhibition by AqB011 of AQP1 ionic conductance was consistent with molecular docking studies suggesting the site of interaction is at the intracellular face of the central pore. Results revealed that AqB011 is the most energetically favored compound followed by AqB007. The predicted interaction site of AqB011 and AqB007 with AQP1 is at the loop D domain. Differences in the structures and efficacies of AqB006, AqB007 and AqB011 indicate that the structure-activity relationship of ion channel inhibition is sensitive to specific chemical modifications at the carboxylic acid position of bumetanide. The length and structure of the modification appears to be critical, and appears based on *in silico* modeling to be the region that interacts with the AQP1 channel gating loop D domain. The absence of cytotoxic effects of AqB011 at doses sufficient to block the AQP1 ion channel activity indicates that the inhibition of migration is not due indirectly to cell death. The observation that AqB011 inhibited migration in AQP1-expressing HT29 colon cancer cells, but had no effect on the migration of AQP-5 expressing SW480 colon cancer cells provides support for the idea that AqB011 is selective for AQP1. The inhibition of migration seen with AqB011 is unlikely to result from off-target effects on general metabolic function, cytoskeletal organization, actin polymerization, or signaling pathways involved in cell motility, since SW480 cell migration remained unaffected by the presence of AqB011.

AQP1 is present in barrier epithelia involved in fluid movement in the body, including proximal tubule and choroid plexus (Agre et al., 1993). It is also expressed in peripheral microvasculature, dorsal root ganglion cells, eye ciliary epithelium and trabecular meshwork, heart ventricle, and other regions in which a direct role for osmotic water flux is less evident (Yool, 2007). Additional roles suggested for AQP1 include angiogenesis (Nicchia et al., 2013); signal transduction (Oshio et al., 2006); increased mechanical compliance to changes in pressure (Baetz et al., 2009); axonal

regeneration of spinal nerves (Zhang and Verkman, 2015); recovery from injury (Hara-Chikuma and Verkman, 2006); and exocytosis (Arnaoutova et al., 2008). Relative contributions of the ion and the water channel functions in these diverse processes remain to be defined.

A possible role for the AQP1 ionic conductance (potentially in combination with water fluxes) in the control of cell volume associated with migration was supported by the results of the wound closure assays with AQP1-expressing HT29 cells. Cell migration was significantly impaired by AqB011 and AqB007, but not by AqB006. The greatest efficacy of migration block was seen with administration of AqB011. The comparable orders of efficacy for block of AQP1 ion channels in the oocyte expression system, and for block of cell migration in HT29 cultures, support the idea that the AqB011 effect on migration is mediated by block of the AQP1 ion channels directly. These data provide evidence that the ion channel activity of AQP1 has physiological relevance. Further work is needed to evaluate effects of blocking both water and ion channel activities of AQP1 together in migrating cells.

AqB011 is a new research tool for probing the physiological role of the AQP1 ion channel function in biological systems. This compound holds future promise as a possible adjunct clinical intervention in cancer metastasis. Exciting opportunities are likely to emerge from continuing discovery of pharmacological modulators for aquaporins for new treatments in cancers and other diseases.

Authorship Contributions

Participated in research design: Kourghi, Pei, De Ieso, Yool

Conducted experiments: Kourghi, Pei, De Ieso

Contributed new reagents or analytic tools: Flynn

Performed data analysis: Kourghi, Pei, De Ieso, Yool

Wrote or contributed to the writing of the manuscript: Kourghi, Pei, Flynn, Yool

References

- Agre P, Preston GM, Smith BL, Jung JS, Raina S, Moon C, Guggino WB and Nielsen S (1993) Aquaporin CHIP: the archetypal molecular water channel. *Am J Physiol* **265**(4 Pt 2):F463-476.
- Anthony TL, Brooks HL, Boassa D, Leonov S, Yanochko GM, Regan JW and Yool AJ (2000) Cloned human aquaporin-1 is a cyclic GMP-gated ion channel. *Mol Pharmacol* **57**(3):576-588.
- Arnautova I, Cawley NX, Patel N, Kim T, Rathod T and Loh YP (2008) Aquaporin 1 is important for maintaining secretory granule biogenesis in endocrine cells. *Molecular endocrinology* **22**(8):1924-1934.
- Baetz NW, Hoffman EA, Yool AJ and Stamer WD (2009) Role of aquaporin-1 in trabecular meshwork cell homeostasis during mechanical strain. *Experimental eye research* **89**(1):95-100.
- Boassa D, Stamer WD and Yool AJ (2006) Ion channel function of aquaporin-1 natively expressed in choroid plexus. *J Neurosci* **26**(30):7811-7819.
- Boassa D and Yool AJ (2003) Single amino acids in the carboxyl terminal domain of aquaporin-1 contribute to cGMP-dependent ion channel activation. *BMC Physiol* **3**:12.
- Brooks HL, Regan JW and Yool AJ (2000) Inhibition of aquaporin-1 water permeability by tetraethylammonium: involvement of the loop E pore region. *Mol Pharmacol* **57**(5):1021-1026.
- Campbell EM, Ball A, Hoppler S and Bowman AS (2008) Invertebrate aquaporins: a review. *J Comp Physiol B* **178**(8):935-955.

- Campbell EM, Birdsell DN and Yool AJ (2012) The activity of human aquaporin 1 as a cGMP-gated cation channel is regulated by tyrosine phosphorylation in the carboxyl-terminal domain. *Mol Pharmacol* **81**(1):97-105.
- Chen TR, Drabkowski D, Hay RJ, Macy M and Peterson W, Jr. (1987) WiDr is a derivative of another colon adenocarcinoma cell line, HT-29. *Cancer Genet Cytogenet* **27**(1):125-134.
- Detmers FJ, de Groot BL, Muller EM, Hinton A, Konings IB, Sze M, Flitsch SL, Grubmuller H and Deen PM (2006) Quaternary ammonium compounds as water channel blockers. Specificity, potency, and site of action. *J Biol Chem* **281**(20):14207-14214.
- El Hindy N, Bankfalvi A, Herring A, Adamzik M, Lambertz N, Zhu Y, Siffert W, Sure U and Sandalcioglu IE (2013) Correlation of aquaporin-1 water channel protein expression with tumor angiogenesis in human astrocytoma. *Anticancer research* **33**(2):609-613.
- Finn RN, Chauvigne F, Hlidberg JB, Cutler CP and Cerda J (2014) The lineage-specific evolution of aquaporin gene clusters facilitated tetrapod terrestrial adaptation. *PLoS One* **9**(11):e113686.
- Fu D, Libson A, Miercke LJ, Weitzman C, Nollert P, Krucinski J and Stroud RM (2000) Structure of a glycerol-conducting channel and the basis for its selectivity. *Science* **290**(5491):481-486.
- Hara-Chikuma M and Verkman AS (2006) Aquaporin-1 facilitates epithelial cell migration in kidney proximal tubule. *Journal of the American Society of Nephrology : JASN* **17**(1):39-45.
- Hu J and Verkman AS (2006) Increased migration and metastatic potential of tumor cells expressing aquaporin water channels. *FASEB journal : official*

publication of the Federation of American Societies for Experimental Biology
20(11):1892-1894.

Huber VJ, Tsujita M and Nakada T (2009) Identification of aquaporin 4 inhibitors using in vitro and in silico methods. *Bioorg Med Chem* **17**(1):411-417.

Ishibashi K (2009) New members of mammalian aquaporins: AQP10-AQP12. *Handb Exp Pharmacol*(190):251-262.

Jiang Y (2009) Aquaporin-1 activity of plasma membrane affects HT20 colon cancer cell migration. *IUBMB Life* **61**(10):1001-1009.

Jung JS, Bhat RV, Preston GM, Guggino WB, Baraban JM and Agre P (1994) Molecular characterization of an aquaporin cDNA from brain: candidate osmoreceptor and regulator of water balance. *Proceedings of the National Academy of Sciences of the United States of America* **91**(26):13052-13056.

McCoy E and Sontheimer H (2007) Expression and function of water channels (aquaporins) in migrating malignant astrocytes. *Glia* **55**(10):1034-1043.

Migliati E, Meurice N, DuBois P, Fang JS, Somasekharan S, Beckett E, Flynn G and Yool AJ (2009) Inhibition of aquaporin-1 and aquaporin-4 water permeability by a derivative of the loop diuretic bumetanide acting at an internal pore-occluding binding site. *Molecular pharmacology* **76**(1):105-112.

Monzani E, Shtil AA and La Porta CA (2007) The water channels, new druggable targets to combat cancer cell survival, invasiveness and metastasis. *Curr Drug Targets* **8**(10):1132-1137.

Nicchia GP, Stigliano C, Sparaneo A, Rossi A, Frigeri A and Svelto M (2013) Inhibition of aquaporin-1 dependent angiogenesis impairs tumour growth in a mouse model of melanoma. *J Mol Med (Berl)* **91**(5):613-623.

- Oshio K, Watanabe H, Yan D, Verkman AS and Manley GT (2006) Impaired pain sensation in mice lacking Aquaporin-1 water channels. *Biochemical and biophysical research communications* **341**(4):1022-1028.
- Park JH and Saier MH, Jr. (1996) Phylogenetic characterization of the MIP family of transmembrane channel proteins. *J Membr Biol* **153**(3):171-180.
- Preston GM, Jung JS, Guggino WB and Agre P (1993) The mercury-sensitive residue at cysteine 189 in the CHIP28 water channel. *The Journal of biological chemistry* **268**(1):17-20.
- Reizer J, Reizer A and Saier MH, Jr. (1993) The MIP family of integral membrane channel proteins: sequence comparisons, evolutionary relationships, reconstructed pathway of evolution, and proposed functional differentiation of the two repeated halves of the proteins. *Critical reviews in biochemistry and molecular biology* **28**(3):235-257.
- Saparov SM, Kozono D, Rothe U, Agre P and Pohl P (2001) Water and ion permeation of aquaporin-1 in planar lipid bilayers. Major differences in structural determinants and stoichiometry. *J Biol Chem* **276**(34):31515-31520.
- Schwab A, Nechyporuk-Zloy V, Fabian A and Stock C (2007) Cells move when ions and water flow. *Pflug Arch Eur J Phy* **453**(4):421-432.
- Seeliger D, Zapater C, Krenc D, Haddoub R, Flitsch S, Beitz E, Cerda J and de Groot BL (2013) Discovery of novel human aquaporin-1 blockers. *ACS Chem Biol* **8**(1):249-256.
- Sogaard R and Zeuthen T (2008) Test of blockers of AQP1 water permeability by a high-resolution method: no effects of tetraethylammonium ions or acetazolamide. *Pflugers Arch* **456**(2):285-292.

- Sui H, Han B-G, Lee JK, Walian P and Jap BK (2001) Structural basis of water-specific transport through the AQP1 water channel. *Nature* **414**(6866):872-878.
- Trott O and Olson AJ (2010) AutoDock Vina: improving the speed and accuracy of docking with a new scoring function, efficient optimization, and multithreading. *J Comput Chem* **31**(2):455-461.
- Tsunoda SP, Wiesner B, Lorenz D, Rosenthal W and Pohl P (2004) Aquaporin-1, nothing but a water channel. *J Biol Chem* **279**(12):11364-11367.
- Yool AJ (2007) Functional domains of aquaporin-1: keys to physiology, and targets for drug discovery. *Curr Pharm Des* **13**(31):3212-3221.
- Yool AJ, Brown EA and Flynn GA (2009) Roles for novel pharmacological blockers of aquaporins in the treatment of brain oedema and cancer. *Clin Exp Pharmacol Physiol* **37**(4):403-409.
- Yool AJ and Campbell EM (2012) Structure, function and translational relevance of aquaporin dual water and ion channels. *Mol Aspects Med* **33**(5):443-561.
- Yool AJ, Morelle J, Cnops Y, Verbavatz JM, Campbell EM, Beckett EA, Booker GW, Flynn G and Devuyst O (2013) AqF026 is a pharmacologic agonist of the water channel aquaporin-1. *J Am Soc Nephrol* **24**(7):1045-1052.
- Yool AJ, Stamer WD and Regan JW (1996) Forskolin stimulation of water and cation permeability in aquaporin-1 water channels. *Science* **273**(5279):1216-1218.
- Yoshida T, Hojo S, Sekine S, Sawada S, Okumura T, Nagata T, Shimada Y and Tsukada K (2013) Expression of aquaporin-1 is a poor prognostic factor for stage II and III colon cancer. *Mol Clin Oncol* **1**(6):953-958.

Yu J, Yool AJ, Schulten K and Tajkhorshid E (2006) Mechanism of gating and ion conductivity of a possible tetrameric pore in aquaporin-1. *Structure* **14**(9):1411-1423.

Zhang H and Verkman AS (2015) Aquaporin-1 water permeability as a novel determinant of axonal regeneration in dorsal root ganglion neurons. *Exp Neurol* **265**:152-159.

Zhang W, Zitron E, Homme M, Kihm L, Morath C, Scherer D, Hegge S, Thomas D, Schmitt CP, Zeier M, Katus H, Karle C and Schwenger V (2007) Aquaporin-1 channel function is positively regulated by protein kinase C. *J Biol Chem* **282**(29):20933-20940.

Footnotes

MK and JVP are co-first authors.

This work was supported in part by the National Institutes of Health [Grant R01 GM059986]; and a 2015 pilot grant from The Institute for Photonics & Advanced Sensing, University of Adelaide.

Figure Legends

Figure 1. Chemical structures of selected bumetanide derivatives and electrophysiology traces showing representative effects of AqB001, AqB006, AqB007, and AqB011 on the ionic conductance responses activated by bath application of CPT-cGMP, before and after 2 h incubation in saline with and without the AqB compounds. See Methods for details.

Figure 2. Trend plots showing the ionic conductance responses for individual oocytes measured prior to cGMP (initial), after the first cGMP application, after 2 h incubation in saline without cGMP containing DMSO (vehicle) or AqB agents, and after the second application of cGMP. Reversible cGMP-dependent activation of an ionic conductance in AQP1-expressing oocytes (A) was not seen in non-AQP1 control oocytes (B). Inhibition was seen after treatment with AqB007, and AqB011, but not with vehicle, AqB001, or AqB006.

Figure 3. Dose-dependent block of the AQP1 ionic conductance. (A) Compiled box plot data showing statistically significant block of the cGMP-activated ionic conductance in AQP1-expressing oocytes by AqB007 and AqB011, but not with vehicle, AqB001, or AqB006. See Methods for details. (B) Dose response curves showing percent block of the activated ionic conductance in AQP1 expressing oocytes and estimated IC_{50} values. *n* values for dose-response data (in order of increasing concentration) for AqB007 were 8, 4, 2, 8; and for AqB011 were 8, 2, 2, 3, 6, 4, 3.

Figure 4. Lack of effect of AqB compounds on AQP1 osmotic water permeability measured by optical swelling assays. (A) Mean oocyte volume, standardized as a percentage of the initial volume for each oocyte, as a function of time after introduction into 50% hypotonic saline, with and without 2 h pre-treatment with AqB

compounds at 200 μ M, or vehicle (0.1% DMSO). (B) Compiled boxplot data showing the absence of any statistically significant differences between the first and second swelling rates, measured before (S1) and after (S2) 2 h incubations in saline alone or saline with 200 μ M AqB compounds as indicated. See Methods for details.

Figure 5. In silico modeling of the energetically favored binding site for AqB011 in the center of the tetrameric channel of AQP1 (grey) at the intracellular side, bracketed by the gating loop D domains (green). The putative binding site suggests an interaction with two of the loop D domains from adjacent subunits. (A) is the full view of the tetramer, and (B) is a closer view slightly rotated to show proximity of the ligand to the conserved arginine residues in loop D.

Figure 6. Block of cell migration in AQP1-expressing HT29 but not SW480 cells treated with AqB011. (A) Illustrative diagram of the circular wound healing method, showing substantial closure of the wounded area in normal culture medium by 24 hours. (B) Compiled boxplot data from wound closure assays showing the dose-dependent inhibitory effects of AqB007 and AqB011, compared to DMSO and AqB006, on wound closure at 24 h in HT29 cell cultures. Migration of SW480 cells was not altered by AqB011.

Supplemental Data. Molecular modelling data in Protein Data Bank (pdb) format showing the compound AqB011 docked at the intracellular side of the tetrameric human AQP1 channel (PDB ID: 1FQY), and interacting with loop D domains of subunits surrounding the central pore.

Table 1. HT29 cell levels of cytotoxicity after treatment with furfural, structurally related compounds, or HgCl₂ in the culture medium.

Agent [AqB011] (μM)	Mean normalized cell viability (%) ± SEM §	n value	
0 (untreated)	100.0 ± 0.70	8	---
0 (0.1% DMSO)	103.9 ± 0.91	8	NS
1	104.0 ± 1.06	4	NS
5	102.3 ± 2.26	4	NS
10	110.6 ± 2.12	4	NS
20	114.0 ± 0.84	4	NS
40	111.8 ± 1.33	4	NS
80	102.4 ± 2.95	4	NS
HgCl ₂ (100 μM)	16.2 ± 0.20	3	**

§ Percent viability was standardized as a percentage of the untreated mean value, measured as changes in alumarBlue fluorescence signal intensity. See Methods for details.

Figure 1

vehicle

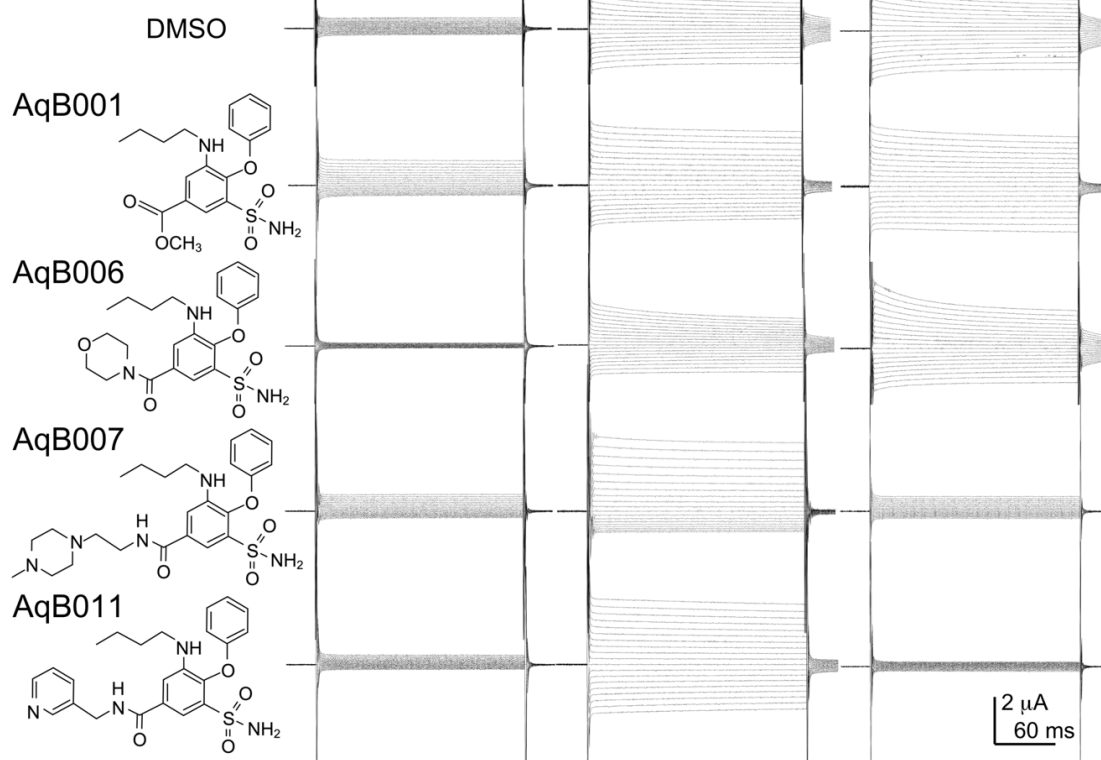


Figure 2

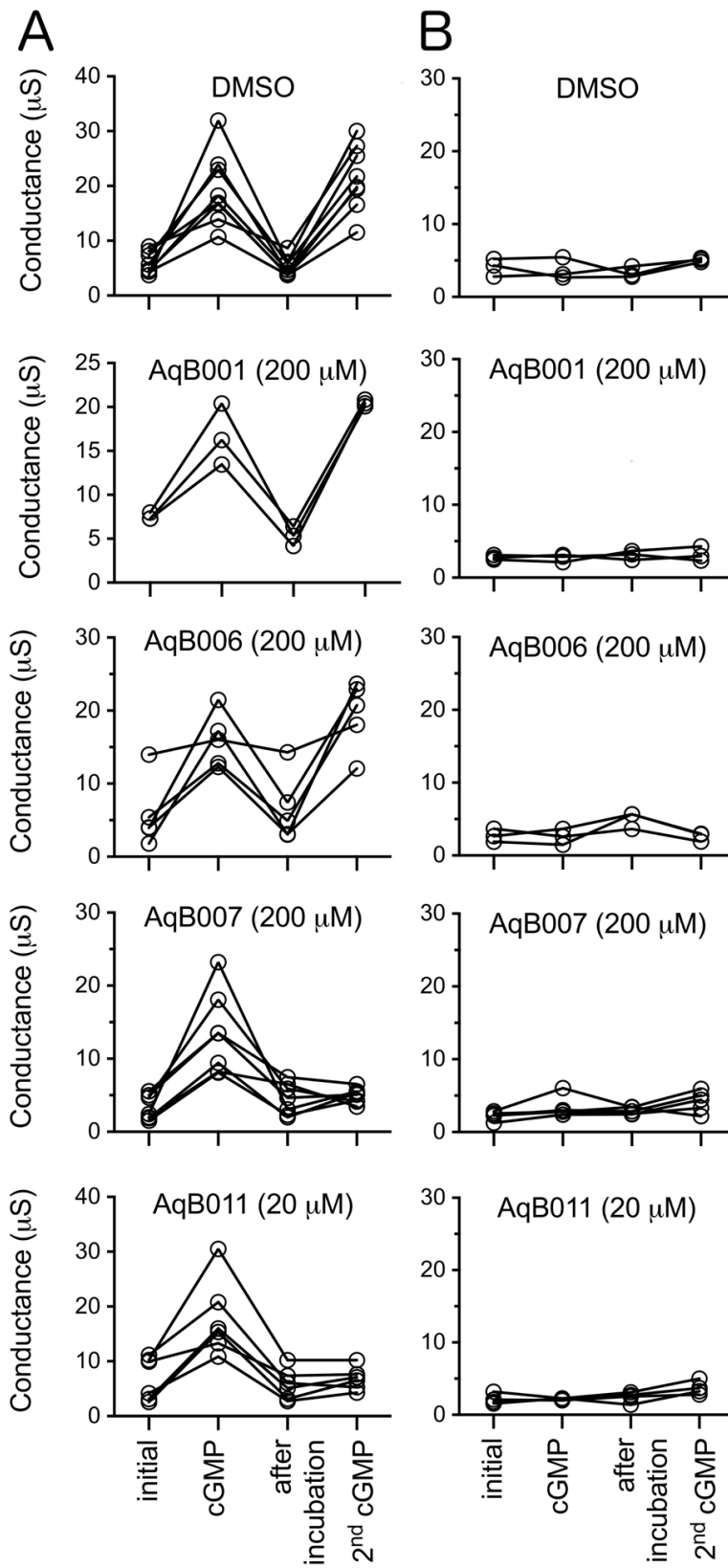


Figure 3

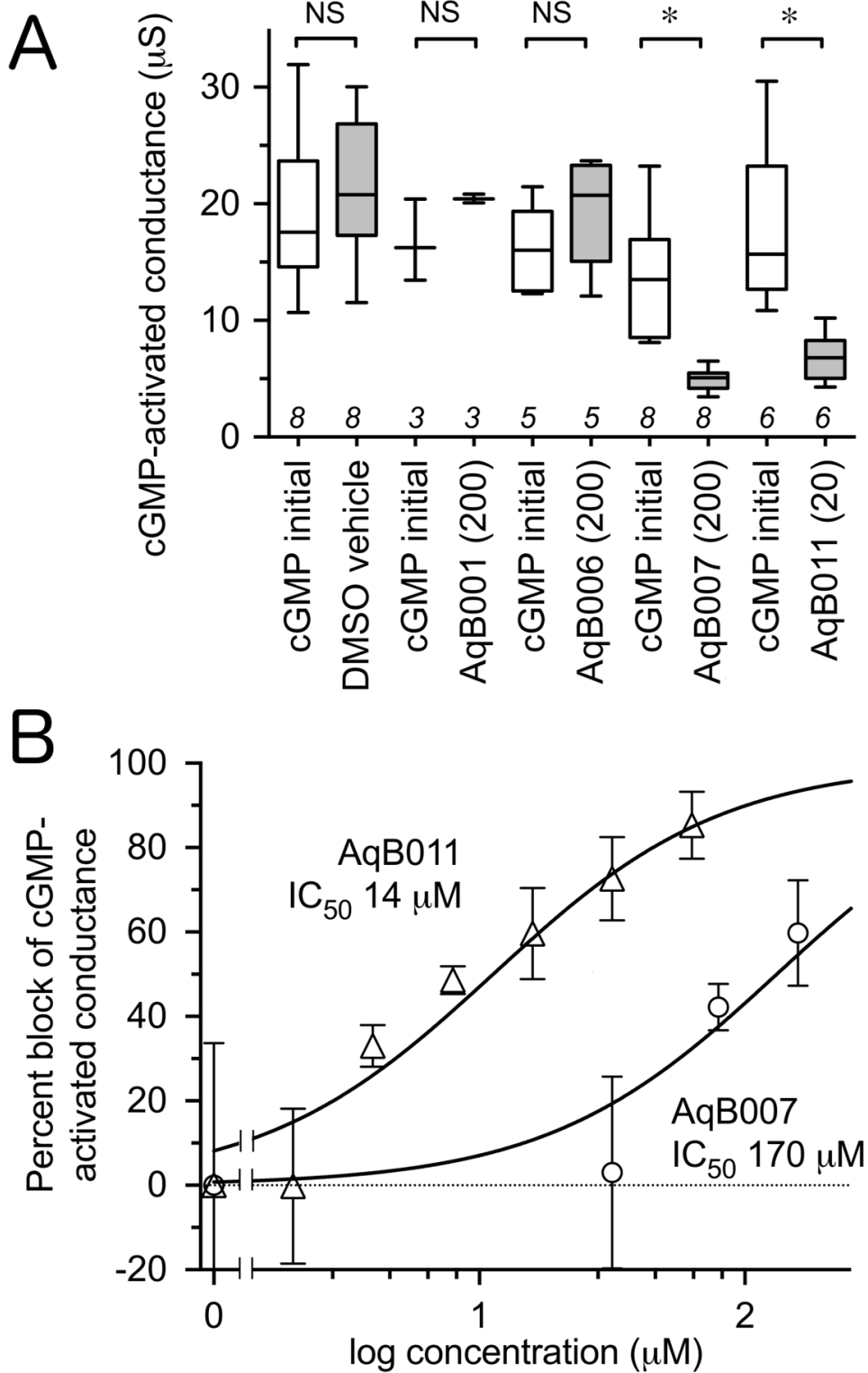


Figure 4

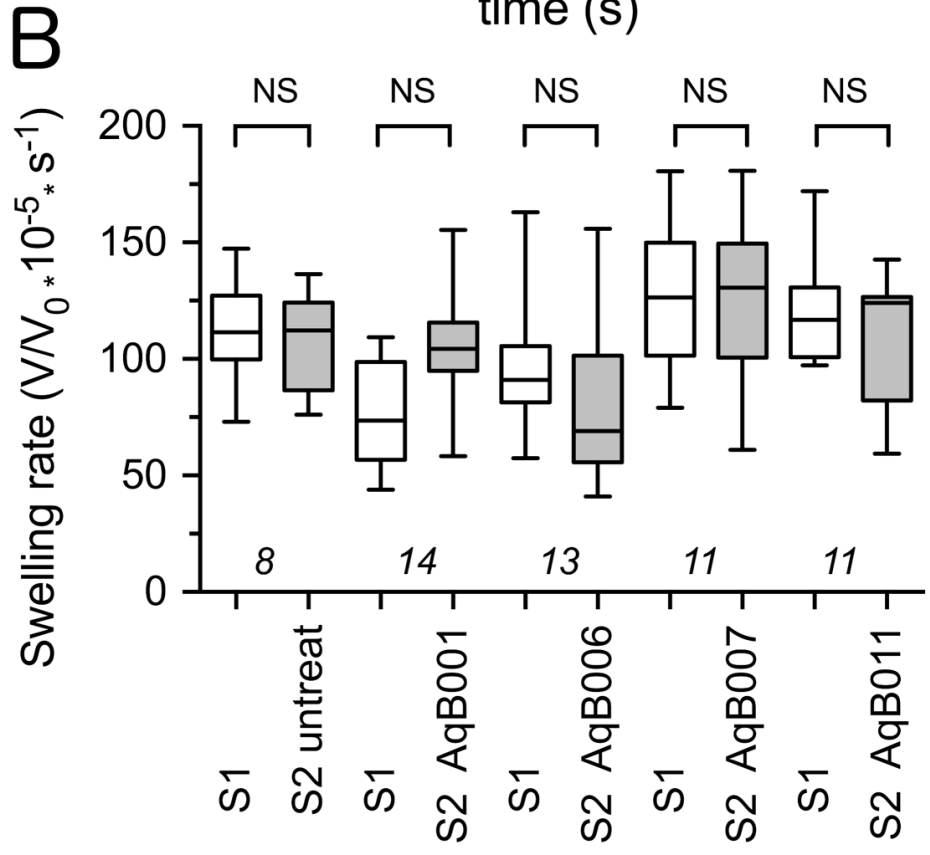
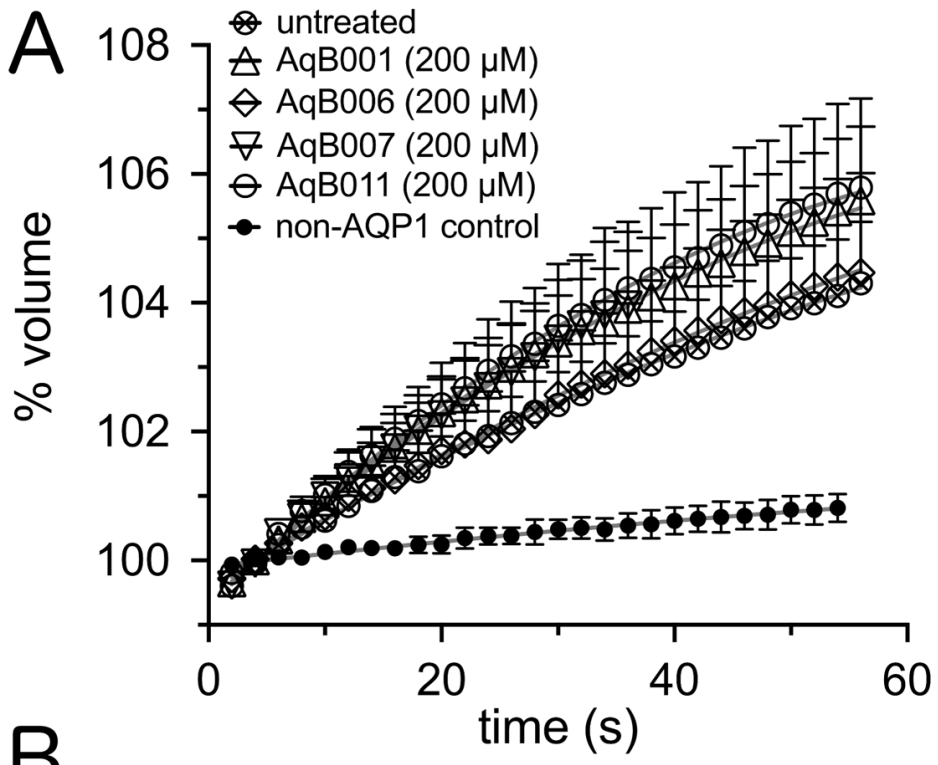


Figure 5

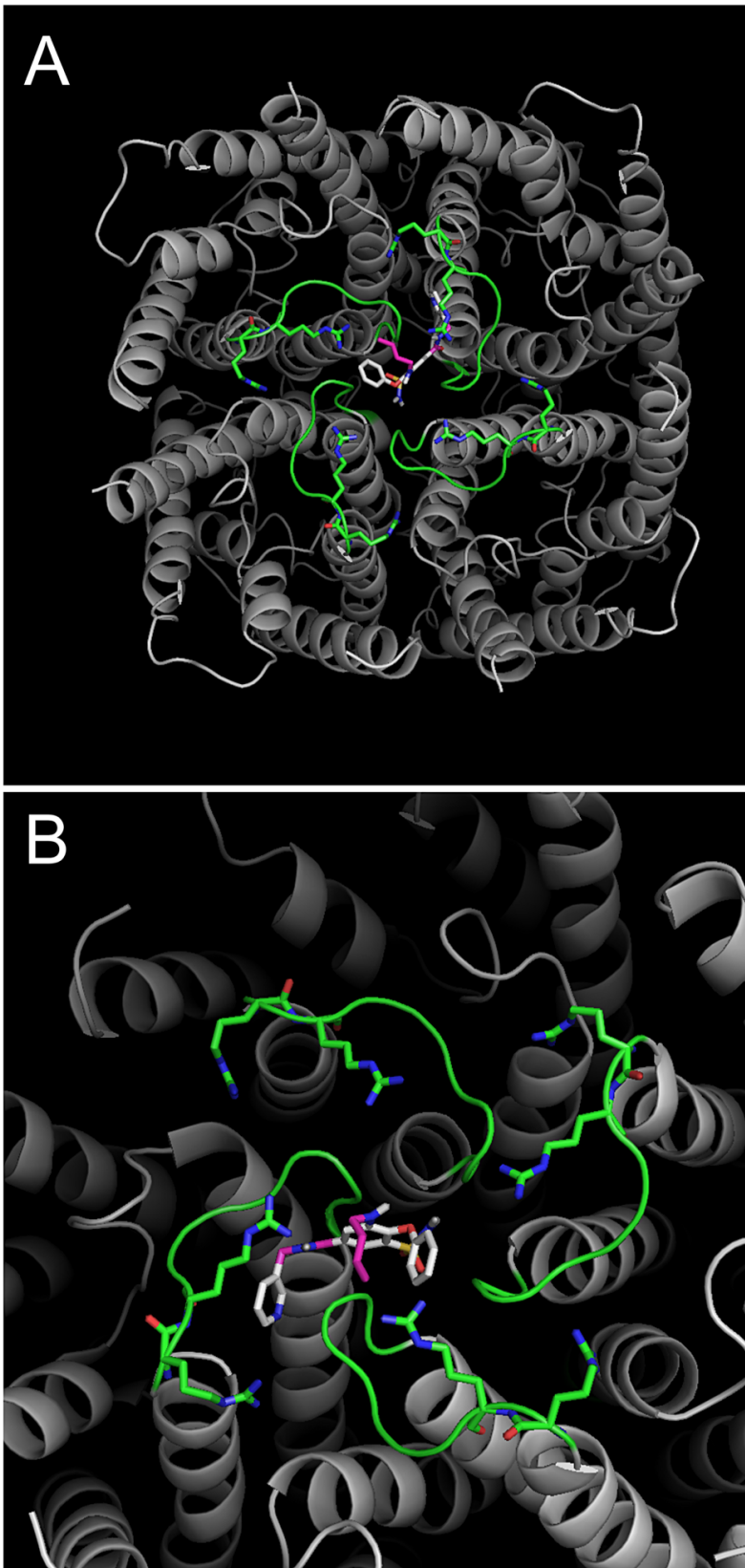
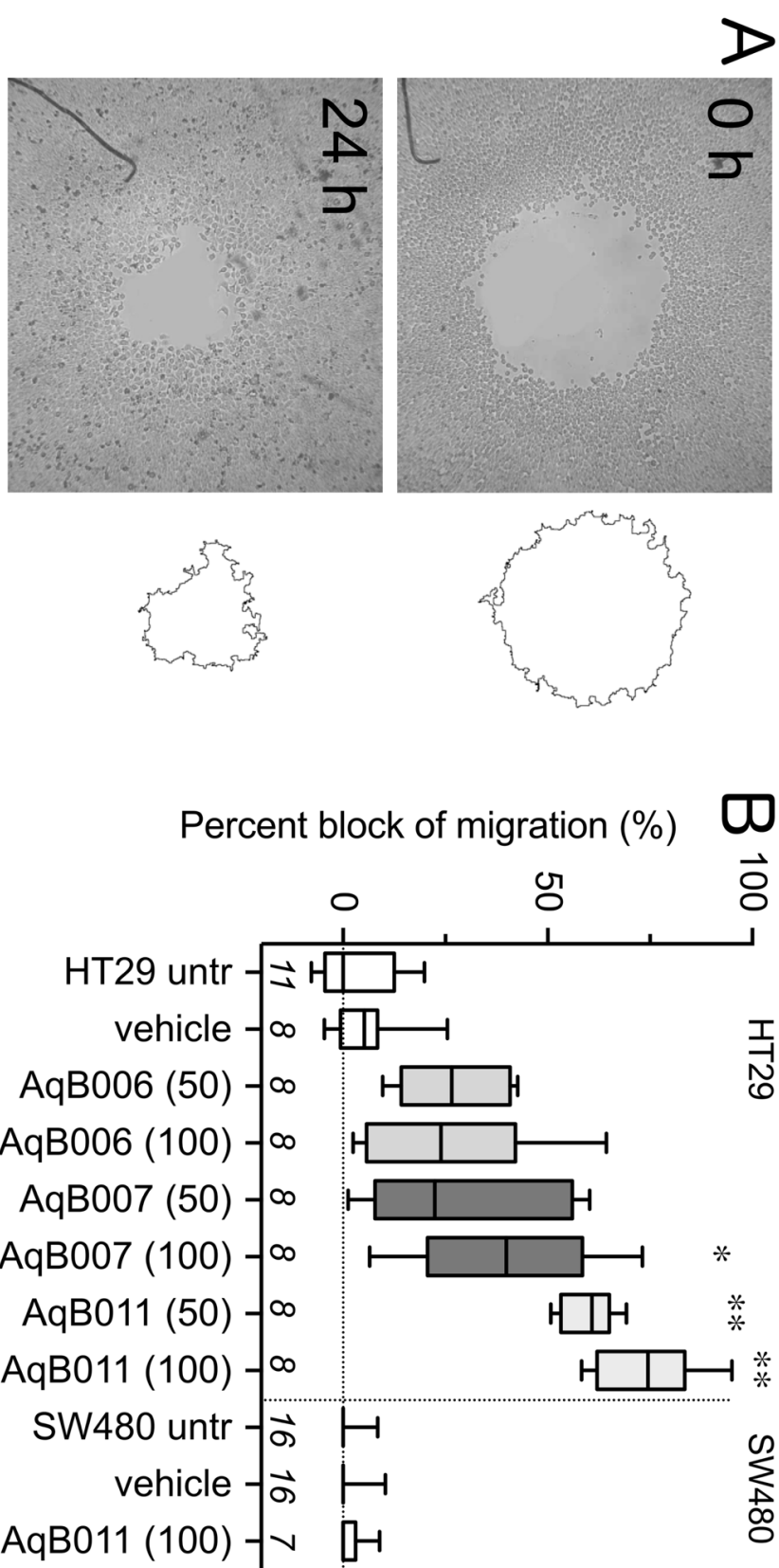


Figure 6



CHAPTER 3: THE DISCOVERY OF NOVEL PHYTOCHEMICALS THAT SLOW CANCER CELL MIGRATION

CONTEXTUAL STATEMENT

Differential inhibition of water and ion channel activities of mammalian Aquaporin-1 by two structurally related bacopaside compounds derived from the medicinal plant *Bacopa monnieri*.

AIM: To test the effect of two structurally related bacopaside compounds on AQP1 and AQP4 water and ionic conductance and to test the effect of both compounds on cancer cell migration.

HYPOTHESIS: Two bacopaside compounds can block either AQP1 or AQP4 water or ionic conductance at various degrees based on their structural differences. Both bacopaside compounds can impair cancer cell migration.

CONCLUSIONS:

1. Medicinal plant *Bacopa monnieri* was selected as the candidate from meta-analysis of literature conducted in Chapter 1.
2. Two triterpene saponins (Bacopaside I and Bacopaside II) were isolated and identified from the crude plant extract that were able to block AQP1 water permeability.
3. Results showed bacopaside I blocked both the water (IC_{50} 117 μ M) and ion channel activities of AQP1 but did not alter AQP4 activity, whereas bacopaside II selectively blocked the AQP1 water channel (IC_{50} 18 μ M) without impairing the ionic conductance.

4. Bacopaside I (IC₅₀ 48 μM) and bacopaside II (IC₅₀ 14 μM) impaired migration of HT29 cells which has higher AQP1 expression, but had minimal effect on SW480 cell migration, which has lower AQP1 expression.
5. Bacopasides could serve as novel lead compounds for pharmaceutical development of selective aquaporin modulators.

COMMENTARY:

The discovery of new AQPs modulators, as presented in this chapter, adds to the portfolio of compounds available for altering AQP-mediated functions, and expands our understanding of the structure-activity relationship of pharmacological blockers of AQP1 channels. This work was the evidence for some of the conclusions summarized in Chapter 1, and the first to demonstrate that identified phytochemical compounds from traditional herbal medicines are valuable candidates for new AQP modulators. The proposal that AQP1 is a key target for anti-cancer drug development is confirmed by results here. Cancer cell migration was impaired by blocking the AQP1 ionic conductance. This chapter, together with Chapter 2, highlight a broad array of pharmacological tools that can be developed as subtype selective probes for AQP research.

Statement of Authorship

Title of Paper	Differential Inhibition of Water and Ion Channel Activities of Mammalian Aquaporin-1 by Two Structurally Related Bacopaside Compounds Derived from the Medicinal Plant <i>Bacopa monnieri</i>
Publication Status	<input checked="" type="checkbox"/> Published <input type="checkbox"/> Accepted for Publication <input type="checkbox"/> Submitted for Publication <input type="checkbox"/> Unpublished and Unsubmitted work written in manuscript style
Publication Details	Pei, J.V. et al. Differential Inhibition of Water and Ion Channel Activities of Mammalian Aquaporin-1 by Two Structurally Related Bacopaside Compounds Derived from the Medicinal Plant <i>Bacopa monnieri</i> . <i>Mol Pharmacol</i> 90, 496-507 (2016).

Principal Author

Name of Principal Author (Candidate)	Jinxin Pei				
Contribution to the Paper	Initiated and performed experiments, analysis on all samples, interpreted data, wrote the manuscript.				
Overall percentage (%)	70%				
Certification:	This paper reports on original research I conducted during the period of my Higher Degree by Research candidature and is not subject to any obligations or contractual agreements with a third party that would constrain its inclusion in this thesis. I am the primary author of this paper.				
Signature	<table border="1" style="width: 100%;"> <tr> <td style="width: 80%;"></td> <td style="width: 20%;">Date</td> </tr> <tr> <td></td> <td>23/5/17</td> </tr> </table>		Date		23/5/17
	Date				
	23/5/17				

Co-Author Contributions

By signing the Statement of Authorship, each author certifies that:

- i. the candidate's stated contribution to the publication is accurate (as detailed above);
- ii. permission is granted for the candidate to include the publication in the thesis; and
- iii. the sum of all co-author contributions is equal to 100% less the candidate's stated contribution.

Name of Co-Author	Mohamad Kourghi				
Contribution to the Paper	Performed experiment and wrote the manuscript.				
Signature	<table border="1" style="width: 100%;"> <tr> <td style="width: 80%;"></td> <td style="width: 20%;">Date</td> </tr> <tr> <td></td> <td>23/05/2017</td> </tr> </table>		Date		23/05/2017
	Date				
	23/05/2017				

Name of Co-Author	Michael L. De Ieso				
Contribution to the Paper	Performed experiment.				
Signature	<table border="1" style="width: 100%;"> <tr> <td style="width: 80%;"></td> <td style="width: 20%;">Date</td> </tr> <tr> <td></td> <td>23/5/17</td> </tr> </table>		Date		23/5/17
	Date				
	23/5/17				

Name of Co-Author	Ewan M. Campbell
Contribution to the Paper	Initiated the project.
Signature	Date 6/6/17.

Name of Co-Author	Hilary S. Doward
Contribution to the Paper	Performed experiments.
Signature	Date 31/5/17

Name of Co-Author	Jennifer E. Hardingham
Contribution to the Paper	Initiated the project.
Signature	Date 1/6/17

Name of Co-Author	Andrea J. Yool
Contribution to the Paper	Initiated project, wrote the manuscript.
Signature	Date 23 May 2017

Published manuscript

**Differential inhibition of water and ion channel activities of mammalian
Aquaporin-1 by two structurally related bacopaside compounds derived from
the medicinal plant *Bacopa monnieri*.**

Jinxin V Pei, Mohamad Kourghi, Michael L De Ieso, Ewan M Campbell, Hilary S
Doward, Jennifer E. Hardingham and
Andrea J Yool

School of Medicine, University of Adelaide; Adelaide SA 5005 Australia (JVP, MK,
MLDI, JEH, AJY)

Institute for Photonics and Advanced Sensing, University of Adelaide; Adelaide SA
5005 Australia (JVP, AJY)

School of Biological Sciences, University of Aberdeen; Aberdeen AB242TZ Scotland
(EMC)

Molecular Oncology Laboratory, Basil Hetzel Institute, The Queen Elizabeth Hospital,
Woodville, SA, 5011 Australia. (HSD, JEH)

Running title:

Inhibition of aquaporin-1 by bacopasides

Corresponding author:

Prof Andrea J Yool

Medical School South level 4, Frome Rd

Adelaide SA 5005 AUSTRALIA

ph: +61 8 8313 3359

email: andrea.yool@adelaide.edu.au

fax: +61 8 8313 5384

Number of text pages: 35

Number of tables: 1

Number of figures: 7

Supplemental data files: 2

Number of words:

abstract 225

introduction 728

discussion 1478

Non-standard abbreviations: AQP (aquaporin); AqBxxx (numbered series of aquaporin blocking agents derived from bumetanide); AqFxxx (numbered series of aquaporin blocking agents derived from furosemide); methanol extract of whole *Bacopa* (meWB)

Abstract

Aquaporin-1 (AQP1) is a major intrinsic protein that facilitates flux of water and other small solutes across cell membranes. In addition to its function as a water channel in maintaining fluid homeostasis, AQP1 also acts as a non-selective cation channel gated by cGMP, a property shown previously to facilitate rapid cell migration in a AQP1-expressing colon cancer cell line. Here we report two new modulators of AQP1 channels, bacopaside I and bacopaside II, isolated from the medicinal plant *Bacopa monnieri*. Screening was conducted in the *Xenopus* oocyte expression system, using quantitative swelling and two-electrode voltage clamp techniques. Results showed bacopaside I blocked both the water (IC_{50} 117 μ M) and ion channel activities of AQP1 but did not alter AQP4 activity, whereas bacopaside II selectively blocked the AQP1 water channel (IC_{50} 18 μ M) without impairing the ionic conductance. These results fit with predictions from in silico molecular modeling. Both bacopasides were tested in migration assays using HT29 and SW480 colon cancer cell lines, with high and low levels of AQP1 expression respectively. Bacopaside I (IC_{50} 48 μ M) and bacopaside II (IC_{50} 14 μ M) impaired migration of HT29 cells, but had minimal effect on SW480 cell migration. Results here are the first to identify differential AQP1 modulators isolated from a medicinal plant. Bacopasides could serve as novel lead compounds for pharmaceutical development of selective aquaporin modulators.

Introduction

Aquaporin (AQP) water channels are in the family of major intrinsic proteins found from bacteria to humans (Agre et al., 1993; Calamita et al., 1995; Reizer et al., 1993), and are targets for the discovery of selective pharmacological modulators. Classes of aquaporins transport water and small uncharged molecules such as glycerol and urea through individual pores located in each subunit (Fu et al., 2000; Tajkhorshid et al., 2002).

An expanding role for aquaporins as multifunctional channels is being recognized (Yool and Campbell, 2012). In addition to facilitating water flux through intrasubunit pores, AQP1 also functions as a non-selective monovalent cation channel using the central pore at the four-fold axis of symmetry (Campbell et al., 2012; Yool and Weinstein, 2002; Yu et al., 2006). The ion channel conductance is activated by interaction of cGMP in the intracellular Loop D domain, and modulated by the carboxyl terminal domain (Anthony et al., 2000; Boassa and Yool, 2003; Saparov et al., 2001; Zhang et al., 2007). cGMP appears to trigger opening of cytoplasmic hydrophobic barriers in the central pore, allowing hydration and cation permeation (Yu et al., 2006). Inhibition of the AQP1 ion channel has been shown to slow cell migration rates in a colon cancer cell line that expresses high levels of AQP1 (Kourghi et al., 2016).

Defining pharmacological modulators of aquaporins has been an area of keen interest (Devuyst and Yool, 2010; Papadopoulos and Verkman, 2008; Seeliger et al., 2013). Early work identified blockers such as mercury (Preston et al., 1993), silver and gold (Niemi et al., 2002), acetazolamide (Gao et al., 2006), and tetraethylammonium ion (Brooks et al., 2000; Detmers et al., 2006; Yool et al., 2002), but these remained limited in usefulness because of toxicity, lack of specificity, or variable efficacy across experimental systems (Yang et al., 2006; Yool, 2007). More

recently, small molecule pharmacological agents with therapeutic potential have been identified. Complexes of gold-based compounds have promise for the selective block of specific classes of aquaporins; functionalized bipyrene and terpyridines coordinating Au(III) were shown to block aquaglyceroporin AQP3 with little effect on AQP1 (Martins et al., 2013). Intracellular arylsulfonamide modulators of AQP1 include the bumetanide derivative, AqB013, which blocks AQP1 and AQP4 water permeability (Migliati et al., 2009); AqB011 which blocks the AQP1 cation channel (Kourghi et al., 2016); and the furosemide derivative AqF026 which potentiates water channel activity of AQP1 (Yool et al., 2013). Other arylsulfonamide agents have been proposed as blockers of AQP4 (Huber et al., 2009; Huber et al., 2007). Growing evidence is demonstrating that specific arylsulfonamides act as AQP modulators in vitro and in vivo (Pei et al., 2016). Diverse small molecules acting at the extracellular side present a valuable array of novel inhibitors of AQP1 (Seeliger et al., 2013), indicating that other compounds in addition to coordinated metal ligands and arylsulfonamides are of interest for the development of AQP modulators. Lack of effects for a broad panel of AQP modulators tested in one study might reflect problems with synthesis or solubilization of the agents, or could indicate that the type of bioassay used influences apparent drug efficacy (Esteva-Font et al., 2016).

The present study was aimed at broadening the panel of AQP modulatory agents by evaluating natural medicinal plants as sources of active compounds. Quantitative swelling assays of mammalian AQP1 and AQP4 channels in the *Xenopus* expression system were used for screening extracts from a variety of traditional medicinal herbs, and identified *Bacopa monnieri* as one of several promising sources. Work here tested the hypothesis that chemical constituents of *B. monnieri* could be identified and

characterized as pharmacological agents that modulate mammalian AQP1 by interacting at domains associated with pore functions.

Data here show that bacopaside I blocks both the water and ion channel activities of AQP1 but does not alter AQP4 activity, and bacopaside II selectively blocks the AQP1 water channel without impairing the ionic conductance. Results fit well with in silico docking for predicted energies of interaction at a pore-occluding intracellular site. Bacopasides I and II showed the same order of efficacy in blocking migration of AQP1-expressing HT29 colon cancer cells, with minimal effects on SW480 cells that express AQP1 at low levels. Results here are the first to identify AQP1 channels as one of the candidate targets of action of the Ayurvedic medicinal plant, water hyssop, and to define new lead compounds for the development of AQP modulators.

Materials and Methods

Bacopa methanol extraction and fractionation

Bacopa monnieri stems and leaves were obtained with permission from The Botanic Gardens of Adelaide (Adelaide, South Australia). Chopped bacopa plant material (100 g) was dried, then refluxed in 500ml of methanol for 2 hours at room temperature. The suspension was filtered using Whatman No. 1 paper to obtain a methanol extract of whole bacopa (meWB). Half of the meWB extract was aliquoted into microfuge tubes, dried under vacuum (SpeedVac) into a solid brown paste, and reconstituted in saline for oocyte swelling assays. The other half of the meWB was fractionated using small-scale reverse phase C18 silica column (Alltech Prevail C18, Grace; Deerfield, IL). The mobile phases used for fractionation were a series of six water-methanol mixtures with H₂O:CH₃OH ratios ranging from 5:0 to 0:5. The fractions were dried in under vacuum and reconstituted in saline for oocyte swelling assays. Fractions containing AQP1 blocking activity were analyzed with mass spectrometry by Flinders Analytical (Flinders University, South Australia). Bacopaside I was identified by precise molecular weight as a major component in the active fractions, and bacopasides I and II were purchased from a commercial source (Chromadex; Irvine CA USA), solubilized in methanol to yield 100x stock solutions, and stored at -20°C. Experimental solutions were prepared by mixing the bacopaside stocks (1 part in 100) with isotonic saline or culture medium to yield final concentrations of 10 to 200 µM. Vehicle control salines were made using the same volume of methanol alone in isotonic saline or culture medium.

Oocyte preparation and cRNA injection

Unfertilized oocytes were isolated from *Xenopus laevis* frogs in accord with University Animal Ethics Committee-approved protocols, defolliculated by treatment with

collagenase (type 1A, 2 mg/ml; Sigma, St. Louis, MO) and trypsin inhibitor (0.67 mg/ml; Sigma, St. Louis, MO) in OR-2 saline (82 mM NaCl, 2.5 mM KCl, 1 mM MgCl₂, and 5 mM HEPES; pH 7.6) at 16°C for 1.5 hours, washed in OR-2 saline, and then incubated in isotonic oocyte saline [96 mM NaCl, 2 mM KCl, 0.6 mM CaCl₂, 5 mM MgCl₂, and 5 mM HEPES supplemented with 10% horse serum (Sigma, St. Louis, MO), 100 U/ml penicillin, 100 µg/ml streptomycin and 50 µg/ml tetracycline, pH 7.6] at 16°C. Oocytes were injected with 1-4 ng of AQP1, AQP4 or AQP1 R159A+R160A cRNA in 50 nl sterile water and incubated for 2 to 3 days at 16-18°C to allow protein expression. Oocytes not injected with cRNA served as non-AQP-expressing control cells.

Human AQP1 (National Center for Biotechnology Information NCBI GenBank: BC022486.1) and rat AQP4 (AF144082.1) cDNAs from P. Agre (The Johns Hopkins University, Baltimore, MD) were subcloned into a modified *Xenopus* β-globin expression plasmid. The double mutant construct human AQP1 R159A+R160A cDNA was generated by site-direct mutation (QuikChange; Stratagene, La Jolla, CA) and sequenced to confirm no errors were introduced (Yu et al., 2006). cDNAs were linearized with BamHI and transcribed using T3 polymerase (T3 mMessage mMachine; Ambion Inc., Austin, TX). cRNAs were resuspended in sterile water and stored at -80°C.

Quantitative oocyte swelling assays

Immediately prior to swelling assays, control and AQP-expressing oocytes were preincubated in isotonic saline (serum- and antibiotic-free) with or without meWB or bacopaside compounds or with methanol vehicle at 16-18°C, for incubation periods as indicated. Osmotic water permeability was determined as the linear rate of change in volume as a function of time, immediately after introduction into 50% hypotonic

saline (isotonic saline diluted with equal volume of water). Oocytes were imaged using a computer controlled charge-coupled-device grayscale camera (Cohu, San Diego, CA) mounted on a dissecting microscope (Olympus SZ-PT; NSW Australia). Images were taken at 0.5 frames per second for 60 seconds; cross-sectional areas were quantified using ImageJ software (Research Services Branch; National Institutes of Health, MD USA). Swelling rates were calculated as the slopes of linear regression fits of volume as a function of time in hypotonic saline. Data were analyzed and compiled for multiple batches of oocytes for statistical analyses and to generate dose-response curves, which were fit by sigmoidal non-linear variable-slope dose-response regression functions using Prism (GraphPad Software Inc., San Diego, CA USA).

Molecular docking

In silico modeling was done with methods reported previously (Yool et al., 2013). The protein crystal structures for human AQP1 (PDB ID. 1FQY) and human AQP4 (PDB ID. 3GDB) were obtained from the protein data bank (NCBI Structure). Bacopaside I and II structures were obtained from PubChem (NCBI) and converted into a software-compatible 3D structures in .pdb format using the Online SMILES Translator and Structure File Generator (National Cancer Institute, US Dept Health and Human Services). Ligand and receptor coordinates were prepared for docking using Autodock (Version 4.2, Scripps Research Institute, La Jolla, CA USA). Autodock Vina (Trott and Olson, 2010) was used to run the flexible ligand docking simulations with two docking grids covering both intracellular and extracellular faces of the monomeric pores. 3D docking result files and docking energy values were exported from Autodock, and results were viewed using PyMol software (Version 1.8, Schrödinger, LLC). Data for AQP1 and AQP4 docking results in .pse format are provided as Supplemental Files 1 and 2.

Electrophysiology

For two-electrode voltage clamp, capillary glass electrodes (1–3 M Ω) were filled with 1 M KCl. Recordings were done in standard isotonic Na⁺ bath saline containing 100 mM NaCl, 2 mM KCl, 4.5 mM MgCl₂, and 5 mM HEPES, pH 7.3. cGMP was applied extracellularly at a final concentration of 10-20 μ M using the membrane-permeable cGMP analog [Rp]-8-[para-chlorophenylthio]-cGMP (Sigma Chemical, Castle Hill NSW Australia). Ionic conductance was monitored for at least 20 min after cGMP addition to allow development of maximal plateau responses. Conductance was determined by linear fit of the current amplitude as a function of voltage, with a step protocol from +60 to -110mV and holding potential of -40 mV. After the first activation by cGMP, oocytes were incubated in isotonic saline with or without bacopaside I or bacopaside II for two hours to allow recovery. After incubation, a second application of cGMP was used to test for reactivation, to determine if any block of the ionic conductance was evident. Using the same protocol, AQP1-expressing oocytes were demonstrated previously to show cGMP-dependent activation, complete recovery during a 2 h incubation in saline alone, and full reactivation of the ionic conductance response to a second application of cGMP, whereas non-AQP1-expressing control oocytes showed a low ionic conductance and no significant response to drug treatments throughout the same protocol (Kourghi et al., 2016). Recordings were made with a GeneClamp amplifier and pClamp 9.0 software (Molecular Devices, Sunnyvale CA USA).

Cancer cell culture and migration assays

HT29 and SW480 colon cancer cell lines (from American Type Culture Collection ATCC, Manassas, VA USA) were cultured in complete medium composed of Dulbecco's Modified Eagles Medium (DMEM) supplemented with 1 x glutaMAX™ (Life

Technologies Mulgrave, VIC, Australia), penicillin and streptomycin (100 U/ml each) and 10% fetal bovine serum (FBS). Cultures were maintained in 5% CO₂ at 37°C. Cells were seeded in a flat-bottom 96-well plates at 1.25 x 10⁶ cells/ml to produce a confluent monolayer. For 12 to 18 hours prior to wounding, cells were serum-starved in 2% FBS, in the presence of 400 nM of the mitotic inhibitor 5-fluoro-2'-deoxyuridine, FUDR (Parsels et al., 2004). For wounding, a sterile p10 pipette tip was attached to the end of a vacuum tube, and a circular wound was created by brief perpendicular contact of the tip with base of the well. Each well was then washed three times with phosphate buffered saline (PBS) to remove detached cell debris. Cultures were maintained during the wound closure assay in 2% FBS medium with FUDR. Wound images were imaged at 10x magnification with a Canon 6D camera mounted on a Olympus inverted microscope. Image dimensions and pixel density were standardized across each image series using XnConvert software. Linear outlines and areas of the wound were generated using ImageJ software (National Institutes of Health). Wound closure data as a function of time were calculated as a percentage of the initial wound areas for the same wells.

Quantitative RT-PCR

Cells at 70-80% confluence were harvested and RNA extracted using the PureLink™ RNA Mini kit (Life Technologies). RNA was quantified using the NanoDrop 2000 spectrophotometer (Thermo Scientific, Waltham, MA, USA) and the integrity (RIN score) assessed using the 2100 Bioanalyzer (Agilent Technologies, Santa Clara, CA, USA). RNA (500 ng) was reverse transcribed using the iScript™ cDNA synthesis kit (Bio-rad, Carlsbad, CA, USA). qPCR of AQP1 and the reference gene phosphomannose mutase 1 (PMM1) was performed using multiplex Taqman

expression assays (Life Technologies) and SsoFast™ probes supermix (Bio-rad) in triplicate in the Rotorgene 6000 (Qiagen).

Western blot

Cultured cells were lysed with RIPA buffer containing 1% β-mercaptoethanol, 1% HALT protease inhibitor 100X solution, 150 U Benzonase (all from Sigma, St Louis, MO, USA) on ice for 10 minutes, homogenized by passing through a 21 gauge syringe and centrifuged 14,000 x g for 15 minutes at 4°C to pellet the cell debris. Protein was quantified (EZQ® assay, Life Technologies). Each sample (50 µg) was resolved by SDS-PAGE on a 12% Mini-PROTEAN® TGX Stain-Free™ Gels (Bio Rad) and transferred to PVDF membranes using the Trans-Blot® Turbo™ Transfer Pack and System (Bio Rad). Membranes were blocked with TBST containing 5% skim milk for 1 hour and incubated overnight at 4°C with anti- AQP1 (H-55) (1/500; Santa Cruz, USA). Following three washes in TBST, membranes were incubated with goat anti-rabbit IgG HRP secondary antibody (1/ 2000) and Streptactin-HRP Conjugate (1/10000) (both Bio-Rad) at room temperature for 1h, and washed. Chemiluminescence using Clarity™ Western ECL Blotting Substrate (Bio-Rad) was used for detection and blots imaged using the ChemiDoc™ Touch Imaging System (Bio-Rad). Image Lab™ Software was used to validate western blotting data via total protein normalization (Bio-Rad).

Immunocytochemistry

HT29 and SW480 cells grown on coverslips to 50% confluence were fixed with 4% paraformaldehyde and permeabilized with 0.5% Triton X-100. Image-iT® FX Signal Enhancer (Life Technologies) was used as per manufacturer's instructions. AQP1 was labelled with a 1/400 dilution of rabbit polyclonal anti-human AQP1 (Abcam®, Cambridge, UK), visualized with a secondary antibody at 1/200 dilution (goat anti

rabbit IgG H&L Alexa Fluor® 568; Life Technologies). Cells were counterstained with NucBlue® Fixed Cell Ready Probes™ Reagent (Life Technologies). Coverslips were mounted in ProLong® Gold antifade reagent (Life Technologies) and imaged with a Zeiss LSM 700 microscope (Carl Zeiss, Jena, Germany).

Live cell imaging

Cells were seeded on an 8-well uncoated Ibidi μ -Slide (Ibidi, Munich Germany) at a density of 1.0×10^6 cells/ml. For 12 to 18 hours prior to wounding, cells were serum-starved in medium with 2% FBS in the presence of FUDR (400 nM). Five circular wounds were created in each well using techniques described for the migration assays (above). The slide was mounted on a Nikon Ti E Live Cell Microscope (Nikon, Tokyo Japan) in an enclosed chamber kept at 37 °C with 5% CO₂. Images were taken at 5 min intervals for 24 hours, using Nikon NIS-Elements software (Nikon, Japan). AVI files were exported from NIS-Elements and converted into TIFF files using ImageJ (NIH). Converted files were analyzed using Fiji software (Schindelin et al., 2012) with the Manual Tracking plug-in.

Cytotoxicity assay

HT29 cell viability was quantified using the AlamarBlue assay (Molecular Probes, Eugene, OR USA). Cells were plated at 10^4 cells/well in 96-well plates, and fluorescence signal levels were measured with a FLUOstar Optima microplate reader after 24 h incubation with concentrations of bacopaside I from 0 to 100 μ M or bacopaside II from 0 to 30 μ M, to obtain quantitative measures of cell viability. Mercuric chloride (100 μ M) was used as a positive control for cytotoxicity.

Results

Extracted compounds from Bacopa monnieri inhibited AQP1 water channel

activity. Methanol-extracted whole Bacopa (meWB) reconstituted in isotonic saline inhibited the water permeability of AQP1-expressing oocytes (Fig 1A). After 2 hours preincubation in 1 mg/ml meWB, swelling rates of AQP1-expressing oocytes were significantly reduced ($p < 0.001$) as compared with untreated AQP1-expressing oocytes. Fractionated samples of meWB reconstituted at 0.1 mg/ml each were tested for biological activity using oocyte swelling assays (Fig 1B) after 2 hours preincubation. AQP1-mediated swelling was significantly decreased by fractions 3 and 4; other fractions had no effect. Combined fractions 3 and 4 were analyzed by mass spectrometry and revealed the presence of a major compound identified by precise molecular weight as bacopaside I. Commercially purchased bacopasides I and II were found to block osmotic water permeability in AQP1-expressing oocytes (Fig 1C) and showed a dose-dependent effect (Fig 1D). The inhibition of AQP1-mediated osmotic water fluxes showed IC_{50} values of approximately 18 μ M for bacopaside II, and approximately 117 μ M for bacopaside I.

Inhibition bacopasides I and II was time-dependent and reversible. AQP4-expressing oocytes showed no block of water channel activity after 2 h preincubation in isotonic saline containing bacopaside I at 178 μ M (Fig 2A). The blocking effect of bacopaside was specific for AQP1. The inhibitory effect of bacopasides I and II on AQP1 water channel activity took time to develop, with near maximum block achieved by approximately 2 h (Fig 2B). The magnitude of inhibition of AQP water flux increased as a function of the duration of preincubation in 178 μ M bacopaside I or 35 μ M bacopaside II. For bacopaside I, half-maximal block was reached after approximately 50 min, and maximum block after 120 min of preincubation. For bacopaside II, half-

maximal block was reached after approximately 30 min, and maximum block after 80 min of preincubation. Longer times provided no appreciable further enhancement of the magnitude of inhibition. Comparably slow time-dependent onset of block has been noted previously for other AQP1 ligands such as AqB013, AqB011 and AqF026, which are thought to bind at the intracellular side of the channel (Kourghi et al., 2016; Migliati et al., 2009; Yool et al., 2013), and require time to travel across the plasma membrane to the cytoplasmic side.

The blocking effects of bacopasides I and II on AQP1 water channel activity were reversible (Fig 2C). AQP1 channels were preincubated 2 hours with 178 μ M bacopaside I or 35 μ M bacopaside II, followed by washout of the drug with isotonic saline. The osmotic water permeability showed approximately 25% recovery by 120 min after the washout of bacopaside I, and half-maximal recovery by 160 min. For bacopaside II, water permeability showed 25% recovery by 150 min after washout of the blocker, and half-maximal recovery by 200 min.

The ion channel conductance of AQP1 was inhibited by bacopaside I but not by bacopaside II. Two-electrode voltage clamp recordings from AQP1-expressing oocytes demonstrated the cGMP-dependent activation of the ionic conductance (Fig 3A) as described previously (Anthony et al., 2000), which was reversible by 2 h incubation in saline without membrane-permeable cGMP (Kourghi et al., 2016). Re-activation of the ionic response by a second dose of cGMP was partly blocked in AQP1-expressing oocytes after 2 h incubation in 50 μ M bacopaside I, and strongly blocked at 100 μ M bacopaside I. In contrast, the reactivation of the ion conductance was unimpaired after incubation with 10 μ M or 20 μ M bacopaside II (Fig 3B).

Identification of candidate intracellular binding sites. Protein crystal structures of AQP1 and AQP4, and three-dimensional structural renditions of bacopaside I and

bacopaside II were prepared and run on interaction simulations using Autodock Vina software to identify predicted binding sites. An array of candidate docking sites for bacopasides I and II on AQP1 and -4 channels were considered with in silico computational docking analyses. Of a total of 8 possible positions evaluated for bacopaside I, the dominant energetically-favored configurations for intracellular binding yielded values of -9.2 Kcal/mol for AQP1, and -8.0 Kcal/mol for AQP4. Similarly out of all possible positions evaluated, the energetically-favored configurations for bacopaside II yielded values of -9.3 Kcal/mol for AQP1, and -7.8 Kcal/mol for AQP4.

In the poses reflecting the most favored docking positions, the intracellular face of the water pore was effectively occluded by bacopasides I and II in AQP1, but not in AQP4 channels (Fig 4A,B,C,D). For AQP1, the bacopasides appeared to nest well into the internal vestibule of the intrasubunit water pore. For AQP4 the optimal interaction was seen for bacopaside sitting in a groove between transmembrane domains 4 and 5, a position where subunits interface near the central pore that might not be accessible in the assembled tetrameric channel.

Closer inspection of specific amino acid residues in the predicted AQP1 docking site (using Chimera visualization software) suggested that the poly-arginine motif in the Loop D domain could enable hydrogen bond formation with the sulfonyl moiety on the glucopyranosyl sugar of bacopaside I (Fig 4E) at residues corresponding to R159 and R160 in human AQP1. These arginines are part of a highly conserved amino acid pattern seen in AQP1 channels from diverse species, and required for cGMP gating of the AQP1 ionic conductance (Yu et al., 2006). The site-directed double mutation of arginines R159 and R160 to alanines did not prevent normal expression of AQP1-mediated osmotic water permeability, indicating that the AQP1 mutant constructs were

expressed and targeted to the oocyte plasma membrane as described previously (Yu et al., 2006); however, the efficacy of bacopaside I in inhibiting osmotic water permeability was abolished in the mutant construct at doses up to 100 μ M (Figure 1D, supporting the suggested role of the loop D arginine residues in stabilizing the docking of the bacopaside I ligand.

Bacopaside II was more effective than bacopaside I in blocking migration of AQP1-expressing colon cancer cells. HT29 cells have a higher endogenous level of AQP1 expression as compared with SW480 cells, as demonstrated by quantitative RT-PCR (Fig. 5A), western blot (Fig. 5B), and immunocytochemistry (Fig 5C) analyses.

Wound closure assays showed robust migration of HT29 cells in medium with vehicle (Fig 6A), resulting in little open area remaining at 24 h. In contrast, treatment with bacopaside II (Fig. 6B) substantially reduced the amount of wound closure. Dose-dependent block of cell migration measured by wound closure (Fig 6C) was observed for both bacopaside I and bacopaside II on HT29 cells. The calculated IC_{50} value for bacopaside I was approximately 48 μ M and for bacopaside II was 14 μ M in HT29 cells. There was a small reduction of migration observed for SW480 cells treated with bacopaside II (Fig 6C), which was consistent with the relatively low expression of AQP1 channels in this cell line.

Time-lapse imaging demonstrated bacopasides I and II differentially decreased the rate of migration of AQP1-expressing HT29 colon cancer cells. Cultured HT29 cancer cells showed different rates of migration into the open wound areas in vehicle, bacopaside I and bacopaside II treatment conditions (Fig 7A,B,C). Time lapse images showed the rates of cell migration were significantly impeded in 50 μ M bacopaside I and in 15 μ M bacopaside II (Fig 7B,C) as compared with vehicle-treated

HT29 cells (Fig 7A). No appreciable difference in cell viability was observed in any of the treatment groups during the 24 time course of the experiment.

In the vehicle-treated group, trajectory plots of individual cells sampled at 50 min intervals over 24 h (Fig 7D) showed generally directional movements of HT29 cells into the open wound spaces. In bacopaside I treatment group, the HT29 cells lacked directional migration and moved short distances between successive frames. In the bacopaside II treated group, the impairment of movement was evident but less severe. The collective trend of trajectories of the vehicle-treated group appeared to be linear and extended, whereas that in the bacopaside I treated group was recursive and compressed; the bacopaside II group showed an intermediate level of restriction of movement.

The net displacement (distance travelled) per time interval was greater in the vehicle treated than the bacopasides I or II treated groups. Frequency histograms showing the number of events observed were compiled as binned values of distances travelled per 50 min interval (Fig 7E), and showed that more cells travelled longer distances in the vehicle treated group as compared with the bacopasides I and II treated groups. Distances moved per 50 min interval were well fit by Gaussian distributions. The decreased mean distances moved in both bacopaside I and II treated groups were seen as a left shift in the peaks of the frequency histograms. Compiled data in a summary histogram (Fig 7F) confirmed the significant decrease in mean total distance travelled by cells during the 24 hours of tracking in bacopaside I or II as compared with vehicle treated cells. Analysis of cytotoxicity by AlamarBlue assay showed that bacopaside I had no significant effect on cell viability at 50 or 75 μM , and bacopaside II had no effect on viability at 15 or 20 μM (Table 1). Concentrations of bacopasides

that significantly blocked AQP1 water channel activity and HT29 cell migration were not appreciably cytotoxic.

Discussion

Results here demonstrated that two structurally similar compounds, bacopaside I and bacopaside II derived from a medicinal herb, act differentially as pharmacological inhibitors of mammalian aquaporin channels. *In silico* modeling predicted that bacopasides I and II have favorable energies of interaction at the intracellular vestibule of AQP1, occluding the intrasubunit water pore. Modeling results were consistent with observed effects of these agents as AQP1 inhibitors. Predicted energies of interaction for docking on AQP1 were higher for bacopaside II than bacopaside I, fitting the observed order of efficacy in blocking AQP1-mediated swelling of oocytes and the same order of efficacy in blocking migration of AQP1-expressing HT29 colon cancer cells, with minimal effects on SW480 cells that express little AQP1. The docking of bacopasides I and II to occlude the water pore appeared principally to involve the trisaccharide rings, which projected down into the AQP1 intrasubunit pore. Future work exploring polysaccharides and related osmolytes as endogenous modulators of AQP channels could be of interest. The lack of a favorable docking interaction of bacopaside with the AQP4 water pore was consistent with the insensitivity of AQP-4 expressing oocytes to bacopaside I in osmotic swelling assays. Based on the docking model, candidate residues that could contribute to the proposed binding of bacopaside sugar rings in the hAQP1 intracellular water pore appear to include amino acids serine 71 in the loop B region, and tyrosine 97 in the adjacent membrane spanning domains, but remain to be defined.

Inhibition of AQP1 water channel activity by bacopasides I and II showed a slow onset that was consistent with prerequisite transit of the agent across the plasma membrane to access the intracellular side. The latency period (approximately 2 h) was

comparable to that described for other aquaporin modulators AqB013 and AqF026, also thought to act at the cytoplasmic side (Migliati et al., 2009; Yool et al., 2013).

Accumulating evidence suggests pharmacological agents can be defined with subtype selectivity for AQP classes. Prior work showed that external application of AqF026 potentiated water permeability in AQP1 (EC_{50} 3.3 μ M), but a 15-fold higher concentration was required to potentiate AQP4 (Yool et al., 2013). Metal complexes acted as blockers of glycerol permeability in AQP3 (at an external site predicted to involve cysteine (C40) and arginine (R218) residues), with comparatively small effects on AQP1 water permeability (Martins et al., 2013). Results here for bacopaside I showed block of osmotic water permeability for AQP1 but not AQP4 channels. This difference in bacopaside sensitivity between related aquaporins suggests that the inhibitory effects seen for AQP1 are exerted directly on the heterologously expressed channel, and not due to side effects on endogenous oocyte channels or transporters. The reversibility of block indicated that functional properties and expression of the channels in plasma membrane were not impaired. Data here cannot rule out possible actions of bacopasides on other molecules not yet assessed; however, the lack of effect of bacopaside treatment on migration in a cancer cell line SW480 with low AQP1 expression suggests the mechanism of action is reasonably selective, and does not appreciably impact diverse signaling and transport processes needed for basic maintenance and non-AQP1 dependent motility. Cytotoxicity assays showed that the viability of AQP1-expressing HT29 cancer cells was not affected by bacopasides I and II at doses that significantly blocked ion flux and cell migration.

Bacopasides I and II are triterpene glycosides, composed of a hydrophobic pentacyclic terpene backbone (estimated logP value approximately 9; enabling membrane permeability), and three linked polar sugar groups (arabinofuranosyl—

glucopyranosyl—arabinopyranose in bacopaside I; and arabinofuranosyl—sulfonyl-glucopyranosyl—glucopyranose in bacopaside II) that appear from in silico modeling to lodge via H-bonds into the water pore entrance of AQP1, with the exception of the sulfonyl group which appears to require an interface with positively charged residues (arginines in the adjacent AQP1 Loop D domain). Mutation of the key Loop D arginines to alanines appeared to cause destabilization of the overall binding of the bacopaside I compound on AQP1, seen as a decreased efficacy of water pore block and increased IC_{50} value in the R159A+R160A mutant.

The ability of modulators to differentially block the ionic conductance is an important consideration in processes such as rapid cell migration which appear to require AQP1 cation channel function (Kourghi et al., 2016). Interaction of the sulfonyl group with Loop D arginines was consistent with the observed block of the cGMP-activated ionic conductance by bacopaside I not II. Bacopaside I showed a lower IC_{50} value for inhibiting HT29 cancer cell migration ($\sim 48 \mu\text{M}$) than for inhibiting the AQP1 ionic conductance alone ($\sim 117 \mu\text{M}$), and the cell migration trajectories in bacopaside I-treated group were more compressed than those in the bacopaside II-treated group, suggesting that simultaneous block of both water and ion channel activities of AQP1 might be more effective in blocking AQP1-dependent cell migration than impairing either function alone.

Although the overall amino acid sequence similarity between AQP1 and AQP4 channels is high (>40% identity and 60% homology), AQP4-mediated osmotic swelling was not sensitive to block by bacopaside I. The docking model suggested the bulky terpene might sterically hinder docking near the AQP4 water pore. As well, the Loop D domain of AQP4 lacks the key arginines 159 and 160 suggested here to be

important for the sulfonyl group coordination, showing instead serine and lysine in the equivalent positions, which might be less effective as putative coordination sites.

The identification of bacopasides as novel AQP modulators expands the database of pharmacophore properties of AQP ligands. Bacopasides I and II themselves might not be ideal as drug candidates, exceeding limits of Lipinski's Rule of Five for molecular weight, hydrophobicity, and numbers of hydrogen bond donors and acceptors— although natural products often show biological activity as exceptions to the rule (Ganesan, 2008). Bacopasides administered in vivo are likely to act as metabolic derivatives as well as intact compounds. More work is needed to define in vivo metabolites of bacopasides and characterize their effects on aquaporins. Nonetheless, bacopasides could serve as lead compounds for the design of small-molecule blockers of aquaporins. Results here suggest the trisaccharide moiety is a key component. An intriguing idea would be to design compact membrane-permeable trisaccharides for blocking water flux; while addition of key sulfonyl or other groups could inhibit parallel AQP functions. Endogenous polysaccharide osmolytes in cells might function as natural modulators of aquaporin channels, a concept that has not to our knowledge been considered previously.

Bacopa monnieri extract (also known as brahmi) has been used in Ayurvedic remedies since ancient times to improve memory and treat anxiety and depression (Russo and Borrelli, 2005). Brahmi has been suggested to have beneficial effects on psychological state, cognitive performance, and memory in human subjects and animal models; neuroprotective effects after ischemic brain injury; and anti-inflammatory actions in processes linked to neurodegenerative disorders (Aguiar and Borowski, 2013; Downey et al., 2013; Kongkeaw et al., 2014; Liu et al., 2013; Rehni et al., 2007; Sairam et al., 2002; Saraf et al., 2010; Singh and Dhawan, 1982; Williams et al., 2014; Zhou

et al., 2007). A meta-analysis of human clinical studies (generally with *B. monnieri* administered 250-450 mg/day for up to several months) improved mental response time and attention, and had potential benefits on memory (Kongkeaw et al., 2014). No serious adverse events were noted; minor side effects included diarrhea and dry mouth.

Beneficial outcomes ascribed to brahmi could in part involve block of AQP1 channels. AQP1 is expressed abundantly in brain choroid plexus where cerebral spinal fluid is produced (Boassa and Yool, 2005; Johansson et al., 2005), and in proximal kidney to facilitate water reabsorption (Nielsen and Agre, 1995). AQP1 is found in peripheral vasculature endothelia, red blood cells, and other cell types (Nielsen et al., 1993). Block of AQP1 could contribute to the anti-inflammatory benefits of brahmi treatment. Macrophages express AQP1 channels, which are required for IL-1 β release and neutrophilic inflammation responses (Rabolli et al., 2014). An alcoholic extract of *B. monnieri* decreased TNF-alpha production in mouse macrophages preincubated for 1 h, with an IC₅₀ near 1 mg/ml (Williams et al., 2014).

Pharmacological inhibitors of AQP1 channels could be useful for intervention in many conditions, including slowing metastasis in AQP1-positive cancer subtypes. In a subset of aggressive cancers, AQP1 expression is upregulated (El Hindy et al., 2013; Moon et al., 2003; Saadoun et al., 2002; Yool et al., 2009). AQP1 channels located at lamellipodial edges have been implicated in enhancing migration and metastasis (Hu and Verkman, 2006; McCoy and Sontheimer, 2007). Block of the AQP1 ion channel has been shown to slow migration in AQP1-expressing HT29 colon cancer cells (Kourghi et al., 2016).

A comprehensive portfolio of effective and selective aquaporin modulators is needed for clinical and basic research. Further exploration of AQP modulators in traditional

herbal medicines is merited (Pei et al., 2016). New ligand modulators of aquaporin channel activity could be present in the armamentarium of traditional herbal medicines, but remain to be discovered.

Acknowledgments

Thanks to John Sandham and The Botanic Gardens of Adelaide for identified samples of the water hyssop *Bacopa monnieri*; and to Dr Agatha Labrinidis and the Adelaide Microscopy core facility for access to equipment, support and training in live cell imaging.

Footnote

This work was supported by funding from the University of Adelaide Institute for Photonics and Advanced Sensing 2015 Pilot Grant program, and Australian Research Council Discovery Project grant DP160104641.

Authorship contributions

Participated in the research design: Pei, Campbell, Yool, Hardingham

Conducted experiments: Pei, Kourghi, De Ieso, Campbell, Doward

Performed data analysis: Pei, Kourghi, De Ieso, Yool

Wrote or contributed to writing of the manuscript: Pei, Kourghi, De Ieso, Yool

References cited

- Agre P, Preston GM, Smith BL, Jung JS, Raina S, Moon C, Guggino WB and Nielsen S (1993) Aquaporin CHIP: the archetypal molecular water channel. *The American journal of physiology* **265**(4 Pt 2):F463-476.
- Aguiar S and Borowski T (2013) Neuropharmacological review of the nootropic herb *Bacopa monnieri*. *Rejuvenation Res* **16**(4):313-326.
- Anthony TL, Brooks HL, Boassa D, Leonov S, Yanochko GM, Regan JW and Yool AJ (2000) Cloned human aquaporin-1 is a cyclic GMP-gated ion channel. *Mol Pharmacol* **57**(3):576-588.
- Boassa D and Yool AJ (2003) Single amino acids in the carboxyl terminal domain of aquaporin-1 contribute to cGMP-dependent ion channel activation. *BMC Physiol* **3**:12.
- Boassa D and Yool AJ (2005) Physiological roles of aquaporins in the choroid plexus. *Curr Top Dev Biol* **67**:181-206.
- Brooks HL, Regan JW and Yool AJ (2000) Inhibition of aquaporin-1 water permeability by tetraethylammonium: involvement of the loop E pore region. *Molecular pharmacology* **57**(5):1021-1026.
- Calamita G, Bishai WR, Preston GM, Guggino WB and Agre P (1995) Molecular cloning and characterization of AqpZ, a water channel from *Escherichia coli*. *The Journal of biological chemistry* **270**(49):29063-29066.
- Campbell EM, Birdsell DN and Yool AJ (2012) The activity of human aquaporin 1 as a cGMP-gated cation channel is regulated by tyrosine phosphorylation in the carboxyl-terminal domain. *Mol Pharmacol* **81**(1):97-105.
- Detmers FJ, de Groot BL, Muller EM, Hinton A, Konings IB, Sze M, Flitsch SL, Grubmuller H and Deen PM (2006) Quaternary ammonium compounds as

water channel blockers. Specificity, potency, and site of action. *J Biol Chem* **281**(20):14207-14214.

Devuyst O and Yool AJ (2010) Aquaporin-1: new developments and perspectives for peritoneal dialysis. *Perit Dial Int* **30**(2):135-141.

Downey LA, Kean J, Neme F, Lau A, Poll A, Gregory R, Murray M, Rourke J, Patak B, Pase MP, Zangara A, Lomas J, Scholey A and Stough C (2013) An Acute, Double-Blind, Placebo-Controlled Crossover Study of 320 mg and 640 mg Doses of a Special Extract of *Bacopa monnieri* (CDRI 08) on Sustained Cognitive Performance. *Phytother Res* **27**:1407-1413.

El Hindy N, Bankfalvi A, Herring A, Adamzik M, Lambertz N, Zhu Y, Siffert W, Sure U and Sandalcioglu IE (2013) Correlation of aquaporin-1 water channel protein expression with tumor angiogenesis in human astrocytoma. *Anticancer research* **33**(2):609-613.

Esteva-Font C, Jin BJ, Lee S, Phuan PW, Anderson MO and Verkman AS (2016) Experimental Evaluation of Proposed Small-Molecule Inhibitors of Water Channel Aquaporin-1. *Mol Pharmacol* **89**(6):686-693.

Fu D, Libson A, Miercke LJ, Weitzman C, Nollert P, Krucinski J and Stroud RM (2000) Structure of a glycerol-conducting channel and the basis for its selectivity. *Science* **290**(5491):481-486.

Ganesan A (2008) The impact of natural products upon modern drug discovery. *Curr Opin Chem Biol* **12**(3):306-317.

Gao J, Wang X, Chang Y, Zhang J, Song Q, Yu H and Li X (2006) Acetazolamide inhibits osmotic water permeability by interaction with aquaporin-1. *Analytical biochemistry* **350**(2):165-170.

- Hu J and Verkman AS (2006) Increased migration and metastatic potential of tumor cells expressing aquaporin water channels. *FASEB journal : official publication of the Federation of American Societies for Experimental Biology* **20**(11):1892-1894.
- Huber VJ, Tsujita M, Kwee IL and Nakada T (2009) Inhibition of aquaporin 4 by antiepileptic drugs. *Bioorg Med Chem* **17**(1):418-424.
- Huber VJ, Tsujita M, Yamazaki M, Sakimura K and Nakada T (2007) Identification of arylsulfonamides as Aquaporin 4 inhibitors. *Bioorg Med Chem Lett* **17**(5):1270-1273.
- Johansson PA, Dziegielewska KM, Ek CJ, Habgood MD, Mollgard K, Potter A, Schuliga M and Saunders NR (2005) Aquaporin-1 in the choroid plexuses of developing mammalian brain. *Cell Tissue Res* **322**(3):353-364.
- Kongkeaw C, Dilokthornsakul P, Thanarangsarit P, Limpeanchob N and Norman Scholfield C (2014) Meta-analysis of randomized controlled trials on cognitive effects of Bacopa monnieri extract. *J Ethnopharmacol* **151**(1):528-535.
- Kourghi M, Pei JV, De Ieso ML, Flynn G and Yool AJ (2016) Bumetanide Derivatives AqB007 and AqB011 Selectively Block the Aquaporin-1 Ion Channel Conductance and Slow Cancer Cell Migration. *Mol Pharmacol* **89**(1):133-140.
- Liu X, Yue R, Zhang J, Shan L, Wang R and Zhang W (2013) Neuroprotective effects of bacopaside I in ischemic brain injury. *Restorative neurology and neuroscience* **31**(2):109-123.
- Martins AP, Ciancetta A, de Almeida A, Marrone A, Re N, Soveral G and Casini A (2013) Aquaporin inhibition by gold(III) compounds: new insights. *ChemMedChem* **8**(7):1086-1092.

- McCoy E and Sontheimer H (2007) Expression and function of water channels (aquaporins) in migrating malignant astrocytes. *Glia* **55**(10):1034-1043.
- Migliati E, Meurice N, DuBois P, Fang JS, Somasekharan S, Beckett E, Flynn G and Yool AJ (2009) Inhibition of aquaporin-1 and aquaporin-4 water permeability by a derivative of the loop diuretic bumetanide acting at an internal pore-occluding binding site. *Mol Pharmacol* **76**(1):105-112.
- Moon C, Soria JC, Jang SJ, Lee J, Obaidul Hoque M, Sibony M, Trink B, Chang YS, Sidransky D and Mao L (2003) Involvement of aquaporins in colorectal carcinogenesis. *Oncogene* **22**(43):6699-6703.
- Nielsen S and Agre P (1995) The aquaporin family of water channels in kidney. *Kidney Int* **48**(4):1057-1068.
- Nielsen S, Smith BL, Christensen EI and Agre P (1993) Distribution of the aquaporin CHIP in secretory and resorptive epithelia and capillary endothelia. *Proc Natl Acad Sci U S A* **90**(15):7275-7279.
- Niemietz CM and Tyerman SD (2002) New potent inhibitors of aquaporins: silver and gold compounds inhibit aquaporins of plant and human origin. *FEBS letters* **531**(3):443-447.
- Papadopoulos MC and Verkman AS (2008) Potential utility of aquaporin modulators for therapy of brain disorders. *Prog Brain Res* **170**:589-601.
- Parsels LA, Parsels JD, Tai DC, Coughlin DJ and Maybaum J (2004) 5-fluoro-2'-deoxyuridine-induced cdc25A accumulation correlates with premature mitotic entry and clonogenic death in human colon cancer cells. *Cancer Res* **64**(18):6588-6594.
- Pei JV, Burton JL, Kourghi M, De Ieso ML and Yool AJ (2016) Drug discovery and therapeutic targets for pharmacological modulators of aquaporin channels., in

Aquaporins in Health and Disease: New Molecular Targets For Drug Discovery (Soveral G, Casinin A and Nielsen S eds) pp 275-297., CRC Press, Oxfordshire, UK.

- Preston GM, Jung JS, Guggino WB and Agre P (1993) The mercury-sensitive residue at cysteine 189 in the CHIP28 water channel. *The Journal of biological chemistry* **268**(1):17-20.
- Rabolli V, Wallemme L, Lo Re S, Uwambayinema F, Palmari-Pallag M, Thomassen L, Tyteca D, Octave JN, Marbaix E, Lison D, Devuyst O and Huaux F (2014) Critical role of aquaporins in interleukin 1beta (IL-1beta)-induced inflammation. *J Biol Chem* **289**(20):13937-13947.
- Rehni AK, Pantlya HS, Shri R and Singh M (2007) Effect of chlorophyll and aqueous extracts of *Bacopa monniera* and *Valeriana wallichii* on ischaemia and reperfusion-induced cerebral injury in mice. *Indian journal of experimental biology* **45**(9):764-769.
- Reizer J, Reizer A and Saier MH, Jr. (1993) The MIP family of integral membrane channel proteins: sequence comparisons, evolutionary relationships, reconstructed pathway of evolution, and proposed functional differentiation of the two repeated halves of the proteins. *Critical reviews in biochemistry and molecular biology* **28**(3):235-257.
- Russo A and Borrelli F (2005) *Bacopa monniera*, a reputed nootropic plant: an overview. *Phytomedicine : international journal of phytotherapy and phytopharmacology* **12**(4):305-317.
- Saadoun S, Papadopoulos MC, Davies DC, Bell BA and Krishna S (2002) Increased aquaporin 1 water channel expression in human brain tumours. *British journal of cancer* **87**(6):621-623.

- Sairam K, Dorababu M, Goel RK and Bhattacharya SK (2002) Antidepressant activity of standardized extract of *Bacopa monniera* in experimental models of depression in rats. *Phytomedicine : international journal of phytotherapy and phytopharmacology* **9**(3):207-211.
- Saparov SM, Kozono D, Rothe U, Agre P and Pohl P (2001) Water and ion permeation of aquaporin-1 in planar lipid bilayers. Major differences in structural determinants and stoichiometry. *J Biol Chem* **276**(34):31515-31520.
- Saraf MK, Prabhakar S and Anand A (2010) Neuroprotective effect of *Bacopa monniera* on ischemia induced brain injury. *Pharmacology, biochemistry, and behavior* **97**(2):192-197.
- Schindelin J, Arganda-Carreras I, Frise E, Kaynig V, Longair M, Pietzsch T, Preibisch S, Rueden C, Saalfeld S, Schmid B, Tinevez JY, White DJ, Hartenstein V, Eliceiri K, Tomancak P and Cardona A (2012) Fiji: an open-source platform for biological-image analysis. *Nat Methods* **9**(7):676-682.
- Seeliger D, Zapater C, Krenc D, Haddoub R, Flitsch S, Beitz E, Cerda J and de Groot BL (2013) Discovery of novel human aquaporin-1 blockers. *ACS Chem Biol* **8**(1):249-256.
- Singh HK and Dhawan BN (1982) Effect of *Bacopa monniera* Linn. (brahmi) extract on avoidance responses in rat. *Journal of ethnopharmacology* **5**(2):205-214.
- Tajkhorshid E, Nollert P, Jensen MO, Miercke LJ, O'Connell J, Stroud RM and Schulten K (2002) Control of the selectivity of the aquaporin water channel family by global orientational tuning. *Science* **296**(5567):525-530.
- Trott O and Olson AJ (2010) AutoDock Vina: improving the speed and accuracy of docking with a new scoring function, efficient optimization, and multithreading. *Journal of computational chemistry* **31**(2):455-461.

- Williams R, Munch G, Gyengesi E and Bennett L (2014) *Bacopa monnieri* (L.) exerts anti-inflammatory effects on cells of the innate immune system in vitro. *Food Funct* **5**(3):517-520.
- Yang B, Kim JK and Verkman AS (2006) Comparative efficacy of HgCl₂ with candidate aquaporin-1 inhibitors DMSO, gold, TEA⁺ and acetazolamide. *FEBS Lett* **580**(28-29):6679-6684.
- Yool AJ (2007) Functional domains of aquaporin-1: keys to physiology, and targets for drug discovery. *Curr Pharm Des* **13**(31):3212-3221.
- Yool AJ, Brokl OH, Pannabecker TL, Dantzler WH and Stamer WD (2002) Tetraethylammonium block of water flux in Aquaporin-1 channels expressed in kidney thin limbs of Henle's loop and a kidney-derived cell line. *BMC physiology* **2**:4.
- Yool AJ, Brown EA and Flynn GA (2009) Roles for novel pharmacological blockers of aquaporins in the treatment of brain oedema and cancer. *Clin Exp Pharmacol Physiol* **37**(4):403-409.
- Yool AJ and Campbell EM (2012) Structure, function and translational relevance of aquaporin dual water and ion channels. *Mol Aspects Med* **33**(5):443-561.
- Yool AJ, Morelle J, Cnops Y, Verbavatz JM, Campbell EM, Beckett EA, Booker GW, Flynn G and Devuyst O (2013) AqF026 is a pharmacologic agonist of the water channel aquaporin-1. *Journal of the American Society of Nephrology : JASN* **24**(7):1045-1052.
- Yool AJ and Weinstein AM (2002) New roles for old holes: Ion channel function in aquaporin-1. *News Physiological Sciences* **17**:68-72.

- Yu J, Yool AJ, Schulten K and Tajkhorshid E (2006) Mechanism of gating and ion conductivity of a possible tetrameric pore in aquaporin-1. *Structure* **14**(9):1411-1423.
- Zhang W, Zitron E, Homme M, Kihm L, Morath C, Scherer D, Hegge S, Thomas D, Schmitt CP, Zeier M, Katus H, Karle C and Schwenger V (2007) Aquaporin-1 channel function is positively regulated by protein kinase C. *J Biol Chem* **282**(29):20933-20940.
- Zhou Y, Shen YH, Zhang C, Su J, Liu RH and Zhang WD (2007) Triterpene saponins from *Bacopa monnieri* and their antidepressant effects in two mice models. *Journal of natural products* **70**(4):652-655.

Table 1. Analysis of cytotoxicity in HT29 colon cancer cells at 24 h treatment, using an AlumarBlue fluorescence assay.

Concentration (μM)	Mean normalized cell viability (%), mean \pm SEM [§]	n value	signif
bacopaside I			
0	108 \pm 4.8	17	NS
0 (vehicle)	100 \pm 3.1	17	---
50	97 \pm 2.1	8	NS
75	79 \pm 4.2	8	NS
100	59 \pm 3.2	8	*
bacopaside II			
0	113 \pm 6.2	16	NS
0 (vehicle)	100 \pm 5.7	16	---
15	104 \pm 18	8	NS
20	123 \pm 17	8	NS
30	47 \pm 5.7	8	*
HgCl₂			
100	16.1 \pm 4.6	6	*

[§] Percent viability was standardized as a percentage of the vehicle-treated mean value, measured as changes in AlumarBlue fluorescence signal intensity. See Methods for details.

* Statistically significant differences ($p < 0.05$), compared with vehicle-treated, were analyzed by ANOVA with post-hoc Dunnett's multiple comparison test (GraphPad Prism). NS is not significant.

Figure Legends

Figure 1. Block of osmotic water permeability in AQP1-expressing oocytes by water hyssop (*Bacopa monnieri*) extract, and constituent compounds bacopaside I and bacopaside II. **A.** Mean swelling responses of AQP1-expressing oocytes in 50% hypotonic saline, standardized to the initial volume V_0 , were blocked by 2 h preincubation in reconstituted extract of water hyssop (at 1 mg/ml). Control non-AQP1 oocytes showed little change in volume. Data are mean values for all oocytes assessed from a single batch of oocytes; error bars are SEM; n values are 6 per treatment group. **B.** Column elution of methanol-extracted *Bacopa* identified two active fractions which caused block of AQP1 osmotic water permeability at 0.1 mg/ml each (which were further analyzed by mass spectroscopy to identify candidate compounds). Data are mean \pm SEM, n values in italics are above the x-axis. **C.** Candidate compounds bacopaside I and bacopaside II at 50 μ M differentially blocked osmotic water permeability in AQP1-expressing oocytes, causing a decrease in the rate of swelling as compared with untreated AQP1-expressing oocytes. Data are mean \pm SEM; n values are 8 (AQP1 untreated), 5 (bacopaside I), 7 (bacopaside II), and 8 (non-AQP1 control). **D.** Dose-dependent block of AQP1-mediated osmotic swelling by bacopasides I and II, with estimated IC_{50} values of 117 μ M and 18 μ M, respectively. No sensitivity to bacopaside I was seen for the AQP1 R159,160A double mutant at doses up to 100 μ M. **E.** Chemical structures of bacopasides I and II.

Figure 2. Subtype selectivity and temporal properties of block onset and recovery with bacopaside I in AQP1-but not AQP4-expressing oocytes. **A.** Mean swelling responses of AQP4-expressing oocytes in 50% hypotonic saline were not affected

after 2 h preincubation in 178 μM bacopaside I. Data are mean \pm SEM; n values are 8 (AQP4 alone), 8 (AQP4 with bacopaside I), and 6 (non-AQP4 control). **B.** Time-dependent establishment of block of AQP1-mediated osmotic water permeability required preincubation of oocytes in 178 μM bacopaside I or 35 μM bacopaside II, with approximately 2 h needed to achieve maximal inhibition. n values are 12 to 14 oocytes per time point; each oocyte was used for a single measurement. **C.** Time-dependent recovery from block in AQP1-expressing oocytes preincubated 2 h in 178 μM bacopaside I or 35 μM bacopaside II, and assessed at different intervals after transfer back into standard isotonic saline at time 0 ('washout'). n values are 10 to 13 oocytes per time point; each oocyte was used for a single measurement.

Figure 3. Block of the cGMP-dependent ionic conductance of AQP1-expressing oocytes by bacopaside I, but not bacopaside II. **A.** Representative sets of traces recorded by two-electrode voltage clamp of AQP1-expressing oocytes showing the initial conductance; the response induced by the first application of membrane-permeable cGMP; the recovery of the response to near initial levels after 2 h incubation in isotonic saline containing bacopaside I (50 or 100 μM) or bacopaside II (10 or 20 μM); and the final response to a second application of cGMP. **B.** Trend plots showing the amplitude of the ionic currents, before and after the first activation by GMP, the recovery after incubation, and the response reactivated by a second cGMP application. Consistent recovery was seen after 10 or 20 μM bacopaside II, but not after incubation with 50 or 100 μM bacopaside I indicating establishment of ion channel block. n values are between 3 to 6 for each treatment.

Figure 4. In silico docking models illustrating predictions for the most favorable sites of interaction of bacopaside I and bacopaside II on AQP1 and AQP4 subunit proteins. AQP subunit models were assembled from crystal structural data for human AQP1 (PDB ID. 1FQY) and human AQP4 (PDB ID. 3GDB); see Methods for details. Subunit views are from the cytoplasmic side with the water pore in the center. The intracellular domain for Loop D, adjacent to the channel tetrameric axis of symmetry, is highlighted in dark gold. **A.** Bacopaside I is predicted by in silico docking to occlude the cytoplasmic side of the intrasubunit water pore in AQP1. **B.** Favorable interactions at the AQP4 water pore are not evident for bacopaside I; this ligand appears to interact poorly with AQP4, and the best fit is seen near membrane-spanning domains distant from the pore (inset). **C.** Bacopaside II is predicted to have the most favorable energy of interaction at a position occluding the cytoplasmic side of the AQP1 water pore. **D.** Predicted binding of bacopaside II with AQP4 is distant from the water pore (inset), in a position similar to that seen for bacopaside I. **E.** Enlarged view of the predicted interaction of the sugar-linked sulfur group of bacopaside I with the conserved Loop D arginine residues in AQP1. **F.** Enlarged view of the predicted binding of the trisaccharide moiety of bacopaside II deep into the cytoplasmic vestibule of the AQP1 water pore.

Figure 5. HT29 cells have higher level of AQP1 expression than SW480 cells. **A.** The AQP1 RNA level was higher in HT29 cell line as compared to SW480 cells demonstrated using quantitative RT-PCR. **B.** The AQP1 protein level was higher in HT29 than SW480 cells as demonstrated by western blot. **C.** The AQP1 positive signal (green) was stronger in HT29 than in SW480 cells. Cell nuclei were counterstained (blue). See Methods for details.

Figure 6. Dose-dependent inhibition of migration by bacopasides I and II in AQP1-expressing HT29 cells, but not in SW480 cells with low AQP1 expression. Cell migration was assessed in the presence of a mitotic inhibitor by rates of closure of circular wounds created by aspiration with a pipette tip in confluent cultures (see Methods for details). **A, B.** Cell migration was assessed in vehicle (A) or with 15 μ M bacopaside II (B), added immediately after wounding. Images are shown for confluent HT29 cultures after initial wounding at time 0 (upper panels) and at 24 h (lower panels). **C.** Dose-dependent block of HT29 cell migration was seen with bacopasides I and II, with IC_{50} values estimated at 48 and 14 μ M respectively. Partial block of SW480 migration at the highest doses tested did not exceed 20%. Doses beyond the ranges shown were not considered valid due to the onset of concomitant cytotoxicity.

Figure 7. Live-cell imaging of the inhibitory effect of bacopaside I and II on migration of HT29 cells. Single cells at the boundaries of circular wounds were tracked with time-lapse images taken at 25 minute intervals for 10 hours at 37°C. **A, B, C.** Panels of six images each from time-lapse series for clarity shown at 50 minute intervals. (A) HT29 cells with vehicle treatment (upper set); **(B)** HT29 cells treated with 50 mM bacopaside I; and **(C)** HT29 cells treated with 15 mM bacopaside II. **D.** Trajectory plots of 10 individual cells per treatment group, monitored by cell nucleus position as a function of time. Data were converted to absolute values and referenced to the starting position at time 0. Plots illustrate the cumulative total movement of 10 single cells over a duration of 600 min, with vehicle, bacopaside I

or with bacopaside II. **E.** Frequency histograms of the distances moved by individual cells per 50-minute interval over 600 min of imaging, sampled for 10 cells per treatment group. Histograms were fit with Gaussian distribution functions (R^2 values >0.94); best-fit values for the mean distances moved per cell per 50 min interval were 10.1 ± 0.5 for untreated, 4.7 ± 0.2 for bacopaside I treated and 7.8 ± 0.2 for bacopaside II treated (mean \pm SEM). **F.** Summary histogram showing the total distance travelled by single cells in 600 min, showing significant inhibition of cell motility by both bacopaside I and II compared to vehicle treated cells (ANOVA test; $p < 0.05$). Data are mean \pm SEM; n values are 10 cells per treatment group. Distances shown are in pixels; the conversion is 7.45 pixels per 1mm.

Figure 1

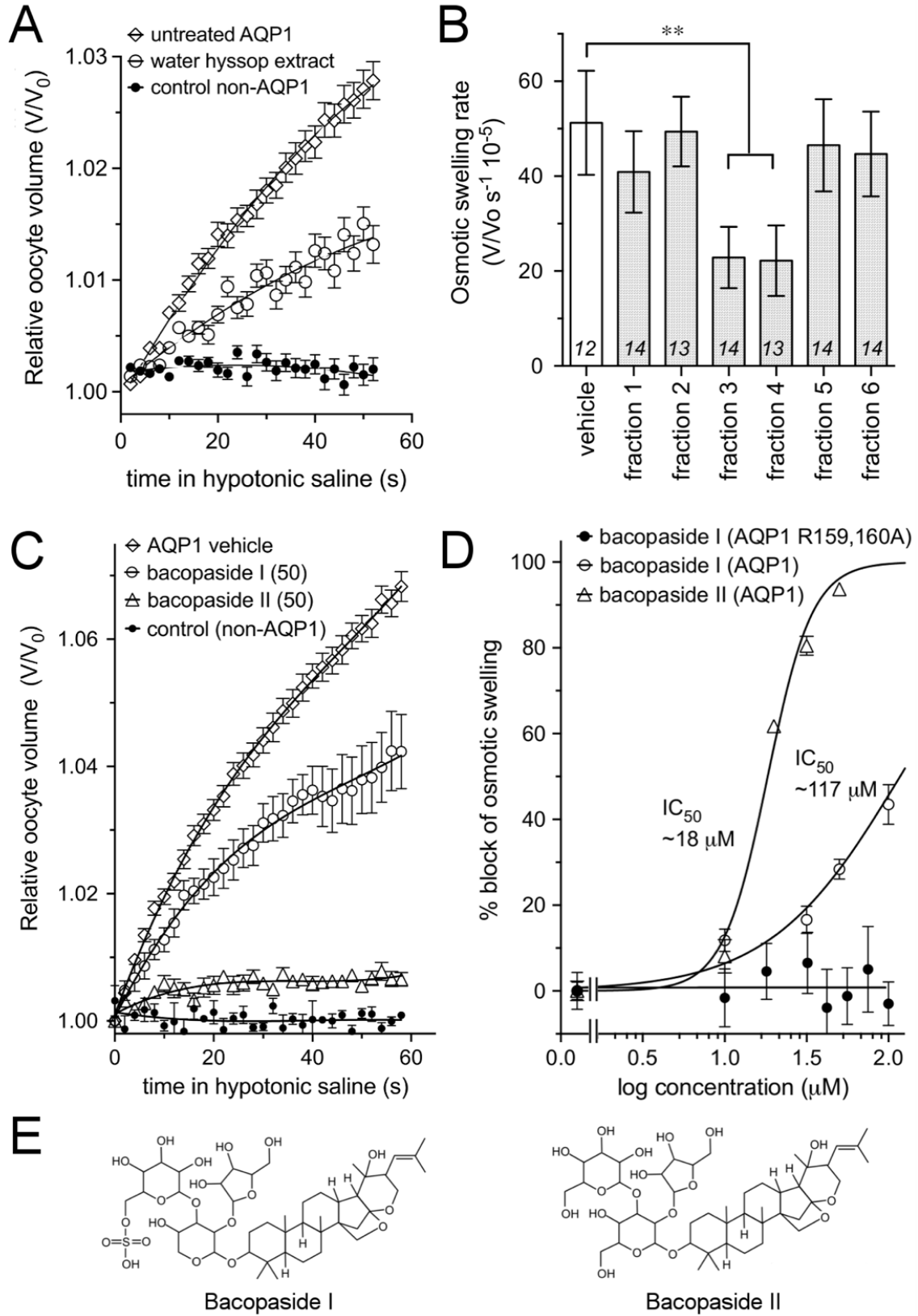


Figure 2

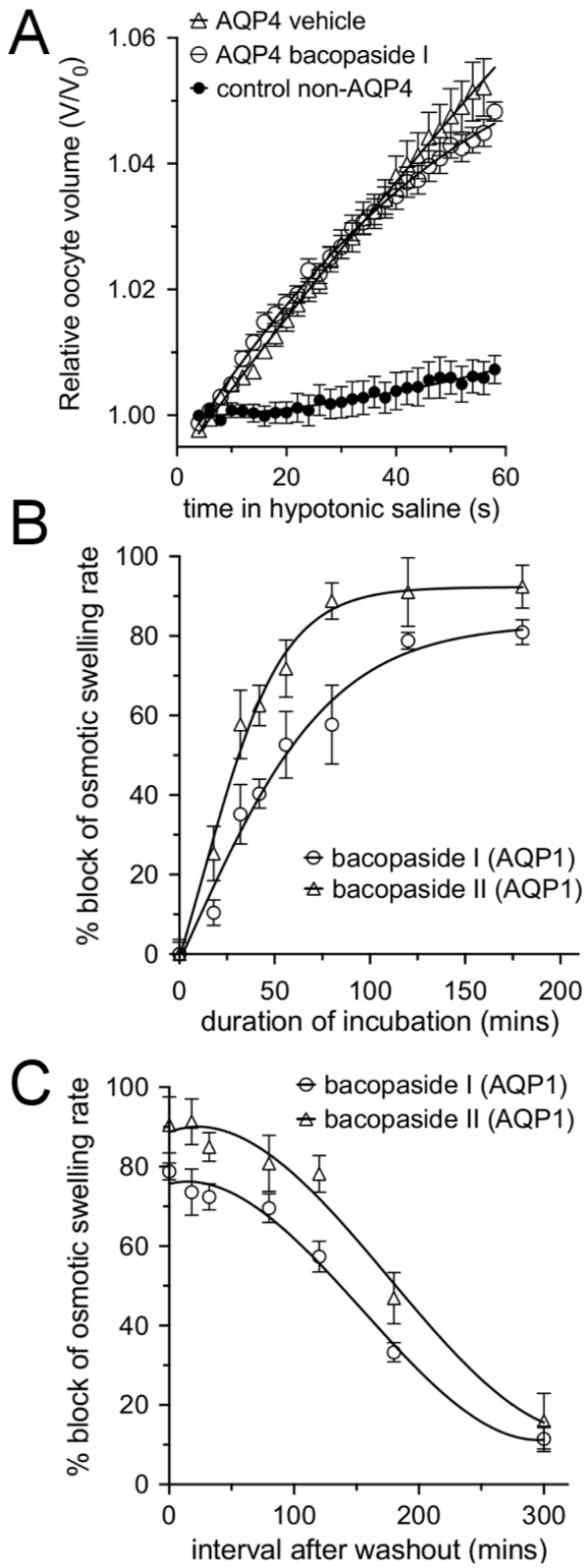


Figure 3

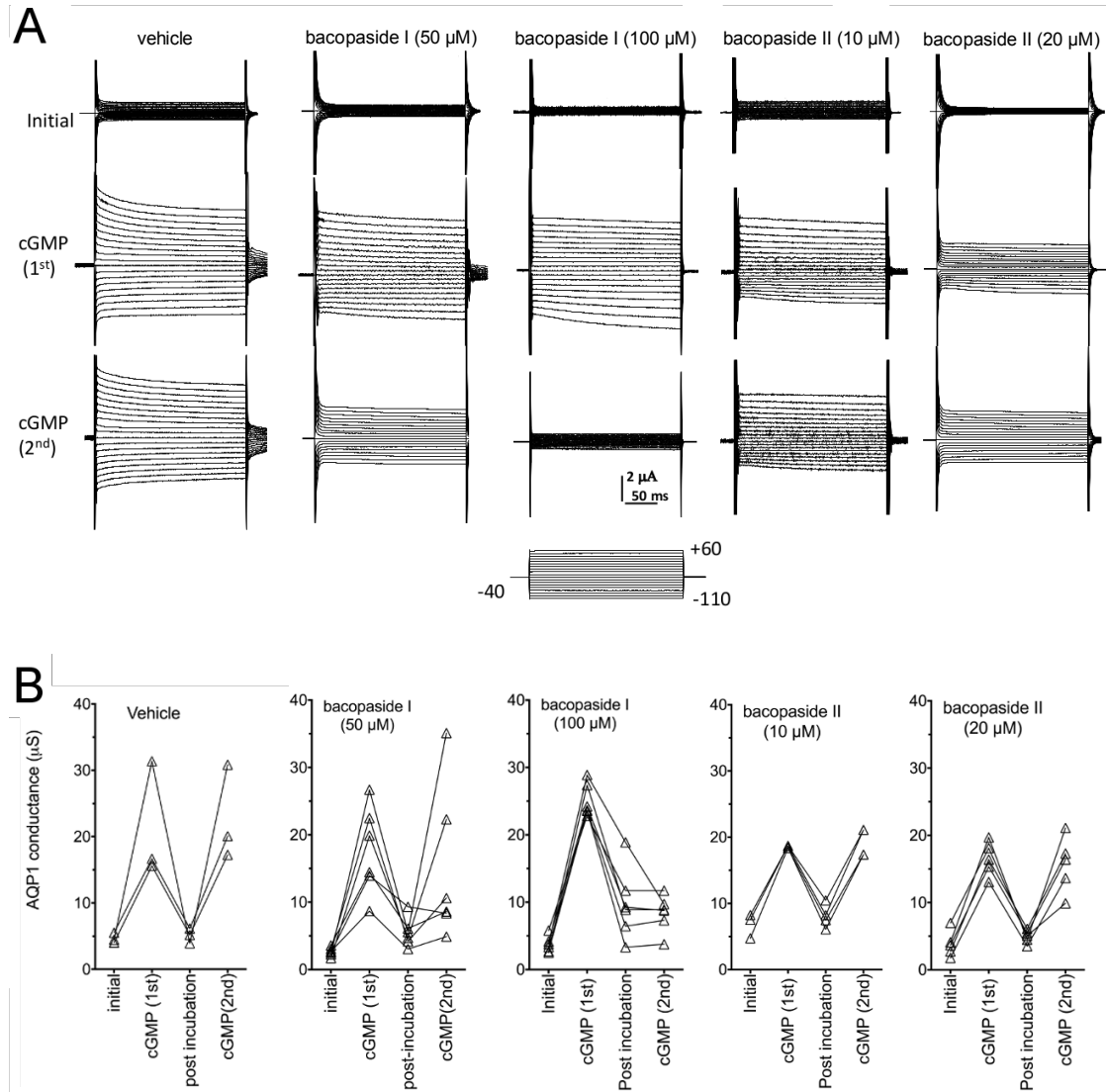


Figure 5

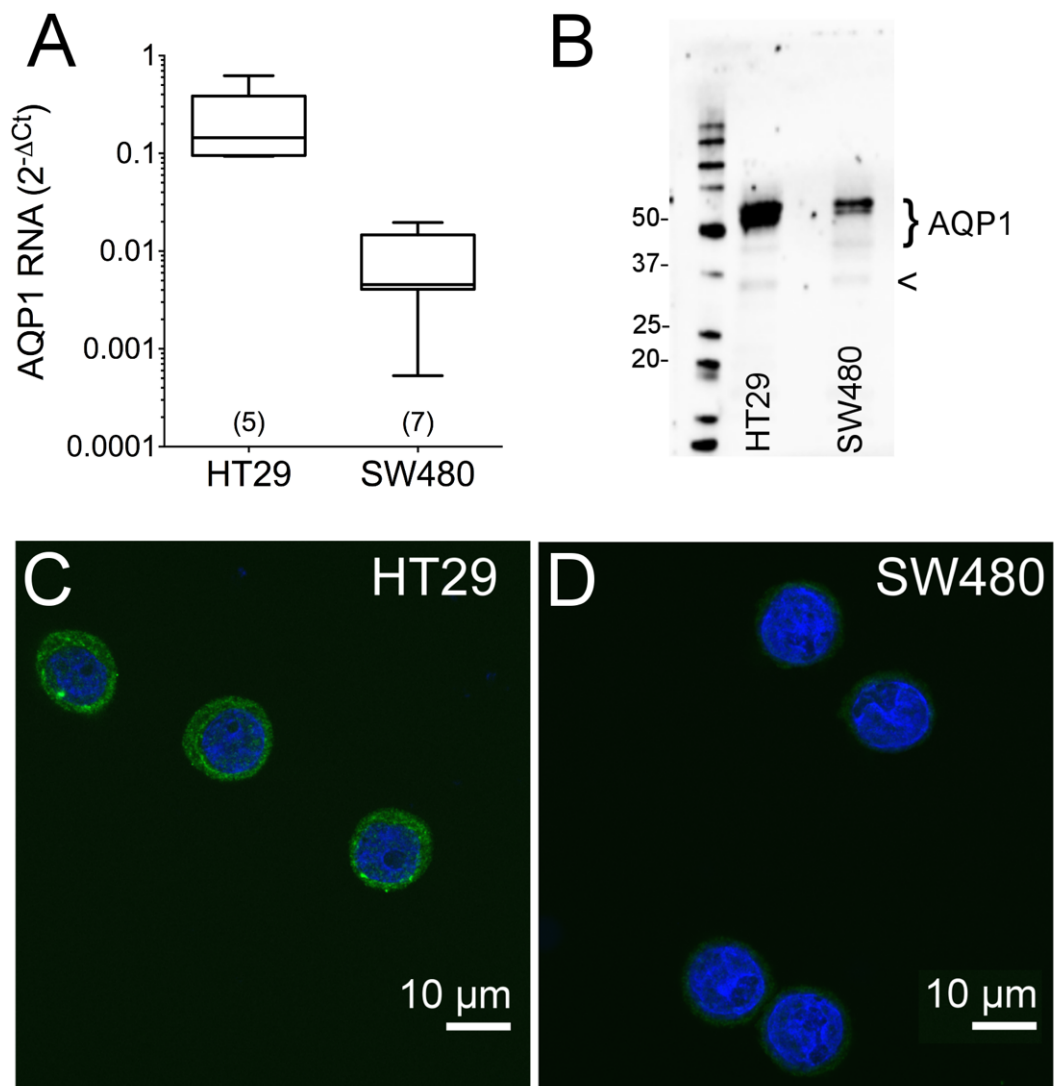
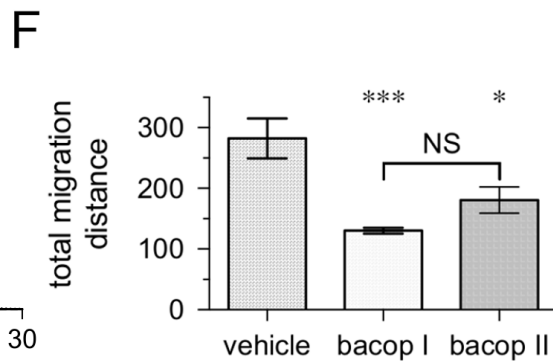
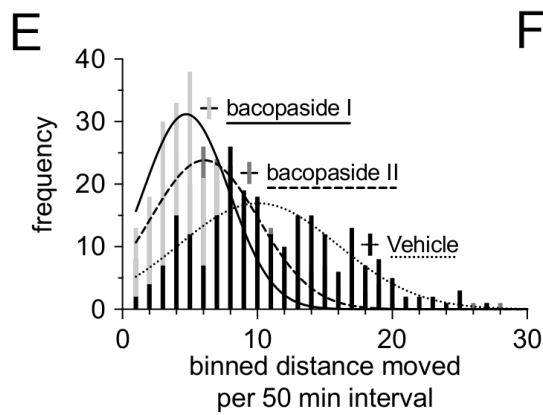
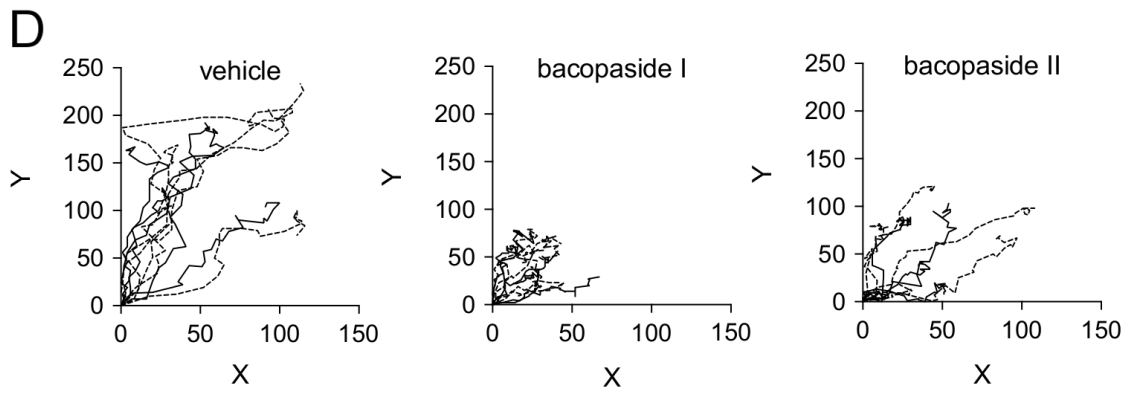
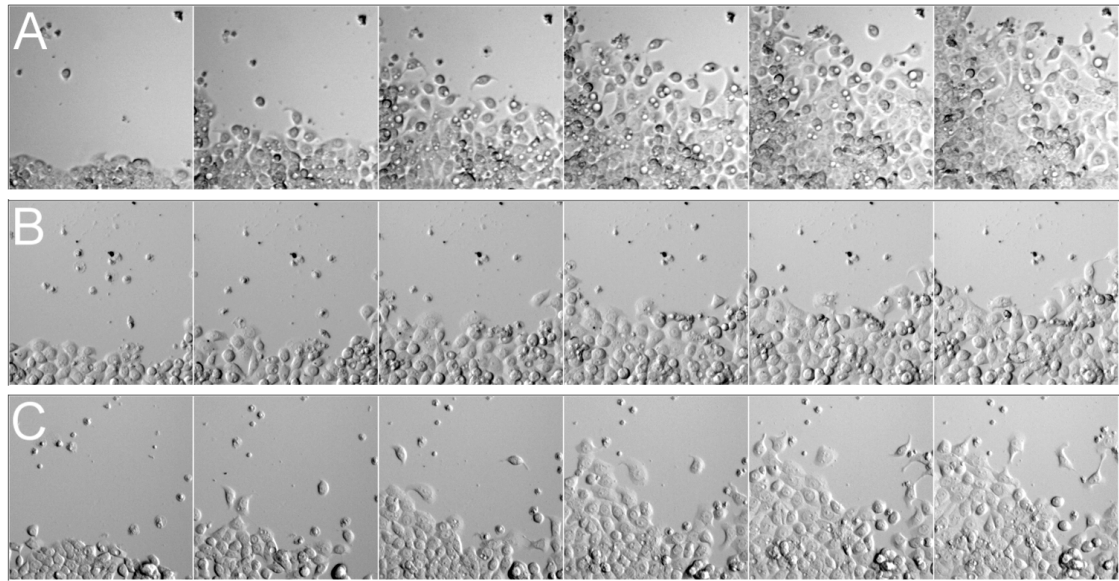


Figure 6



CHAPTER 4: DISCOVERY OF A NOVEL LITHIUM SENSOR FOR THE REAL-TIME ANALYSIS OF ION CONDUCTANCE IN AQP1

CONTEXTUAL STATEMENT

Lithium 'Hot-spots':

Real-time Analysis of Ion Conductance in Aquaporin-1

AIM: To synthesize a novel photo-switchable Li^+ ion sensor and to visualize the real-time ion conductance mediated by (Aquaporin-1) AQP1 channels in living cells.

HYPOTHESIS: A novel photo-switchable lithium probe (designated "SHL") can be used to demonstrate the sites of transmembrane cation influx across plasma membrane that are colocalized with AQP1 channels.

CONCLUSIONS:

1. A novel synthetic cation sensor designated as SHL is highly specific for Li^+ in the monovalent cation family. SHL contains a photochromic spiropyran that can be reversibly switched between a non-fluorescent isomer (SP) and a charge-delocalized fluorescent merocyanine isomer (MC) when interacting with an appropriate metal ion such as Li^+ .
2. SHL yielded a sensitive Li^+ -dependent signal that could be photoswitched repeatedly in living cells, in accord with characterized chemical properties of the probe.
3. In AQP1- expressing colon cancer HT29 cells, punctate Li^+ hot spots were observed submembrane domains. Application of the AQP1 ion channel blocker AqB011 or the replacement of extracellular Li^+ with an equivalent concentration

of tetraethylammomium ion (TEA^+) abolished the SHL hot spot signals, demonstrating the responses were due to Li^+ entry across the membrane, and relied on functional AQP1 ion channels.

4. Li^+ hot spots were observed at the leading edges of migrating HT29 cells but were not observed in colonn cancer SW620 cells lacking comparable AQP1 expression.
5. Hot spots of monovalent cation entry are colocalized with AQP1 channels in migrating HT29 cells.

COMMENTARY:

The novel synthesis, characterization and biological application of a photo-switchable sensor that detects Li^+ ions is reported in this chapter. Results show this sensor will be a valuable tool for monitoring cation fluxes across cell membranes. The ionic conductance of AQP (reviewed in Chapter 1), and its physiological relevance (for example in cancer migration as shown in Chapters 2 and 3), has been difficult to evaluate in full in the past because of the lack of pharmacological agents (Jeyaseelan et al., 2006; Verkman et al., 2008), prior to the discovery of the AQP1 ion channel blocker AqB011 (Kourghi et al, 2016). In this chapter, we demonstrate for the first time the imaging of real-time ion fluxes associated with AQP1, providing another compelling line of evidence that AQP1 functions as an ion channel.

Statement of Authorship

Title of Paper	Lithium 'Sparks', real-time Analysis of Ion Conductance in Aquaporin
Publication Status	<input type="checkbox"/> Published <input type="checkbox"/> Accepted for Publication <input type="checkbox"/> Submitted for Publication <input checked="" type="checkbox"/> Unpublished and Unsubmitted work written in manuscript style
Publication Details	Pei JV, Heng S, De Ieso ML, Sylvia G, Kourghi M, Nourmohammadi S, Abell AD, and Yool AJ (2017) Lithium 'Sparks', real-time analysis of ion conductance in Aquaporin.

Principal Author

Name of Principal Author (Candidate)	Jinxin Pei
Contribution to the Paper	Initiated and performed experiments, analysis on all samples, interpreted data, wrote the manuscript.
Overall percentage (%)	70%
Certification:	This paper reports on original research I conducted during the period of my Higher Degree by Research candidature and is not subject to any obligations or contractual agreements with a third party that would constrain its inclusion in this thesis. I am the primary author of this paper.
Signature	Date 28/5/17

Co-Author Contributions

By signing the Statement of Authorship, each author certifies that:

- i. the candidate's stated contribution to the publication is accurate (as detailed above);
- ii. permission is granted for the candidate to include the publication in the thesis; and
- iii. the sum of all co-author contributions is equal to 100% less the candidate's stated contribution.

Name of Co-Author	Sabrina Heng
Contribution to the Paper	Invented the tool, initiated and performed experiment and wrote the manuscript.
Signature	Date 23/06/17

Name of Co-Author	Michael L. De Ieso
Contribution to the Paper	Performed experiment and wrote the manuscript.
Signature	Date 23/5/17

Name of Co-Author	Georgina Sylvia		
Contribution to the Paper	Invented the tool.		
Signature		Date	23/06/2017

Name of Co-Author	Mohamed Kourghi		
Contribution to the Paper	Performed experiment and wrote the manuscript.		
Signature		Date	23/05/2017

Name of Co-Author	Saeed Nourmohammadi		
Contribution to the Paper	Performed experiment.		
Signature		Date	27-June-17

Name of Co-Author	Andrew D. Abell		
Contribution to the Paper	Initiated the project and edited the manuscript.		
Signature		Date	26/6/2017

Name of Co-Author	Andrea J. Yool		
Contribution to the Paper	Initiated the project and edited the manuscript.		
Signature		Date	23 May 2017

Manuscript

Lithium 'Hot-spots':

Real-time Analysis of Ion Conductance in Aquaporin-1

Jinxin V Pei¹, Sabrina Heng², Michael De Ieso¹, Georgina Sylvia², Mohamad Kourghi¹, Saeed Nourmohammadi¹, Andrew D Abell², and Andrea J Yool¹

¹ Adelaide Medical School, Institute for Photonics and Advanced Sensing (IPAS), The University of Adelaide, Adelaide, SA 5005, Australia.

² ARC Centre of Excellence for Nanoscale BioPhotonics (CNBP), IPAS, School of Physical Sciences, Department of Chemistry, The University of Adelaide, Adelaide, SA 5005, Australia.

Abstract

Aquaporin 1 channels are located at the leading edges of certain classes of aggressive cancer cells, where they are necessary to enable fast migration. AQP1 has pores for water present in each of the four channel subunits, thought to enable local volume changes needed for process extension. An additional contribution of the AQP1 monovalent cation conductance (via the central pore of the tetrameric channel) in cancer cell migration has been suggested previously from selective pharmacological inhibition, but not demonstrated directly. Work here is the first to use a newly designed Li^+ -selective photoswitchable probe named 'SHL' in living colon cancer cells to monitor AQP1 ion channel activity in real time by the appearance of lithium hot spots, detected by confocal microscopy. The Li^+ hot spots are clustered in the lamellipodial leading edges of AQP1-expressing HT29 colon cancer cells, and are blocked by the AQP1-ion channel antagonist AqB011. Lithium hot spots are not evident in a poorly-migrating colon cancer cell line SW620 that lacks comparable membrane expression of AQP1. The Li^+ probe loaded in living cells shows the expected chemical signature properties of ionic selectivity, and the capacity to be reset for fluorescence signaling by illumination at bandwidths that induce photoswitching. The correlation between the subcellular distribution and the visualized ion channel activity of AQP1 channels in cancer cells supports the proposed role of the AQP1 ion channel in cell migration. The AQP1 ion channel is a novel candidate for therapeutic interventions that could be used to manage metastasis in aggressive AQP1-dependent cancers.

INTRODUCTION

Aquaporins enable the flux of water and small solutes across membranes¹. In addition to regulating fluid balance, they provide a key role in cell migration and hence the development and maintenance of multicellular organisms.^{2,3} They are central to critical processes of repair, regeneration, immune protection and cancer metastasis.⁴⁻⁶ Thirteen classes of human AQP subtypes are known, with aquaporin-1 (AQP1) playing a pivotal role in enhancing mobility in some of the most motile cells such as T-cells, fibroblasts, cancer and amoebae.⁷ While the exact mechanism for this has yet to be determined, we do know that elevated expression of AQP1 is apparent at the leading edges of lamellipodia in certain classes of migrating cells. Genetic knockdown of AQP1 expression has been shown to impair cell migration significantly^{8,9} whereas reintroduction of AQP1 restored motility. With substitution of aquaporin-4 (AQP4), also a strong water channel, cell motility remained impaired. A major difference between the channel classes is that AQP1 but not AQP4 also functions as an ion channel that can be gated by cGMP¹⁰⁻¹². Thus, while the mechanism of AQP1 action on cell migration remains unknown, it seems likely to involve ion fluxes. Unravelling the unique properties of AQP1, and defining the role of AQP1 ion channel function in rapid cell motility would advance our knowledge of how aquaporin channels enable enhanced cell motility seen in cancer, stem cells and regenerating tissues, and uncover the basic mechanisms governing cell migration that might be targeted for intervention, for example in cancer metastasis.

Here we confirm the role of AQP1 as a nonselective monovalent cation channel, demonstrate AQP1-mediated ion influx using real-time imaging, and show the punctate signals are clustered in the lamellipodia of migrating cancer cells. This was

accomplished using a reversible lithium sensor (SHL) in combination with an ion channel blocker (AqB011), to modulate the AQP1-mediated Li^+ entry in the cells. SHL was specifically developed to be selective for a low abundance monovalent ions such as Li^+ over Na^+ or K^+ . Results here show that ion binding to the sensor intracellularly is dependent on exogenous Li^+ transport into the cell. Selective blocking of AQP1 with AqB011 shows that Li^+ transport is occurring through AQP1. These results provide the first evidence of 'hot-spots' that correlate with ion movement through AQP1 channels, as confirmed by properties of pharmacological sensitivity, ion selectivity, and levels of AQP1 expression.

Results and Discussion

Design and characterization of the reversible and selective lithium (Li^+) sensor (SHL).

The sensor described here (see Figure 1A for sensor SHL structure) contains a photochromic spiropyran that can be reversibly switched between a non-fluorescent isomer (SP) and a charge-delocalized fluorescent merocyanine isomer (MC) when interacting with an appropriate metal ion such as Li^+ (see Figure 1A)¹³. The ability to switch between the two states is advantages for visualizing Li^+ transport into the cell as SHL will only have enhanced fluorescence when complexed to Li^+ (e.g. MC- Li^+ complex in Figure 1A), while maintaining low background fluorescence in the absence of the ion (SP isomer in Figure 1A). This is a desirable sensor characteristic for visualizing ion binding with confocal microscopy and would result in better resolution

in terms of signal-to-background as compared with standard fluorescent probes.^{14,15} A more critical sensor characteristic is the selectivity of SHL for Li⁺ over other biologically relevant ions. Spiropyrans can be readily modified to bear cation ion binding domains that will interact with phenolate group in the ring-opened MC isomer (Figure 1A) to achieve ion affinity and selectivity. This was achieved by incorporating a 1-aza-15-crown-5 substituent at C8' and a hydroxyethyl substituent at N1 respectively (labeled in Figure 1A). Finally, we incorporated a NO₂ substituent at C6' of the benzopyran ring as electron-withdrawing groups at that position are known to stabilize the ring-opened MC form thus favoring ion binding. Details on the synthesis of SHL are reported in the Synthesis section of the Supporting Information. Briefly, the Li⁺ sensor was prepared from 1-aza-15-crown-5 and 1-(2-hydroxyethyl)-2,3,3-trimethyl-3*H*-indol-1-ium to give SHL with an overall yield of 40 - 50 % using a modification to existing methodology^{16,17}.

The addition of excess Li⁺ (100 μM) to SHL (50 μM) gave rise to strong fluorescence ($\lambda_{\text{ex}} = 532 \text{ nm}$) at approximately $\lambda_{\text{em}} = 635 \text{ nm}$ as shown in Figure 1B (insert), which is consistent with the formation of the MC(SHL)-Li⁺ complex as expected based on our sensor design. Importantly, the red fluorescence is advantageous as it represents an emission bandwidth that is distinct from the blue nuclear stain (Hoescht 33258) and green cellular auto-fluorescence emissions. Additional spectroscopic properties of SHL such as absorbance, detection limits, photoswitching and quantum yields are detailed in the 'Supporting information' section. More importantly, the selectivity of SHL for Li⁺ against other biologically relevant ions was confirmed through ion binding assay with excess Li⁺ and other biologically relevant metal ions (Na⁺, K⁺, Cs⁺, Mg²⁺, Mn²⁺, Cu²⁺ and Zn²⁺). Results in Figure 1B showed that SHL has highest affinity for Li⁺, and

relatively little response to similar monovalent ions such as Na^+ and K^+ . The red-emitting properties and selectivity of SHL for Li^+ are critical for demonstrating that the emission observed in the cell is not due auto fluorescence or interaction of the sensor with other endogenous ions; the signal is specific to the MC(SHL)- Li^+ complex.

AQP1 ion channel is permeable to Li^+ and can be blocked by AqB011.

AQP1-expressing *Xenopus* oocytes were recorded by two-electrode voltage clamp in isotonic saline with 137 mM Li^+ substituted for Na^+ . Currents (Fig 2A) in isotonic Li^+ saline were measured for AQP1-expressing *Xenopus* oocytes and non-expressing control oocytes before ('initial') and after treatment with a membrane permeable analog of cGMP (CPT-cGMP; See Supporting Information for details), confirming activation of the ionic conductance. Oocytes were then incubated 2 h in 30 μM AqB011 and reactivated by cGMP ("AqB011") in Li^+ saline. Results (Figure 2B) showed that approximately 90% of the cGMP-induced current in AQP1-expressing oocytes was successfully blocked by AqB011; whereas control oocytes (AQP1-) lacked appreciable cGMP-activated current responses.

Real time analysis of the kinetics and magnitude of Li^+ fluxes in live cells.

The relative ability of SHL to chelate and sense Li^+ in live cells was investigated using confocal microscopy. HT29 colon cancer cells were used in this study as they are known to have high AQP1 expression¹⁹, providing a good model for cellular imaging of Li^+ passage through AQP1.

SHL (50 μM in physiological saline) was incubated with the HT29 cells for 2 h prior to imaging to allow the uptake of SHL by the cells. The cells were co-labelled with

Hoescht 33258 as a counterstain for the nuclei. The cells were illuminated with green laser light to activate the MC(SHL)-Li⁺ complex, which resulted intracellularly in a red fluorescence signal characteristic of this chemical interaction (see Figure 3). Subsequent exposure of the cells to visible light for 10 min restored a low level of fluorescence, consistent with the expected photoswitching from the fluorescent MC(SHL)-Li⁺ complex to back to the non-fluorescent SP isomer (see Figure 1A). Fluorescence intensity decreased as a function of time following a single-phase decay when the cells were illuminated with standard white light, with measurements taken every 2 min. Specifically, the normalized intensity decreased from 100 Relative Fluorescence Units (RFU) to 44.51 RFU after 10 min of visible light radiation (labelled OFF2 in Figure 3C). Under these experimental conditions, the half-life was determined to be 4.13 minutes with a τ value estimated at 5.95 minutes. The images of cells after each episode of visible light radiation are illustrated in Figure 3B. The cells were then incubated in the dark for 10 min to allow the formation of the MC isomer, and the binding of Li⁺ to form the MC(SHL)-Li⁺ complex (labelled ON1 in Figure 3A) with the normalized intensity at 84.65 RFU (labelled ON2 in Figure 3A). Repeated cycles of photoswitching performed on same cells gave reproducible changes in fluorescence, demonstrating the ability of SHL to reversibly photoswitch in living cells. This innovation defines a new probe for monitoring changes in intracellular Li⁺ in a biological sample over time, without loss of sensitivity imposed by photobleaching of the sensor. The photoswitching property allows direct comparison of functions over multiple experimental parameters, and provides additional advantages in biological assays where sample availability is often limited.

Importantly, results in Figure 4C show distinct punctate Li⁺ signals in the HT29 cells when imaged in Li⁺ substituted extracellular saline (Figure. 4C-1), which we refer to

as lithium 'hot spots'. The removal of Li^+ from the extracellular saline by equimolar substitution of Na^+ , caused a loss of 'hot spot' events. Similar losses of 'hot spot' events were observed after treatment with 20 μM AqB011 for 2 h, after which only a faint background fluorescence was observed (Figure 4C-2). Further validation that the observed 'hot spots' are a result of Li^+ induced binding was achieved using HT29 cells that were imaged in saline with equimolar tetraethylammonium (TEA) substituted for Na^+ or Li^+ (as detailed in the Supporting Information section), where a similar loss of 'hot spot' activity was observed. The Li^+ -selective fluorescent signal was two-fold greater in normal HT29 cells imaged in Li^+ saline, as compared with HT29 cells in which Li^+ entry was compromised by pharmacological block (AqB011) or removal of Li^+ ion from the saline by equimolar replacement with other cations such as Na^+ or TEA^+ (Figure 4D). Collectively, these results confirm that the bright punctate Li^+ signals are dependent on the presence of extracellular Li^+ and the presence of functional AQP1 ion channels (Figure 4C-3 and -4). These data rule out the possibility that the observed 'hot spots' were generated by non-selective interaction of SHL with other intracellular cations. This finding is significant in that it shows the flux of Li^+ across the membrane is required to activate the intracellular Li^+ signal seen with SHL, and supports the conclusion that intracellular lithium hot spots are caused by Li^+ entry into the cell through AQP1 cation channel.

Li^+ hot spots at the leading edges of migrating HT29 cells were not observed in SW620 cells lacking comparable AQP1 expression.

The role of AQP1 ion channels in mediating the lithium 'hot spot' events was tested by evaluation of another colon cancer cell line (SW620), that is similar to HT29 in having an adherent epithelial phenotype²⁰, but different in that rates of migration are very slow

and levels of AQP1 expression are 2.6-fold lower in SW620 than HT29 cells (Figure 4A). HT29 cells and SW620 cells were pre-incubated in SHL for 2 hours in Li⁺-substituted saline and imaged as described above. Results in Figure 4 show that the lithium 'hot spots' were more abundant and brighter in HT29 cells (Figures 4B 1-3) than in SW620 cells (Figures 4B 4-6). In migrating HT29 cells, lithium 'hot spots' were concentrated in leading edges of the cells (Figures 4B 2 and 3) compared to uniformly distributed in non-migrating cells (Figure 4B 1). This observation is consistent with the known clustering of AQP1 channels in the leading edges of specific classes of cells during migration, where it is proposed to facilitate fluid movement needed for volume change during extension, and to compensate for changes in osmotic pressure associated with actin polymerization and depolymerisation^{8,19}.

AQP1 Expression levels were as determined by immunofluorescent imaging with confocal microscopy (as detailed in the Supporting Information section). AQP1 channels were localized using excitation of the immunolabeled cells with 488 nm laser to cause green fluorescence emission characteristic of AQP1 immunolabeling and visualization with a AlexaFluor 488 tagged secondary antibody. HT29 cells demonstrated significantly higher AQP1 expression compared to SW620 cells (Figure 4A).

Results with SW620 cells demonstrate that the observed lithium 'hot spots' are directly dependent on the presence of AQP1 channels, and cannot readily be attributed to fluxes through other membrane channels and transporters. In combination, results here from pharmacology, ion substitution and comparison of cell lines with different

patterns of AQP1 expression provide evidence that lithium 'hot spots' measured by the novel probe SHL mark the locations of active AQP1 ion channels.

Lithium hot spots are colocalized with AQP1 channels in HT29 cells

The spatial correlation between the locations of the lithium 'hot-spots' and the AQP1 channels was assessed using confocal microscopy. The signal intensities using Z-stacked compiled images were measured as a function of distance across the cell diameter (indicated by straight lines crossing the cell centers; for two cross-sections per cell). Signals were plotted as a function of X-Y distance to quantify the correspondence between the SHL Li⁺ fluorescence intensity (red channel; MC(SHL)-Li⁺ complex) and the AQP1 protein signal intensity (green channel; autofluorescence). Results in Figure 5A show that the two fluorescence signals were strongly co-localized in HT29 cells (with superimposed red and green signals being represented by yellow), yielding relative fluorescence units (RFU) ranging from 50 to 200 which were consistent with data shown in Figure 4A. The spatial profiles of red and green signal distributions as a function of position across the diameters of cell are illustrated by plots of signal intensity (Figure 5C). Li⁺ and AQP1 signals in HT29 cells were found to be strongly correlated with R² values ranging 0.61 to 0.68. In contrast, SW620 cells (Figures 5C 3 and 4), showed poor spatial correlation and low intensities, with most signal values ranging from 0 to 50 RFU. Signal intensity data from SW620 cells showed little correlation with R² values ranging from 0.06 to 0.09. This work opens avenues never before imagined for the real-time visualization of cation channel function and the localization of active channel domains in living cells, with particular insight into the relevance of AQP1 ion channels in dynamic cellular responses.

Conclusion

Our results define a new Li^+ selective sensor, SHL, and demonstrate its translational potential in addressing fundamental signaling mechanisms, here explored by the visual monitoring of cation entry through AQP1 cation channels in cancer cell migration. The SHL photoswitchable sensor, which maintains stable emission after prolonged excitation, offers exciting potential applications for optical studies of dynamic ion fluxes in active moving cells. The novel Li^+ selective fluorophore SHL promises to be a valuable addition to the ion sensor field.

The initial proposal that AQP1 works as a non-selective cation channel in addition to its known role as a water channel¹⁸ generated controversy. Subsequent analyses from different groups confirmed the capacity of AQP1 to function as a dual water and ion channel, showing the ion channel activity is gated directed by intracellular cGMP and indirectly regulated by intracellular signalling cascades including tyrosine phosphorylation^{10,11,12}, but left unclear the physiological relevance of the dual water and ion channel function. Recent work has since demonstrated that the AQP1 ion conductance is essential for rapid cell movement in a subset of cancer cells that show high metastasis or invasiveness and a corresponding upregulation of AQP1 channels in the leading edges^{8,9,19}, demonstrating a functional role for the AQP1 ion channel in cell motility.

Here confocal imaging confirmed cation entry through AQP1 ion channels monitored using a permeable monovalent cation Li^+ that could be monitored visually with the new probe SHL. The two colon cell lines used in this study that have different endogenous levels of AQP1 expression; AQP1 is high in fast moving HT29 cells, and low in the

slowly migrating SW620 cells. Lithium hot spots were abundant in HT29 cells, and rare in SW620 cells. The spatial resolution of AQP1 ion channel sites of activity at the leading edges of HT29 cells was an exciting observation, suggesting future studies might go further in the characterization of the temporal and spatial dynamic properties of the ion fluxes in migrating responding cells

AQP1 channels are not the only pathway for Li^+ transport across cell membranes. For example, Li^+ is permeable through voltage-gated Na^+ channels^{22,23,24} and Na^+ -proton exchanger²¹. Some of the Li signal described here might involve additional channels or transporters. However, the alternative hypothesis that the lithium signal observed in HT29 cancer cells was due entirely to other mechanisms unrelated to AQP1 seems unlikely for several reasons. First, results here showed that pharmacological inhibition with the AQP1 ion channel blocker, AqB011, significantly diminished the Li^+ signal to a level similar to the response observed in cells imaged in saline with TEA⁺ (which does not bind to SHL). Other AQP modulators in the library of bumetanide derivatives that include AqB011 have been shown to be selective for specific AQP classes without off-target effects on other signaling and transport mechanisms^{25,26}. Second, the punctate Li^+ signal pattern was not evident in SW620 cells that have low levels of AQP1 expression but otherwise express various channels and transporters required for basic cellular function and low level motility. Third, the cells used for the studies would not be expected to have appreciable levels of voltage-gated Na channel expression. Lastly, the co-localization of AQP1 expression and Li^+ signals showed a strong correlation, and was consistent with other work indicating that the expression of AQP1 in migrating cells is localized strongly in the leading edges. In sum, evidence presented here supports the proposal that AQP1 is not just a water channel, but also

works as a monovalent cation channel. The AQP1 ion channel is an attractive candidate for the development of therapeutic interventions that could be used to manage metastasis and invasiveness in aggressive AQP1-dependent cancers.

METHODS

Electrophysiology

Two electrode voltage clamp recordings were used to investigate if AQP1 ionic pore is permeable to Lithium ions. Recording were performed at room temperature, in standard isotonic Na⁺ saline and in Li⁺ substituted isotonic saline containing 100 mM NaCl or 100mM LiCl, 2 mM KCl, 4.5 mM MgCl₂, and 5 mM HEPES, pH 7.3. 1 M KCl was used to fill capillary glass electrodes (1–3 MΩ) for recordings. cGMP was applied to the bath saline at a final concentration of 10-20 μM using the membrane-permeable cGMP analog [Rp]-8-[para-chlorophenylthio]-cGMP (Sigma-Aldrich, Castle Hill NSW Australia). Ion conductance was determined by linear fit of the current amplitude as a function of voltage, with a step protocol from +60 to -110 mV and holding potential of -40 mV. Ionic conductance was monitored over 25 minutes after the bath application of cGMP to allow sufficient time to achieve maximal response. Conductance was determined by linear fit of the current amplitude as a function of voltage, with a step protocol from +60 to -110mV and holding potential of -40 mV. Recordings were made with a GeneClamp amplifier and pClamp 9.0 software (Molecular Devices, Sunnyvale CA USA).

Immunohistochemistry

Cells were cultured using 8 well Ibidi μ-Slide (Ibidi, Munich Germany) to achieve 50% confluency prior to experiment. To begin the immunostaining procedure cells were rinsed with PBS and fixed in 4% paraformaldehyde for 20 minutes at room temperature (RT). Then washed 4 times in PBS (5 minute washes at RT) on a rocker. Cells were permeabilised with 0.1% PBS Tween for 5 minutes and washed three times with PBS

at room temperature for 5 minutes, on a rocker. Next cells were blocked with 10% horse serum in PPS (GS/PBS) for 40 minutes at room temperature on a rocker and incubated with the rabbit anti-AQP1 antibody (ab15080, Abcam, Victoria, Australia) in 0.1%GS/PBS for 2 hours at room temperature. The cells were then washed three times in PBS for 7 minutes at room temperature on a rocker and incubate with Alexa488 conjugated sheep anti-rabbit antibody (ab150181, Abcam, Victoria, Australia) diluted in 0.1%GS/PBS for 35 minutes at room temperature in the dark. Next cells were washed three times in PBS for 7 minutes at room temperature, on a rocker and incubated with Hoescht (diluted 1:1000 in PBS) for 5 minutes in the dark. The cells were rinsed with PBS twice and mounted using hydromount mounting media (Sigma-Aldrich, Castle Hill NSW Australia).

Cancer cell culture and Confocal imaging

HT29 and SW620 colorectal cancer cell lines and the MDA-293 breast cancer cell line (American Type Culture Collection ATCC, Manassas, VA USA) were cultured in complete medium composed of Dulbecco's Modified Eagles Medium (DMEM) supplemented with 10% fetal bovine serum (FBS), penicillin and streptomycin (100 U/ml each) and 1 x glutaMAX™ (Life Technologies Mulgrave, VIC, Australia). Cultures were maintained in 5% CO₂ at 37°C. Cells were seeded on an 8-well uncoated Ibidi μ-Slide (Ibidi, Munich Germany) at a density of 1.0×10^5 cells/ml and allowed 24 hours to settle.

All imaging experiment was performed in a darkroom. Prior to imaging, cells were incubated with 50 μM of sensor for 2 hours then washed twice with lukewarm

phosphate buffered saline (PBS). For AqB011 treated group, cells were then incubated with 20 μ M AqB011 for 2 hours. All cells were treated with 0.5 mg/mL of Hoechst 34580 for 20 mins. Either Li⁺ saline (137 mM LiCl, 3.5 mM KCl, 0.68 mM KH₂PO₄, 5 mM HEPES, 10 mM glucose and 4.4 mM MgSO₄) or TEA⁺ saline (137 mM TEACl, 3.5 mM KCl, 0.68 mM KH₂PO₄, 5 mM HEPES, 10 mM glucose and 4.4 mM MgSO₄) was used for the imaging. The μ -Slide was mounted on a Leica TCS SP5 laser scanning confocal microscope (Leica, Germany) with 63x objective selected. For signal emitted by sensor, Ex=513 nM/Em=550 nm~700 nM setting was used. For signal emitted by Hoechst 34580 staining, Ex=405 nM/Em= 425 nM~ 500 nM setting was used.

In cell photo switching experiment

Plate was mounted on microscope with UV lamp and table light over hanging. First image was taken after the plate was transferred from incubator to microscope and been exposed under white light for 10 minutes (OFF1). Then the plate was exposed under UV (632nm) light for 10 minutes and second image was taken (ON1). In the next 10 minutes, one image was taken after every 2 minutes of white light exposure. The seventh image was labelled as OFF2. Last image was taken after the plate was incubated in total dark for 10 minutes (ON2). Fluorescent intensity was quantified using Image J software (National Institutes of Health, MD USA).

ACKNOWLEDGEMENTS

SH is an ARC Senior Research Fellow. AJY and SH are funded by ARC Grant # DP160104641.

AUTHOR CONTRIBUTIONS

JVP and SH contributed equally to this work. JVP, GS, MK performed the experiments and analyzed the data. JVP, SH and AJY designed the research and wrote the paper. SH and AA developed the ion sensitive probe. All authors discussed the results and conclusions and commented on the manuscript.

COMPETING FINANCIAL INTERESTS

The authors declare no competing financial interests.

References

1. Agre, P. et al. Aquaporin CHIP: the archetypal molecular water channel. *Am J Physiol* 265, F463-76 (1993).
2. Petrie, R.J., Doyle, A.D. & Yamada, K.M. Random versus directionally persistent cell migration. *Nat Rev Mol Cell Biol* 10, 538-49 (2009).
3. Krummel, M.F., Bartumeus, F. & Gerard, A. T cell migration, search strategies and mechanisms. *Nat Rev Immunol* 16, 193-201 (2016).
4. Friedl, P. & Wolf, K. Plasticity of cell migration: a multiscale tuning model. *The Journal of cell biology, jcb.* 200909003 (2009).
5. Vicente-Manzanares, M. & Horwitz, A.R. Cell migration: an overview. *Cell Migration: Developmental Methods and Protocols*, 1-24 (2011).
6. Olson, M.F. & Sahai, E. The actin cytoskeleton in cancer cell motility. *Clinical & experimental metastasis* 26, 273 (2009).
7. King, L.S., Kozono, D. & Agre, P. From structure to disease: the evolving tale of aquaporin biology. *Nat Rev Mol Cell Biol* 5, 687-98 (2004).
8. Hu, J. & Verkman, A.S. Increased migration and metastatic potential of tumor cells expressing aquaporin water channels. *FASEB J* 20, 1892-4 (2006).
9. McCoy, E. & Sontheimer, H. Expression and function of water channels (aquaporins) in migrating malignant astrocytes. *Glia* 55, 1034-1043 (2007).
10. Anthony, T.L. et al. Cloned human aquaporin-1 is a cyclic GMP-gated ion channel. *Molecular Pharmacology* 57, 576-588 (2000).
11. Yool, A.J. & Campbell, E.M. Structure, function and translational relevance of aquaporin dual water and ion channels. *Mol Aspects Med* 33, 553-61 (2012).

12. Boassa, D. & Yool, A.J. Single amino acids in the carboxyl terminal domain of aquaporin-1 contribute to cGMP-dependent ion channel activation. *BMC physiology* 3, 12-12 (2003).
13. Rivera-Fuentes, P. et al. A Far-Red Emitting Probe for Unambiguous Detection of Mobile Zinc in Acidic Vesicles and Deep Tissue. *Chem Sci* 6, 1944-1948 (2015).
14. Kolmakov, K. et al. Red-emitting rhodamine dyes for fluorescence microscopy and nanoscopy. *Chemistry* 16, 158-66 (2010).
15. Klajn, R. Spiropyran-based dynamic materials. *Chemical Society reviews* 43, 148-84 (2014).
16. Heng, S., Nguyen, M., Kostecky, R., Monroe, T.M. & Abell, A.D. Nanoliter-scale, regenerable ion sensor: sensing with a surface functionalized microstructured optical fiber. *RSC Advances* 3, 8308-8317 (2013).
17. Stubing, D.B., Heng, S. & Abell, A.D. Crowned spiropyran fluoroionophores with a carboxyl moiety for the selective detection of lithium ions. *Organic & biomolecular chemistry* 14, 3752-7 (2016).
18. Yool, A.J., Stamer, W.D. & Regan, J.W. Forskolin stimulation of water and cation permeability in aquaporin 1 water channels. *Science* 273, 1216-8 (1996).
19. Pei, J.V. et al. Differential Inhibition of Water and Ion Channel Activities of Mammalian Aquaporin-1 by Two Structurally Related Bacopaside Compounds Derived from the Medicinal Plant *Bacopa monnieri*. *Mol Pharmacol* 90, 496-507 (2016).
20. Fogh, J., Fogh, J.M. & Orfeo, T. One hundred and twenty-seven cultured human tumor cell lines producing tumors in nude mice. *J Natl Cancer Inst* 59, 221-6 (1977).

21. Lenox, R.H., McNamara, R.K., Papke, R.L. & Manji, H.K. Neurobiology of lithium: an update. *The Journal of clinical psychiatry* 59, 37-47 (1997).
22. Hille, B. The permeability of the sodium channel to metal cations in myelinated nerve. *The Journal of general physiology* 59, 637-658 (1972).
23. Richelson, E. Lithium ion entry through the sodium channel of cultured mouse neuroblastoma cells: a biochemical study. *Science* 196, 1001-1002 (1977).
24. Timmer, R.T. & Sands, J.M. Lithium intoxication. *Journal of the American Society of Nephrology* 10, 666-674 (1999).
25. Migliati, E. et al. Inhibition of aquaporin-1 and aquaporin-4 water permeability by a derivative of the loop diuretic bumetanide acting at an internal pore-occluding binding site. *Mol Pharmacol* 76, 105-12 (2009).
26. Yool, A.J. et al. AqF026 is a pharmacologic agonist of the water channel aquaporin-1. *J Am Soc Nephrol* 24, 1045-1052 (2013).

FIGURE LEGENDS

Figure 1. (A) Spiropyran (SP) and merocyanine-lithium complex of sensor **SHL** (MC(**SHL**)-Li⁺). The ring-closed spiropyran is weakly fluorescent. The ring-opened merocyanine is expected to be more fluorescent. Shown is the proposed mode for reversible binding of Li⁺ to **SHL**. (B) insert. Fluorescence spectra of **SHL** in water (50 μM). Black spectra represent **SHL** with no added Li⁺; blue spectra represent **SHL** with excess Li⁺ (100 μM). (B) Bar graph showing fluorescence of **SHL** (50 μM) in the presence of Li⁺ or other biologically relevant metal ions. Excitation wavelength = 532 nm; emission wavelength = 625 nm for (B)

Figure 2. Electrophysiology traces demonstrating that AQP1 central ion pore is permeable to Li²⁺ ions and blocked by AqB011 compound. (A) Recordings were performed in Li⁺ substituted isotonic saline. After the initial recordings (Initial), the ionic conductance response in oocytes expressing AQP1 was activated by CPT-cGMP over 25 min in Li⁺ saline (cGMP), which was not observed in non-AQP1 expressing controls. Post 2 h incubation in AqB011, the channels remain closed and inactivated to second application of cGMP (AqB011). (B) Trend plots showing the ionic conductance responses for individual oocytes measured before (initial), after the application of first bath cGMP (cGMP), post 2hour incubation in saline containing 30 μM AqB011 (AqB011). The cGMP activated cationic response in AQP1-expressing oocytes is not observed in non-AQP1 control oocytes. After incubation in saline containing AqB011, the AQP1 cationic conductance remains closed and unresponsive to second bath application of cGMP, which is not observed in control oocytes.

Figure 3. Confocal images of SHL in HT29 cells. HT29 cells were incubated with 50 μM **SHL** for 2 h prior to imaging. Cell nucleus were labelled with Hoescht 33258 (Blue)

and **SHL** sensors (Red) were activated with green laser light. **(A)** Four distinctive states of the sensor during the photoswitch cycles were illustrated here. Cells were first illuminated under visible light radiation for 10 min to convert majority of the sensor back to non-fluorescent SP isomer (OFF1). Then, cells were illuminated under UV light for 10 min to convert SP isomer to fluorescent MC(**SHL**)-Li⁺ complex (ON1), followed by exposure under white light for 10 min with measurement taken every 2 min (OFF2). Finally, cells were incubated in the dark for 10 min to allow the formation of the MC isomer, and the binding of Li⁺ to form the MC(**SHL**)-Li⁺ complex (OFF2). **(B)** 10 min white light illumination was applied to cells after ON1 state, images were taken every 2 min and illustrated here. Red SHL signals were gradually fade away with time. **(C)** Red fluorescent signals were measured for individual cells in the field of view and values were normalized to ON1 state. Data are mean ± S.E.M.; n value is 43. A single-phase decay function was fitted to values between ON1 (100 RFU) and OFF2 (44.51 RFU) state, the half-life was determined to be 4.13 minutes with a τ value estimated at 5.95 minutes. After 10 min incubation in dark, sensors were converted back to MC isomer, and the normalized intensity increased from 44.51 RFU (OFF2) to 84.65 RFU (ON2).

Figure 4. Characterization of lithium hot spots. **(A)** Cells were labeled with Hoescht for nucleus (blue) and AQP1 antibody (Green). HT29 cells have 2.6-fold higher AQP1 expression than SW620 cells. **(B)** HT29 cells (1, 2, 3) and SW620 cells (4, 5, 6) were incubated with SHL for 2 h prior to imaging. Strong Li⁺ signal was observed in all HT29 cells compared with minimal Li⁺ signal observed in SW620 cells. In non-migrating HT cells, Li⁺ 'hot spots' were observed across the whole cytosolic area (1). In migrating HT29 cells, lithium 'hot spots' were concentrated in leading edges of the cells (2, 3).

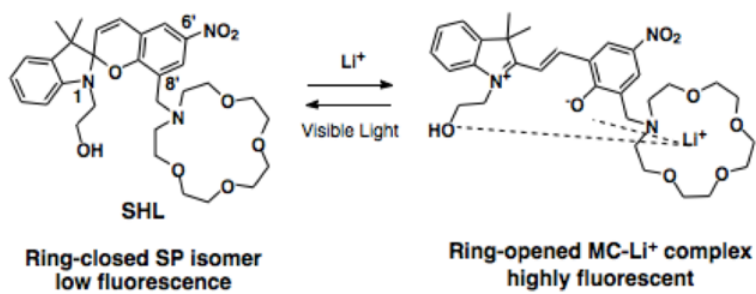
(C) Distinctive punctate Li⁺ hot spots were observed in HT29 cells imaged in Li substituted extracellular saline (1). In cells that were pre-treated with 20 μM AqB011 for 2 h, Li⁺ hot spots were not observed (2). Similar losses of 'hot spot' events were observed after the removal of Li⁺ from the extracellular saline by equimolar substitution of TEA⁺ (3). Pre-incubation in 20 μM AqB011 for 2 h didn't cause any further decrease of Li⁺ signal (4). (D) Li⁺-selective fluorescent signals were quantified by measuring red fluorescent intensity of each individual cells. Intensities were normalized to normal HT29 cells imaged in Li⁺ saline. Li⁺ entry was significantly compromised by pharmacological block (AqB011) or removal of Li⁺ ion from the saline by equimolar replacement with other cations such as TEA⁺. White scale bars represent 5 μm.

Figure 5. Quantitative analysis of confocal images. HT29 cells (A) and SW620 cells (B) were pre-incubated with SHL (Red) and then fixed and labelled with AQP1 primary antibody together with AlexaFluro-488 conjugated secondary antibody (Green). Nucleus were stained with Hoescht (Blue). All three channels were stacked and illustrated in the far-right panel. Consistent with data shown above, both Li⁺ and AQP1 signals were more abundant in HT29 cells compared with SW620 cells. In the stacked images, fluorescence signals from MC(SHL)-Li⁺ complex and AQP1 are strongly co-localized in HT29 cells but not in SW620 cells (combined red and green signals are colored yellow). C 2 cross-sections were chosen for each cell, 1 and 2 for HT29 cell, 3 and 4 for SW620 cell. Both red Li⁺ signals and green AQP1 signals along the cross-sections were plotted as a function of X-Y distance across the cell. In HT29 cells, high levels of Li⁺ signals and AQP1 expression were observed and 2 traces were strongly correlated. In contrast, SW620 cells showed poor spatial correlation and low intensities for both Li⁺ signals and AQP1 expression. D Li⁺ signals and AQP1

expression in C were plotted against each other to illustrate the correlation between them. Linear regression was fitted and R^2 values were calculated in Prism 7. Two channels were strongly correlated in HT29 cells with R^2 values ranging 0.61 to 0.68. In contrast, signals were poorly correlated in SW620 cells and with R^2 values ranging from 0.06 to 0.09.

Figure 1

(A)



(B)

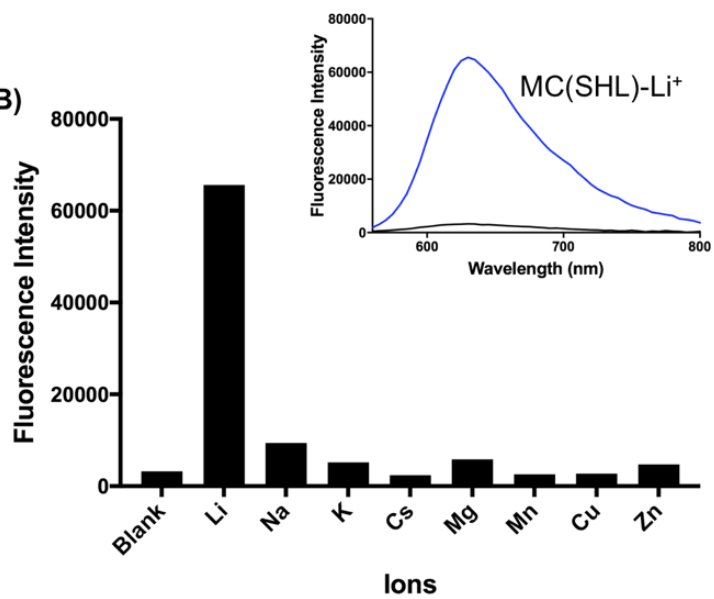


Figure 2

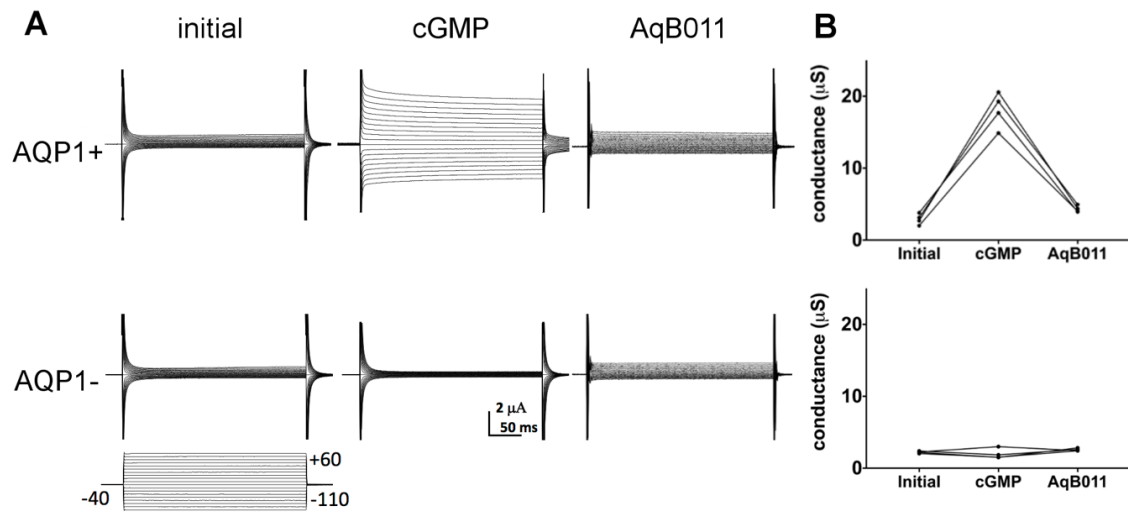


Figure 3

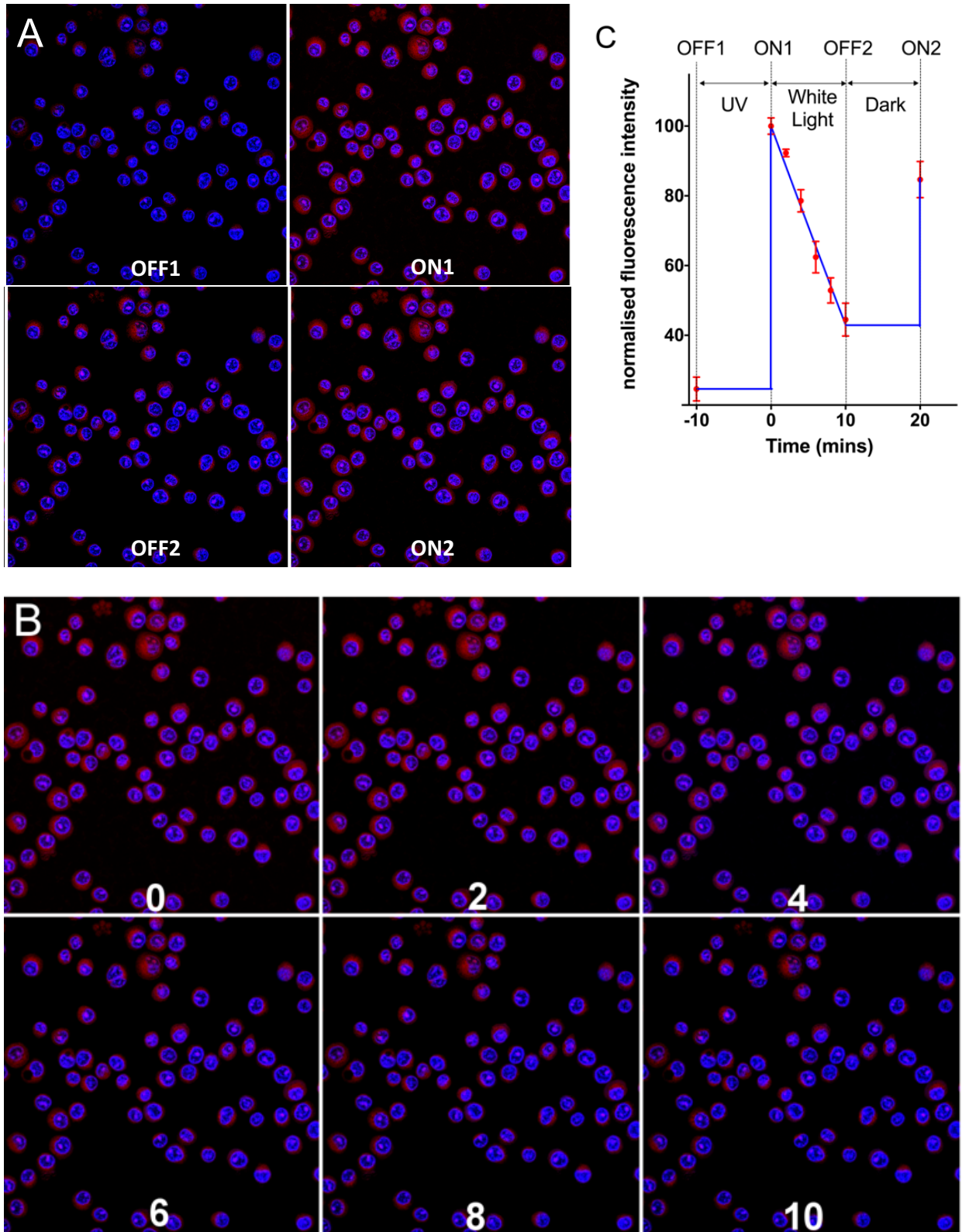


Figure 4

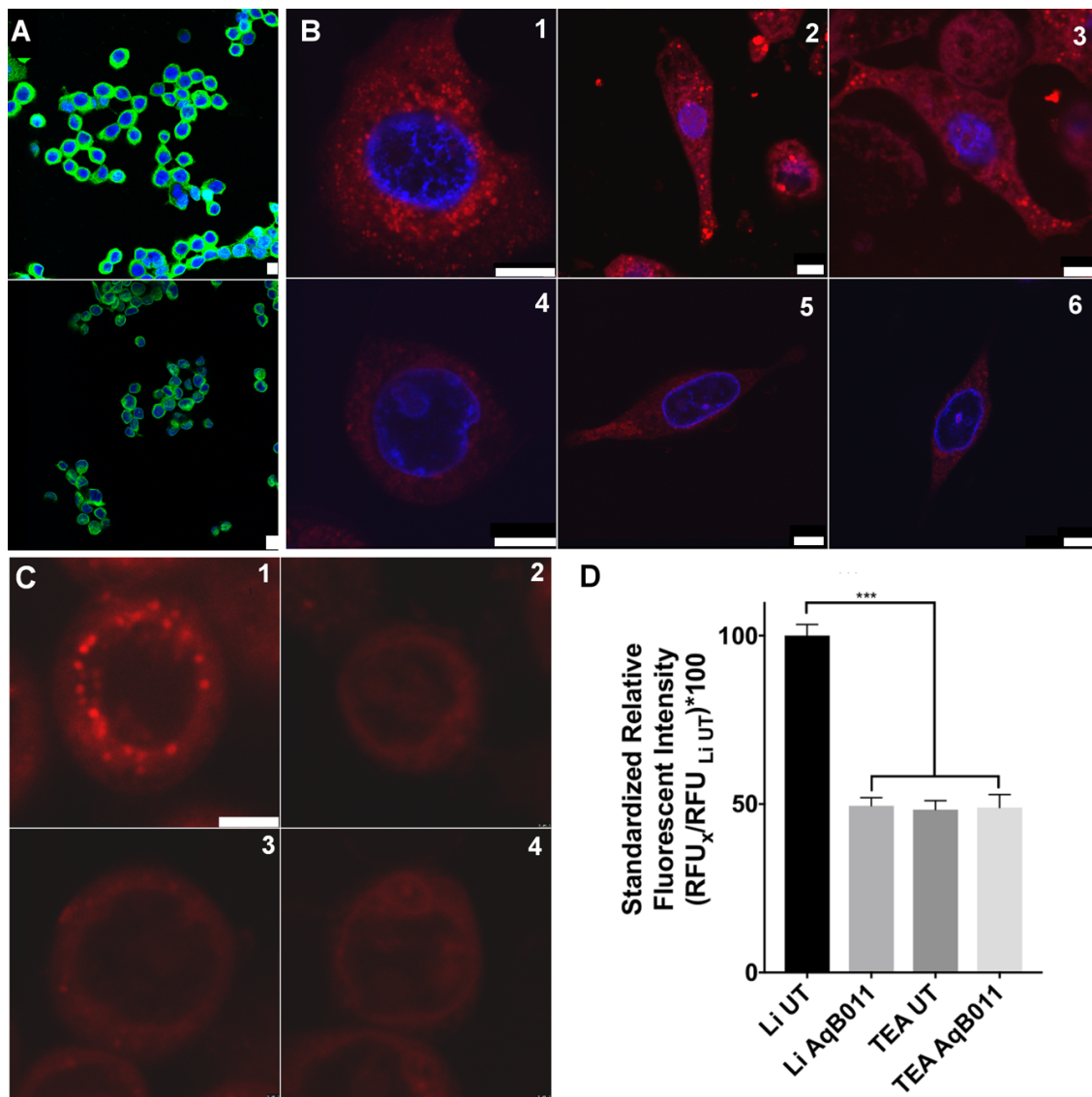
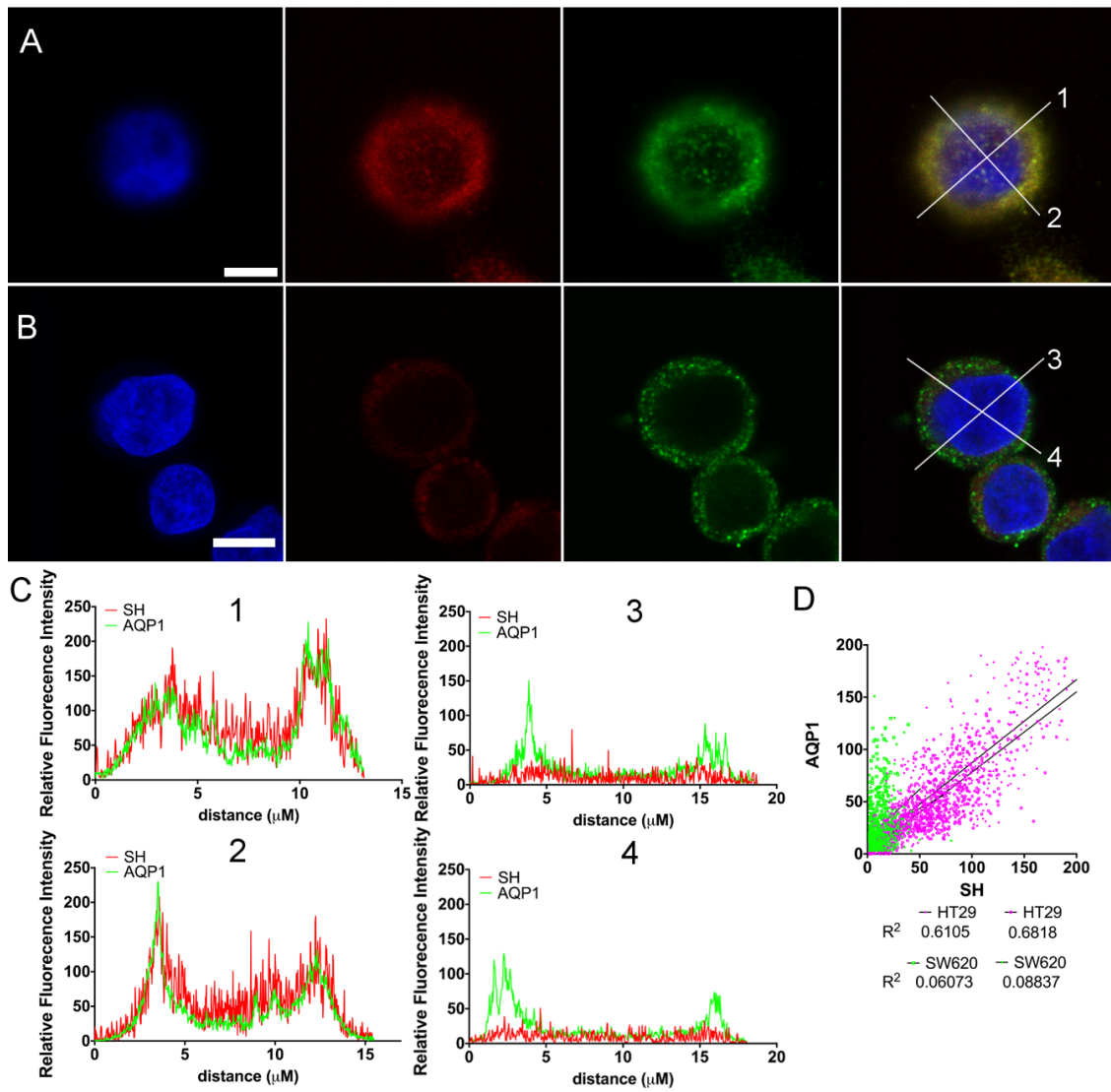


Figure 5



CONCLUSIONS AND THOUGHTS ON FUTURE DIRECTIONS IN AQUAPORIN RESEARCH

Jinxin V Pei

With approximately 60% of human body being composed of water¹, maintaining water homeostasis is critical for basic functions of the human body such as urine concentration², spinal cord fluid formation³. Multiple classes of ion channels and transporters play important roles in regulating body fluid homeostasis^{4,5}, including Na⁺-K⁺-ATPase pumps⁶, Na⁺, K⁺ and Cl⁻ channels⁷⁻⁹, transporters¹⁰, and the aquaporin family¹¹. The ancient family of aquaporin channels, present across many kingdoms of life¹², are well-known pathways for passive water flux¹³. As described in this thesis, a handful of plant, invertebrate, and vertebrate aquaporins have been found to conduct ions, including human aquaporin-1 (AQP1). In addition to the well-characterised water transport role, AQP1 plays an important role in the conduction of monovalent cations (Na⁺ and K⁺) in physiological conditions¹⁴.

Cell migration plays a critical role in many aspects of cell physiology. It is essential for embryogenesis, development, and cancer metastasis¹⁵. During oogenesis in the drosophila ovary, several epithelial cells are recruited by anterior polar cells to form a cluster to initiate cell migration. These recruited epithelial cells can extend protrusions and sense chemoattractant signals^{16,17}. During the development of *Xenopus laevis*, the neural crest initially formed in the dorsal part of the embryo followed by the migration alongside the neural tube¹⁸. In order to initiate migration, neural crest cells first undergo epithelial-mesenchymal transition (EMT). Disassociated cells migrate as a cluster by exchanging chemotactic signals within the cluster¹⁹. Another physiological process that involves cell migration is cancer metastasis. Melanoma cells, for example, can spread from the epidermis of the skin to distal organs. Melanoma cells also migrate in cluster and along extra cellular matrix²⁰.

In a migrating cell, actin filaments are assembled and polymerised at the leading edge of the cell, which create the physical driving force for cell protrusion²¹. Actin polymerization is accompanied by specific classes of membrane proteins in the domains of membrane extension. Various classes of aquaporins have been shown to enhance cell migration and invasion, including AQP1, -3, and -4. AQP1 has been observed at the leading edge of lamellipodia in migrating cells, and knockdown of AQP1 expression has been shown to impair cell migration significantly^{22,23}. For example, experiments have demonstrated that the knockdown of AQP1 in the endothelial cell will reduce the cell migration, thus limiting tumour angiogenesis and proliferation²⁴. AQP3 and -4 are also crucial for cell migration and invasion as demonstrated via in-vitro AQP1-knockdown studies, or in-vivo AQP1-deficient studies. The decreasing AQP4 expression in astrocytes slows cell migration²⁵. Impaired cell migration also been observed in cells from AQP3-deficient animal²⁶. Thus, it is important to understand the mechanisms of AQP-facilitated cell migration.

Similar to AQP1, AQP4 also facilitates osmotic water permeability, but the over-expression of AQP4 does not mimic the function of AQP1 in terms of enhancing cell motility²⁷. Unlike AQP4, AQP1 also functions as monovalent cation channel that can be gated by cGMP^{11,28,29}. The ion channel function of AQP1 is essential for cell migration in a subset of cell types that express the channel in their leading edges^{30,31}. As reviewed in Chapter 1, pharmacological modulators are important in order to evaluate and understand the function of AQP1 in cancer metastasis and in normal cell motility. Since the first evidence showing that AQP1 channels function as a non-selective cation channel by Yool and colleagues in 1996, this novel finding

has attracted interest and controversy in the field^{32,33}. The ion channel activity was replicated in other laboratories^{33,34}, though the physiological relevance of the dual water and ion channel function of AQP1 remained to be defined. Differences in experimental outcomes across preparations suggested multiple levels of regulation controlled the ion channel activity levels of AQP1 channels, including tyrosine phosphorylation in the carboxyl terminal domain³⁵. Characterizing the ion conductance of AQP1 was essential for enabling the additional roles of AQP1 to be considered for understanding the mechanisms that govern cell migration.

My studies have advanced the field of aquaporin pharmacology. Prior to the work presented in this thesis, no modulators that targeted the AQP1 ionic conductance had been discovered. My dissertation research has defined two new AQP1 ion channel antagonists (AqB011 and bacopaside I) and one new AQP1 water channel antagonist (bacopaside II), all now published. The ion channel blocker AqB011 was used to selectively block the AQP1 ion channel and was found to inhibit migration without altering viability or proliferation of AQP1-expressing colon cancer cells³⁰. The water channel blocker bacopaside II was found to only block the AQP1 water channel but not ion channel and slow cell migration when treated on AQP1 expressing cancer cells³¹. The agent bacopaside I interestingly is a blocker of both the water and ion channel activities of AQP1, and was also found to inhibit the migration of cancer cells³¹. In summary, the novel pharmacological tools identified in my dissertation research have created a powerful pharmacological toolbox targeting AQP1 and may have potential significance in future anti-metastasis drug development.

Ion currents through AQP1 have been recorded using electrophysiology techniques, but have not previously been visualized with ion-selective probes. Other types of ionic sparks have been characterized by imaging with ion-selective sensors^{36,37}. Fluo-4 AM, a commercially available Ca^{2+} sensor has been used to detect Ca^{2+} sparks in various tissue sections, which contribute new sights in excitation contraction in cardiomyocytes and the circadian rhythm origin in suprachiasmatic nucleus^{37,38}. Results in this dissertation demonstrated the first real-time analysis and imaging of AQP1-mediated ion entry into lamellipodia of migrating cancer cells. This was achieved with a reversible and selective lithium (Li^+) sensor (SHL). By performing the imaging of Li^+ entry through AQP1 channels, the function of AQP1 as ion channels has been further substantiated. SHL is a novel spiropyran-based ion sensor that is specific for lithium ions (Li^+) in the monovalent cation family. Beside the specificity, SHL also works as a photoswitchable sensor. The ring-opened spiropyran isomer (OFF) and ring-opened merocyanine- Li^{2+} (ON) complex can be switched repeatedly under different wavelength without significant lose of fluorescent intensity. This photo-switchable property is consistent with other spiropyran-based ion sensors³⁹⁻⁴¹. This is not the first example of ion channel activity leading to the appearance of spark-like events monitored optically in living cells. Other studies have successfully monitored the zinc –sparks during the very early stage of fertilization in mouse oocytes^{42,43}. This zinc-sparks can be used clinically as a bio-marker for oocyte quality⁴³.

For *Bacopa monnieri*, two phytochemicals (Bacopaside I and II) were successfully identified and characterised as reported in Chapter III of this dissertation. Future work could follow on from unpublished pilot studies conducted during my PhD work.

For example, during the screening for medicinal plant candidates as AQP1 modulators, in addition to *Bacopa monnieri*, I found three more plants with promise as sources of new modulators. These medicinal herbs were selected based on reports in literature of traditional uses for dysfunctions or diseases potentially linked to AQP1-mediated activity. There were *Poria cocos*, *Rheum rhuababarum* and *Panax ginseng*. The details of these plants and possible active compounds are listed in Table 1. The crude extracts of the three plants were tested on AQP1-expressing oocytes, and all acted as antagonists of the AQP1 water flux (data not shown). Due to limited time available, no extended follow-up studies were carried out for *Poria cocos* or *Panax ginseng*, but these merit investigations in future work. For *Rheum rhuababarum*, active phytochemicals were enriched by extraction and column separation, but identification of the final pure active compound was handicapped by technical limitations given the highly glycosylated composition of the enriched crude extract. Chemicals with properties consistent with an expected partition into the enriched active fraction were selected for study; these were Epicatechin gallate (ECG) and Epigallocatechin gallate (EGCG), which are present in extracts of in *Rheum rhuababarum*. Both ECG and EGCG belong to the catechin flavonoid family known to have high bioactivity⁴⁴. Preliminary tests demonstrated that both ECG and EGCG were able to block AQP1 water conductance significantly at 50 μ M; and when tested on cancer cell migration, both chemicals were able to slow down SW480 colorectal cancer cell migration at 50 μ M (data not shown). These preliminary studies have successfully lead to a new PhD project that is currently in progress.

In this dissertation, my focus has been on human AQP, but I have had the opportunity to evaluate AQPs from different species during my PhD studies that

have resulted in co-authored publications that are not included as chapters in this thesis, but are available in the Appendix of Published Work.

(i) Insect aquaporins: New AQPs from two different insect species were identified and characterized in collaboration with Jeff Fabric's research group in Arizona USA. From *Lygus hesperus*, a pest insect that impacts crops in western North America, five new AQPs were cloned and I carried out their functional characterization using the *Xenopus* oocyte expression system. The published results showed that all five identified *Lygus* AQPs (LhAQP1-5) transported water but not glycerol, placing them as members of the classical AQP family¹⁵. Further investigation of the candidate pharmacological blockers for these LhAQPs might shed light to the development of new species-targeted pesticides. A possible future project will be to screen all the AQP modulators reported in this dissertation and their structural homologs for possible block of the insets LhAQPs.





(ii) Molluscan aquaporin: A candidate AQP gene was cloned from the squid (*Doryteuthis opalescens*) by Dan Morse and colleagues in California USA. In the squid, the AQP (DoAQP) channel is expressed in iridocytes, which are cells that can reflect specific wavelength via controlling using neurotransmitters. I carried out the functional swelling assays, showing DoAQP1 is a classical AQP that is permeable to water but not glycerol (data not shown). This finding may contribute to ongoing work in the Morse lab aimed at answering the question of how squid regulate the changes in their skin iridescence needed for camouflage. Inside the iridocytes, protein plates called reflectin are stacked together. Reflectin with high refractive index is separated by low refractive index space to form multilayer reflectors, thus enable the iridocyte to reflect certain wavelengths. Data thus far have shown that iridescence changes via the rapid polymerization and depolymerisation of reflectin

proteins in the iridocyte. This rapid change requires fast water flow which appears to be conducted through DoAQPs expressed on the surface of iridocytes. These findings of new AQPs from different species contribute to the diversity of functions, expanding understanding in the AQP research field.

For future directions, there are an array of projects that can lead on from my PhD studies based on the preliminary findings outlined above. One area of particular interest would be a detailed study of all the medicinal plants that could potentially contribute new compounds to the AQP modulator collection. Some of the natural agents could serve as lead compounds that might be further refined and optimised. For example, both of the bacopasides have relative high molecular weight and do not fit into the Lipinski's five rules⁴⁵ for a pro-drug molecule, I noted that from my *in silico* docking results that the key moiety which interfaced with the AQP protein in both bacopaside chemicals is the tri-saccharide, not the terpene backbone. In the next stage of research, it would be of interest to chemically isolate the tri-saccharide part and test it directly for a role as an AQP blocker. In this way, the molecular weight of the active compounds could be reduced dramatically and still in theory retain the essential docking domain, which is predicted to cause water channel block. Initial studies are now in progress through collaboration with Dr Sabrina Heng in the synthetic chemistry group at University of Adelaide. A commercial with structural similarities to the tri-saccharide component of bacopasides was selected as the template. The candidate agent is being modified to increase the lipophilicity, as the proposed blocking site is positioned at the intracellular face of the AQP1 water pore. The candidate blocker will be tested both in the oocyte expression system and in various cancer cell lines for its possible function as an AQP channel modulator, and an inhibitor of cancer cell migration.

In this dissertation, diverse agents such as bacopasides and other medicinal plant products, as well as synthetic AqB modulators were studied *in vitro*; however, a systematic study *in vivo* is needed reveal the translational values of these diverse modulators in terms of effective anti-metastatic effects. Preliminary studies are being carried out by collaborators in Adelaide. Tail-vein injections of tagged cancer cells in mice are being used to test whether intraperitoneal administration of AqB013, an AQP1 water channel blocker, can slow down the proliferation and migration of cancer cells *in vivo*. Both live animal CT scan and autopsy studies will be performed in this study. Other modulators reported in this dissertation can be tested using the same protocol. A new and expanding array of pharmacological modulators of AQP1 and other AQPs is likely to offer exciting opportunities for intervention in diseases involving mechanisms of fluid and volume homeostasis mediated by aquaporin channels.

Table 1. Summary of Selected Candidate Medicinal Plants

Plant Name	Picture	Extraction Part	Extraction Method	Possible Compound(s)
Bacopa <i>Bacopa monnieri</i>		Leaves and stem	Ethanol	Bacopasides (I, II and A)
Fuling <i>Poria cocos</i>		Cortex of root	Water	Poriatic acid
Rhubarb <i>Rheum rhuababarum</i>		Stem	Water	Epicatechin gallate (ECG), Epigallocatechin gallate (EGCG)
Ginseng <i>Panax ginseng</i>		Root	Ethanol	Ginsenosides

1. Mitchell, H.H., Hamilton, T.S., Steggerda, F.R. & Bean, H.W. THE CHEMICAL COMPOSITION OF THE ADULT HUMAN BODY AND ITS BEARING ON THE BIOCHEMISTRY OF GROWTH. *J. Biol. Chem.* **158**, 625-637 (1945).
2. Jung, H.J. & Kwon, T.H. Molecular mechanisms regulating aquaporin-2 in kidney collecting duct. *American Journal of Physiology-Renal Physiology* **311**, F1318-F1328 (2016).
3. Nesic, O. et al. Aquaporins in Spinal Cord Injury: The Janus Face of Aquaporin 4. *Neuroscience* **168**, 1019-1035 (2010).
4. Kortenoeven, M.L. & Fenton, R.A. Renal aquaporins and water balance disorders. *Biochim Biophys Acta* **1840**, 1533-49 (2014).
5. Matalon, S., Bartoszewski, R. & Collawn, J.F. Role of epithelial sodium channels in the regulation of lung fluid homeostasis. *Am J Physiol Lung Cell Mol Physiol* **309**, L1229-38 (2015).
6. Matchkov, V.V. & Krivoi, I.I. Specialized Functional Diversity and Interactions of the Na,K-ATPase. *Frontiers in Physiology* **7**(2016).
7. Sorensen, C.M., Braunstein, T.H., Holstein-Rathlou, N.H. & Salomonsson, M. Role of vascular potassium channels in the regulation of renal hemodynamics. *American Journal of Physiology-Renal Physiology* **302**, F505-F518 (2012).
8. Schild, L. The epithelial sodium channel and the control of sodium balance. *Biochimica Et Biophysica Acta-Molecular Basis of Disease* **1802**, 1159-1165 (2010).
9. Li, C.Y. & Naren, A.P. CFTR chloride channel in the apical compartments: spatiotemporal coupling to its interacting partners. *Integrative Biology* **2**, 161-177 (2010).
10. Benfenati, V. & Ferroni, S. Water Transport between Cns Compartments: Functional and Molecular Interactions between Aquaporins and Ion Channels. *Neuroscience* **168**, 926-940 (2010).
11. Yool, A.J. & Campbell, E.M. Structure, function and translational relevance of aquaporin dual water and ion channels. *Mol Aspects Med* **33**, 553-61 (2012).
12. Campbell, E.M., Ball, A., Hoppler, S. & Bowman, A.S. Invertebrate aquaporins: a review. *Journal of Comparative Physiology B-Biochemical Systemic and Environmental Physiology* **178**, 935-955 (2008).
13. Yool, A.J. & Weinstein, A.M. New roles for old holes: ion channel function in aquaporin-1. *News Physiol Sci* **17**, 68-72 (2002).
14. Anthony, T.L. et al. Cloned human aquaporin-1 is a cyclic GMP-gated ion channel. *Mol Pharmacol* **57**, 576-88 (2000).
15. Mayor, R. & Etienne-Manneville, S. The front and rear of collective cell migration. *Nat Rev Mol Cell Biol* **17**, 97-109 (2016).
16. Ducheck, P. & Rorth, P. Guidance of cell migration by EGF receptor signaling during *Drosophila* oogenesis. *Science* **291**, 131-133 (2001).
17. Ducheck, P., Somogyi, K., Jekely, G., Beccari, S. & Rorth, P. Guidance of cell migration by the *Drosophila* PDGF/VEGF receptor. *Cell* **107**, 17-26 (2001).
18. Mayor, R. & Theveneau, E. The neural crest. *Development* **140**, 2247-2251 (2013).
19. Theveneau, E. et al. Collective Chemotaxis Requires Contact-Dependent Cell Polarity. *Developmental Cell* **19**, 39-53 (2010).
20. Friedl, P. & Gilmour, D. Collective cell migration in morphogenesis, regeneration and cancer. *Nature Reviews Molecular Cell Biology* **10**, 445-457 (2009).

21. Le Clairche, C. & Carlier, M.F. Regulation of actin assembly associated with protrusion and adhesion in cell migration. *Physiol Rev* **88**, 489-513 (2008).
22. Nico, B. & Ribatti, D. Role of aquaporins in cell migration and edema formation in human brain tumors. *Exp Cell Res* **317**, 2391-6 (2011).
23. Papadopoulos, M.C., Saadoun, S. & Verkman, A.S. Aquaporins and cell migration. *Pflugers Arch* **456**, 693-700 (2008).
24. Saadoun, S., Papadopoulos, M.C., Hara-Chikuma, M. & Verkman, A.S. Impairment of angiogenesis and cell migration by targeted aquaporin-1 gene disruption. *Nature* **434**, 786-92 (2005).
25. Saadoun, S. et al. Involvement of aquaporin-4 in astroglial cell migration and glial scar formation. *J Cell Sci* **118**, 5691-8 (2005).
26. Hara-Chikuma, M. & Verkman, A.S. Aquaporin-3 facilitates epidermal cell migration and proliferation during wound healing. *J Mol Med (Berl)* **86**, 221-31 (2008).
27. McCoy, E. & Sontheimer, H. Expression and function of water channels (aquaporins) in migrating malignant astrocytes. *Glia* **55**, 1034-1043 (2007).
28. Anthony, T.L. et al. Cloned human aquaporin-1 is a cyclic GMP-gated ion channel. *Molecular Pharmacology* **57**, 576-588 (2000).
29. Boassa, D. & Yool, A.J. Single amino acids in the carboxyl terminal domain of aquaporin-1 contribute to cGMP-dependent ion channel activation. *BMC physiology* **3**, 12-12 (2003).
30. Kourghi, M., Pei, J.V., De Ieso, M.L., Flynn, G. & Yool, A.J. Bumetanide Derivatives AqB007 and AqB011 Selectively Block the Aquaporin-1 Ion Channel Conductance and Slow Cancer Cell Migration. *Mol Pharmacol* **89**, 133-40 (2016).
31. Pei, J.V. et al. Differential Inhibition of Water and Ion Channel Activities of Mammalian Aquaporin-1 by Two Structurally Related Bacopaside Compounds Derived from the Medicinal Plant *Bacopa monnieri*. *Mol Pharmacol* **90**, 496-507 (2016).
32. Tsunoda, S.P., Wiesner, B., Lorenz, D., Rosenthal, W. & Pohl, P. Aquaporin-1, nothing but a water channel. *Journal of Biological Chemistry* **279**, 11364-11367 (2004).
33. Saparov, S.M., Kozono, D., Rothe, U., Agre, P. & Pohl, P. Water and ion permeation of aquaporin-1 in planar lipid bilayers. Major differences in structural determinants and stoichiometry. *J Biol Chem* **276**, 31515-20 (2001).
34. Zhang, W. et al. Aquaporin-1 channel function is positively regulated by protein kinase C. *Journal of Biological Chemistry* **282**, 20933-20940 (2007).
35. Campbell, E.M., Birdsell, D.N. & Yool, A.J. The activity of human aquaporin 1 as a cGMP-gated cation channel is regulated by tyrosine phosphorylation in the carboxyl-terminal domain. *Mol Pharmacol* **81**, 97-105 (2012).
36. Que, E.L. et al. Quantitative mapping of zinc fluxes in the mammalian egg reveals the origin of fertilization-induced zinc sparks. *Nat Chem* **7**, 130-9 (2015).
37. Llach, A. et al. Detection, properties, and frequency of local calcium release from the sarcoplasmic reticulum in teleost cardiomyocytes. *PLoS One* **6**, e23708 (2011).
38. Hong, J.H. et al. Intracellular calcium spikes in rat suprachiasmatic nucleus neurons induced by BAPTA-based calcium dyes. *PLoS One* **5**, e9634 (2010).

39. Zhang, X., Heng, S. & Abell, A.D. Photoregulation of alpha-Chymotrypsin Activity by Spiropyran-Based Inhibitors in Solution and Attached to an Optical Fiber. *Chemistry* **21**, 10703-13 (2015).
40. Heng, S. et al. Microstructured optical fibers and live cells: a water-soluble, photochromic zinc sensor. *Biomacromolecules* **14**, 3376-9 (2013).
41. Warren-Smith, S.C., Heng, S., Ebendorff-Heidepriem, H., Abell, A.D. & Monro, T.M. Fluorescence-based aluminum ion sensing using a surface-functionalized microstructured optical fiber. *Langmuir* **27**, 5680-5 (2011).
42. Duncan, F.E. et al. The zinc spark is an inorganic signature of human egg activation. *Sci Rep* **6**, 24737 (2016).
43. Zhang, N., Duncan, F.E., Que, E.L., O'Halloran, T.V. & Woodruff, T.K. The fertilization-induced zinc spark is a novel biomarker of mouse embryo quality and early development. *Sci Rep* **6**, 22772 (2016).
44. Du, G.J. et al. Epigallocatechin Gallate (EGCG) is the most effective cancer chemopreventive polyphenol in green tea. *Nutrients* **4**, 1679-91 (2012).
45. Lipinski, C.A., Lombardo, F., Dominy, B.W. & Feeney, P.J. Experimental and computational approaches to estimate solubility and permeability in drug discovery and development settings. *Adv Drug Deliv Rev* **46**, 3-26 (2001).

Appendix

PAPERS IN PUBLISHED FORMAT

Drug Discovery and Therapeutic Targets for Pharmacological Modulators of Aquaporin Channels

Jinxin V. Pei, Joshua L. Ameliorate, Mohamad Kourghi,
Michael L. De Ieso and Andrea J. Yool

CONTENTS

Abstract	273
14.1 Introduction	274
14.2 Overview of Aquaporin Channel Functions in Brain Fluid	
Homeostasis and Cell Migration	274
14.2.1 AQP4 in Cerebral Edema	275
14.2.2 AQP1 in Cell Migration	277
14.3 Small Molecule Drug Discovery for Aquaporin Channels	278
14.4 Translational Promise of Pharmacological Modulators of Aquaporin Channels in Brain Edema, Cancer and Other Disorders	281
14.4.1 Targeting AQP4 Channels in Brain Edema	281
14.4.2 Differential Regulation of Expression of AQP Channel Types in Cancer Cells	281
14.4.3 Targeting AQP1 Channels in Cell Migration and Metastasis	283
14.5 New Avenues for Aquaporin Drug Discovery from Traditional and Alternative Medicines	284
References	287

ABSTRACT

FLUID HOMEOSTASIS IN THE body is well known to be regulated by ion channels and transporters, but equally important are the co-expressed classes of aquaporin (AQP) water channels that facilitate transmembrane water movement. The field of AQP

pharmacology is expanding rapidly with the new identification of small molecule drug-like agents with distinctive properties in AQP modulation, allowing exploration of potential therapeutic applications in brain edema, cancer and other disorders. Pharmacological agents could modulate AQPs by direct occlusion of the water pore itself, by acting at distinct sites that confer other channel properties, or by altering levels of protein expression or membrane targeting. Expanding the pharmacological portfolio will benefit basic research and promote new therapeutic strategies in many conditions involving AQPs in the symptoms or disease processes. Exploring herbal alternative medicines as sources of pharmacological agents for AQPs is likely to have a substantial impact on the field of AQP research, which has keenly awaited the development of chemical interventions as a platform for therapeutic approaches. Recent work is providing an enhanced understanding of the molecular mechanisms of action of traditional herbal medicines as novel sources of AQP modulators.

14.1 INTRODUCTION

Aquaporins (AQPs) found throughout the kingdoms of life (Zardoya, 2005) are channel proteins which facilitate water and small solute movement across plasma membranes based on chemical, osmotic and hydrostatic gradients (Hachez and Chaumont, 2010; Ishibashi et al., 2011; Madeira et al., 2014). The existence of water channels in red blood cells and barrier membranes and their hallmark sensitivity to block by mercury (Benga et al., 1986; Macey, 1984; Macey et al., 1972; Naccache and Sha'afi, 1974) was deduced before AQP1 cDNA was cloned and characterized in the early 1990s (Preston and Agre, 1991; Preston et al., 1992). Progress since has defined 13 mammalian subtypes of AQPs, their relative protein abundance, tissue-specific distributions and expression levels under various conditions. AQP crystal structures have provided insights into the homotetrameric channel structure and the location of the water pores within each of the four subunits (Ishibashi et al., 2009; Jensen et al., 2003; Sui et al., 2001). AQP1 is a tetrameric channel with water pores located within each of the four individual subunits (Fu et al., 2000; Sui et al., 2001). Review articles have emphasized the compelling need for development of AQP modulators as candidate treatments for a variety of disorders (Castle, 2005; Frigeri et al., 2007; Huber et al., 2012; Jeyaseelan et al., 2006). However, prior to 2009, the discovery of AQP pharmacological agents had not progressed substantially beyond mercuric compounds, which lacked translational potential due to toxicity, and agents that affected multiple targets and lacked potency. Recent advances have shown that drug-like lead compounds are emerging, complementing work that has investigated the functional roles of AQPs by overexpression or targeted genetic knockdown and deletion.

14.2 OVERVIEW OF AQUAPORIN CHANNEL FUNCTIONS IN BRAIN FLUID HOMEOSTASIS AND CELL MIGRATION

Fluid homeostasis in the body is regulated by partnerships of ion channels and transporters with co-expressed classes of AQP channels (Conde et al., 2010; Fischbarg, 2010). The 13 classes of mammalian AQP water channels (AQPs 0–12) are expressed in tissue-specific patterns in the body and are essential in regulating the movement of fluid across barrier

membranes and contributing to control of cell volume, production of cerebral spinal fluid, edema formation and recovery, mediating renal function and more (Ishibashi, 2009; Nielsen et al., 2007). Under pathological conditions, dysfunctions in the control of fluid movement create serious problems. The physiological importance of AQP channels and their compelling potential value as therapeutic targets has motivated researchers to work toward defining a pharmacological panel of chemical modulators for AQPs. A comprehensive pharmacological portfolio for all classes of AQPs will provide an array of new therapeutic opportunities that will continue to expand as new roles for AQP channels are uncovered. Two major areas of current interest in AQP-based mechanisms of disease are brain swelling after injury or stroke and the migration of cancer cells in the process of metastasis.

14.2.1 AQP4 in Cerebral Edema

An area of intense interest for new therapies directed at AQPs is aimed at reducing brain swelling after acute traumatic injury or stroke (Mack and Wolburg, 2013; Yool et al., 2009). Cerebral edema and increased intracranial pressure are life-threatening sequelae of severe brain injuries, associated with a poor prognosis as evidenced by a mortality rate near 60%–80% (Feickert et al., 1999; Hacke et al., 1996). Traumatic brain injury affects an estimated 10 million people annually; according to the World Health Organization, it will be the major cause of death and disability by the year 2020 (Hyder et al., 2007). Nearly one-third of hospitalized traumatic brain injury patients die from injuries that are secondary to the initial trauma, including neuroinflammation, excitotoxicity, brain edema and intracranial hypertension (Miller et al., 1992). Traumatic brain injury reduces life expectancy and compromises the quality of life (Schiehser et al., 2014) with increased incidences of seizures, sleep disorders, neurodegenerative disease, neuroendocrine dysregulation, psychiatric problems and non-neurological disorders that can persist years after the injury event (Masel and DeWitt, 2010). The burden of mortality and morbidity makes traumatic brain injury a pressing public health and medical concern, but there is currently no targeted pharmacological treatment for reducing the secondary damage (Park et al., 2008).

Cerebral ischemia following severe traumatic brain injury involves a combination of cytotoxic and vasogenic events (Hossmann, 1994; Papadopoulos et al., 2004; Shi et al., 2012; Tourdias et al., 2011). Brain edema commonly occurs when cerebral blood flow drops beneath 10 mL/100 g/min and essential ionic pump activity is impaired. During the first 5 h of ischemia, blood–brain barrier integrity can be maintained without substantial brain swelling (Betz et al., 1989), but upon reperfusion, a rise in brain water content can occur in conjunction with an elevation in intracranial pressure depending on the extent of ischemia and the delay until cerebral blood flow is restored (Avery et al., 1984). Conventional treatments focus on reducing edema and intracranial pressure using hyperventilation, mannitol, diuretics, corticosteroids or barbiturates (Manno et al., 1999; Winter et al., 2005). Decompressive craniectomy involves the surgical removal of a part of the skull, creating a space for the swollen brain tissue to expand. This surgical method improves survival but does not fully address pathological outcomes as many patients are left moderately or severely disabled (Fischer et al., 2011; Vahedi et al., 2007).

Work in animal models relies on optimizing the reliability and reproducibility of the injury event. The middle cerebral artery occlusion model in rodents has been a standard method for testing experimental therapeutic agents but is difficult in part because of unexplained variability in infarct volumes. When analyzed with computed tomography cerebral blood volume maps, variability was found to result from unintended occlusion of a second artery (the anterior choroidal artery) in a subset of animals, causing expanded infarct areas (McLeod et al., 2013). Brain computed tomography perfusion imaging provides a powerful tool for improving the experimental method by fully defining the arteries affected by occlusion and accurately identifying the infarct core and penumbra domains (McLeod et al., 2011).

The concept of edema as being the primary cause of increased intracranial pressure has been challenged; small ischemic strokes in rats resulted in minimal amounts of edema but were associated with a substantial elevation in intracranial pressure at 24 h, which was effectively countered by application of hypothermia soon after the stroke event. Mechanisms in addition to cerebral edema alone must be considered as important drivers of intracranial pressure elevation (Murtha et al., 2014a,b). Assessing the regulated contributions of transporters and channels including AQP1 and AQP4 might offer insight into possible molecular mechanisms generating the distinct outcomes.

AQP4 is the predominant water channel in the brain, localized to the blood–brain barrier, ependymal cells lining the ventricles, subependymal astrocytes and the glia limitans (Amiry-Moghaddam and Ottersen, 2003; Nagelhus and Ottersen, 2013; Xiao and Hu, 2014) for their involvement in water movement both in and out of the brain (Mack and Wolburg, 2013). Studies in AQP4-deficient mouse models showing partial protection from water intoxication and edema after stroke (Manley et al., 2000; Papadopoulos and Verkman, 2008) support the idea that ligand modulators of AQP4 could revolutionize clinical treatment of brain edema. To date, progress in the field has been limited by the lack of availability of pharmacologic modulators of the AQP channels. Identification of agonists and antagonists of AQP4 remains an important goal in the field of cerebral edema research. AQP4 channels subserve water movement during cerebral edema formation (Jullienne and Badaut, 2013; Manley et al., 2000), highlighting them as an attractive therapeutic target for non-surgical management of cerebral edema (Yool, 2007a; Yool et al., 2009).

Alterations in levels of AQP expression in response to cerebral fluid imbalance can offer clues for understanding the functional roles of water channels, assuming the goal is to restore homeostasis. In experimental models of cerebral ischemia, expression levels of AQP4 were reduced in the initial period post injury and significantly increased thereafter (Taniguchi et al., 2000; Yamamoto et al., 2001). Regulation of AQP4 expression appears to correlate with levels of the transcription factor hypoxia-inducible factor 1- α (HIF-1 α) (Kaur et al., 2006). Early after traumatic brain injury (5 h), levels of HIF-1 α were low and increased to peak at 24–48 h post injury (Ding et al., 2009; Higashida et al., 2011). Inhibition of HIF-1 α correlated with decreased AQP4 and attenuated swelling post injury (Shenag et al., 2012). The temporal pattern of AQP4 regulation suggests that downregulation of channels early after injury could be a protective response to limit the influx of fluid into the brain, whereas delayed upregulation might serve to enable fluid export and to restore

fluid homeostasis. However, altered gene expression responses are not spatially uniform. A reduction in AQP4 expression occurred in astrocytes within the ischemic core, while an elevation in AQP4 expression was seen in glial endfeet in the surrounding penumbra, in a middle cerebral artery occlusion model (Frydenlund et al., 2006). Spatially selective regulation of AQP4 might limit water influx into the ischemic core without preventing the amelioration of vasogenic edema in the penumbra. The loss of AQP4 was not linked to a decrease in the astrocyte marker, glial fibrillary acidic protein (Friedman et al., 2009), indicating that decreased AQP4 expression was not an indirect effect of glial cell loss in the injured domain.

AQP4 water channels are dynamically regulated components of brain fluid homeostasis, being mobilized or deactivated as needed to reduce damage arising from shifts or disturbances in cerebral fluid homeostasis. The temporal and spatial patterns of AQP4 regulation are contingent upon the extent and duration of injury and stage of pathology. AQP pharmacological agents will be advantageous for intervention in brain fluid disorders particularly if administered with an understanding of the dynamic mechanisms of AQP channel regulation.

14.2.2 AQP1 in Cell Migration

Cell migration is essential in development, repair, regeneration and immune protection in multicellular organisms. In 1937, the neuroanatomist Ramon y Cajal pondered: ‘What mysterious forces stimulate the migrations of cells...?’ (Kater and Letourneau, 1985). Currently, it is thought that branched assemblies of actin filaments, actively polymerizing at the leading edge, generate the primary force, which pushes out thin ruffled membrane extensions known as lamellipodia (Le Clainche and Carlier, 2008). Parallel arrays of actin are stalled by small loads on the order of 1 pN (Footer et al., 2007), but branched actin networks with many points of contact can generate nN of force per μm^2 , on the scale needed for movement through viscous extracellular environments (Marcy et al., 2004; Parekh et al., 2005). Cell adhesions at the leading edge hold the new position, while the trailing edge detaches, and the cell resets for the next push forward.

AQPs found in all the kingdoms of life facilitate fluxes of water and small solutes across membranes (King et al., 2004). In diverse motile cells from amoeba to human, specific AQPs are localized in lamellipodial leading edges. When these cells are made AQP deficient (e.g. by genetic knockout or RNA-interference techniques), cell migration is greatly impaired. Reintroduction of AQP restores rates of movement, but interestingly, the effects of different AQPs are not interchangeable (McCoy and Sontheimer, 2007).

Of the 13 known mammalian classes of AQPs, the three often associated with migration thus far are AQPs 1, 3 and 5. In the ‘World Cell Race’ event held at the *American Society for Cell Biology* meeting in 2011, cell lines were submitted by teams around the world; the winner was a bone marrow stem cell which covered the 400 μm track at a speed of 5.2 $\mu\text{m}/\text{min}$. Bone marrow stem cells express lamellipodial AQP1 that is required for migration (Meng et al., 2014). The need for AQPs in migration extends to life forms other than mammals. The amoeba *Dictyostelium discoideum* migrates in a chemotactic response to external cyclic adenosine monophosphate (cAMP) signals and expresses an AQP orthologous to human

AQP1 (48% amino acid sequence similarity) which is localized in lamellipodia (von Bulow et al., 2012). If *D. discoideum* had been in the competition, it might have taken the honors, moving at up to 11 $\mu\text{m}/\text{min}$ in response to cAMP chemotactic stimuli (Van Duijn and Inouye, 1991). Other contenders could have included activated T-cells moving at $>10 \mu\text{m}/\text{min}$ (Katakai et al., 2013), which express AQPs 1, 3 and 5 (Moon et al., 2004), and fibroblasts moving at up to 9 $\mu\text{m}/\text{min}$ (Ware et al., 1998), which express AQP1 (Minami et al., 2001).

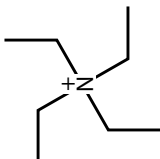
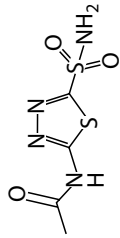
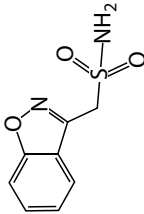
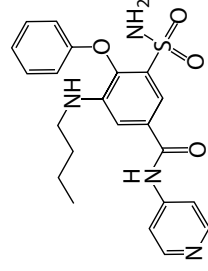
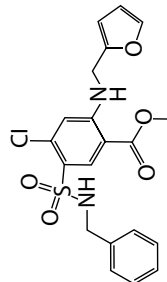
Even though AQP1 and AQP4 are both highly functional water channels, the expression of AQP1 enables rapid cell movement, whereas expression of AQP4 does not. One important difference is that AQP1 but not AQP4 can function as a gated monovalent cation channel (Anthony et al., 2000; Yool and Campbell, 2012). AQP1 ion channel activity has been replicated in other laboratories (Saparov et al., 2001; Zhang et al., 2007), but its physiological significance remains unknown. During migration, changes in cytoplasmic volume are required. Fluid flux is commonly thought of as a passive process in which water follows salt. Yet the observation that water channels cannot simply be swapped between cells suggests that other properties in addition to water channel function are needed. The pro-migratory effect of AQP1 and its orthologs appears to be a convergent target of evolution across phyla.

14.3 SMALL MOLECULE DRUG DISCOVERY FOR AQUAPORIN CHANNELS

Inhibitors of AQPs have long been heralded as an important goal in the field. A database of structurally diverse compounds will be of substantial value in expanding our understanding of drug structure–activity relationships and molecular sites of action for AQP pharmacological modulators. Pharmacological agents could modulate AQPs by direct occlusion of the water pore itself, by acting at distinct sites that confer other channel properties or by altering levels of protein expression or membrane targeting. Regulatory domains in AQPs can control membrane localization, interaction with proteins to create signalling complexes and scaffolds, and gated permeation of small solutes other than water through AQPs (Cowan et al., 2000; Yool, 2007a,b).

Much of the work to date has focused on the agents that act to occlude the water pore. The existence of water channels in cell membranes and their hallmark sensitivity to block by mercury was deduced before the first AQP1 cDNA was cloned (Preston and Agre, 1991; Preston et al., 1992). Finding non-mercurial AQP blockers has been essential for AQP drug discovery (Table 14.1). Silver and gold compounds were reported to block water channel activity of both plant and human AQPs (Niemi et al., 2002; Tyerman et al., 2002). Membrane-permeable derivatives of the loop diuretic drugs bumetanide and furosemide have proven useful as pharmacological antagonist AqB013 (Migliati et al., 2009) and agonist AqF026 (Yool et al., 2013) agents for AQP1 and AQP4 water channel activities. Characterized in vitro and in rodent models in vivo, these candidate AQP drugs appear to be effective and well tolerated. In a mouse model of peritoneal dialysis, the lack of effect of the agonist AqF026 in AQP1 knockout animals indicated specificity of action without appreciable off-target effects (Yool et al., 2013). Other groups also have investigated arylsulfonamides as AQP blockers (Gao et al., 2006; Huber et al., 2007; Ma et al., 2004; Seeliger et al., 2013). Acetazolamide (AZA)

TABLE 14.1 Summary of Aquaporin Pharmacological Modulators and Proposed Interaction Sites

Name	Structure	Proposed Binding Site	References
Mercuric chloride HgCl ₂	Cl-Hg-Cl	Cys-189 in AQP1	Preston et al. (1993)
Silver and gold compounds: AgNO ₃ , HAuCl ₄	$\text{Ag}^+ \left[\begin{array}{c} \text{O} \\ \parallel \\ \text{O}-\text{N}-\text{O}^- \end{array} \right]^-$ $\text{H}^+ \left[\begin{array}{c} \text{Cl} \\ \\ \text{Cl}-\text{Au}-\text{Cl} \\ \\ \text{Cl} \end{array} \right]^-$	Cys-189 in AQP1	Niemietz and Tyerman (2002)
Tetraethylammonium (TEA ⁺)		Loop-E region	Brooks et al. (2000), Yool et al. (2002)
Acetazolamide (AZA)		Ag-216 and Gly-209 in AQP4	Huber et al. (2009, 2007)
Zonisamide		Possibly Arg-216 and Gly-209 in AQP4	Huber et al. (2009)
AqB013		Intracellular vestibule of the water pore	Migliati et al. (2009)
AqF026		Intracellular loop D domain	Yool et al. (2013)

has been reported to inhibit AQP4 water permeability with an IC_{50} value of 0.9 μ M. In silico docking suggested an interaction between the sulfonamide group of AZA and both arginine 216 and glycine 209 (Huber et al., 2007). As compared to AQP4, AQP1 was less sensitive to AZA, with an IC_{50} value estimated at $5.5 \pm 0.5 \mu$ M (Seeliger et al., 2013).

The passage of water and ions occurs through pharmacologically distinct pathways in AQP1 (Saparov et al., 2001; Yool et al., 2002). The cyclic guanosine monophosphate (cGMP)-gated cation permeation pathway is thought to be in the central pore of the tetramer, based on molecular dynamic simulations (Yu et al., 2006) and effects of site-directed mutations on altering ionic conductance properties (Campbell et al., 2012). Conduction of ions in AQP1 channels is inhibited by Cd^{2+} but not tetraethylammonium ion (TEA^+), whereas water transport which occurs through the individual pores located in each subunit is sensitive to TEA^+ , AqB013, AqF026 but not Cd^{2+} (Boassa et al., 2006; Brooks et al., 2000; Migliati et al., 2009; Yool et al., 2002, 2013). In silico docking identified possible extracellular binding by TEA^+ (Detmers et al., 2006) but indicated intracellular sites of action for the arylsulfonamides, supported by results of site-directed mutations and biological assays. AqB013 is thought to occlude the water pore at the internal vestibule, whereas the AQP agonist, AqF026, appears to potentiate water channel activity by interacting with an intracellular gate (loop D) between the fourth and fifth transmembrane domains (Yool et al., 2013).

The loop D domain serves as a gate for AQP channel activity in mammalian AQP1 (Yu et al., 2006), AQP4 (Zelenina et al., 2002), amoeba AQP-B (von Bulow et al., 2012) and plant AQP (Tornroth-Horsefield et al., 2006). In AQP1, loop D domain is involved in the regulation of cation channel activity activated by cGMP (Yu et al., 2006). The loop D sequence is highly conserved across species in AQP1 channels from fish to mammals, yet mutations in this domain do not impact water channel activity, suggesting that loop D is essential for AQP1 functions other than water permeability. Mutations at specific loop D positions in AQP1 remove ion channel activity without impairing water channel activity (Yu et al., 2006). The retention of water channel functionality showed that the mutation did not interfere with expression, trafficking or assembly of AQP1 channel.

Other regulatory domains in AQP1 have been suggested in the carboxyl terminal domain. A putative cGMP-dependent modulatory domain with sequence similarity to the cGMP-phosphodiesterase selectivity domain was identified in the AQP1 C-terminus (Boassa and Yool, 2002, 2003). Mutations of conserved phosphodiesterase-like residues in this domain did not remove cGMP-dependent activation of AQP1 but reduced the efficacy of cGMP by right shifting the dose–response curve. An EF-hand motif found in calcium-binding proteins (Grabarek, 2006) has been proposed in the carboxyl terminal domain of AQP1, but its functional role has not yet been defined (Fotiadis et al., 2002). A tyrosine phosphorylation site in the carboxyl terminal serves a modulatory role in governing the availability of AQP1 to be gated as a cGMP-dependent cation channel (Campbell et al., 2012). A PDZ protein–protein ligand domain identified in AQP1 (Ile260 to Arg264) in the C-terminus was shown to be important for targeting AQP1 into a membrane complex needed to maintain vestibular fluid balance in the inner ear (Cowan et al., 2000). Regulatory domains and transmembrane pore regions in AQPS are both attractive candidates for the development of drug agents.

14.4 TRANSLATIONAL PROMISE OF PHARMACOLOGICAL MODULATORS OF AQUAPORIN CHANNELS IN BRAIN EDEMA, CANCER AND OTHER DISORDERS

14.4.1 Targeting AQP4 Channels in Brain Edema

Conventional approaches have relieved intracranial pressure with hyperventilation, hyperosmotic agents, diuretics and decompressive craniectomy (Diedler et al., 2009; Park et al., 2008; Werner and Engelhard, 2007) but are limited in effectiveness by treating symptoms rather than causes of edema. A major challenge has been the lack of interventions for controlling fluid movement in brain edema. Pharmacological control of the direct fluid flow pathways between blood and brain could provide for invaluable therapeutic interventions in cerebral pathologies involving abnormal water fluxes such as stroke, hydrocephalus and brain tumours. AQP4 is a logical choice as a molecular target for drug development (Papadopoulos and Verkman, 2007; Yool et al., 2009). It is abundantly expressed in the central nervous system near the blood–brain barrier at glial cell endfeet and provides a major pathway for fluid homeostasis (Amiry-Moghaddam and Ottersen, 2003). Astrocytes have been proposed to have a bimodal contribution, with a positive role in fluid homeostasis and limiting brain injury, and a negative role in worsening the neuroinflammation, cerebral edema and elevated intracranial pressure associated with secondary brain injury following neurotrauma (Laird et al., 2008).

Now with the characterization of novel AQP agonists and antagonists, it will be possible to investigate potential pharmacological treatments for cerebral edema (Yool et al., 2009) with an intriguing capacity for bimodal regulation of AQP water channel activity. For example, in a rat model of cerebral edema induced by diffuse traumatic brain injury, a single intravenous application of the AQP antagonist AqB013 within 5 h post-injury dramatically reduced edema formation, and single administration of the AQP agonist AqF026 at 1–2 days post-injury accelerated the resolution of brain edema (Burton et al., unpublished data). Each modulator was beneficial alone; however, of interest was the observation that a sequential treatment of antagonist followed by agonist each at their optimal single time points provided a powerful combination that further enhanced the protection of motor function, reduced brain swelling and decreased brain albumin content post injury. Understanding the biphasic role of AQP4 in cerebral edema and the actions of AQP pharmacological modulators will be likely to open new avenues for the development of therapeutic interventions after traumatic brain injury.

14.4.2 Differential Regulation of Expression of AQP Channel Types in Cancer Cells

Evidence emerging within the past decade is providing increasingly strong support for the role of selected classes of AQPs as important constituents in cancer cell biological mechanisms. Data show a strong positive correlation between AQP expression levels and tumor severity (Machida et al., 2011). Tumor cells selectively increase levels of expression of different specific types of AQPs; in some cases, there is an increase in an AQP class normally expressed in the cell type (Saadoun et al., 2002a), but in other cancers, the upregulated class of AQP is not found at appreciable levels in the original tissue (Moon et al., 2003). AQPs are linked with a variety of properties of cancer cells, such as tumour size expansion, edema,

cell adhesion, migration and proliferation, which enhance tumour growth and metastasis (Hu and Verkman, 2006; Saadoun et al., 2002a,b).

For AQP1 and AQP5 channels, *de novo* expression has been observed in early stage colorectal carcinoma development but is not detectable in normal colonic epithelium (Moon et al., 1997, 2003) for purposes that remain incompletely understood in the context of cancer progression. When transfected into melanoma and breast cancer cell lines, increased AQP1 expression was associated with an increase in both *in vitro* cell migration and *in vivo* metastasis (Hu and Verkman, 2006). When melanoma cells B16F10 were implanted subcutaneously, AQP1 null mice showed slower melanoma tumour growth and impaired tumour angiogenesis as compared with wild-type mice (Saadoun et al., 2005).

AQP1 contributes to cell migration and angiogenesis and facilitates tumour growth and metastasis through mechanisms that remain to be defined. In its proposed activity as a dual water and ion channel (Yool and Weinstein, 2002), AQP1 could be one mechanism used for enhancing migration rate in a subset of classes of aggressive cancers. Facilitation of cell migration appears to be achieved in other types of cells by colocalization of water-selective AQPs in combination with ion transporters (Chai et al., 2013; Stroka et al., 2014).

AQP3 increased migration and proliferation of corneal epithelial cells in wild type as compared with *Aqp1* null mice and was important in peritoneal fibrosis and wound healing (Ryu et al., 2012). In squamous skin cell carcinomas and bronchioloalveolar carcinomas, AQP3 upregulation influenced metastasis and proliferation (Hara-Chikuma and Verkman, 2008a; Machida et al., 2011). After si-RNA knockdown of AQP3 expression, weaker cell adhesion and impaired cell growth were observed (Kusayama et al., 2011). In non-small cell lung cancer, AQP3 knockdown suppressed tumour growth and reduced angiogenesis (Xia et al., 2014). In agreement, AQP3 null mice show reduced glycerol transport and were more resistant to skin cancer formation (Hara-Chikuma and Verkman, 2008b).

AQP4 appears to assist with water balance in the tumour environment and has been postulated to play a role in cell–cell adhesion, possibly via an extracellular helical domain in loop C that could interact with adjacent cells. Expression of AQP4 conferred adhesive properties in cells that lacked classic adhesion molecules, as shown by L-cell cluster formation in AQP4-positive cells but not control cells (Hiroaki et al., 2006); however, other work has not confirmed the idea (Zhang and Verkman, 2008). More studies will be required to determine what factors influence a putative role of AQP4 in tumour cell adhesion. AQP4 can be phosphorylated by protein kinase C (PKC) at Ser-180. Phosphorylation level is inversely proportional to water permeability. Mutation of Ser-180 to alanine increased AQP4 water permeability by approximately twofold (McCoy et al., 2010). In AQP4-transfected glioma D54MG cells, both AQP4 water permeability and tumour cell migration were decreased when PKC was activated by phorbol ester treatment. It is postulated that cells with suppressed AQP4 activity have a compromised ability to adjust cell shape during migration (McCoy et al., 2010). In contrast, when D54MG cells were transfected with AQP1, neither of the properties of water channel activity or cell migration were affected by PKC modulators (McCoy et al., 2010).

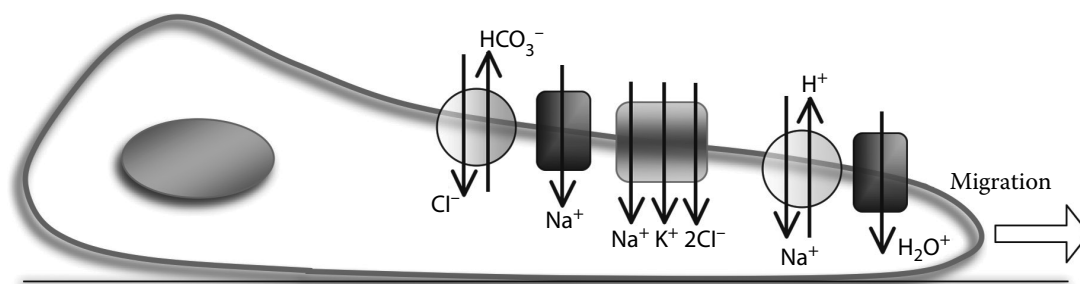


FIGURE 14.1 Schematic diagram of the colocalization of AQP channels with ion transporters, other channels and exchangers at the leading edge of a lamellipodium in a migrating cell.

AQP5 expression is increased in pancreatic, colon cancers and myelogenous leukemia cells (Machida et al., 2011; Woo et al., 2008). Proliferation of human ovarian cancer cells has also been correlated with AQP5 expression levels (Chae et al., 2008a). The involvement of AQP5 in cancer invasion has been demonstrated to depend on phosphorylation of Ser-156 located in the loop D domain through a cellular sarcoma kinase (c-Src) signalling pathway (Chae et al., 2008b). Deletion of AQP5 but not AQP1 nor AQP3 was correlated with decreased activation of the epithelial growth factor receptor signal cascade (EGFR/ERK/MAPK) which regulated cancer cell migration and proliferation (Zhang et al., 2010). Results from many studies now show that AQP3 and AQP5 contribute to processes of tumour proliferation, but the link from AQP function to the regulation of growth remains to be defined.

As depicted in Figure 14.1, AQP expression can be polarized in the lamellipodia of migrating cells, together with transporters such as the Na^+/H^+ , the $\text{Cl}^-/\text{HCO}_3^-$ exchanger or the $\text{Na}^+-\text{K}^+-\text{Cl}^-$ co-transporter. Localized ion fluxes are proposed to create a driving force for osmotic water fluxes, in parallel with the osmotic effects of actin polymerization and depolymerization, that could drive the membrane protrusions. This concept has been presented as an ‘osmotic engine model’ (Stroka et al., 2014) based on studies of AQP5 and Na^+/H^+ exchangers polarized to the leading edges in mouse S180 sarcoma cells migrating in a confined environment.

14.4.3 Targeting AQP1 Channels in Cell Migration and Metastasis

Tumour cell migration enables metastasis and tissue invasion and is a major cause of death in patients with cancer (Bogenrieder and Herlyn, 2003). A review of literature shows that AQP1 expression is upregulated in a subset of aggressive cancers, whereas AQP1 deletion or downregulation impedes migration of AQP1-expressing cancer cells *in vitro* and reduces metastasis *in vivo* (Deb et al., 2012; Verkman et al., 2008; Yool et al., 2009). Wound-healing and transwell migration assays have demonstrated impaired migration of tumour cells lacking AQP1 as compared to wild type (Jiang, 2009; Jiang et al., 2009; Jiang and Jiang, 2010; Li et al., 2006). Cell migration rate in AQP1 knockdown cells can be rescued by adenovirus-mediated AQP1 expression. Similarly, transfection of AQP1 into tumour cells that lack endogenous AQP1 show accelerated cell migration rate *in vitro* as compared to control cells (Hu and Verkman, 2006; McCoy and Sontheimer, 2007).

Manipulation of tumour cell migration rate via AQP1 expression levels has been explored in rodent models *in vivo*. Increased AQP1 expression increased tumour cell

extravasation, quantified by the numbers of fluorescently tagged tumour cells which infiltrated mouse lung tissue after injection into tail vein (Hu and Verkman, 2006). In a mouse model that spontaneously developed well-differentiated, luminal-type breast adenomas with lung metastases, genetic deletion of AQP1 correlated with reductions in lung metastases, tumour mass and tumour volume with abnormal microvascular anatomy and reduced vessel density as compared to wild-type mice (Esteva-Font et al., 2014). AQP1 expression facilitated endothelial cell migration and augmented tumour growth in vivo by the facilitation of angiogenesis (El Hindy et al., 2013; Nicchia et al., 2013). Impaired melanoma growth was observed in AQP1 null mice after subcutaneous tumour cell implantation and attributed to reduced aortic endothelial cell migration (Saadoun et al., 2005).

AQP1 is an attractive therapeutic target for controlling tumour growth and migration. Pharmacological modulation of AQP1 could be a pivotal adjunct to existing cancer therapies, improving the prognosis for cancer patients by slowing cancer angiogenesis and metastases.

14.5 NEW AVENUES FOR AQUAPORIN DRUG DISCOVERY FROM TRADITIONAL AND ALTERNATIVE MEDICINES

Complementary and alternative medicine practices provide an intriguing starting point in searches for novel pharmacological modulators for AQP channels, drawing on cultural insights of native botanical agents from Asian, indigenous Australian, American, Indian and other sources of cultural knowledge. Given the importance of AQPs in human health and disease, AQP modulatory agents have a compelling potential to benefit research and health care globally. Scientific evidence is needed to understand the molecular mechanisms that underlay therapeutic actions of alternative medicines which have been used around the world from ancient times to treat fluid imbalance disorders and diseases (de Moraes Lima et al., 2011; Karou et al., 2011; Kong et al., 2015; Nie et al., 2013). Possible agents for AQP channels might be present in native botanical agents used for treating conditions such as kidney and gastrointestinal disorders, swelling, brain edema and inflammation, which in theory could be benefiting from altered AQP channel activity in mitigating the dysfunctions.

Botanical compounds over many centuries have been an important source of useful drugs. As reviewed by Wachtel-Galor and Benzie (2011; CRC Press *Herbal Medicines: Biomolecular and Clinical Aspects*), about 25% of the drugs prescribed worldwide are derived from plants, including morphine derived from poppy seeds (*Papaver somniferum*), digoxin from foxglove (*Digitalis lanata*), aspirin from willow bark, antimalarials such as quinine from cinchona bark (*Cinchona officinalis*) and artemisinin derived from *Artemisia annua*. The potential value for translation into a novel pharmacology for AQP channels is immense. Expanding the pharmacological portfolio for AQPs will not only benefit basic research but could also prompt strategies for therapeutic interventions in cancers, lung and cardiac edema, secretory and digestive dysfunctions, and other conditions involving tissues in which AQPs are expressed.

Two principal groups of phytochemicals of interest appear to be emerging from the data available thus far: (1) polysaccharides (glucans) extracted from aqueous fractions and

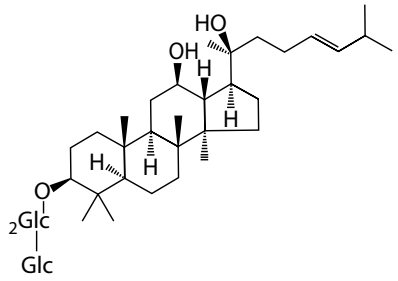
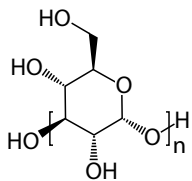
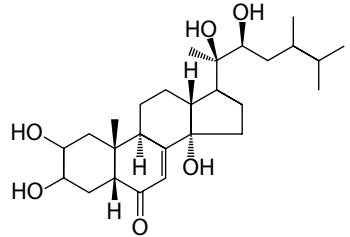
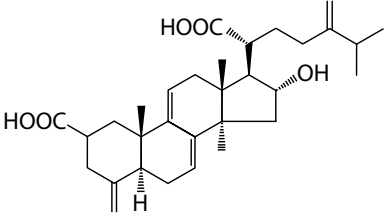
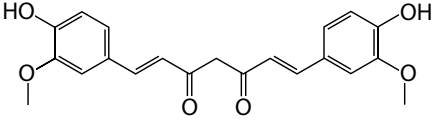
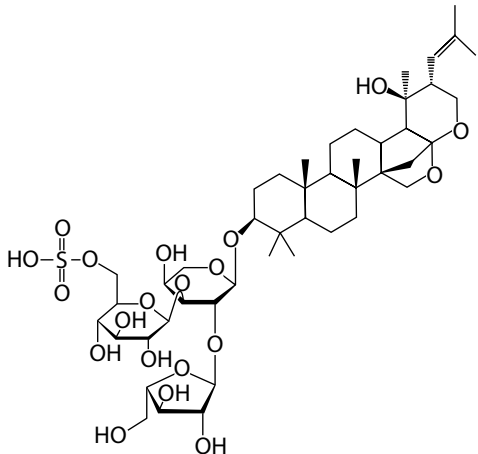
(2) triterpenes (polyporosterones) extracted from organic fractions of medicinal plants. A meta-analysis of published data on extracts and isolated compounds from an edible mushroom *Polyporus umbellatus* shows it acts as a diuretic, anti-cancer, immunostimulant and hepatoprotective agent (Zhao, 2013). An aqueous fraction of the Chinese medicinal fungus Fu Ling *Poria cocos* contains multiple saccharides and has been reported to attenuate renal AQP2 expression at the transcription and translational levels (Lee et al., 2012b). Extracts of Fu Ling also act as a diuretic and suppress the growth and invasiveness of various tumour cell lines (Cheng et al., 2013; Ling et al., 2011; Zhao et al., 2012). Similar to *P. umbellatus*, various triterpenes have been extracted and identified from *P. cocos* (Rios, 2011). In a study of papilloma carcinogenesis, poricoic acid C was demonstrated to decrease the incidence to 27% as compared with 100% in the control group (Akihisa et al., 2007). A bioactive compound (ginsenoside Rg3) found in the ginseng root extract was shown to attenuate cell migration via inhibition of AQP1 expression in PC-3M prostate cancer cells in vitro and demonstrated the potential usefulness of pharmacological modulation of AQP1 in manipulating tumour cell migration (Pan et al., 2012).

Diverse classes of channels and transporters are modulated by curcumin (isolated from turmeric in the ginger family), including voltage-gated K⁺ and Ca²⁺ channels, the volume-regulated anion channel (VRAC), the Ca²⁺ release-activated Ca²⁺ channel (CRAC), AQP4 channels, glucose transporters and others (Zhang et al., 2014). As compared with vehicle-injected rats, a lower level of AQP4 expression was observed in rats injected with 40 mg/kg curcumin. In the same experiment, a neuroprotective effect of curcumin was demonstrated in a rat model of hypoxic ischemic brain damage (Yu et al., 2012).

Bacopa (*Bacopa monnieri*), a water hyssop also known as Brahmi in traditional Indian medicine, has been used in complementary medicine remedies for centuries to improve memory and treat anxiety and depression (Russo and Borrelli, 2005). The main active components are triterpenes (bacosides, bacopasides and bacosaponins) (Russo and Borrelli, 2005). Some of the beneficial effects of bacopa could potentially involve AQP channels; however, the diverse group of candidate targets of action remains to be investigated. Tumour size decreased when mice with subcutaneously implanted S180 sarcoma cells were treated with bacopa extracts (Peng et al., 2010). Bacopa confers neuroprotective effects after ischemic brain injury (Liu et al., 2013; Saraf et al., 2010), which might suggest testing for a possible link with AQP4, known to be a key contributor in pathological outcomes of brain injury (Kim et al., 2010; Lee et al., 2012a; Shin et al., 2011). Bacopa also has also been used for control of epilepsy (Shanmugasundaram et al., 1991), and some anti-epileptic drugs have been demonstrated to inhibit AQP4 water permeability (Huber et al., 2009).

Plant-derived polysaccharide and triterpene compounds possess diverse pharmacological functions. A subset of them appear to have theoretical potential (based simply on the nature of their cellular and systemic effects in vivo) to regulate AQP levels of expression or function directly or indirectly. A sample of interesting phytochemical candidates and their structures is listed in Table 14.2. While still speculative at this point, the concept is worth further investigation. More research is needed focusing on phytochemicals as sources of candidate pharmacological agents for AQPs. Intriguing connections between botanical

TABLE 14.2 Phytochemicals Derived from Medicinal Plants Traditionally Used for Treating Potentially Aquaporin-Related Diseases

Plant Source	Compound	Structure
<i>Panax ginseng</i>	Ginsenoside Rg3	
<i>Polyporus umbellatus</i>	(1→3)- α -D-glucan	
	Polyporusterone A	
<i>Poria cocos</i>	Poricoic acid A	
<i>Curcuma longa</i>	Curcumin	
<i>Bacopa monnieri</i>	Bacopaside I	

(Continued)

TABLE 14.2 (Continued) Phytochemicals Derived from Medicinal Plants Traditionally Used for Treating Potentially Aquaporin-Related Diseases

Plant Source	Compound	Structure
	Bacopaside II	

medicinal agents and AQPs remain to be investigated but could be a valuable source of new lead compounds for broadening the field of AQP pharmacology and better understanding the molecular mechanisms of action of alternative medicinal agents.

REFERENCES

- Akihisa T, Nakamura Y, Tokuda H, Uchiyama E, Suzuki T, Kimura Y, Uchikura K and Nishino H (2007) Triterpene acids from *Poria cocos* and their anti-tumor-promoting effects. *Journal of Natural Products* **70**(6):948–953.
- Amiry-Moghaddam M and Ottersen OP (2003) The molecular basis of water transport in the brain. *Nature Reviews Neuroscience* **4**(12):991–1001.
- Anthony TL, Brooks HL, Boassa D, Leonov S, Yanochko GM, Regan JW and Yool AJ (2000) Cloned human aquaporin-1 is a cyclic GMP-gated ion channel. *Molecular Pharmacology* **57**(3):576–588.
- Avery S, Crockard HA and Russell RR (1984) Evolution and resolution of oedema following severe temporary cerebral ischaemia in the gerbil. *Journal of Neurology, Neurosurgery, and Psychiatry* **47**(6):604–610.
- Benga G, Popescu O, Pop VI and Holmes RP (1986) p-(Chloromercuri) benzenesulfonate binding by membrane proteins and the inhibition of water transport in human erythrocytes. *Biochemistry* **25**(7):1535–1538.
- Betz AL, Iannotti F and Hoff JT (1989) Brain edema: A classification based on blood-brain barrier integrity. *Cerebrovascular and Brain Metabolism Reviews* **1**(2):133–154.
- Boassa D, Stamer WD and Yool AJ (2006) Ion channel function of aquaporin-1 natively expressed in choroid plexus. *Journal of Neuroscience* **26**(30):7811–7819.
- Boassa D and Yool AJ (2002) A fascinating tail: cGMP activation of aquaporin-1 ion channels. *Trends in Pharmacology Sciences* **23**(12):558–562.
- Boassa D and Yool AJ (2003) Single amino acids in the carboxyl terminal domain of aquaporin-1 contribute to cGMP-dependent ion channel activation. *BMC Physiology* **3**:12.

- Bogenrieder T and Herlyn M (2003) Axis of evil: Molecular mechanisms of cancer metastasis. *Oncogene* **22**(42):6524–6536.
- Brooks HL, Regan JW and Yool AJ (2000) Inhibition of aquaporin-1 water permeability by tetraethylammonium: Involvement of the loop E pore region. *Molecular Pharmacology* **57**(5):1021–1026.
- Campbell EM, Birdsall DN and Yool AJ (2012) The activity of human aquaporin 1 as a cGMP-gated cation channel is regulated by tyrosine phosphorylation in the carboxyl-terminal domain. *Molecular Pharmacology* **81**(1):97–105.
- Castle NA (2005) Aquaporins as targets for drug discovery. *Drug Discovery Today* **10**(7):485–493.
- Chae YK, Kang SK, Kim MS, Woo J, Lee J, Chang S, Kim DW et al. (2008a) Human AQP5 plays a role in the progression of chronic myelogenous leukemia (CML). *PLoS One* **3**(7):e2594.
- Chae YK, Woo J, Kim MJ, Kang SK, Kim MS, Lee J, Lee SK et al. (2008b) Expression of aquaporin 5 (AQP5) promotes tumor invasion in human non small cell lung cancer. *PLoS One* **3**(5):e2162.
- Chai RC, Jiang JH, Kwan Wong AY, Jiang F, Gao K, Vatcher G and Hoi Yu AC (2013) AQP5 is differentially regulated in astrocytes during metabolic and traumatic injuries. *Glia* **61**(10):1748–1765.
- Cheng S, Eliaz I, Lin J, Thyagarajan-Sahu A and Sliva D (2013) Triterpenes from *Poria cocos* suppress growth and invasiveness of pancreatic cancer cells through the downregulation of MMP-7. *International Journal of Oncology* **42**(6):1869–1874.
- Conde A, Diallinas G, Chaumont F, Chaves M and Geros H (2010) Transporters, channels, or simple diffusion? Dogmas, atypical roles and complexity in transport systems. *The International Journal of Biochemistry and Cell Biology* **42**(6):857–868.
- Cowan CA, Yokoyama N, Bianchi LM, Henkemeyer M and Fritzsche B (2000) EphB2 guides axons at the midline and is necessary for normal vestibular function. *Neuron* **26**(2):417–430.
- de Moraes Lima GR, de Albuquerque Montenegro C, de Almeida CL, de Athayde-Filho PF, Barbosa-Filho JM and Batista LM (2011) Database survey of anti-inflammatory plants in South America: A review. *International Journal of Molecular Science* **12**(4):2692–2749.
- Deb P, Pal S, Dutta V, Boruah D, Chandran VM and Bhatoe HS (2012) Correlation of expression pattern of aquaporin-1 in primary central nervous system tumors with tumor type, grade, proliferation, microvessel density, contrast-enhancement and perilesional edema. *Journal of Cancer Research and Therapeutics* **8**(4):571–577.
- Detmers FJ, de Groot BL, Muller EM, Hinton A, Konings IB, Sze M, Flitsch SL, Grubmuller H and Deen PM (2006) Quaternary ammonium compounds as water channel blockers. Specificity, potency, and site of action. *Journal of Biological Chemistry* **281**(20):14207–14214.
- Diedler J, Sykora M, Blatow M, Juttler E, Unterberg A and Hacke W (2009) Decompressive surgery for severe brain edema. *Journal of Intensive Care Medicine* **24**(3):168–178.
- Ding JY, Kreipke CW, Speirs SL, Schafer P, Schafer S and Rafols JA (2009) Hypoxia-inducible factor-1 α signaling in aquaporin upregulation after traumatic brain injury. *Neuroscience Letters* **453**(1):68–72.
- Downey LA, Kean J, Nemeh F, Lau A, Poll A, Gregory R, Murray M et al. (2013) An acute, double-blind, placebo-controlled crossover study of 320 mg and 640 mg doses of a special extract of *Bacopa monnieri* (CDRI 08) on sustained cognitive performance. *Phytotherapy Research* **27**(9):1407–1413.
- El Hindy N, Bankfalvi A, Herring A, Adamzik M, Lambertz N, Zhu Y, Siffert W, Sure U and Sandalcioglu IE (2013) Correlation of aquaporin-1 water channel protein expression with tumor angiogenesis in human astrocytoma. *Anticancer Research* **33**(2):609–613.
- Esteva-Font C, Jin B-J and Verkman A (2014) Aquaporin-1 gene deletion reduces breast tumor growth and lung metastasis in tumor-producing MMTV-PyVT mice. *FASEB Journal* **28**(3):1446–1453.
- Feickert HJ, Drommer S and Heyer R (1999) Severe head injury in children: Impact of risk factors on outcome. *Journal of Trauma* **47**(1):33–38.

- Fischbarg J (2010) Fluid transport across leaky epithelia: Central role of the tight junction and supporting role of aquaporins. *Physiological Reviews* **90**(4):1271–1290.
- Fischer U, Taussky P, Gralla J, Arnold M, Brekenfeld C, Reinert M, Meier N et al. (2011) Decompressive craniectomy after intra-arterial thrombolysis: Safety and outcome. *Journal of Neurology, Neurosurgery & Psychiatry* **82**(8):885–887.
- Footer MJ, Kerssemakers JW, Theriot JA and Dogterom M (2007) Direct measurement of force generation by actin filament polymerization using an optical trap. *Proceedings of National Academy Science USA* **104**(7):2181–2186.
- Fotiadis D, Suda K, Tittmann P, Jenó P, Philippsen A, Müller DJ, Gross H and Engel A (2002) Identification and structure of a putative Ca²⁺-binding domain at the C terminus of AQP1. *Journal of Molecular Biology* **318**(5):1381–1394.
- Friedman B, Schachtrup C, Tasi PS, Shih AY, Akassoglou K, Kellinfield D and Lyden PD (2009) Acute vascular disruption and aquaporin 4 loss after stroke. *Stroke* **40**:2182–2190.
- Frigeri A, Nicchia GP and Svelto M (2007) Aquaporins as targets for drug discovery. *Current Pharmaceutical Design* **13**(23):2421–2427.
- Frydenlund DS, Bhardwaj A, Otsuka T, Mylonakou MN, Yasumura T, Davidson KG, Zeynalov E et al. (2006) Temporary loss of perivascular aquaporin-4 in neocortex after transient middle cerebral artery occlusion in mice. *Proceedings of the National Academy of Sciences* **103**:13532–13536.
- Fu D, Libson A, Miercke LJ, Weitzman C, Nollert P, Krucinski J and Stroud RM (2000) Structure of a glycerol-conducting channel and the basis for its selectivity. *Science* **290**(5491):481–486.
- Gao J, Wang X, Chang Y, Zhang J, Song Q, Yu H and Li X (2006) Acetazolamide inhibits osmotic water permeability by interaction with aquaporin-1. *Analytical Biochemistry* **350**(2):165–170.
- Grabarek Z (2006) Structural basis for diversity of the EF-hand calcium-binding proteins. *Journal of Molecular Biology* **359**(3):509–525.
- Hachez C and Chaumont F (2010) Aquaporins: A family of highly regulated multifunctional channels. *Advances in Experimental Medicine and Biology* **679**:1–17.
- Hacke W, Schwab S, Horn M, Spranger M, De Georgia M and von Kummer R (1996) ‘Malignant’ middle cerebral artery territory infarction: Clinical course and prognostic signs. *Archives of Neurology* **53**(4):309–315.
- Hara-Chikuma M and Verkman AS (2008a) Aquaporin-3 facilitates epidermal cell migration and proliferation during wound healing. *Journal of Molecular Medicine* **86**(2):221–231.
- Hara-Chikuma M and Verkman AS (2008b) Prevention of skin tumorigenesis and impairment of epidermal cell proliferation by targeted aquaporin-3 gene disruption. *Molecular and Cellular Biology* **28**(1):326–332.
- Higashida T, Kreipke CW, Rafols JA, Peng C, Schafer S, Schafer P, Ding JY et al. (2011) The role of hypoxia-inducible factor-1 α , aquaporin-4, and matrix metalloproteinase-9 in blood-brain barrier disruption and brain edema after traumatic brain injury. *Journal of Neurosurgery* **114**(1):92–101.
- Hiroaki Y, Tani K, Kamegawa A, Gyobu N, Nishikawa K, Suzuki H, Walz T et al. (2006) Implications of the aquaporin-4 structure on array formation and cell adhesion. *Journal of Molecular Biology* **355**(4):628–639.
- Hossmann YA (1994) Viability thresholds and the penumbra of focal ischemia. *Annals of Neurology* **36**:557–565.
- Hu J and Verkman AS (2006) Increased migration and metastatic potential of tumor cells expressing aquaporin water channels. *FASEB Journal* **20**(11):1892–1894.
- Huber VJ, Tsujita M, Kwee IL and Nakada T (2009) Inhibition of aquaporin 4 by antiepileptic drugs. *Bioorganic & Medicinal Chemistry* **17**(1):418–424.
- Huber VJ, Tsujita M and Nakada T (2012) Aquaporins in drug discovery and pharmacotherapy. *Molecular Aspects of Medicine* **33**(5–6):691–703.

- Huber VJ, Tsujita M, Yamazaki M, Sakimura K and Nakada T (2007) Identification of arylsulfonamides as aquaporin 4 inhibitors. *Bioorganic & Medicinal Chemistry Letters* **17**(5):1270–1273.
- Hyder AA, Wunderlich CA, Puvanachandra P, Gururaj G, Kobusingye OC (2007) The impact of traumatic brain injuries: A global perspective. *NeuroRehabilitation* **22**(5):341–53.
- Ishibashi K (2009) New members of mammalian aquaporins: AQP10–AQP12. *Handbook of Experimental Pharmacology* **2009**(190):251–262.
- Ishibashi K, Hara S and Kondo S (2009) Aquaporin water channels in mammals. *Clinical and Experimental Nephrology* **13**(2):107–117.
- Ishibashi K, Kondo S, Hara S and Morishita Y (2011) The evolutionary aspects of aquaporin family. *American Journal of Physiology. Regulatory Integrative Comparative Physiology* **300**(3):R566–R576.
- Jensen MO, Tajkhorshid E and Schulten K (2003) Electrostatic tuning of permeation and selectivity in aquaporin water channels. *Biophysical Journal* **85**(5):2884–2899.
- Jeyaseelan K, Sepramaniam S, Armugam A and Wintour EM (2006) Aquaporins: A promising target for drug development. *Expert Opinion on Therapeutic Targets* **10**(6):889–909.
- Jiang Y (2009) Aquaporin-1 activity of plasma membrane affects HT20 colon cancer cell migration. *IUBMB Life* **61**(10):1001–1009.
- Jiang Y, Chen K, Zhang T and Luo X (2009) Down-regulation of aquaporin-1 in W489 colon cancer cells inhibits cell migration, *Bioinformatics and Biomedical Engineering*. Paper presented at Third International Conference on Bioinformatics and Biomedical Engineering, Beijing, pp. 1–5, Piscataway, New Jersey: IEEE.
- Jiang Y and Jiang Z-B (2010) Aquaporin 1-expressing MCF-7 mammary carcinoma cells show enhanced migration in vitro. *Journal of Biomedical Science and Engineering* **3**(01):95.
- Jullienne A and Badaut J (2013) Molecular contributions to neurovascular unit dysfunctions after brain injuries: Lessons for target-specific drug development. *Future Neurology* **8**(6):677–689.
- Karou SD, Tchacondo T, Ilboudo DP and Simpore J (2011) Sub-Saharan Rubiaceae: A review of their traditional uses, phytochemistry and biological activities. *Pakistan Journal of Biological Sciences* **14**(3):149–169.
- Katakai T, Habiro K and Kinashi T (2013) Dendritic cells regulate high-speed interstitial T cell migration in the lymph node via LFA-1/ICAM-1. *Journal of Immunology* **191**(3):1188–1199.
- Kater S and Letourneau P (1985) *Biology of the Nerve Growth Cone*. Alan R Liss, New York.
- Kaur C, Sivakumar V, Zhang Y and Ling EA (2006) Hypoxia-induced astrocytic reaction and increased vascular permeability in the rat cerebellum. *Glia* **54**(8):826–839.
- Kim JH, Lee YW, Park KA, Lee WT and Lee JE (2010) Agmatine attenuates brain edema through reducing the expression of aquaporin-1 after cerebral ischemia. *Journal of Cerebral Blood Flow and Metabolism* **30**(5):943–949.
- King LS, Kozono D and Agre P (2004) From structure to disease: The evolving tale of aquaporin biology. *Nature Review Molecular Cell Biology* **5**(9):687–698.
- Kong G, Zhao Y, Li GH, Chen BJ, Wang XN, Zhou HL, Lou HX, Ren DM and Shen T (2015) The genus *Litsea* in traditional Chinese medicine: An ethnomedical, phytochemical and pharmacological review. *Journal of Ethnopharmacology* **164**:256–264.
- Kusayama M, Wada K, Nagata M, Ishimoto S, Takahashi H, Yoneda M, Nakajima A, Okura M, Kogo M and Kamisaki Y (2011) Critical role of aquaporin 3 on growth of human esophageal and oral squamous cell carcinoma. *Cancer Science* **102**(6):1128–1136.
- Laird MD, Vender JR and Dhandapani KM (2008) Opposing roles for reactive astrocytes following traumatic brain injury. *Neurosignals* **16**(2–3):154–164.
- Le Clainche C and Carlier MF (2008) Regulation of actin assembly associated with protrusion and adhesion in cell migration. *Physiological Reviews* **88**(2):489–513.
- Lee K, Jo IY, Park SH, Kim KS, Bae J, Park JW, Lee BJ, Choi HY and Bu Y (2012a) Defatted sesame seed extract reduces brain oedema by regulating aquaporin 4 expression in acute phase of transient focal cerebral ischaemia in rat. *Phytotherapy Research: PTR* **26**(10):1521–1527.

- Lee SM, Lee YJ, Yoon JJ, Kang DG and Lee HS (2012b) Effect of *Poria cocos* on hypertonic stress-induced water channel expression and apoptosis in renal collecting duct cells. *Journal of Ethnopharmacology* **141**(1):368–376.
- Li Y, Feng X, Yang H and Ma T (2006) Expression of aquaporin-1 in SMMC-7221 liver carcinoma cells promotes cell migration. *Chinese Science Bulletin* **51**(20):2466–2471.
- Ling H, Zhang Y, Ng KY and Chew EH (2011) Pachymic acid impairs breast cancer cell invasion by suppressing nuclear factor-kappaB-dependent matrix metalloproteinase-9 expression. *Breast Cancer Research and Treatment* **126**(3):609–620.
- Liu X, Yue R, Zhang J, Shan L, Wang R and Zhang W (2013) Neuroprotective effects of bacopa-side I in ischemic brain injury. *Restorative Neurology and Neuroscience* **31**(2):109–123.
- Ma B, Xiang Y, Mu SM, Li T, Yu HM and Li XJ (2004) Effects of acetazolamide and anordiol on osmotic water permeability in AQP1-cRNA injected *Xenopus* oocyte. *Acta Pharmacologica Sinica* **25**(1):90–97.
- Macey R (1984) Transport of water and urea in red blood cells. *American Journal of Cell Physiology* **246**:C195–C203.
- Macey RI, Karan DM and Farmer RE (1972) Properties of water channels in human red cells. *Biomembranes* **3**:331–340.
- Machida Y, Ueda Y, Shimasaki M, Sato K, Sagawa M, Katsuda S and Sakuma T (2011) Relationship of aquaporin 1, 3, and 5 expression in lung cancer cells to cellular differentiation, invasive growth, and metastasis potential. *Human Pathology* **42**(5):669–678.
- Mack AF and Wolburg H (2013) A novel look at astrocytes: Aquaporins, ionic homeostasis, and the role of the microenvironment for regeneration in the CNS. *Neuroscientist* **19**(2):195–207.
- Madeira A, Moura TF and Soveral G (2014) Aquaglyceroporins: Implications in adipose biology and obesity. *Cellular and Molecular Life Science*. **72**(4):759–771.
- Manley GT, Fujimura M, Ma T, Noshita N, Filiz F, Bollen AW, Chan P and Verkman AS (2000) Aquaporin-4 deletion in mice reduces brain edema after acute water intoxication and ischemic stroke. *Nature Medicine* **6**(2):159–163.
- Manno EM, Adams RE, Derdeyn CP, Powers WJ and Diringer MN (1999) The effects of mannitol on cerebral edema after large hemispheric cerebral infarct. *Neurology* **52**(3):583–587.
- Marcy Y, Prost J, Carlier MF and Sykes C (2004) Forces generated during actin-based propulsion: A direct measurement by micromanipulation. *Proceedings of National Academy of Sciences of United States of America* **101**(16):5992–5997.
- Masel BE, DeWitt DS (2010) Traumatic brain injury: a disease process, not an event. *Journal of Neurotrauma* **27**(8):1529–1540.
- McCoy E and Sontheimer H (2007) Expression and function of water channels (aquaporins) in migrating malignant astrocytes. *Glia* **55**(10):1034–1043.
- McCoy ES, Haas BR and Sontheimer H (2010) Water permeability through aquaporin-4 is regulated by protein kinase C and becomes rate-limiting for glioma invasion. *Neuroscience* **168**(4):971–981.
- McLeod DD, Beard DJ, Parsons MW, Levi CR, Calford MB and Spratt NJ (2013) Inadvertent occlusion of the anterior choroidal artery explains infarct variability in the middle cerebral artery thread occlusion stroke model. *PLoS One* **8**(9):e75779.
- McLeod DD, Parsons MW, Levi CR, Beaument S, Buxton D, Roworth B and Spratt NJ (2011) Establishing a rodent stroke perfusion computed tomography model. *International Journal of Stroke* **6**(4):284–289.
- Meng F, Rui Y, Xu L, Wan C, Jiang X and Li G (2014) Aqp1 enhances migration of bone marrow mesenchymal stem cells through regulation of FAK and beta-catenin. *Stem Cells and Development* **23**(1):66–75.
- Migliati E, Meurice N, DuBois P, Fang JS, Somasekharan S, Beckett E, Flynn G and Yool AJ (2009) Inhibition of aquaporin-1 and aquaporin-4 water permeability by a derivative of the loop diuretic bumetanide acting at an internal pore-occluding binding site. *Molecular Pharmacology* **76**(1):105–112.

- Miller LP, Hsu C (1992) Therapeutic potential for adenosine receptor activation in ischemic brain injury. *Journal of Neurotrauma* **2**:563–577.
- Minami S, Kobayashi H, Yamashita A, Yanagita T, Uezono Y, Yokoo H, Shiraishi S et al. (2001) Selective expression of aquaporin 1, 4 and 5 in the rat middle ear. *Hearing Research* **158**(1–2):51–56.
- Moon C, King LS and Agre P (1997) Aqp1 expression in erythroleukemia cells: Genetic regulation of glucocorticoid and chemical induction. *The American Journal of Physiology* **273**(5 Part 1):C1562–1570.
- Moon C, Rousseau R, Soria JC, Hoque MO, Lee J, Jang SJ, Trink B, Sidransky D and Mao L (2004) Aquaporin expression in human lymphocytes and dendritic cells. *American Journal of Hematology* **75**(3):128–133.
- Moon C, Soria JC, Jang SJ, Lee J, Obaidul Hoque M, Sibony M, Trink B, Chang YS, Sidransky D and Mao L (2003) Involvement of aquaporins in colorectal carcinogenesis. *Oncogene* **22**(43):6699–6703.
- Murtha LA, McLeod DD, McCann SK, Pepperall D, Chung S, Levi CR, Calford MB and Spratt NJ (2014a) Short-duration hypothermia after ischemic stroke prevents delayed intracranial pressure rise. *International Journal of Stroke* **9**(5):553–559.
- Murtha LA, McLeod DD, Pepperall D, McCann SK, Beard DJ, Tomkins AJ, Holmes WM, McCabe C, Macrae IM and Spratt NJ (2014b) Intracranial pressure elevation after ischemic stroke in rats: Cerebral edema is not the only cause, and short-duration mild hypothermia is a highly effective preventive therapy. *Journal of Cerebral Blood Flow & Metabolism*. **35**(4):592–600.
- Naccache P and Sha'afi RI (1974) Effect of PCMBS on water transfer across biological membranes. *Journal of Cell Physiology* **83**(3):449–456.
- Nagelhus EA, Ottersen OP (2013) Physiological roles of aquaporin-4 in brain. *Physiological Review* **93**(4):1543–1562.
- Nicchia GP, Stigliano C, Sparaneo A, Rossi A, Frigeri A and Svelto M (2013) Inhibition of aquaporin-1 dependent angiogenesis impairs tumour growth in a mouse model of melanoma. *Journal of Molecular Medicine (Berlin, Germany)* **91**(5):613–623.
- Nie Y, Dong X, He Y, Yuan T, Han T, Rahman K, Qin L and Zhang Q (2013) Medicinal plants of genus *Curculigo*: Traditional uses and a phytochemical and ethnopharmacological review. *Journal of Ethnopharmacology* **147**(3):547–563.
- Nielsen S, Kwon TH, Frokiaer J and Agre P (2007) Regulation and dysregulation of aquaporins in water balance disorders. *Journal of Internal Medicine* **261**(1):53–64.
- Niemietz CM and Tyerman SD (2002) New potent inhibitors of aquaporins: Silver and gold compounds inhibit aquaporins of plant and human origin. *FEBS Letters* **531**(3):443–447.
- Pan XY, Guo H, Han J, Hao F, An Y, Xu Y, Xiaokaiti Y, Pan Y and Li XJ (2012) Ginsenoside Rg3 attenuates cell migration via inhibition of aquaporin 1 expression in PC-3M prostate cancer cells. *European Journal of Pharmacology* **683**(1–3):27–34.
- Papadopoulos MC, Manley GT, Krishna S and Verkman AS (2004) Aquaporin-4 facilitates reabsorption of excess fluid in vasogenic brain edema. *The Federation of American Societies for Experimental Biology Journal* **18**:1291–1293.
- Papadopoulos MC and Verkman AS (2007) Aquaporin-4 and brain edema. *Pediatric Nephrology* **22**(6):778–784.
- Papadopoulos MC and Verkman AS (2008) Potential utility of aquaporin modulators for therapy of brain disorders. *Progress in Brain Research* **170**:589–601.
- Parekh SH, Chaudhuri O, Theriot JA and Fletcher DA (2005) Loading history determines the velocity of actin-network growth. *Nature Cell Biology* **7**(12):1219–1223.
- Park E, Bell JD and Baker AJ (2008) Traumatic brain injury: Can the consequences be stopped? *Canadian Medical Association Journal* **178**(9):1163–1170.
- Peng L, Zhou Y, Kong de Y and Zhang WD (2010) Antitumor activities of dammarane triterpene saponins from *Bacopa monniera*. *Phytotherapy Research: PTR* **24**(6):864–868.

- Preston GM and Agre P (1991) Isolation of the cDNA for erythrocyte integral membrane protein of 28 kilodaltons: Member of an ancient channel family. *Proceedings of National Academy of Sciences of United States of America* **88**(24):11110–11114.
- Preston GM, Carroll TP, Guggino WB and Agre P (1992) Appearance of water channels in *Xenopus* oocytes expressing red cell CHIP28 protein. *Science* **256**(5055):385–387.
- Rios JL (2011) Chemical constituents and pharmacological properties of *Poria cocos*. *Planta Medica* **77**(7):681–691.
- Rohini G and Devi CS (2008) *Bacopa monniera* extract induces apoptosis in murine sarcoma cells (S-180). *Phytotherapy Research: PTR* **22**(12):1595–1598.
- Russo A and Borrelli F (2005) *Bacopa monniera*, a reputed nootropic plant: An overview. *Phytomedicine: International Journal of Phytotherapy and Phytopharmacology* **12**(4):305–317.
- Ryu HM, Oh EJ, Park SH, Kim CD, Choi JY, Cho JH, Kim IS et al. (2012) Aquaporin 3 expression is up-regulated by TGF-beta1 in rat peritoneal mesothelial cells and plays a role in wound healing. *American Journal of Pathology* **181**(6):2047–2057.
- Saadoun S, Papadopoulos MC, Davies DC, Bell BA and Krishna S (2002a) Increased aquaporin 1 water channel expression in human brain tumours. *British Journal of Cancer* **87**(6):621–623.
- Saadoun S, Papadopoulos MC, Davies DC, Krishna S and Bell BA (2002b) Aquaporin-4 expression is increased in oedematous human brain tumours. *Journal of Neurology, Neurosurgery, and Psychiatry* **72**(2):262–265.
- Saadoun S, Papadopoulos MC, Hara-Chikuma M and Verkman AS (2005) Impairment of angiogenesis and cell migration by targeted aquaporin-1 gene disruption. *Nature* **434**(7034):786–792.
- Sairam K, Dorababu M, Goel RK and Bhattacharya SK (2002) Antidepressant activity of standardized extract of *Bacopa monniera* in experimental models of depression in rats. *Phytomedicine: International Journal of Phytotherapy and Phytopharmacology* **9**(3):207–211.
- Saparov SM, Kozono D, Rothe U, Agre P and Pohl P (2001) Water and ion permeation of aquaporin-1 in planar lipid bilayers. Major differences in structural determinants and stoichiometry. *Journal of Biological Chemistry* **276**(34):31515–31520.
- Saraf MK, Prabhakar S and Anand A (2010) Neuroprotective effect of *Bacopa monniera* on ischemia induced brain injury. *Pharmacology, Biochemistry, and Behavior* **97**(2):192–197.
- Seeliger D, Zapater C, Krenc D, Haddoub R, Flitsch S, Beitz E, Cerda J and de Groot BL (2013) Discovery of novel human aquaporin-1 blockers. *ACS Chemical Biology* **8**(1):249–256.
- Shanmugasundaram ER, Akbar GK and Shanmugasundaram KR (1991) Brahmighritham, an Ayurvedic herbal formula for the control of epilepsy. *Journal of Ethnopharmacology* **33**(3):269–276.
- Shenaq M, Kassem H, Peng C, Schafer S, Ding JY, Fredrickson V, Guthikonda M, Kreipke CW, Rafols JA and Ding Y (2012) Neuronal damage and functional deficits are ameliorated by inhibition of aquaporin and HIF1alpha after traumatic brain injury (TBI). *Journal of the Neurological Sciences* **323**(1–2):134–140.
- Shi W-Z, Qi L-L, Fang S-H, Lu Y-B, Zhang W-P and Wei E-Q (2012) Aggravated chronic brain injury after focal cerebral ischemia in aquaporin-4-deficient mice. *Neuroscience Letters* **520**(1):121–125.
- Shin JA, Choi JH, Choi YH and Park EM (2011) Conserved aquaporin 4 levels associated with reduction of brain edema are mediated by estrogen in the ischemic brain after experimental stroke. *Biochimica et Biophysica Acta* **1812**(9):1154–1163.
- Singh HK and Dhawan BN (1982) Effect of *Bacopa monniera* Linn. (brahmi) extract on avoidance responses in rat. *Journal of Ethnopharmacology* **5**(2):205–214.
- Stroka KM, Jiang H, Chen SH, Tong Z, Wirtz D, Sun SX and Konstantopoulos K (2014) Water permeation drives tumor cell migration in confined microenvironments. *Cell* **157**(3):611–623.
- Sui H, Han BG, Lee JK, Walian P and Jap BK (2001) Structural basis of water-specific transport through the AQP1 water channel. *Nature* **414**(6866):872–878.

- Taniguchi M, Yamashita T, Kumura E, Tamatani M, Kobayashi A, Yokawa T, Maruno M et al. (2000) Induction of aquaporin-4 water channel mRNA after focal cerebral ischemia in rat. *Brain Research Molecular Brain Research* **78**(1–2):131–137.
- Tornroth-Horsefield S, Wang Y, Hedfalk K, Johanson U, Karlsson M, Tajkhorshid E, Neutze R and Kjellbom P (2006) Structural mechanism of plant aquaporin gating. *Nature* **439**(7077):688–694.
- Tourdias T, Mori N, Dragonu I, Cassagno N, Boiziau C, Aussudre J, Brochet B, Moonen C, Petry KG and Douset V (2011) Differential aquaporin 4 expression during edema build-up and resolution phases of brain inflammation. *Journal of Neuroinflammation* **8**:143.
- Tyerman SD, Niemietz CM and Bramley H (2002) Plant aquaporins: Multifunctional water and solute channels with expanding roles. *Plant Cell & Environment* **25**(2):173–194.
- Ukiya M, Akihisa T, Tokuda H, Hirano M, Oshikubo M, Nobukuni Y, Kimura Y, Tai T, Kondo S and Nishino H (2002) Inhibition of tumor-promoting effects by poricoic acids G and H and other lanostane-type triterpenes and cytotoxic activity of poricoic acids A and G from *Poria cocos*. *Journal of Natural Products* **65**(4):462–465.
- Vahedi K, Vicaut E, Mateo J, Kurtz A, Orabi M, Guichard JP, Boutron C et al. (2007) Sequential-design, multicenter, randomized, controlled trial of early decompressive craniectomy in malignant middle cerebral artery infarction (DECIMAL trial). *Stroke* **38**(9):2506–2517.
- Van Duijn B and Inouye K (1991) Regulation of movement speed by intracellular pH during *Dictyostelium discoideum* chemotaxis. *Proceedings of National Academy of Sciences on United States of America* **88**(11):4951–4955.
- Verkman A, Hara-Chikuma M and Papadopoulos MC (2008) Aquaporins—New players in cancer biology. *Journal of Molecular Medicine* **86**(5):523–529.
- von Bulow J, Muller-Lucks A, Kai L, Bernhard F and Beitz E (2012) Functional characterization of a novel aquaporin from *Dictyostelium discoideum* amoebae implies a unique gating mechanism. *Journal of Biological Chemistry* **287**(10):7487–7494.
- Ware MF, Wells A and Lauffenburger DA (1998) Epidermal growth factor alters fibroblast migration speed and directional persistence reciprocally and in a matrix-dependent manner. *Journal of Cell Science* **111**(Part 16):2423–2432.
- Werner C and Engelhard K (2007) Pathophysiology of traumatic brain injury. *British Journal of Anaesthesia* **99**(1):4–9.
- Winter CD, Adamides AA, Lewis PM and Rosenfeld JV (2005) A review of the current management of severe traumatic brain injury. *Surgeon* **3**(5):329–337.
- Woo J, Lee J, Chae YK, Kim MS, Baek JH, Park JC, Park MJ et al. (2008) Overexpression of AQP5, a putative oncogene, promotes cell growth and transformation. *Cancer Letters* **264**(1):54–62.
- Xia H, Ma YF, Yu CH, Li YJ, Tang J, Li JB, Zhao YN and Liu Y (2014) Aquaporin 3 knockdown suppresses tumour growth and angiogenesis in experimental non-small cell lung cancer. *Experimental Physiology* **99**(7):974–984.
- Xiao M, Hu G (2014) Involvement of aquaporin 4 in astrocyte function and neuropsychiatric disorders. *CNS Neuroscience & Therapeutics* **20**(5):385–390.
- Yamamoto N, Yoneda K, Asai K, Sobue K, Tada T, Fujita Y, Katsuya H et al. (2001) Alterations in the expression of the AQP family in cultured rat astrocytes during hypoxia and reoxygenation. *Brain Research Molecular Brain Research* **90**(1):26–38.
- Yool AJ (2007a) Aquaporins: Multiple roles in the central nervous system. *Neuroscientist* **13**(5):470–485.
- Yool AJ (2007b) Functional domains of aquaporin-1: Keys to physiology, and targets for drug discovery. *Current Pharmaceutical Design* **13**(31):3212–3221.
- Yool AJ, Brokl OH, Pannabecker TL, Dantzler WH and Stamer WD (2002) Tetraethylammonium block of water flux in aquaporin-1 channels expressed in kidney thin limbs of Henle's loop and a kidney-derived cell line. *BMC Physiology* **2**:4.

- Yool AJ, Brown EA and Flynn GA (2009) Roles for novel pharmacological blockers of aquaporins in the treatment of brain oedema and cancer. *Clinical and Experimental Pharmacology & Physiology* **37**(4):403–409.
- Yool AJ and Campbell EM (2012) Structure, function and translational relevance of aquaporin dual water and ion channels. *Molecular Aspects of Medicine* **33**(5–6):553–561.
- Yool AJ, Morelle J, Cnops Y, Verbavatz JM, Campbell EM, Beckett EA, Booker GW, Flynn G and Devuyt O (2013) AqF026 is a pharmacologic agonist of the water channel aquaporin-1. *Journal of the American Society of Nephrology: JASN* **24**(7):1045–1052.
- Yool AJ and Weinstein AM (2002) New roles for old holes: Ion channel function in aquaporin-1. *News Physiological Sciences* **17**:68–72.
- Yu J, Yool AJ, Schulten K and Tajkhorshid E (2006) Mechanism of gating and ion conductivity of a possible tetrameric pore in aquaporin-1. *Structure* **14**(9):1411–1423.
- Yu L, Yi J, Ye G, Zheng Y, Song Z, Yang Y, Song Y, Wang Z and Bao Q (2012) Effects of curcumin on levels of nitric oxide synthase and AQP-4 in a rat model of hypoxia-ischemic brain damage. *Brain Research* **1475**:88–95.
- Zardoya R (2005) Phylogeny and evolution of the major intrinsic protein family. *Biology of the Cell* **97**(6):397–414.
- Zelenina M, Zelenin S, Bondar AA, Brismar H and Aperia A (2002) Water permeability of aquaporin-4 is decreased by protein kinase C and dopamine. *American Journal of Physiology. Renal Physiology* **283**(2):F309–F318.
- Zhang H and Verkman AS (2008) Evidence against involvement of aquaporin-4 in cell-cell adhesion. *Journal of Molecular Biology* **382**(5):1136–1143.
- Zhang W, Zitron E, Homme M, Kihm L, Morath C, Scherer D, Hegge S et al. (2007) Aquaporin-1 channel function is positively regulated by protein kinase C. *Journal of Biological Chemistry* **282**(29):20933–20940.
- Zhang X, Chen Q, Wang Y, Peng W and Cai H (2014) Effects of curcumin on ion channels and transporters. *Frontiers in Physiology* **5**:94.
- Zhang Z, Chen Z, Song Y, Zhang P, Hu J and Bai C (2010) Expression of aquaporin 5 increases proliferation and metastasis potential of lung cancer. *The Journal of Pathology* **221**(2):210–220.
- Zhao YY (2013) Traditional uses, phytochemistry, pharmacology, pharmacokinetics and quality control of *Polyporus umbellatus* (Pers.) fries: A review. *Journal of Ethnopharmacology* **149**(1):35–48.
- Zhao YY, Feng YL, Du X, Xi ZH, Cheng XL and Wei F (2012) Diuretic activity of the ethanol and aqueous extracts of the surface layer of *Poria cocos* in rat. *Journal of Ethnopharmacology* **144**(3):775–778.

Bumetanide Derivatives AqB007 and AqB011 Selectively Block the Aquaporin-1 Ion Channel Conductance and Slow Cancer Cell Migration[Ⓢ]

Mohamad Kourghi,¹ Jinxin V. Pei,¹ Michael L. De Ieso, Gary Flynn, and Andrea J. Yool

School of Medicine (M.K., J.V.P., M.L.D.I., A.J.Y.) and Institute for Photonics and Advanced Sensing (J.V.P., A.J.Y.), University of Adelaide, Adelaide, South Australia, Australia; and Spacefill Enterprises LLC, Oro Valley, Arizona (G.F.)

Received September 3, 2015; accepted October 13, 2015

ABSTRACT

Aquaporins (AQPs) in the major intrinsic family of proteins mediate fluxes of water and other small solutes across cell membranes. AQP1 is a water channel, and under permissive conditions, a nonselective cation channel gated by cGMP. In addition to mediating fluid transport, AQP1 expression facilitates rapid cell migration in cell types including colon cancers and glioblastoma. Work here defines new pharmacological derivatives of bumetanide that selectively inhibit the ion channel, but not the water channel, activity of AQP1. Human AQP1 was analyzed in the *Xenopus laevis* oocyte expression system by two-electrode voltage clamp and optical osmotic swelling assays. The aquaporin ligand bumetanide derivative AqB011 was the most potent blocker of the AQP1 ion conductance (IC₅₀ of 14 μM), with no effect on water channel activity (at up to

200 μM). The order of potency for inhibition of the ionic conductance was AqB011 > AqB007 >> AqB006 ≅ AqB001. Migration of human colon cancer (HT29) cells was assessed with a wound-closure assay in the presence of a mitotic inhibitor. AqB011 and AqB007 significantly reduced migration rates of AQP1-positive HT29 cells without affecting viability. The order of potency for AQP1 ion channel block matched the order for inhibition of cell migration, as well as in silico modeling of the predicted order of energetically favored binding. Docking models suggest that AqB011 and AqB007 interact with the intracellular loop D domain, a region involved in AQP channel gating. Inhibition of AQP1 ionic conductance could be a useful adjunct therapeutic approach for reducing metastasis in cancers that upregulate AQP1 expression.

Introduction

Osmotic water transport across biologic membranes is facilitated by membrane proteins known as aquaporins (AQPs), which are found in all kingdoms of life (Reizer et al., 1993; Park and Saier, 1996; Campbell et al., 2008). To date, at least 15 mammalian subfamilies have been identified: AQP0–AQP14 (Ishibashi, 2009; Finn et al., 2014). Aquaporin is organized as a tetramer of subunits, each comprising six transmembrane domains and five loops (A–E) and carrying a monomeric pore that allows the movement of water or other small solutes (Jung et al., 1994; Fu et al., 2000; Sui et al., 2001).

There is increasing recognition that certain classes of aggressive cancers depend on upregulation of AQP1 for fast migration and metastasis (Monzani et al., 2007). Although the precise mechanism for AQP1-enhanced motility remains unknown, both ion and water channels are essential in the cellular migration process (Schwab et al., 2007). AQP1

expression has been linked to metastasis and invasiveness of colon cancer cells (Jiang, 2009; Yoshida et al., 2013). In mammary and melanoma cancer cells, AQP1 facilitates tumor cell migration in vitro and metastasis in vivo (Hu and Verkman, 2006). Increased levels of AQP1 expression in astrocytoma correlate with the clinical grade, serving as a diagnostic indicator of poor prognoses (El Hindy et al., 2013). AQP1-facilitated cell migration in glioma cannot be substituted by AQP4, indicating more than a simple water channel function is involved in the migration-enhancing mechanism (McCoy and Sontheimer, 2007).

A subset of aquaporins have been shown to have ion channel function, including AQP0, AQP1, AQP6, plant nodulin, and *Drosophila* big brain (Yool and Campbell, 2012). In AQP1, multiple lines of evidence have shown the cGMP-dependent monovalent cation channel is located in the central pore at the 4-fold axis of symmetry and is pharmacologically distinct from the monomeric water pores (Anthony et al., 2000; Saparov et al., 2001; Boassa and Yool, 2003; Yu et al., 2006; Zhang et al., 2007). The AQP1 ion channel has a unitary conductance of 150 picosiemens in physiologic saline, slow activation and deactivation kinetics, and is permeable to Na⁺, K⁺, and Cs⁺, but not divalent cations (Yool et al., 1996; Anthony et al., 2000). Loop D has been shown previously to be involved in cGMP-dependent gating of AQP1 ion channels (Yu et al.,

This work was supported in part by the National Institutes of Health [Grant R01 GM059986] and a 2015 pilot grant from the Institute for Photonics and Advanced Sensing, University of Adelaide.

¹M.K. and J.V.P. are co-first authors.
dx.doi.org/10.1124/mol.115.101618

[Ⓢ] This article has supplemental material available at molpharm.aspetjournals.org.

ABBREVIATIONS: AqB, aquaporin ligand bumetanide derivative (in numbered series); AQP1, aquaporin-1; DMSO, dimethylsulfoxide; ETOAC, ethyl acetate; MW, molecular weight.

2006). The low proportion of AQP1 water channels that are available to be gated as ion channels in reconstituted bilayers and heterologous expression systems has prompted uncertainty regarding the physiologic relevance of the dual water and ion channel function in AQP1 (Saparov et al., 2001; Tsunoda et al., 2004). Further work has indicated that the availability of AQP1 ion channels to be activated by cGMP depends in part on tyrosine phosphorylation at the carboxyl terminal domain (Campbell et al., 2012).

Our characterization here of selective nontoxic pharmacological blockers of the AQP1 ion channel opens the first opportunity to define the functional roles of the AQP1 ion conductance. Prior to 2009, available AQP1 blockers were limited by low potency, lack of specificity, or toxicity. Mercury potently blocks AQP1 water permeability by covalent modification of a cysteine residue in loop E (Preston et al., 1993), but is highly toxic. The tetraethylammonium ion blocks the AQP1 water pore, although not in all cell types (Brooks et al., 2000; Detmers et al., 2006; Sogaard and Zeuthen, 2008), and the cadmium ion blocks the AQP1 ion channel (Boassa et al., 2006), but both lack selectivity for aquaporins. Effective compounds discovered recently include the arylsulfonamides AqB013, which blocks AQP1 and AQP4 water channel permeability (Migliati et al., 2009), and AqF026, which strongly potentiates AQP1 water channel activity (Yool et al., 2013). Other arylsulfonamides have been proposed as blockers of AQP4 channels (Huber et al., 2009). A distinct class of agents acting on the external side of the membrane to block human AQP1 water flux has been identified as a source of candidate lead compounds for drug development (Seeliger et al., 2013).

Work here characterizes a novel set of aquaporin ligand bumetanide derivative (AqB) compounds that differentially block the AQP1 ion channel without affecting water permeability. The most potent of these, AqB011, is a promising tool for dissecting the role of the AQP1 ion channel while sparing osmotic water permeability. Understanding the functional roles and regulation of AQP1 is essential for determining the full range of physiologic roles it might serve and its possible value as a therapeutic target in cancer metastasis.

Materials and Methods

Oocyte Preparation and Injection. The use of animals in this study has been carried out in accordance with the Guide for the Care and Use of Laboratory Animals, licensed under the South Australian Animal Welfare Act 1985, with protocols approved by the University of Adelaide Animal Ethics Committee. Unfertilized oocytes were harvested from anesthetized *Xenopus laevis* frogs and defolliculated by incubation in type 1A collagenase (2 mg/ml) with a trypsin inhibitor (0.3 mg/ml) in OR-2 saline (82 mM NaCl, 2.5 mM KCl, 1 mM MgCl₂, and 5 mM HEPES; pH 7.3) at 16–18°C for 2 to 3 hours. Human aquaporin-1 cDNA was provided by Professor P. Agre (Preston et al., 1992; GenBank accession number NM_198098). AQP1 subcloned into a *X. laevis* β -globin plasmid was linearized with BamHI and transcribed in vitro (T3 mMessage mMachine; Ambion Inc., Austin, TX), and cRNA was resuspended in sterile water. Prepared oocytes were injected with 50 nl of water (non-AQP1-expressing control oocytes) or 50 nl of water containing 1 ng of AQP1 cRNA and incubated for 2 or more days at 16°C in ND96 saline (96 mM NaCl, 2 mM KCl, 1 mM MgCl₂, 1.8 mM CaCl₂, and 5 mM HEPES, pH 7.3) to allow protein expression. Successful expression was confirmed by osmotic swelling assays. Batches of AQP1-expressing oocytes that lacked robust cGMP-activated conductance responses were further incubated overnight in ND96 saline with the tyrosine phosphatase inhibitor

bisperoxovanadium (100 μ M; Santa Cruz Biotechnology, Dallas, TX) per published methods (Campbell et al., 2012). Chemicals were purchased from Sigma-Aldrich (St. Louis, MO) unless otherwise specified.

AqB Compounds: Synthesis and Preparation. The AqB compounds (custom-designed bumetanide derivatives) were synthesized by Dr. G. Flynn (Spacefill Enterprises LLC, Oro Valley, AZ) as described in U.S. patent 8,835,491-B2. To make AqB001, bumetanide was mixed with diazomethane (CH₂N₂) generated by reaction with Diazald to create bumetanide methyl ester [molecular weight (MW) 344.8; ClogP 2.10], which was dissolved in hot CHCl₃, diluted with hexanes and allowed to cool to provide the purified methyl ester as white flakes, whose mass and NMR spectra were consistent with the desired product. Reaction of bumetanide with 1.2 equivalents of 1,1'-carbonyldiimidazole in ethyl acetate (EtOAc) under argon with heating afforded an intermediate imidazolide, which upon cooling, formed a white solid that could be isolated by filtration and stored under argon for later use. Alternatively, the imidazolide solution could be reacted in situ with two equivalents of an amine to form the corresponding amides. In a typical reaction, the reaction mixture would be partitioned between water and EtOAc, the organic layer would be washed with brine, the solution would be filtered and concentrated, and the residue would be crystallized to form EtOAc/hexanes. AqB-006 (MW 413.9; ClogP 1.04) was prepared using morpholine as the amine; AqB007 (MW 470.0; ClogP 0.79) resulted from 2-(4-methylpiperazine-1-yl) ethylamine; and AqB011 (MW 434.9; ClogP 1.80) was prepared using 2-(morpholine-1-yl)ethylamine. The structures of all the compounds were confirmed by high-resolution mass spectrometry and NMR analysis. Chemicals were purchased from Sigma-Aldrich unless otherwise specified.

Powdered compounds were dissolved in dimethylsulfoxide (DMSO) to create 1000 \times stock solutions for each desired final dosage. An equal dilution of DMSO (0.1%) alone in saline was used as the vehicle control.

Quantitative Swelling Assay. For double-swelling assays, each oocyte served as its own control. Swelling rates were assayed first without drug treatment (S1), and then oocytes incubated for 2 hours in isotonic saline with or without the AqB compounds were reassessed in a second swelling assay (S2). Swelling rates in 50% hypotonic saline (isotonic Na saline diluted with an equal volume of water) were quantified by relative increases in the oocyte cross-sectional area imaged by videomicroscopy (charge-coupled device camera; Cohu, San Diego, CA) at 0.5 frames per second for 30 seconds using National Institutes of Health ImageJ software (Bethesda, MD). Rates were measured as the slopes of the linear regression fits of relative volume as a function of time using Prism (GraphPad Software Inc., San Diego, CA).

Electrophysiology. For the two-electrode voltage clamp, capillary glass electrodes (1–3 M Ω) were filled with 1 M KCl. Recordings were done in standard Na⁺ bath saline containing 100 mM NaCl, 2 mM KCl, 4.5 mM MgCl₂, and 5 mM HEPES, pH 7.3. cGMP was applied extracellularly at a final concentration of 10–20 μ M using the membrane-permeable cGMP analog (Rp)-8-(*para*-chlorophenylthio)-cGMP. Ionic conductance was monitored for at least 20 minutes after cGMP addition to allow development of maximal plateau responses. Conductance was determined by voltage step protocols from +60 to –110 mV from a holding potential of –40 mV. Recordings were made with a GeneClamp amplifier and pClamp 9.0 software (Molecular Devices, Sunnyvale, CA).

Circular Wound Closure Assay. The cancer cell lines used in this study were HT29 human colorectal adenocarcinoma cells (Chen et al., 1987) purchased from American Type Culture Collection (HTB-38; Manassas, VA), which strongly express endogenous AQP1, and SW480 human colorectal adenocarcinoma cells (CCL-228; from American Type Culture Collection), which express AQP5 but show little AQP1 expression. mRNA levels were evaluated by quantitative polymerase chain reaction and protein levels by western blot (H. Dorward et al., submitted manuscript). Confluent cultures of

HT29 and SW480 cells were used in migration assays to measure the effects of AqB treatments on rates of wound closure. Cells were plated in flat-bottom 96-well plates at 1.25×10^5 cells/well in Dulbecco's modified Eagle's medium with 10% fetal bovine serum and incubated at 37°C and 5% CO₂ for 12–18 hours to allow monolayer formation. Circular wounds were created by aspirating a central circle of cells with a p10 pipette. Wells were washed 2 to 3 times with phosphate-buffered saline to remove cell debris. Culture media (Dulbecco's modified Eagle's medium with 2% bovine calf serum) containing either vehicle or drug treatments in the presence of a mitotic inhibitor 5-fluoro-2'-deoxyuridine (100 ng/ml) were administered into the wells. Cultures were imaged at 0 and 24 hours and analyzed using ImageJ software to calculate the percent wound closure by the change in area:

$$[(\text{Area}_0 - \text{Area}_{24})/\text{Area}_0] \times 100$$

Cytotoxicity Assay. Cell viability was quantified using the alamarBlue cell viability assay (Molecular Probes, Eugene, OR). Cells were plated at 10^4 cells/well in 96-well plates, and fluorescence signal levels were measured with a FLUOstar Optima microplate reader (BMG Labtech, Victoria, Australia) after 24-hour incubation, with concentrations of AqB011 ranging from 1 to 80 μM , to obtain quantitative measures of cell viability. Mercuric chloride (20 μM) was used as a positive control for cytotoxicity.

Molecular Modeling. In silico modeling was conducted with methods reported previously (Yool et al., 2013). The crystal structure of human AQP1 was obtained from the Protein Data Bank (PDB) (identity 1FQY). The tetrameric model (Supplemental Material) was generated in Pymol (Version 1.7.4; Schrödinger, LLC; Mannheim, Germany) using coordinates provided in the pdb file. Renderings of the AqB ligands were generated in Chemdraw (Version 13.0; PerkinElmer, MA) and then converted into the pdb format using the online SMILES translation tool (National Cancer Institute, U.S. Department Health and Human Services, Washington, DC). Both AQP1 and ligand coordinates were prepared for docking using MGLtools (Version 1.5.4; Scripps Institute, San Diego, CA). The docking was carried using Autodock Vina (Trott and Olson, 2010), with a docking grid covering the intracellular face of tetrameric pore.

Data Compilation and Statistics. The results compiled from replicate experiments are presented as box plots. The boxes represent

50% of the data, the error bars indicate the full range, and the horizontal bars are the median values. The *n* values are in italics above the *x*-axis. Statistical differences were analyzed with one-way analysis of variance and post hoc Bonferroni tests and reported as ***P* < 0.0001, **P* < 0.05, and N.S. (*P* > 0.05).

Results

AQP1 Ion Channel Inhibition by Novel Bumetanide Derivatives. A set of four related compounds with structural modifications at the carboxylic acid moiety of bumetanide was tested for effects on the cGMP-activated ionic conductance in AQP1-expressing oocytes. Two-electrode voltage clamp recordings of AQP1-expressing oocytes (Fig. 1) illustrate the inhibition of the ionic conductance by extracellular application of AqB007 (200 μM) and AqB011 (20 μM), but no appreciable block of the AQP1 ion channel with 200 μM AqB001 or AqB006. Initial recordings before cGMP application and responses to the first application of cGMP recordings showed typical cGMP-dependent activation, as described previously (Anthony et al., 2000). Oocytes were then transferred into saline with the indicated agents for 2 hours, during which time the ionic conductances uniformly recovered to initial levels (Fig. 2). In response to the second application of cGMP, oocytes treated with vehicle (DMSO), AqB001, or AqB006 showed increases in conductance that were comparable to the first response. However, the cGMP-activated conductance responses were inhibited after treatment with AqB007 or AqB011.

Trend plots (Fig. 2A) show that the ionic conductance in AQP1-expressing oocytes was initially low and activated by the first bath application of membrane-permeable cGMP. The ionic conductance then recovered to the basal level during 2-hour incubation without cGMP and was tested for reactivation by a second application of cGMP after treatment with vehicle or AqB compounds. Recordings for oocytes incubated in saline without DMSO during the recovery period were comparable to

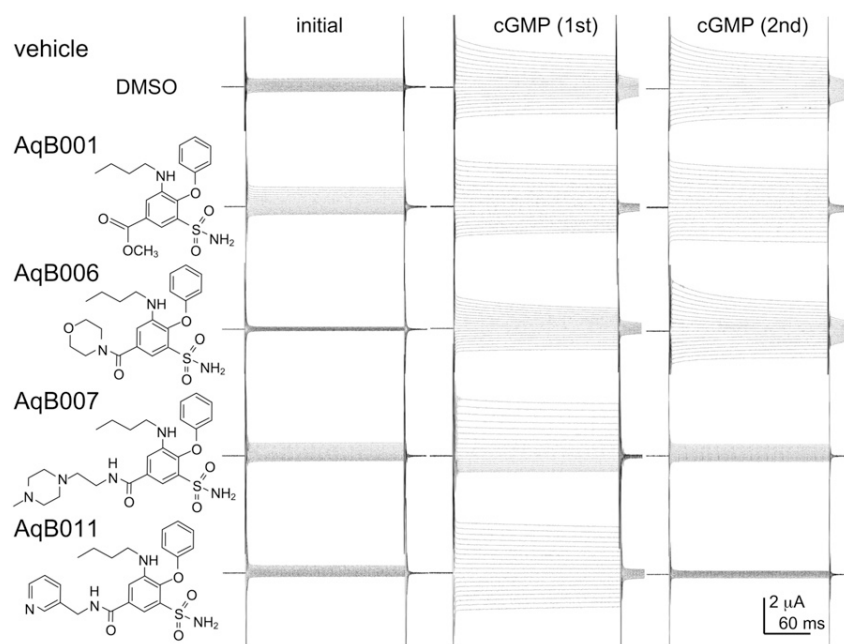


Fig. 1. Chemical structures of selected bumetanide derivatives and electrophysiology traces showing representative effects of AqB001, AqB006, AqB007, and AqB011 on the ionic conductance responses activated by bath application of CPT-cGMP before and after 2-hour incubation in saline with and without the AqB compounds. See *Materials and Methods* for details.

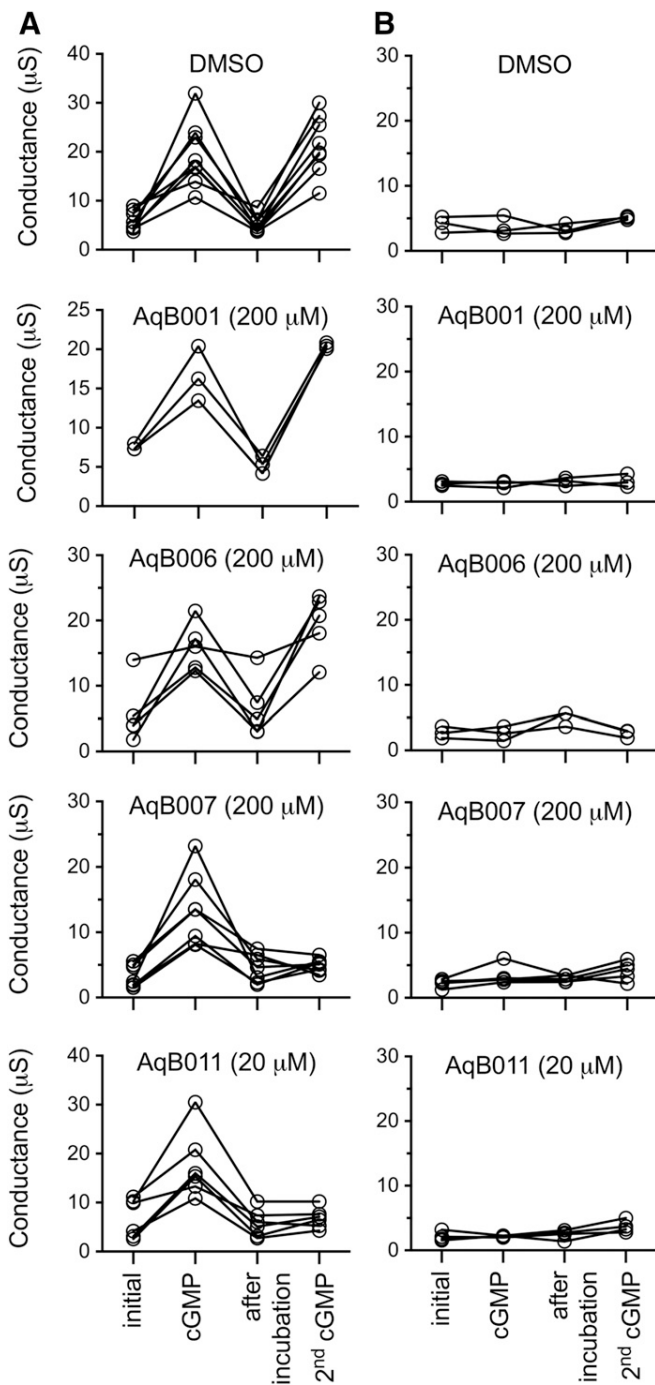


Fig. 2. Trend plots showing the ionic conductance responses for individual oocytes measured prior to cGMP (initial), after the first cGMP application, after 2-hour incubation in saline without cGMP containing DMSO (vehicle) or AqB agents, and after the second application of cGMP. Reversible cGMP-dependent activation of an ionic conductance in AQP1-expressing oocytes (A) was not seen in non-AQP1 control oocytes (B). Inhibition was seen after treatment with AqB007 and AqB011, but not with vehicle, AqB001, or AqB006.

those for the DMSO-treated group (not shown). Non-AQP1-expressing control oocytes showed no ionic conductance response to cGMP and no effect of the vehicle or drug treatments (Fig. 2B).

Compiled data for the cGMP-activated ionic conductance values in AQP1-expressing oocytes are shown in the box plot

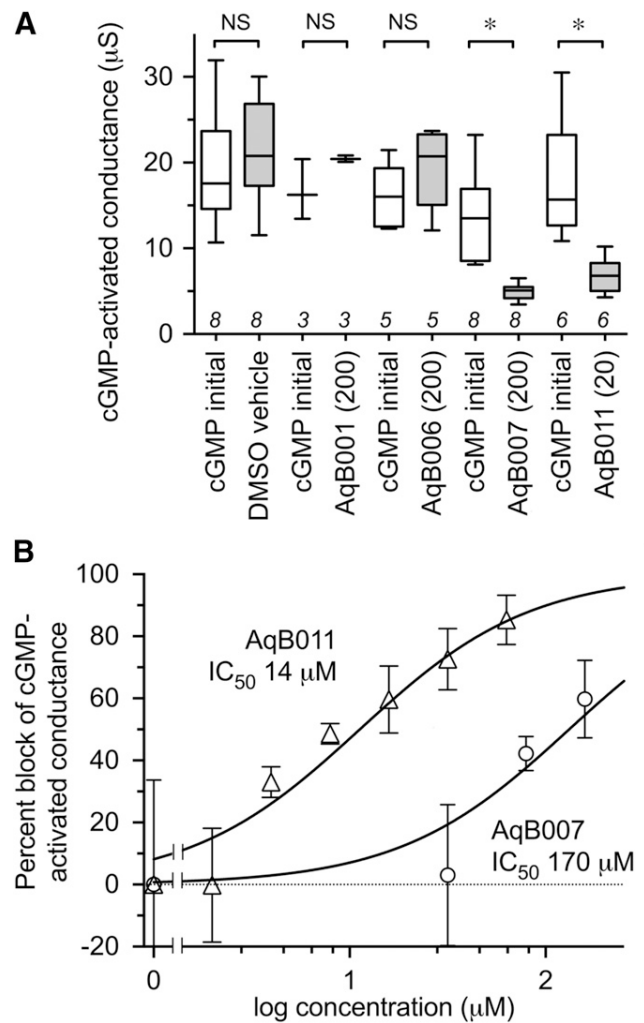


Fig. 3. Dose-dependent block of the AQP1 ionic conductance. (A) Compiled box plot data showing a statistically significant block of the cGMP-activated ionic conductance in AQP1-expressing oocytes by AqB007 and AqB011, but not with vehicle, AqB001, or AqB006. See *Materials and Methods* for details. (B) Dose-response curves showing percent block of the activated ionic conductance in AQP1-expressing oocytes and estimated IC_{50} values. n values for dose-response data (in order of increasing concentration) for AqB007 and AqB011 were 8, 4, 2, 8 and 8, 2, 2, 3, 6, 4, 3, respectively.

(Fig. 3A) and indicate the levels of block by 200 μ M AqB007 and 20 μ M AqB011 were statistically significant as compared with initial responses to cGMP prior to treatment. Dose-response relationships (Fig. 3B) yielded estimated IC_{50} values of 14 μ M for AqB011 and 170 μ M for AqB007.

AqB Ion Channel Blockers Have No Effect on Osmotic Water Permeability. Data for oocyte volumes that were standardized as a percentage of the initial volume at time zero illustrate the mean swelling responses over 60 seconds after introduction of the oocytes into 50% hypotonic saline (Fig. 4A). AQP1-expressing oocytes showed consistent osmotic swelling, which was unaffected by treatment with vehicle (DMSO 0.1%) or AqB compounds at 200 μ M each. Non-AQP1-expressing control oocytes showed little osmotic water permeability.

To analyze the possible effects of the AqB compounds on water channel activity, a double-swelling assay was used (Fig. 4B).

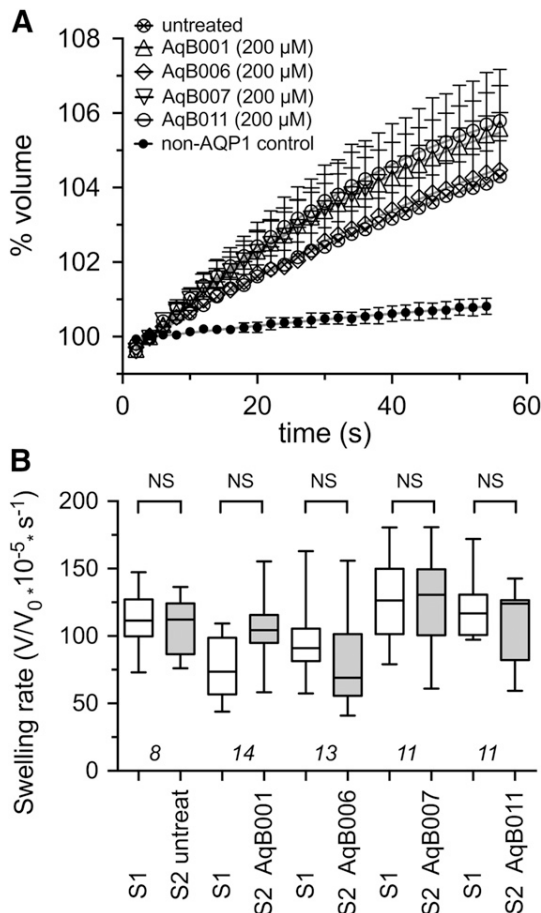


Fig. 4. Lack of effect of AqB compounds on AQP1 osmotic water permeability measured by optical swelling assays. (A) Mean oocyte volume, standardized as a percentage of the initial volume for each oocyte, as a function of time after introduction into 50% hypotonic saline, with and without 2-hour pretreatment with AqB compounds at 200 μ M or vehicle (0.1% DMSO). (B) Compiled box plot data showing the absence of any statistically significant differences between the first and second swelling rates measured before (S1) and after (S2) 2-hour incubations in saline alone or saline with 200 μ M AqB compounds as indicated. See *Materials and Methods* for details.

After the first swelling (S1) in hypotonic saline, oocytes were incubated in isotonic saline with or without the AqB compounds (200 μ M) for 2 hours before assessing the second swelling response (S2). There were no significant differences between the first and second swelling rates in any of the treatment groups, confirming that the AqB ion channel agents did not affect AQP1 osmotic water permeability.

Molecular Modeling of Candidate Intracellular Binding Sites. Putative binding sites on the AQP1 ion pore for AqB011 and AqB007 in the intracellular loop D domain can be suggested based on structural modeling and docking analyses (Fig. 5). In silico modeling suggested the sites for the most favorable energies of interaction for AqB007 and AqB011 were located at the intracellular face of the central pore (Fig. 5A). Interestingly, the model predicted hydrogen bonding between the uniquely elongated moieties of the two effective AqB ligands and the initial pairs of arginine residues in the highly conserved loop D motifs from two adjacent subunits (Fig. 5B). The same arginines (R159 and R160 in human AQP1) have been shown to be involved in

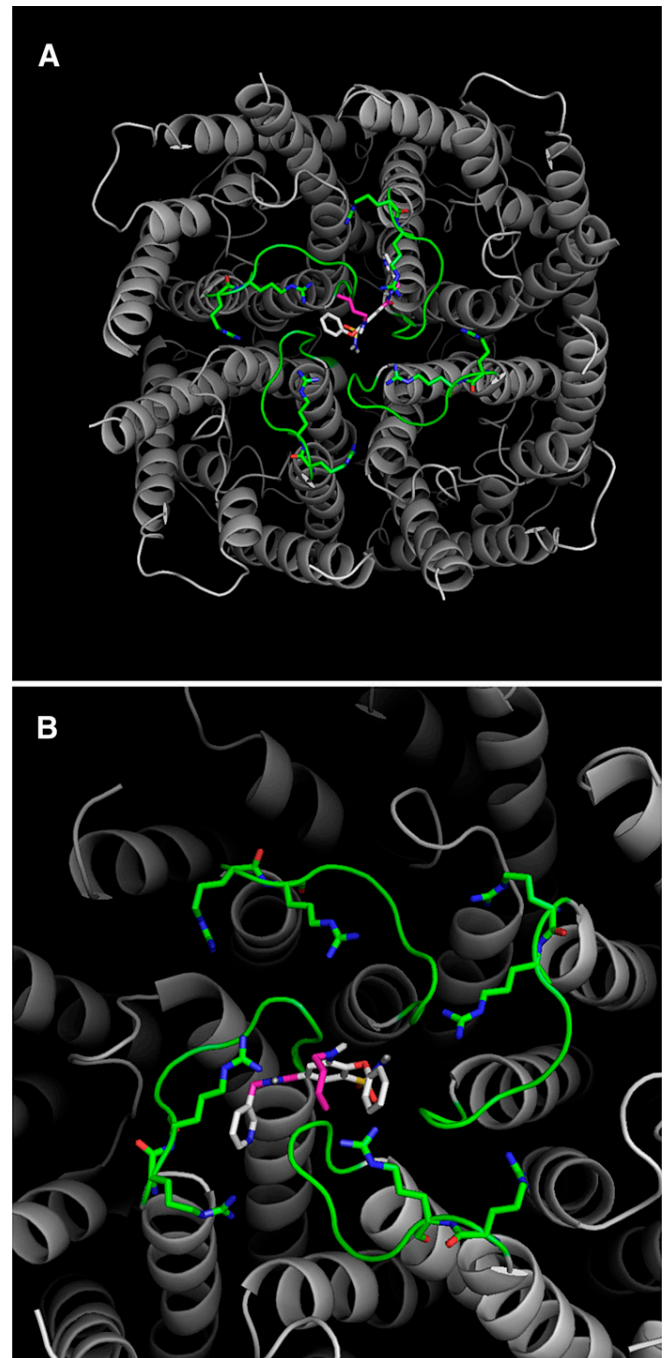


Fig. 5. In silico modeling of the energetically favored binding site for AqB011 in the center of the tetrameric channel of AQP1 (gray) at the intracellular side and bracketed by the gating loop D domains (green). The putative binding site suggests an interaction with two of the loop D domains from adjacent subunits. (A) is the full view of the tetramer, and (B) is a closer view slightly rotated to show proximity of the ligand to the conserved arginine residues in loop D.

AQP1 ion channel gating, but not water channel activity, in prior work (Yu et al., 2006). The more compact AqB006 docked weakly at a different position in the central vestibule (not shown). Although in silico modeling does not define actual binding sites, it provides a testable hypothesis for future work and offers intriguing support for the role of loop D in modulating AQP1 ion channel gating. The most

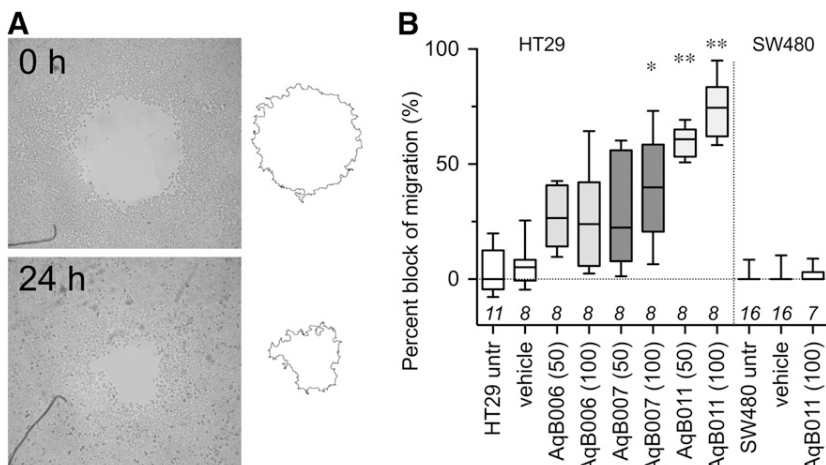


Fig. 6. Block of cell migration in AQP1-expressing HT29, but not SW480, cells treated with AqB011. (A) Illustrative diagram of the circular wound healing method showing substantial closure of the wounded area in normal culture medium by 24 hours. (B) Compiled box plot data from wound closure assays showing the dose-dependent inhibitory effects of AqB007 and AqB011 compared with DMSO and AqB006 on wound closure at 24 hours in HT29 cell cultures. Migration of SW480 cells was not altered by AqB011.

favorable energy of interaction was calculated for AqB011 (at -9.2 kcal/mol). The next most favorable energy of interaction for AqB compounds with the AQP1 channel was for AqB007 (at -7.0 kcal/mol), followed by AqB006 (at -6.0 kcal/mol). This order of interaction strength for the AqB series matched their order of efficacy for inhibition of the AQP1 ion channel conductance (Fig. 3).

Inhibition of AQP1 Ion Channel Activity Slows Cancer Cell Migration. The effects of AqB006, AqB007, and AqB011 were tested in migration assays of human HT29 colon cancer cells (Fig. 6), which natively express AQP1. Net migration rates were calculated from the percent closure of a circular wound area at 24 hours (Fig. 6A). The results showed that cancer cell migration was not impaired by AqB006, but was significantly impaired by AqB007 at $100 \mu\text{M}$ and AqB011 at 50 and $100 \mu\text{M}$, as compared with vehicle-treated control HT29 cells (Fig. 6B). AqB011 was more effective than AqB007 in blocking migration, which is consistent with the relative efficacies of the agents as blockers of the ion channel conductance. In contrast, AqB011 at $100 \mu\text{M}$ had no effect on the migration rate of SW480 colon cancer cells (Fig. 6B), which express AQP5, but not AQP1, suggesting that the inhibitory effect of AqB011 appears to be selective for AQP1.

AqB Compounds Show Low Cytotoxicity. There was no significant difference in the viability of vehicle-treated and untreated cells and no effect of treatment with AqB011 for HT29 cells (Table 1). Cell viability was assessed with alamarBlue assays. The persistence of the fluorescent signal at 24 hours confirmed there was no appreciable cytotoxic effect of AqB011 treatment on HT29 cells at concentrations of up to $80 \mu\text{M}$. Mercuric chloride as a positive control caused significant cell death, which was measured as a decrease in fluorescence. AqB011 at doses used to block the AQP1 ionic conductance and cancer cell migration did not impact cell viability.

Discussion

The aim of this study was to search for selective small-molecule pharmacological agents that are capable of blocking the cGMP-activated cationic conductance in AQP1. Discovery of pharmacological modulators for AQP1 channels has been an important goal in the aquaporin field. AQP1 antagonist and agonist agents are expected to be useful for defining the

complex roles of aquaporins in fundamental biologic processes as well as characterizing AQP1 modulators as potential clinical agents in various conditions, such as cancer metastasis (Yool et al., 2010). AQP1 expression is upregulated in subtypes of aggressive cancer cells, in which it facilitates cancer migration. The results here show that selective blockers of the AQP1 ion channel slow the migration of human colon cancer cells in culture. Pharmacological inhibition of AQP1 is predicted to have a protective effect in reducing metastasis in cancer, but remains to be demonstrated in vivo.

Using bumetanide as a starting scaffold, we created an array of novel synthetic derivatives. Based on pilot data indicating a small inhibitory effect of AqB050 on the AQP1 ion channel at high doses (unpublished data), we investigated a series of structurally related derivatives, AqB006, AqB007, and AqB011, as well as a simple methylated version of bumetanide, AqB001, to test for possible inhibitors of the AQP1 ionic conductance. Our findings demonstrated that AqB007 and AqB011 are effective inhibitors of the central ion pore of AQP1, with estimated IC_{50} values of 170 and $14 \mu\text{M}$, respectively. Both AqB007 and AqB011 showed dose-dependent inhibition of the central ion pore, whereas the intrasubunit water pores were unaffected, enabling the first dissection of physiologic roles of the distinct channel functions. Measuring fluorescence signal intensity with the alamarBlue

TABLE 1

HT29 cell levels of cytotoxicity after 24-hour incubation in culture medium with vehicle, AqB011, or HgCl_2

Agent (AqB011)	Mean Normalized Cell Viability \pm S.E.M. ^a	n Value	Statistical Significance
μM	%		
0 (untreated)	100.0 ± 0.70	8	—
0 (0.1% DMSO)	103.9 ± 0.91	8	N.S.
1	104.0 ± 1.06	4	N.S.
5	102.3 ± 2.26	4	N.S.
10	110.6 ± 2.12	4	N.S.
20	114.0 ± 0.84	4	N.S.
40	111.8 ± 1.33	4	N.S.
80	102.4 ± 2.95	4	N.S.
HgCl_2 ($100 \mu\text{M}$)	16.2 ± 0.20	3	**

^aPercent viability was standardized as a percentage of the untreated mean value measured as changes in alamarBlue fluorescence signal intensity. See *Materials and Methods* for details.

cell viability assay showed that AqB011 was not cytotoxic at doses that produced maximal ion channel inhibition.

The inhibition by AqB011 of AQP1 ionic conductance was consistent with molecular docking studies, suggesting the site of interaction is at the intracellular face of the central pore. The results revealed that AqB011 is the most energetically favored compound, followed by AqB007. The predicted interaction site of AqB011 and AqB007 with AQP1 is at the loop D domain. Differences in the structures and efficacies of AqB006, AqB007, and AqB011 indicate that the structure-activity relationship of ion channel inhibition is sensitive to specific chemical modifications at the carboxylic acid position of bumetanide. The length and structure of the modification appears to be critical and based on *in silico* modeling to be the region that interacts with the AQP1 channel gating loop D domain. The absence of cytotoxic effects of AqB011 at doses sufficient to block the AQP1 ion channel activity indicates that the inhibition of migration is not indirectly due to cell death. The observation that AqB011 inhibited migration in AQP1-expressing HT29 colon cancer cells, but had no effect on the migration of AQP-5-expressing SW480 colon cancer cells, provides support for the idea that AqB011 is selective for AQP1. The inhibition of migration seen with AqB011 is unlikely to result from off-target effects on general metabolic function, cytoskeletal organization, actin polymerization, or signaling pathways involved in cell motility since SW480 cell migration remained unaffected by the presence of AqB011.

AQP1 is present in barrier epithelia involved in fluid movement in the body, including the proximal tubule and choroid plexus (Agre et al., 1993). It is also expressed in peripheral microvasculature, dorsal root ganglion cells, eye ciliary epithelium and trabecular meshwork, heart ventricles, and other regions, in which a direct role for osmotic water flux is less evident (Yool, 2007). Additional roles suggested for AQP1 include angiogenesis (Nicchia et al., 2013), signal transduction (Oshio et al., 2006), increased mechanical compliance to changes in pressure (Baetz et al., 2009), axonal regeneration of spinal nerves (Zhang and Verkman, 2015), recovery from injury (Hara-Chikuma and Verkman, 2006), and exocytosis (Arnaoutova et al., 2008). Relative contributions of the ion and water channel functions in these diverse processes remain to be defined.

A possible role for the AQP1 ionic conductance (potentially in combination with water fluxes) in the control of cell volume associated with migration was supported by the results of the wound closure assays with AQP1-expressing HT29 cells. Cell migration was significantly impaired by AqB011 and AqB007, but not by AqB006. The greatest efficacy of migration block was seen with administration of AqB011. The comparable orders of efficacy for the block of AQP1 ion channels in the oocyte expression system and for the block of cell migration in HT29 cultures support the idea that the AqB011 effect on migration is mediated by direct block of the AQP1 ion channels. These data provide evidence that the ion channel activity of AQP1 has physiologic relevance. Further work is needed to evaluate the effects of blocking both water and ion channel activities of AQP1 together in migrating cells.

AqB011 is a new research tool for probing the physiologic role of the AQP1 ion channel function in biologic systems. This compound holds future promise as a possible adjunct clinical intervention in cancer metastasis. Exciting opportunities

are likely to emerge from continuing discovery of pharmacological modulators for aquaporins for new treatments in cancers and other diseases.

Authorship Contributions

Participated in research design: Kourghi, Pei, De Ieso, Yool.

Conducted experiments: Kourghi, Pei, De Ieso.

Contributed new reagents or analytic tools: Flynn.

Performed data analysis: Kourghi, Pei, De Ieso, Yool.

Wrote or contributed to the writing of the manuscript: Kourghi, Pei, Flynn, Yool.

References

- Agre P, Preston GM, Smith BL, Jung JS, Raina S, Moon C, Guggino WB, and Nielsen S (1993) Aquaporin CHIP: the archetypal molecular water channel. *Am J Physiol* **265**:F463–F476.
- Anthony TL, Brooks HL, Boassa D, Leonov S, Yanochko GM, Regan JW, and Yool AJ (2000) Cloned human aquaporin-1 is a cyclic GMP-gated ion channel. *Mol Pharmacol* **57**:576–588.
- Arnaoutova I, Cawley NX, Patel N, Kim T, Rathod T, and Loh YP (2008) Aquaporin 1 is important for maintaining secretory granule biogenesis in endocrine cells. *Mol Endocrinol* **22**:1924–1934.
- Baetz NW, Hoffman EA, Yool AJ, and Stamer WD (2009) Role of aquaporin-1 in trabecular meshwork cell homeostasis during mechanical strain. *Exp Eye Res* **89**: 95–100.
- Boassa D, Stamer WD, and Yool AJ (2006) Ion channel function of aquaporin-1 natively expressed in choroid plexus. *J Neurosci* **26**:7811–7819.
- Boassa D and Yool AJ (2003) Single amino acids in the carboxyl terminal domain of aquaporin-1 contribute to cGMP-dependent ion channel activation. *BMC Physiol* **3**: 12.
- Brooks HL, Regan JW, and Yool AJ (2000) Inhibition of aquaporin-1 water permeability by tetraethylammonium: involvement of the loop E pore region. *Mol Pharmacol* **57**:1021–1026.
- Campbell EM, Ball A, Hoppler S, and Bowman AS (2008) Invertebrate aquaporins: a review. *J Comp Physiol B* **178**:935–955.
- Campbell EM, Birdsall DN, and Yool AJ (2012) The activity of human aquaporin 1 as a cGMP-gated cation channel is regulated by tyrosine phosphorylation in the carboxyl-terminal domain. *Mol Pharmacol* **81**:97–105.
- Chen TR, Drabkowski D, Hay RJ, Macy M, and Peterson W, Jr (1987) WiDr is a derivative of another colon adenocarcinoma cell line, HT-29. *Cancer Genet Cytogenet* **27**:125–134.
- Detmers FJ, de Groot BL, Müller EM, Hinton A, Konings IB, Sze M, Flitsch SL, Grubmüller H, and Deen PM (2006) Quaternary ammonium compounds as water channel blockers. Specificity, potency, and site of action. *J Biol Chem* **281**: 14207–14214.
- El Hindy N, Bankfalvi A, Herring A, Adamzik M, Lambertz N, Zhu Y, Siffert W, Sure U, and Sandalcioglu IE (2013) Correlation of aquaporin-1 water channel protein expression with tumor angiogenesis in human astrocytoma. *Anticancer Res* **33**: 609–613.
- Finn RN, Chauvigné F, Hlidberg JB, Cutler CP, and Cerdá J (2014) The lineage-specific evolution of aquaporin gene clusters facilitated tetrapod terrestrial adaptation. *PLoS One* **9**:e113686.
- Fu D, Libson A, Miercke LJ, Weitzman C, Nollert P, Krucinski J, and Stroud RM (2000) Structure of a glycerol-conducting channel and the basis for its selectivity. *Science* **290**:481–486.
- Hara-Chikuma M and Verkman AS (2006) Aquaporin-1 facilitates epithelial cell migration in kidney proximal tubule. *J Am Soc Nephrol* **17**:39–45.
- Hu J and Verkman AS (2006) Increased migration and metastatic potential of tumor cells expressing aquaporin water channels. *FASEB J* **20**:1892–1894.
- Huber VJ, Tsujita M, and Nakada T (2009) Identification of aquaporin 4 inhibitors using *in vitro* and *in silico* methods. *Bioorg Med Chem* **17**:411–417.
- Ishibashi K (2009) New members of mammalian aquaporins: AQP10–AQP12. *Handb Exp Pharmacol* **251**–262.
- Jiang Y (2009) Aquaporin-1 activity of plasma membrane affects HT20 colon cancer cell migration. *IUBMB Life* **61**:1001–1009.
- Jung JS, Bhat RV, Preston GM, Guggino WB, Baraban JM, and Agre P (1994) Molecular characterization of an aquaporin cDNA from brain: candidate osmoreceptor and regulator of water balance. *Proc Natl Acad Sci USA* **91**:13052–13056.
- McCoy E and Sontheimer H (2007) Expression and function of water channels (aquaporins) in migrating malignant astrocytes. *Glia* **55**:1034–1043.
- Migliati E, Meurice N, DuBois P, Fang JS, Somasekharan S, Beckett E, Flynn G, and Yool AJ (2009) Inhibition of aquaporin-1 and aquaporin-4 water permeability by a derivative of the loop diuretic bumetanide acting at an internal pore-occluding binding site. *Mol Pharmacol* **76**:105–112.
- Monzani E, Shtil AA, and La Porta CA (2007) The water channels, new druggable targets to combat cancer cell survival, invasiveness and metastasis. *Curr Drug Targets* **8**:1132–1137.
- Nicchia GP, Stigliano C, Sparaneo A, Rossi A, Frigeri A, and Svelto M (2013) Inhibition of aquaporin-1 dependent angiogenesis impairs tumour growth in a mouse model of melanoma. *J Mol Med (Berl)* **91**:613–623.
- Oshio K, Watanabe H, Yan D, Verkman AS, and Manley GT (2006) Impaired pain sensation in mice lacking aquaporin-1 water channels. *Biochem Biophys Res Commun* **341**:1022–1028.
- Park JH and Saier MH, Jr (1996) Phylogenetic characterization of the MIP family of transmembrane channel proteins. *J Membr Biol* **153**:171–180.

- Preston GM, Carroll TP, Guggino WB, and Agre P (1992) Appearance of water channels in *Xenopus* oocytes expressing red cell CHIP28 protein. *Science* **256**:385–387.
- Preston GM, Jung JS, Guggino WB, and Agre P (1993) The mercury-sensitive residue at cysteine 189 in the CHIP28 water channel. *J Biol Chem* **268**:17–20.
- Reizer J, Reizer A, and Saier MH, Jr (1993) The MIP family of integral membrane channel proteins: sequence comparisons, evolutionary relationships, reconstructed pathway of evolution, and proposed functional differentiation of the two repeated halves of the proteins. *Crit Rev Biochem Mol Biol* **28**:235–257.
- Saparov SM, Kozono D, Rothe U, Agre P, and Pohl P (2001) Water and ion permeation of aquaporin-1 in planar lipid bilayers. Major differences in structural determinants and stoichiometry. *J Biol Chem* **276**:31515–31520.
- Schwab A, Nechiporuk-Zloy V, Fabian A, and Stock C (2007) Cells move when ions and water flow. *Pflugers Arch* **453**:421–432.
- Seeliger D, Zapater C, Krenc D, Haddoub R, Flitsch S, Beitz E, Cerdà J, and de Groot BL (2013) Discovery of novel human aquaporin-1 blockers. *ACS Chem Biol* **8**:249–256.
- Søgaard R and Zeuthen T (2008) Test of blockers of AQP1 water permeability by a high-resolution method: no effects of tetraethylammonium ions or acetazolamide. *Pflugers Arch* **456**:285–292.
- Sui H, Han B-G, Lee JK, Walian P, and Jap BK (2001) Structural basis of water-specific transport through the AQP1 water channel. *Nature* **414**:872–878.
- Trott O and Olson AJ (2010) AutoDock Vina: improving the speed and accuracy of docking with a new scoring function, efficient optimization, and multithreading. *J Comput Chem* **31**:455–461.
- Tsunoda SP, Wiesner B, Lorenz D, Rosenthal W, and Pohl P (2004) Aquaporin-1, nothing but a water channel. *J Biol Chem* **279**:11364–11367.
- Yool AJ (2007) Functional domains of aquaporin-1: keys to physiology, and targets for drug discovery. *Curr Pharm Des* **13**:3212–3221.
- Yool AJ, Brown EA, and Flynn GA (2010) Roles for novel pharmacological blockers of aquaporins in the treatment of brain oedema and cancer. *Clin Exp Pharmacol Physiol* **37**:403–409.
- Yool AJ and Campbell EM (2012) Structure, function and translational relevance of aquaporin dual water and ion channels. *Mol Aspects Med* **33**:553–561.
- Yool AJ, Morelle J, Cnops Y, Verbavatz JM, Campbell EM, Beckett EA, Booker GW, Flynn G, and Devuyst O (2013) AqF026 is a pharmacologic agonist of the water channel aquaporin-1. *J Am Soc Nephrol* **24**:1045–1052.
- Yool AJ, Stamer WD, and Regan JW (1996) Forskolin stimulation of water and cation permeability in aquaporin 1 water channels. *Science* **273**:1216–1218.
- Yoshida T, Hojo S, Sekine S, Sawada S, Okumura T, Nagata T, Shimada Y, and Tsukada K (2013) Expression of aquaporin-1 is a poor prognostic factor for stage II and III colon cancer. *Mol Clin Oncol* **1**:953–958.
- Yu J, Yool AJ, Schulten K, and Tajkhorshid E (2006) Mechanism of gating and ion conductivity of a possible tetrameric pore in aquaporin-1. *Structure* **14**:1411–1423.
- Zhang H and Verkman AS (2015) Aquaporin-1 water permeability as a novel determinant of axonal regeneration in dorsal root ganglion neurons. *Exp Neurol* **265**:152–159.
- Zhang W, Zitron E, Hömme M, Kihm L, Morath C, Scherer D, Hegge S, Thomas D, Schmitt CP, and Zeier M et al. (2007) Aquaporin-1 channel function is positively regulated by protein kinase C. *J Biol Chem* **282**:20933–20940.

Address correspondence to: Professor Andrea Yool, Medical School South, Level 4, Frome Rd., University of Adelaide, Adelaide SA 5005 Australia. E-mail: andrea.yool@adelaide.edu.au

Differential Inhibition of Water and Ion Channel Activities of Mammalian Aquaporin-1 by Two Structurally Related Bacopaside Compounds Derived from the Medicinal Plant *Bacopa monnieri*[§]

Jinxin V. Pei, Mohamad Kourghi, Michael L. De Ieso, Ewan M. Campbell, Hilary S. Dorward, Jennifer E. Hardingham, and Andrea J. Yool

School of Medicine (J.V.P., M.K., M.L.D.I., J.E.H., A.J.Y.), and Institute for Photonics and Advanced Sensing (J.V.P., A.J.Y.), University of Adelaide, Adelaide, Australia; School of Biological Sciences, University of Aberdeen, Aberdeen, Scotland, United Kingdom (E.M.C.); Molecular Oncology Laboratory, Basil Hetzel Institute, Queen Elizabeth Hospital, Woodville, Australia (H.S.D., J.E.H.)

Received July 3, 2016; accepted July 26, 2016

ABSTRACT

Aquaporin-1 (AQP1) is a major intrinsic protein that facilitates flux of water and other small solutes across cell membranes. In addition to its function as a water channel in maintaining fluid homeostasis, AQP1 also acts as a nonselective cation channel gated by cGMP, a property shown previously to facilitate rapid cell migration in a AQP1-expressing colon cancer cell line. Here we report two new modulators of AQP1 channels, bacopaside I and bacopaside II, isolated from the medicinal plant *Bacopa monnieri*. Screening was conducted in the *Xenopus* oocyte expression system, using quantitative swelling and two-electrode voltage clamp techniques. Results showed bacopaside I blocked both the water (IC₅₀ 117 μM) and ion channel

activities of AQP1 but did not alter AQP4 activity, whereas bacopaside II selectively blocked the AQP1 water channel (IC₅₀ 18 μM) without impairing the ionic conductance. These results fit with predictions from in silico molecular modeling. Both bacopasides were tested in migration assays using HT29 and SW480 colon cancer cell lines, with high and low levels of AQP1 expression, respectively. Bacopaside I (IC₅₀ 48 μM) and bacopaside II (IC₅₀ 14 μM) impaired migration of HT29 cells but had minimal effect on SW480 cell migration. Our results are the first to identify differential AQP1 modulators isolated from a medicinal plant. Bacopasides could serve as novel lead compounds for pharmaceutical development of selective aquaporin modulators.

Introduction

Aquaporin (AQP) water channels are in the family of major intrinsic proteins found from bacteria to humans (Agre et al., 1993; Reizer et al., 1993; Calamita et al., 1995) and are targets for the discovery of selective pharmacologic modulators. Classes of aquaporins transport water and small uncharged molecules such as glycerol and urea through individual pores located in each subunit (Fu et al., 2000; Tajkhorshid et al., 2002).

An expanding role for aquaporins as multifunctional channels is being recognized (Yool and Campbell, 2012). In addition to facilitating water flux through intrasubunit pores, AQP1 also functions as a nonselective monovalent cation channel using the central pore at the 4-fold axis of symmetry (Yool and Weinstein, 2002; Yu et al., 2006; Campbell et al.,

2012). The ion channel conductance is activated by interaction of cGMP in the intracellular loop D domain, and modulated by the carboxyl terminal domain (Anthony et al., 2000; Saparov et al., 2001; Boassa and Yool, 2003; Zhang et al., 2007). Cyclic GMP appears to trigger opening of cytoplasmic hydrophobic barriers in the central pore, allowing hydration and cation permeation (Yu et al., 2006). Inhibition of the AQP1 ion channel has been shown to slow cell migration rates in a colon cancer cell line that expresses high levels of AQP1 (Kourghi et al., 2016).

Defining pharmacologic modulators of aquaporins has been an area of keen interest (Papadopoulos and Verkman, 2008; Devuyst and Yool, 2010; Seeliger et al., 2013). Early work identified blockers such as mercury (Preston et al., 1993), silver and gold (Niemietz and Tyerman, 2002), acetazolamide (Gao et al., 2006), and tetraethylammonium ion (Brooks et al., 2000; Yool et al., 2002; Detmers et al., 2006), but these remained limited in usefulness because of toxicity, lack of specificity, or variable efficacy across experimental systems (Yang et al., 2006; Yool, 2007).

More recently, small molecule pharmacologic agents with therapeutic potential have been identified. Complexes of

This work was supported by funding from the University of Adelaide Institute for Photonics and Advanced Sensing 2015 Pilot Grant program, and Australian Research Council Discovery Project grant DP160104641.
dx.doi.org/10.1124/mol.116.105882.

[§] This article has supplemental material available at molpharm.aspetjournals.org.

ABBREVIATIONS: AQP, aquaporin; AqBxxx, numbered series of aquaporin modulators derived from bumetanide; AqFxxx, numbered series of aquaporin modulators derived from furosemide; FBS, fetal bovine serum; FUDR, 5-fluoro-2'-deoxyuridine; meWB, methanol extract of whole *Bacopa*; NCBI, National Center for Biotechnology Information; qRT-PCR, quantitative reverse-transcription polymerase chain reaction.

gold-based compounds have promise for the selective block of specific classes of aquaporins; functionalized bipyrene and terpyridines coordinating Au(III) were shown to block aquaglyceroporin AQP3 with little effect on AQP1 (Martins et al., 2013). Intracellular arylsulfonamide modulators of AQP1 include the bumetanide derivative, AqB013, which blocks AQP1 and AQP4 water permeability (Migliati et al., 2009); AqB011, which blocks the AQP1 cation channel (Kourghi et al., 2016); and the furosemide derivative AqF026, which potentiates water channel activity of AQP1 (Yool et al., 2013). Other arylsulfonamide agents have been proposed as blockers of AQP4 (Huber et al., 2007, 2009). Growing evidence has demonstrated that specific arylsulfonamides act as AQP modulators in vitro and in vivo (Pei et al., 2016).

Diverse small molecules acting at the extracellular side present a valuable array of novel inhibitors of AQP1 (Seeliger et al., 2013), indicating that other compounds in addition to coordinated metal ligands and arylsulfonamides are of interest for the development of AQP modulators. Lack of effect for a broad panel of AQP modulators tested in one study might reflect problems with synthesis or solubilization of the agents or could indicate that the type of bioassay used influences apparent drug efficacy (Esteve-Font et al., 2016).

Our study has broadened the panel of AQP modulatory agents by evaluating natural medicinal plants as sources of active compounds. Quantitative swelling assays of mammalian AQP1 and AQP4 channels in the *Xenopus* expression system, used for screening extracts from a variety of traditional medicinal herbs, have identified *Bacopa monnieri* as one of several promising sources. Work here tested the hypothesis that chemical constituents of *B. monnieri* could be identified and characterized as pharmacologic agents that modulate mammalian AQP1 by interacting at domains associated with pore functions.

Data here show that bacopaside I blocks both the water and ion channel activities of AQP1 but does not alter AQP4 activity, and bacopaside II selectively blocks the AQP1 water channel without impairing the ionic conductance. These results fit well with in silico docking for predicted energies of interaction at a pore-occluding intracellular site. Bacopasides I and II showed the same order of efficacy in blocking migration of AQP1-expressing HT29 colon cancer cells, with minimal effects on SW480 cells that express AQP1 at low levels. Our results are the first to identify AQP1 channels as one of the candidate targets of action of the Ayurvedic medicinal plant water hyssop, and to define new lead compounds for the development of AQP modulators.

Materials and Methods

Bacopa Methanol Extraction and Fractionation. *Bacopa monnieri* stems and leaves were obtained with permission from the Botanic Gardens of Adelaide (Adelaide, South Australia). Chopped *Bacopa* plant material (100 g) was dried, then refluxed in 500 ml of methanol for 2 hours at room temperature. The suspension was filtered using Whatman No. 1 paper to obtain a methanol extract of whole *Bacopa* (meWB). Half the meWB extract was aliquoted into microfuge tubes, dried under vacuum (SpeedVac; Thermo Fisher Scientific, Waltham, MA) into a solid brown paste, and reconstituted in saline for oocyte swelling assays. The other half of the meWB was fractionated using small-scale reverse phase C18 silica column (Alltech Prevail C18; Grace, Deerfield, IL). The mobile phases used for fractionation were a series of six water–methanol mixtures with

H₂O:CH₃OH ratios ranging from 5:0 to 0:5. The fractions were dried in under vacuum and reconstituted in saline for oocyte swelling assays.

Fractions containing AQP1 blocking activity were analyzed with mass spectrometry by Flinders Analytical (Flinders University, South Australia). Bacopaside I was identified by precise molecular weight as a major component in the active fractions, and bacopasides I and II were purchased from a commercial source (Chromadex, Irvine CA), solubilized in methanol to yield 100× stock solutions, and stored at -20°C. Experimental solutions were prepared by mixing the bacopaside stocks (1 part in 100) with isotonic saline or culture medium to yield final concentrations of 10 to 200 μM. Vehicle control salines were made using the same volume of methanol alone in isotonic saline or culture medium.

Oocyte Preparation and cRNA Injection. Unfertilized oocytes were isolated from *Xenopus laevis* frogs in accord with the university animal ethics committee-approved protocols, defolliculated by treatment with collagenase (type 1A, 2 mg/ml; Sigma-Aldrich, St. Louis, MO) and trypsin inhibitor (0.67 mg/ml; Sigma-Aldrich) in OR-2 saline (82 mM NaCl, 2.5 mM KCl, 1 mM MgCl₂, and 5 mM HEPES; pH 7.6) at 16°C for 1.5 hours, washed in OR-2 saline, and then incubated in isotonic oocyte saline [96 mM NaCl, 2 mM KCl, 0.6 mM CaCl₂, 5 mM MgCl₂, and 5 mM HEPES supplemented with 10% horse serum (Sigma-Aldrich), 100 U/ml penicillin, 100 μg/ml streptomycin, and 50 μg/ml tetracycline, pH 7.6] at 16°C. Oocytes were injected with 1–4 ng of AQP1, AQP4, or AQP1 R159A+R160A cRNA in 50 nl of sterile water and incubated for 2 to 3 days at 16–18°C to allow protein expression. The oocytes not injected with cRNA served as non-AQP-expressing control cells.

Human AQP1 [National Center for Biotechnology Information (NCBI) GenBank: BC022486.1] and rat AQP4 (AF144082.1) cDNAs from P. Agre (Johns Hopkins University, Baltimore, MD) were subcloned into a modified *Xenopus* β-globin expression plasmid. The double mutant construct human AQP1 R159A+R160A cDNA was generated by site-direct mutation (QuikChange; Stratagene, La Jolla, CA) and sequenced to confirm no errors were introduced (Yu et al., 2006). The cDNAs were linearized with BamHI and transcribed using T3 polymerase (T3 mMessage mMachine; Ambion, Austin, TX). The cRNAs were resuspended in sterile water and stored at -80°C.

Quantitative Oocyte Swelling Assays. Immediately before the swelling assays, the control and AQP-expressing oocytes were preincubated in isotonic saline (serum and antibiotic free) with or without meWB or bacopaside compounds or with methanol vehicle at 16–18°C, for incubation periods as indicated. Osmotic water permeability was determined as the linear rate of change in volume as a function of time, immediately after introduction into 50% hypotonic saline (isotonic saline diluted with equal volume of water).

Oocytes were imaged using a computer controlled charge-coupled-device grayscale camera (Cohu, San Diego, CA) mounted on a dissecting microscope (Olympus SZ-PT; Olympus, Macquarie Park, Australia). Images were taken at 0.5 frames per second for 60 seconds; cross-sectional areas were quantified using ImageJ software (Research Services Branch, National Institutes of Health, Bethesda, MD). Swelling rates were calculated as the slopes of linear regression fits of volume as a function of time in hypotonic saline. Data were analyzed and compiled for multiple batches of oocytes for statistical analyses and to generate dose–response curves, which were fit by sigmoidal nonlinear variable-slope dose–response regression functions using Prism (GraphPad Software, San Diego, CA).

Molecular Docking. In silico modeling was performed with methods reported previously elsewhere (Yool et al., 2013). The protein crystal structures for human AQP1 (PDB ID 1FQY) and human AQP4 (PDB ID 3GDB) were obtained from the protein data bank (NCBI Structure). Bacopaside I and II structures were obtained from PubChem (NCBI) and converted into a software-compatible 3D structures in .pdb format using the Online SMILES Translator and Structure File Generator (National Cancer Institute, U.S. National Institutes of Health, Bethesda, MD). Ligand and receptor coordinates were prepared for docking using Autodock (version 4.2; Scripps

Research Institute, La Jolla, CA). Autodock Vina (Trott and Olson, 2010) was used to run the flexible ligand docking simulations with two docking grids covering both intracellular and extracellular faces of the monomeric pores. The three-dimensional docking result files and docking energy values were exported from Autodock, and the results were viewed using PyMOL software (version 1.8; Schrödinger, Cambridge, MA). Data for AQP1 and AQP4 docking results in .pdb format are provided as supplemental data files.

Electrophysiology. For two-electrode voltage clamp, capillary glass electrodes (1–3 M Ω) were filled with 1 M KCl. Recordings were done in a standard isotonic Na⁺ bath saline containing 100 mM NaCl, 2 mM KCl, 4.5 mM MgCl₂, and 5 mM HEPES, pH 7.3. We applied cGMP extracellularly at a final concentration of 10–20 μ M using the membrane-permeable cGMP analog [Rp]-8-[para-chlorophenylthio]-cGMP (Sigma Chemical, Castle Hill, Australia). Ionic conductance was monitored for at least 20 minutes after cGMP addition to allow development of maximal plateau responses. Conductance was determined by linear fit of the current amplitude as a function of voltage, with a step protocol from +60 to –110 mV and holding potential of –40 mV.

After the first activation by cGMP, oocytes were incubated in isotonic saline with or without bacopaside I or bacopaside II for 2 hours to allow recovery. After incubation, a second application of cGMP was used to test for reactivation, to determine whether any block of the ionic conductance was evident. Using the same protocol, AQP1-expressing oocytes were demonstrated previously to show cGMP-dependent activation, complete recovery during a 2-hour incubation in saline alone, and full reactivation of the ionic conductance response to a second application of cGMP, whereas non-AQP1-expressing control oocytes showed a low ionic conductance and no significant response to drug treatments throughout the same protocol (Kourghi et al., 2016). Recordings were made with a GeneClamp amplifier and pClamp 9.0 software (Molecular Devices, Sunnyvale, CA).

Cancer Cell Culture and Migration Assays. HT29 and SW480 colon cancer cell lines (from American Type Culture Collection [ATCC], Manassas, VA) were cultured in complete medium composed of Dulbecco's modified Eagle's medium supplemented with 1 \times glutamax (Life Technologies, Mulgrave, Australia), penicillin and streptomycin (100 U/ml each), and 10% fetal bovine serum. Cultures were maintained in 5% CO₂ at 37°C. Cells were seeded in a flat-bottom 96-well plates at 1.25 \times 10⁶ cells/ml to produce a confluent monolayer.

For 12 to 18 hours before wounding, cells were serum-starved in 2% fetal bovine serum (FBS), in the presence of 400 nM of the mitotic inhibitor 5-fluoro-2'-deoxyuridine (FU DR) (Parsels et al., 2004). For wounding, a sterile p10 pipette tip was attached to the end of a vacuum tube, and a circular wound was created by brief perpendicular contact of the tip with base of the well. Each well was then washed 3 times with phosphate-buffered saline to remove detached cell debris. Cultures were maintained during the wound closure assay in 2% FBS medium with FU DR.

Wound images were imaged at 10 \times magnification with a Canon EOS 6D camera (Canon, Macquarie Park, Australia) mounted on an Olympus inverted microscope (Olympus Corp., Waltham, MA). Image dimensions and pixel density were standardized across each image series using XnConvert software (XnSoft, Reims, France). Linear outlines and areas of the wound were generated using ImageJ software (National Institutes of Health). Wound closure data as a function of time were calculated as a percentage of the initial wound areas for the same wells.

Quantitative Reverse-Transcription Polymerase Chain Reaction. Cells at 70%–80% confluence were harvested, and the RNA was extracted using the PureLink RNA Mini kit (Life Technologies, Carlsbad, CA). RNA was quantified using the NanoDrop 2000 spectrophotometer (Thermo Scientific) and the integrity (RIN score) assessed using the 2100 Bioanalyzer (Agilent Technologies, Santa Clara, CA). The RNA (500 ng) was reverse transcribed using the iScript cDNA synthesis kit (Bio-Rad Laboratories, Hercules, CA). Quantitative reverse-transcription polymerase chain reaction (qRT-PCR) of AQP1 and the reference gene phosphomannose mutase

1 (PMM1) was performed using multiplex Taqman expression assays (Life Technologies) and SsoFast probes supermix (Bio-Rad Laboratories) in triplicate in the Rotorgene 6000 (Qiagen).

Western Blot Analysis. Cultured cells were lysed with RIPA buffer containing 1% β -mercaptoethanol, 1% HALT protease inhibitor 100 \times solution, 150 U Benzamide (all from Sigma-Aldrich) on ice for 10 minutes, homogenized by passing through a 21-gauge syringe and centrifuged 14,000g for 15 minutes at 4°C to pellet the cell debris. Protein was quantified (EZQ Assay; Life Technologies). Each sample (50 μ g) was resolved by SDS-PAGE on a 12% Mini-PROTEAN TGX Stain-Free Gels (Bio-Rad Laboratories) and transferred to polyvinylidene fluoride membranes using the Trans-Blot Turbo Transfer Pack and System (Bio-Rad Laboratories). Membranes were blocked with Tris-buffered saline with Tween 20 containing 5% skim milk for 1 hour and incubated overnight at 4°C with anti-AQP1 (H-55) (1/500; Santa Cruz). After three washes in Tris-buffered saline with Tween 20, membranes were incubated with goat anti-rabbit IgG horseradish peroxidase secondary antibody (1/2000) and Strep-Tactin-HRP Conjugate (1/10,000) (both Bio-Rad Laboratories) at room temperature for 1 hour, and washed.

Chemiluminescence using Clarity Western ECL Blotting Substrate (Bio-Rad Laboratories) was used for detection and blots imaged using the ChemiDoc Touch Imaging System (Bio-Rad Laboratories). Image Laboratory Software was used to validate the Western blotting data via total protein normalization (Bio-Rad Laboratories).

Immunocytochemistry. HT29 and SW480 cells grown on coverslips to 50% confluence were fixed with 4% paraformaldehyde and permeabilized with 0.5% Triton X-100. Image-iT FX Signal Enhancer (Life Technologies) was used as per manufacturer's instructions. AQP1 was labeled with a 1/400 dilution of rabbit polyclonal anti-human AQP1 (Abcam, Cambridge, United Kingdom) and visualized with a secondary antibody at 1/200 dilution (goat anti rabbit IgG H&L Alexa Fluor 568; Life Technologies). Cells were counterstained with NucBlue Fixed Cell Ready Probes Reagent (Life Technologies). Coverslips were mounted in ProLong Gold antifade reagent (Life Technologies) and imaged with a Zeiss LSM 700 microscope (Carl Zeiss, Jena, Germany).

Live Cell Imaging. Cells were seeded on an eight-well uncoated Ibidi μ -Slide (Ibidi, Munich, Germany) at a density of 1.0 \times 10⁶ cells/ml. For 12 to 18 hours before wounding, cells were serum-starved in medium with 2% FBS in the presence of FU DR (400 nM). Five circular wounds were created in each well using techniques described earlier for the migration assays. The slide was mounted on a Nikon Ti E Live Cell Microscope (Nikon, Tokyo, Japan) in an enclosed chamber kept at 37°C with 5% CO₂. Images were taken at 5-minute intervals for 24 hours, using Nikon NIS-Elements software. AVI files were exported from NIS-Elements and converted into TIFF files using ImageJ (U.S. National Institutes of Health). Converted files were analyzed using Fiji software (Schindelin et al., 2012) with the Manual Tracking plug-in.

Cytotoxicity Assay. HT29 cell viability was quantified using the AlamarBlue assay (Molecular Probes, Eugene, OR). The cells were plated at 10⁴ cells/well in 96-well plates, and the fluorescence signal levels were measured with a FLUOstar Optima microplate reader (BMG Labtech, Ortenberg, Germany) after 24 hours of incubation with concentrations of bacopaside I from 0 to 100 μ M or bacopaside II from 0 to 30 μ M, to obtain quantitative measures of cell viability. Mercuric chloride (100 μ M) was used as a positive control for cytotoxicity.

Results

Extracted Compounds from *Bacopa monnieri* Inhibited AQP1 Water Channel Activity. Methanol-extracted whole *Bacopa* (meWB) reconstituted in isotonic saline ("water hyssop extract") inhibited the water permeability of AQP1-expressing oocytes (Fig. 1A). After 2 hours preincubation in 1 mg/ml meWB, the swelling rates of

AQP1-expressing oocytes were significantly reduced ($P < 0.001$) as compared with untreated AQP1-expressing oocytes. Fractionated samples of meWB reconstituted at 0.1 mg/ml each were tested for biologic activity using oocyte swelling assays (Fig. 1B) after 2 hours of preincubation. AQP1-mediated swelling was significantly decreased by fractions 3 and 4; other fractions had no effect.

Combined fractions 3 and 4 were analyzed by mass spectrometry and revealed the presence of a major compound identified by precise molecular weight as bacopaside I. Commercially purchased bacopasides I and II were found to block osmotic water permeability in AQP1-expressing oocytes (Fig. 1C) and showed a dose-dependent effect (Fig. 1D). The inhibition of AQP1-mediated osmotic water fluxes showed IC_{50} values of approximately 18 μM for bacopaside II, and approximately 117 μM for bacopaside I. The chemical structures are shown in Fig. 1E.

Inhibition by Bacopasides I and II Was Time-Dependent and Reversible. AQP4-expressing oocytes showed no block of water channel activity after 2 hours of

preincubation in isotonic saline containing bacopaside I at 178 μM (Fig. 2A). The blocking effect of bacopaside was specific for AQP1. The inhibitory effect of bacopasides I and II on AQP1 water channel activity took time to develop, with near maximum block achieved by approximately 2 hours (Fig. 2B). The magnitude of inhibition of AQP water flux increased as a function of the duration of preincubation in 178 μM bacopaside I or 35 μM bacopaside II. For bacopaside I, half-maximal block was reached after approximately 50 minutes, and maximum block after 120 minutes of preincubation. For bacopaside II, half-maximal block was reached after approximately 30 minutes, and maximum block after 80 minutes of preincubation. Longer times provided no appreciable further enhancement of the magnitude of inhibition. A comparably slow time-dependent onset of block has been noted previously for other AQP1 ligands such as AqB013, AqB011, and AqF026, which are thought to bind at the intracellular side of the channel (Migliati et al., 2009; Yool et al., 2013; Kourghi et al., 2016) and require time to travel across the plasma membrane to the cytoplasmic side.

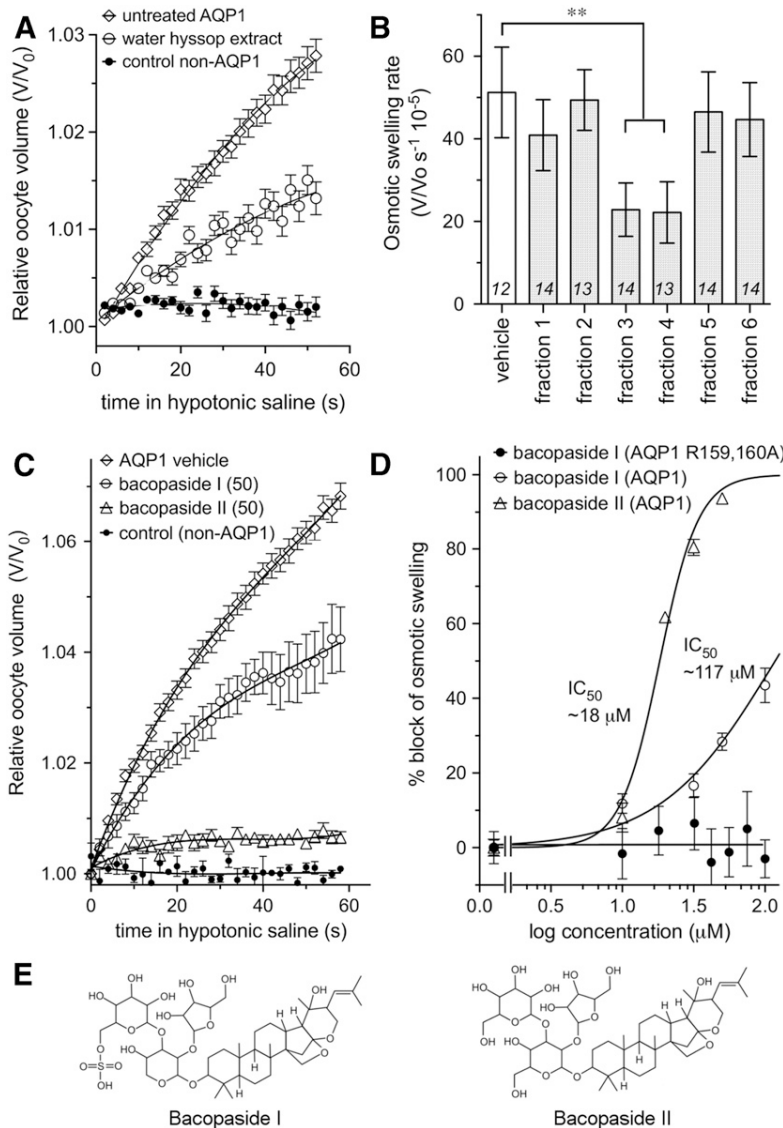


Fig. 1. Block of osmotic water permeability in AQP1-expressing oocytes by water hyssop (*Bacopa monnieri*) extract, and constituent compounds bacopaside I and bacopaside II. (A) Mean swelling responses of AQP1-expressing oocytes in 50% hypotonic saline, standardized to the initial volume V_0 , were blocked by 2 hours of preincubation in reconstituted extract of water hyssop (at 1 mg/ml). Control non-AQP1 oocytes showed little change in volume. Data are mean values for all oocytes assessed from a single batch of oocytes; error bars are S.E.M.; n values are 6 per treatment group. (B) Column elution of methanol-extracted *Bacopa* identified two active fractions which caused block of AQP1 osmotic water permeability at 0.1 mg/ml each (which were further analyzed by mass spectroscopy to identify candidate compounds). Data are mean \pm S.E.M.; n values in italics are above the x -axis. (C) Candidate compounds bacopaside I and bacopaside II at 50 μM differentially blocked osmotic water permeability in AQP1-expressing oocytes, causing a decrease in the rate of swelling as compared with untreated AQP1-expressing oocytes. Data are mean \pm S.E.M.; n values are 8 (AQP1 vehicle), 5 (bacopaside I), 7 (bacopaside II), and 8 (non-AQP1 control). (D) Dose-dependent block of AQP1-mediated osmotic swelling by bacopasides I and II, with estimated IC_{50} values of 117 μM and 18 μM , respectively. No sensitivity to bacopaside I was seen for the AQP1 R159,160A double mutant at doses up to 100 μM . (E) Chemical structures of bacopasides I and II.

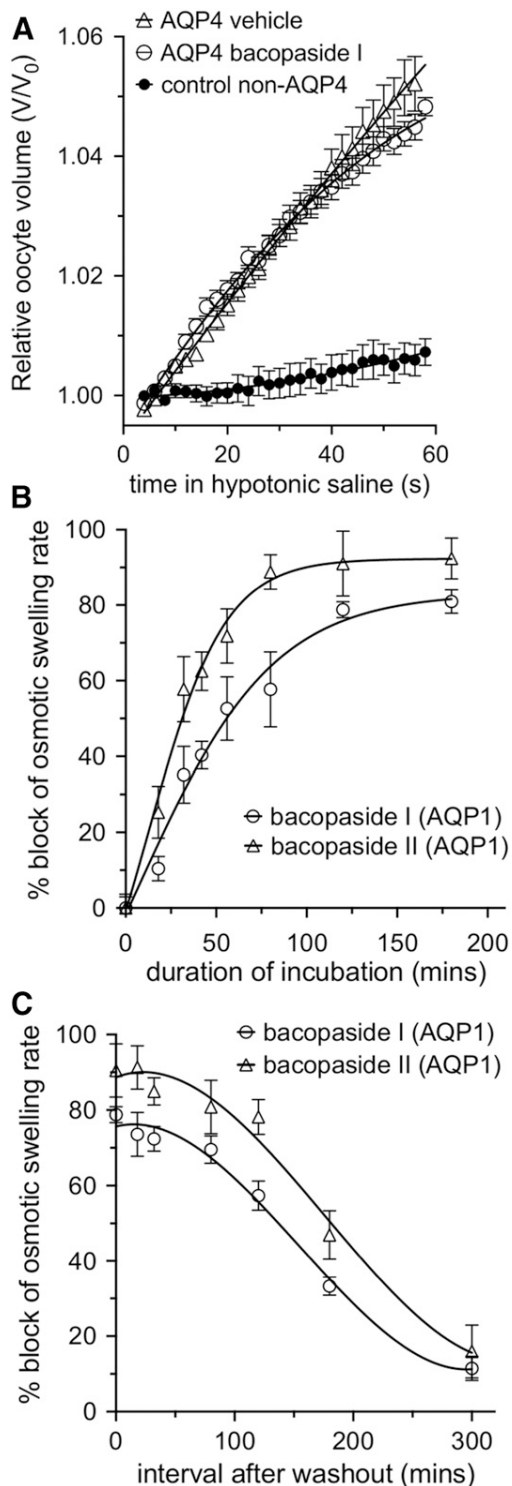


Fig. 2. Subtype selectivity and temporal properties of block onset and recovery with bacopasides I and II in AQP-expressing oocytes. (A) Mean swelling responses of AQP4-expressing oocytes in 50% hypotonic saline were not affected after 2 hours of preincubation in 178 μ M bacopaside I. Data are mean \pm S.E.M.; n values are 8 (AQP4 alone), 8 (AQP4 with bacopaside I), and 6 (non-AQP4 control). (B) Time-dependent establishment of block of AQP1-mediated osmotic water permeability required preincubation of oocytes in 178 μ M bacopaside I or 35 μ M bacopaside II, with approximately 2 hours needed to achieve maximal inhibition. The n values are 12 to 14 oocytes per time point; each oocyte was used for a single measurement. (C) Time-dependent recovery from block in AQP1-expressing oocytes preincubated 2 hours in 178 μ M bacopaside I or 35 μ M

The blocking effects of bacopasides I and II on AQP1 water channel activity were reversible (Fig. 2C). AQP1-expressing oocytes were preincubated 2 hours with 178 μ M bacopaside I or 35 μ M bacopaside II, followed by washout of the drug with isotonic saline. The osmotic water permeability showed approximately 25% recovery by 120 minutes after the washout of bacopaside I, and half-maximal recovery by 160 minutes. For bacopaside II, water permeability showed 25% recovery by 150 minutes after washout of the blocker, and half-maximal recovery by 200 minutes.

Ion Channel Conductance of AQP1 Was Inhibited by Bacopaside I but Not by Bacopaside II. Two-electrode voltage clamp recordings from AQP1-expressing oocytes demonstrated the cGMP-dependent activation of the ionic conductance (Fig. 3A) as described previously elsewhere (Anthony et al., 2000), which was reversible by 2 hours of incubation in saline without membrane-permeable cGMP (Kourghi et al., 2016). Reactivation of the ionic response by a second dose of cGMP was partly blocked in AQP1-expressing oocytes after 2-hour incubation in 50 μ M bacopaside I, and strongly blocked at 100 μ M bacopaside I (Fig. 3B). In contrast, the reactivation of the ion conductance was unimpaired after incubation with 10 μ M or 20 μ M bacopaside II.

Identification of Candidate Intracellular Binding Sites. Protein crystal structures of AQP1 and AQP4, and three-dimensional structural renditions of bacopaside I and bacopaside II were prepared and run on interaction simulations using Autodock Vina software to identify predicted binding sites. An array of candidate docking sites for bacopasides I and II on AQP1 and AQP4 channels were considered with *in silico* computational docking analyses. Of a total of eight possible positions evaluated for bacopaside I, the dominant energetically favored configurations for intracellular binding yielded values of -9.2 kcal/mol for AQP1 (Data Supplement 1), and -8.0 Kcal/mol for AQP4 (Data Supplement 2). Similarly out of all possible positions evaluated, the energetically favored configurations for bacopaside II yielded values of -9.3 kcal/mol for AQP1 (Data Supplement 3), and -7.8 kcal/mol for AQP4 (Data Supplement 4).

In the poses reflecting the most favored docking positions, the intracellular face of the water pore was effectively occluded by bacopasides I and II in AQP1, but not in AQP4 channels (Fig. 4, A–D). For AQP1, the bacopasides appeared to nest well into the internal vestibule of the intrasubunit water pore. For AQP4 the optimal interaction was seen for bacopaside sitting in a groove between transmembrane domains 4 and 5, a position where subunits interface near the central pore that might not be accessible in the assembled tetrameric channel.

Closer inspection of specific amino acid residues in the predicted AQP1 docking site (using Chimera visualization software) suggested that the poly-arginine motif in the loop D domain could enable hydrogen bond formation with the sulfonyl moiety on the glucopyranosyl sugar of bacopaside I (Fig. 4E) at residues corresponding to R159 and R160 in human AQP1. These arginines are part of a highly conserved amino acid pattern seen in AQP1 channels from diverse species, and they are required for cGMP gating of the AQP1 ionic conductance (Yu et al., 2006). The site-directed double

bacopaside II, and assessed at different intervals after transfer back into standard isotonic saline at time 0 (washout). The n values are 10 to 13 oocytes per time point; each oocyte was used for a single measurement.

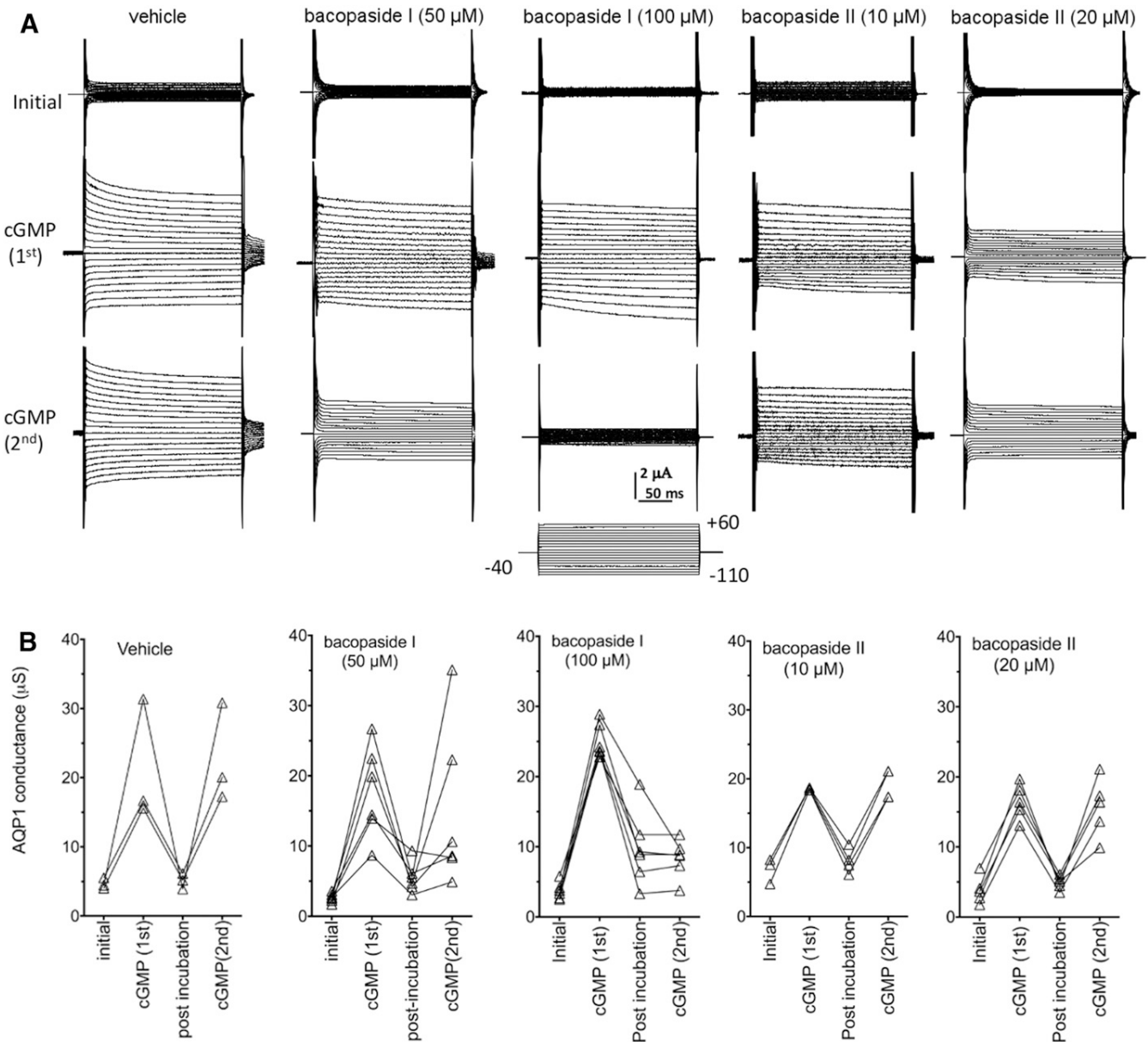


Fig. 3. Block of the cGMP-dependent ionic conductance of AQP1-expressing oocytes by bacopaside I, but not bacopaside II. (A) Representative sets of traces recorded by two-electrode voltage clamp of AQP1-expressing oocytes showing the initial conductance; the response induced by the first application of membrane-permeable cGMP; the recovery of the response to near initial levels after 2 hours of incubation in isotonic saline containing bacopaside I (50 or 100 μM) or bacopaside II (10 or 20 μM); and the final response to a second application of cGMP. (B) Trend plots showing the amplitude of the ionic currents, before and after the first activation by GMP, the recovery after incubation, and the response reactivated by a second cGMP application. Consistent recovery was seen after 10 or 20 μM bacopaside II, but not after incubation with 50 or 100 μM bacopaside I indicating establishment of ion channel block. The *n* values are as shown; each line represents a series of recordings from one oocyte.

mutation of arginines R159 and R160 to alanines did not prevent normal expression of AQP1-mediated osmotic water permeability, indicating that the AQP1 mutant constructs were expressed and targeted to the oocyte plasma membrane as described previously elsewhere (Yu et al., 2006); however, the efficacy of bacopaside I in inhibiting osmotic water permeability was abolished in the mutant construct at doses up to 100 μM (Fig. 1D), supporting the suggested role of the loop D arginine residues in stabilizing the docking of the bacopaside I ligand.

Bacopaside II Was More Effective Than Bacopaside I in Blocking Migration of AQP1-Expressing Colon Cancer Cells. HT29 cells have a higher endogenous level of

AQP1 expression as compared with SW480 cells, as demonstrated by qRT-PCR (Fig. 5A), western blot (Fig. 5B), and immunocytochemistry (Fig. 5C) analyses.

Wound closure assays showed robust migration of HT29 cells in medium with vehicle (Fig. 6A), resulting in little open area remaining at 24 hours. In contrast, treatment with bacopaside II (Fig. 6B) substantially reduced the amount of wound closure. A dose-dependent block of cell migration measured by wound closure (Fig. 6C) was observed for both bacopaside I and bacopaside II on HT29 cells. The calculated IC₅₀ value for bacopaside I was approximately 48 μM and for bacopaside II was 14 μM in HT29 cells. There was a small

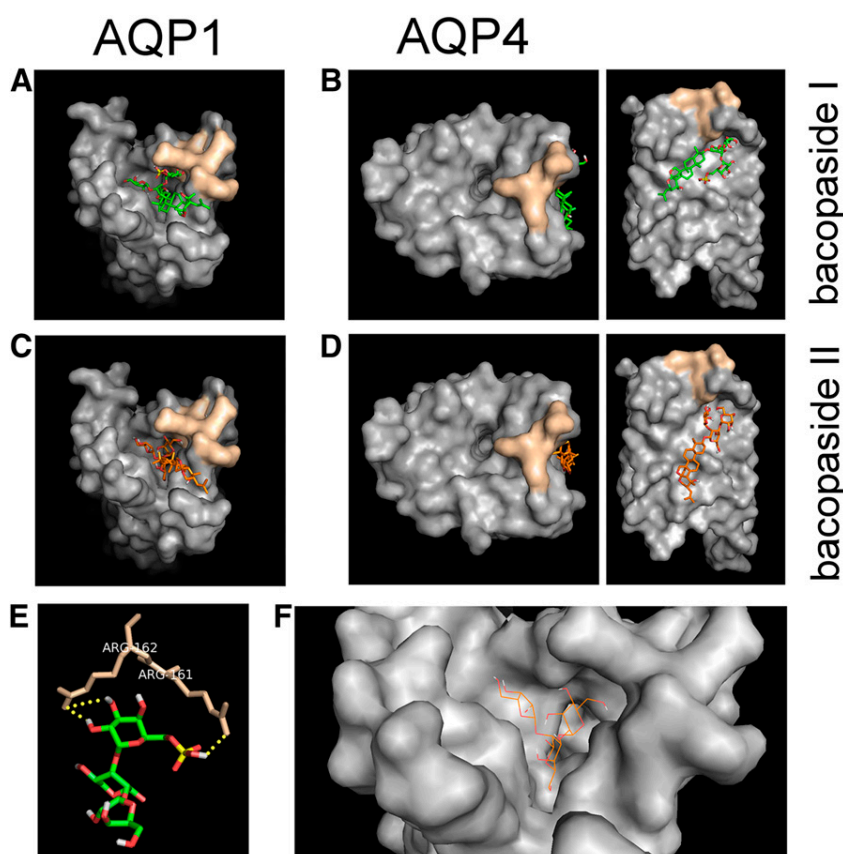


Fig. 4. In silico docking models illustrating predictions for the most favorable sites of interaction of bacopaside I and bacopaside II on AQP1 and AQP4 subunit proteins. AQP subunit models were assembled from crystal structural data for human AQP1 (PDB ID 1FQY) and human AQP4 (PDB ID 3GDB); see *Materials and Methods* for details. Subunit views are from the cytoplasmic side, with the water pore in the center. The intracellular loop D domain, adjacent to the channel tetrameric axis of symmetry, is highlighted in dark gold. (A) Bacopaside I is predicted by in silico docking to occlude the cytoplasmic side of the intrasubunit water pore in AQP1. (B) Favorable interactions at the AQP4 water pore are not evident for bacopaside I; the best fit is seen near membrane-spanning domains distant from the pore (inset). (C) Bacopaside II is predicted to have the most favorable energy of interaction at a position occluding the cytoplasmic side of the AQP1 water pore. (D) Predicted binding of bacopaside II with AQP4 is distant from the water pore (inset), in a position similar to that seen for bacopaside I. (E) Enlarged view of the predicted interaction of the sugar-linked sulfur group of bacopaside I with the conserved loop D arginine residues in AQP1. (F) Enlarged view of the predicted binding of the trisaccharide moiety of bacopaside II deep into the cytoplasmic vestibule of the AQP1 water pore.

reduction of migration observed for SW480 cells treated with bacopasides I and II (Fig. 6C), which was consistent with the relatively low expression of AQP1 channels in this cell line.

Time-Lapse Imaging Demonstrated Bacopasides I and II Differentially Decreased the Rate of Migration of AQP1-Expressing HT29 Colon Cancer Cells. Cultured HT29 cancer cells showed differences in rates of migration into the open wound areas in the vehicle, bacopaside I and bacopaside II treatment conditions (Fig. 7, A–C). Time-lapse images showed the rates of cell migration were significantly impeded in 50 μ M bacopaside I and in 15 μ M bacopaside II (Fig. 7, B and C) as compared with vehicle-treated HT29 cells (Fig. 7A). No appreciable difference in cell viability was observed in any of the treatment groups during the 24-hour time course of the experiment.

In the vehicle-treated group, trajectory plots of individual cells sampled at 50-minute intervals over 24 hours (Fig. 7D) showed generally directional movements of HT29 cells into the open wound spaces. In bacopaside I treatment group, the HT29 cells lacked directional migration and moved short distances between successive frames. In the bacopaside II treated group, the impairment of movement was evident but less severe. The collective trend of trajectories of the vehicle-treated group appeared to be linear and extended, whereas that in the bacopaside I treated group was recursive and compressed; the bacopaside II group showed an intermediate level of restriction of movement.

The net displacement (distance traveled) per time interval was greater in the vehicle-treated group than in the

bacopasides I and II treatment groups. Frequency histograms, summarizing all events observed, were compiled as the binned values of distances traveled per 50-minute interval (Fig. 7E). These histograms showed that more cells traveled longer distances per time interval in the vehicle-treated group than in the bacopaside-treated groups. Distributions moved were well fit by Gaussian functions; the decreased mean distances moved in the bacopaside treatments were seen as left shifts in the peaks of the frequency histograms. Compiled data in a summary histogram (Fig. 7F) confirmed the significant decrease in mean total distance traveled by cells during the 24 hours of tracking in bacopaside I or II as compared with vehicle-treated cells. Analysis of cytotoxicity by AlamarBlue assay showed that bacopaside I had no significant effect on cell viability at 50 or 75 μ M, and bacopaside II had no effect on viability at 15 or 20 μ M (Table 1). Concentrations of bacopasides that significantly blocked AQP1 water channel activity and HT29 cell migration were not appreciably cytotoxic.

Discussion

Our results have demonstrated that two structurally similar compounds, bacopaside I and bacopaside II, derived from a medicinal herb, act differentially as pharmacologic inhibitors of mammalian aquaporin channels. In silico modeling predicted that bacopasides I and II have favorable energies of interaction at the intracellular vestibule of AQP1, occluding the intrasubunit water pore. Modeling results were consistent with the observed effects of these agents as AQP1 inhibitors.

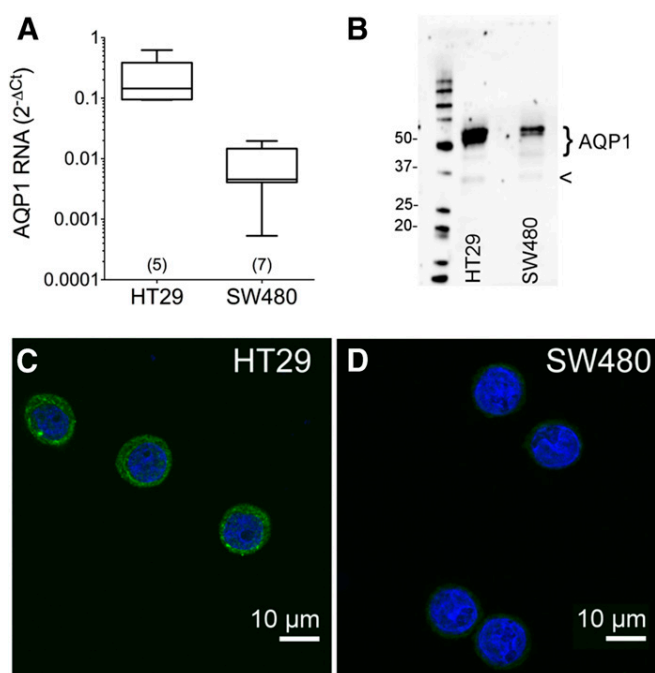


Fig. 5. HT29 cells have higher level of AQP1 expression than SW480 cells. (A) The AQP1 RNA level was higher in HT29 cells as compared with SW480 cells as assessed using qRT-PCR. (B) The AQP1 protein level was higher in HT29 than SW480 cells as demonstrated by Western blot, with monomeric subunit band seen near the predicted size of 28 kD with higher molecular mass glycosylated bands. (C) The AQP1 immunopositive signal (green) associated with the cell membrane was stronger in HT29 than in SW480 cells. Cell nuclei were counterstained (blue). See *Materials and Methods* for details.

The predicted energies of interaction for docking on AQP1 were higher for bacopaside II than bacopaside I, fitting the observed order of efficacy in blocking AQP1-mediated swelling of oocytes and the same order of efficacy in blocking migration of AQP1-expressing HT29 colon cancer cells, with minimal effects on SW480 cells that express little AQP1. The docking of bacopasides I and II to occlude the water pore appeared principally to involve the trisaccharide rings, which projected down into the AQP1 intrasubunit pore.

Future work exploring polysaccharides and related osmolytes as endogenous modulators of AQP channels could be of interest. The lack of a favorable docking interaction of bacopaside with the AQP4 water pore was consistent with the insensitivity of AQP-4 expressing oocytes to bacopaside I in osmotic swelling assays. Based on the docking model, candidate residues that could contribute to the proposed binding of bacopaside sugar rings in the hAQP1 intracellular water pore appear to include amino acids serine 71 in the loop B region, and tyrosine 97 in the adjacent membrane spanning domains, but remain to be defined.

Inhibition of AQP1 water channel activity by bacopasides I and II showed a slow onset that was consistent with pre-requisite transit of the agent across the membrane to access the intracellular side. The latency period (approximately 2 hours) was comparable to that described for other aquaporin modulators AqB013 and AqF026, also thought to act at the cytoplasmic side (Migliati et al., 2009; Yool et al., 2013).

Accumulating evidence suggests pharmacologic agents can be defined with subtype selectivity for AQP classes. Prior work

showed external application of AqF026 potentiated water permeability in AQP1 (EC_{50} 3.3 μ M), but a 15-fold higher concentration was required to potentiate AQP4 (Yool et al., 2013). Metal complexes acted as blockers of glycerol permeability in AQP3 (at an external site predicted to involve cysteine [C40] and arginine [R218] residues), with comparatively small effects on AQP1 water permeability (Martins et al., 2013). Results here for bacopaside I showed block of osmotic water permeability for AQP1 but not AQP4 channels. This difference in bacopaside sensitivity between related aquaporins suggests that the inhibitory effects seen for AQP1 are exerted directly on the heterologously expressed channel and are not due to side effects on endogenous oocyte channels or transporters.

The reversibility of the block indicated that functional properties and expression of the channels in plasma membrane were not impaired. Data here cannot rule out actions of bacopasides on other molecules not yet assessed; however, the

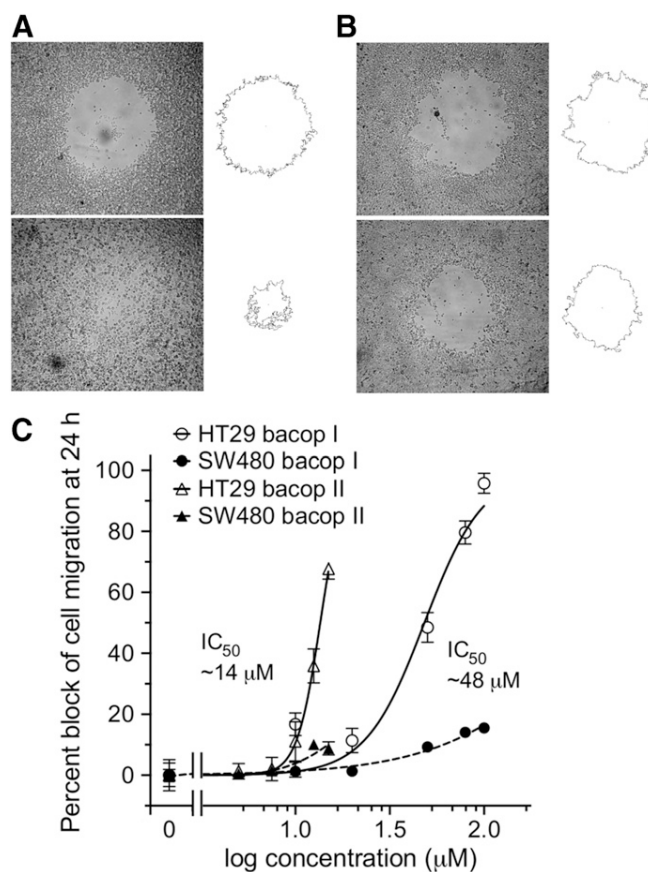


Fig. 6. Dose-dependent inhibition of migration by bacopasides I and II in AQP1-expressing HT29 cells, but not in SW480 cells with low AQP1 expression. Cell migration in the presence of a mitotic inhibitor was assessed by rates of closure of circular wounds, created by aspiration with a pipette tip in confluent cultures (see *Materials and Methods* for details). (A, B) Cell migration was assessed in vehicle (A) or with 15 μ M bacopaside II (B) added immediately after wounding. Images are shown for confluent HT29 cultures after initial wounding at time 0 (upper panels) and at 24 hours (lower panels). (C) Dose-dependent block of HT29 cell migration was seen with bacopasides I and II, with IC_{50} values estimated at 48 and 14 μ M, respectively. Partial block of SW480 migration at the highest doses tested did not exceed 20%. Doses beyond the ranges shown were not considered valid due to the onset of cytotoxicity.

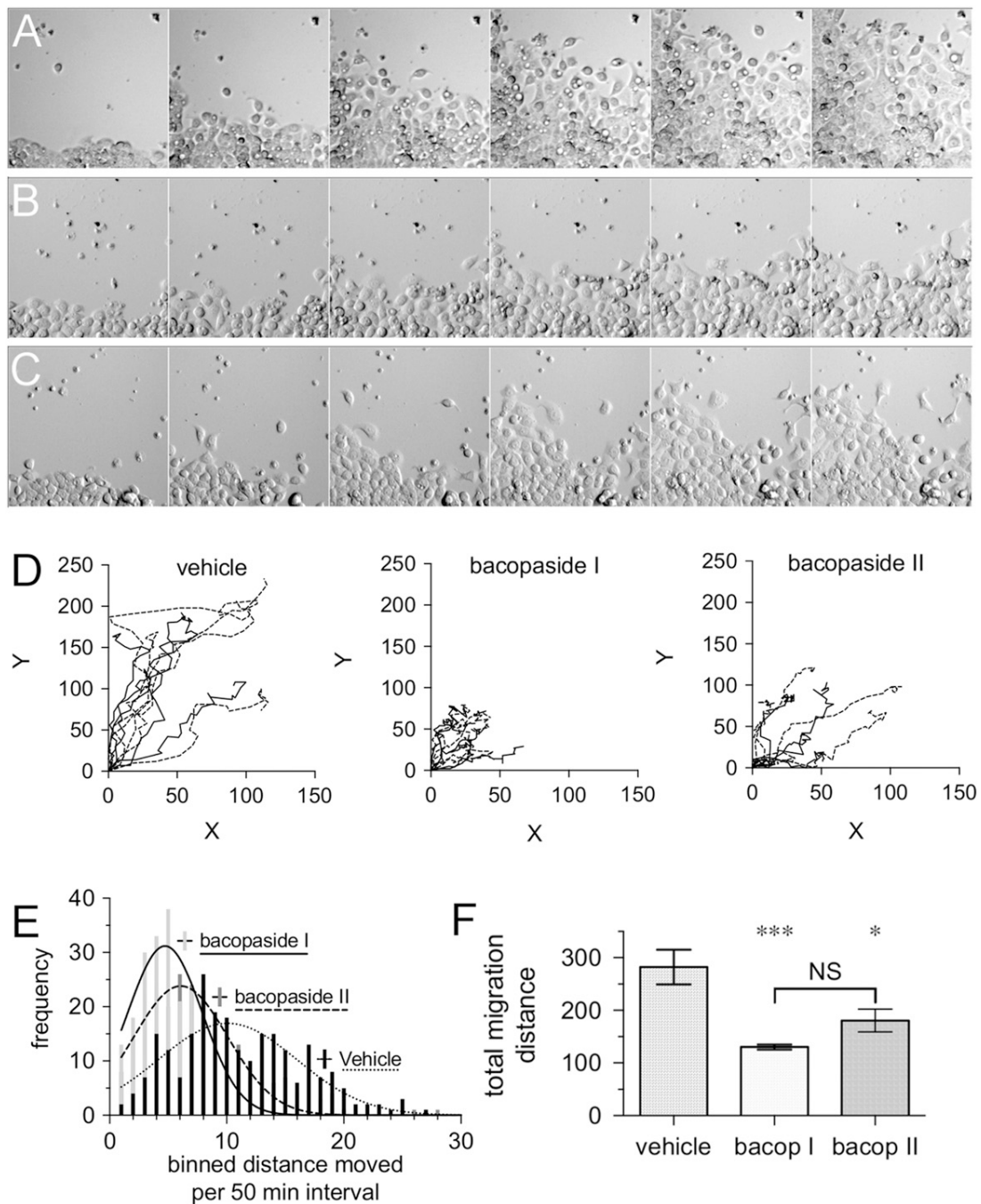


Fig. 7. Live-cell imaging of the inhibitory effects of bacopasides I and II on migration of HT29 cells. Single cells at the boundaries of circular wounds were tracked with time-lapse images taken at 25-minute intervals for 10 hours at 37°C. (A–C) Panels of six images each from time-lapse series are shown at 50-minute intervals: (A) HT29 cells with vehicle treatment. (B) HT29 cells treated with 50 μM bacopaside I. (C) HT29 cells treated with 15 μM bacopaside II. (D) Trajectory plots of 10 individual cells per treatment group, monitored by cell nucleus position as a function of time. Data were converted to absolute values and referenced to the starting position at time 0; X and Y values are in pixels (7.45 pixels per mm). Trajectory plots illustrate the total movement of 10 individual cells per treatment over a duration of 600 minutes, with vehicle, bacopaside I or with bacopaside II. (E) Frequency histograms of the distances moved by individual cells per 50-minute interval over 600 minutes of imaging, for 10 cells per treatment group. Histograms were fit with Gaussian distribution functions (R^2 values > 0.94); best-fit values for the mean distances moved per cell per 50-minute interval were 10.1 ± 0.5 for untreated, 4.7 ± 0.2 for bacopaside I treated, and 7.8 ± 0.2 for bacopaside II treated (mean \pm S.E.M.). (F) Summary histogram showing the mean total distance traveled by cells in 600 minutes, showing significant inhibition of cell motility by both bacopaside I and II as compared with vehicle-treated cells (analysis of variance test $P < 0.05$; post hoc Bonferroni $*P < 0.05$; $***P < 0.001$). Data are mean \pm S.E.M.; n values are 10 cells per treatment group.

lack of effect of bacopaside on migration in SW480 cells with low AQP1 expression suggests the mechanism of action is reasonably selective, and does not appreciably impact diverse signaling and transport processes needed for basic

maintenance and non-AQP1 dependent motility. Cytotoxicity assays showed the viability of AQP1-expressing HT29 cancer cells was not affected by bacopasides I and II at doses that significantly blocked ion flux and cell migration.

TABLE 1
Analysis of cytotoxicity in HT29 colon cancer cells at 24 hours of treatment, using an AlamarBlue fluorescence assay

Concentration (μM)	Mean Normalized Cell Viability (%) ^a	<i>n</i> value	<i>P</i> value
bacopaside I			
0	108 \pm 4.8	17	N.S.
0 (vehicle)	100 \pm 3.1	17	—
50	97 \pm 2.1	8	N.S.
75	79 \pm 4.2	8	N.S.
100	59 \pm 3.2	8	^b
bacopaside II			
0	113 \pm 6.2	16	N.S.
0 (vehicle)	100 \pm 5.7	16	—
15	104 \pm 18	8	N.S.
20	123 \pm 17	8	N.S.
30	47 \pm 5.7	8	^b
HgCl ₂			
100	16.1 \pm 4.6	6	^b

^aMean \pm S.E.M. The percentage of viability was standardized as a percentage of the vehicle-treated mean value, measured as changes in AlamarBlue fluorescence signal intensity. See *Materials and Methods* for details.

^bStatistically significant differences ($P < 0.05$), compared with vehicle-treated, were analyzed by analysis of variance with post hoc Dunnett's multiple comparison test (GraphPad Prism). N.S. is not statistically significant.

Bacopasides I and II are triterpene glycosides, composed of a hydrophobic pentacyclic terpene backbone (estimated log*P* value approximately 9; enabling membrane permeability), and three linked polar sugar groups (arabinofuranosyl—glucopyranosyl—arabinopyranose in bacopaside I; and arabinofuranosyl—sulfonfyl—glucopyranosyl—glucopyranose in bacopaside II) that appear from *in silico* modeling to lodge via H-bonds into the water pore entrance of AQP1, with the exception of the sulfonfyl group which appears to require an interface with positively charged residues (arginines in the adjacent AQP1 loop D domain). Mutation of the key loop D arginines to alanines appeared to cause destabilization of the overall binding of the bacopaside I compound on AQP1, seen as a decreased efficacy of water pore block and increased IC₅₀ value in the R159A+R160A mutant.

The ability of modulators to block the central pore ionic conductance is an important consideration in processes such as rapid cell migration which appear to require the AQP1 cation channel activity (Kourghi et al., 2016). Interaction of the sulfonfyl group with loop D arginines was consistent with the observed block of the cGMP-activated ionic conductance by bacopaside I, not II. Bacopaside II lacked an effect on the ionic conductance, and showed similar IC₅₀ values for the block of AQP1 water channel activity in oocytes, and the block of cell migration in HT29 cells. In contrast, bacopaside I showed a lower IC₅₀ value for inhibiting HT29 cancer cell migration ($\sim 48 \mu\text{M}$) than for inhibiting the AQP1 osmotic water flux in oocytes ($\sim 117 \mu\text{M}$), suggesting that simultaneous block of both water and ion channel activities of AQP1 might be more effective in blocking cell migration. This is consistent with the observed migration trajectories, which were more compressed in bacopaside I-treated group than in the bacopaside II-treated group.

Although the overall amino acid sequence similarity between AQP1 and AQP4 channels is high (>40% identity and 60% homology), AQP4-mediated osmotic swelling was not sensitive to block by bacopaside I. The docking model suggested the bulky terpene might sterically hinder docking near the AQP4 water pore. As well, the loop D domain of AQP4 lacks the key arginines 159 and 160, suggested here to be

important for the sulfonfyl group coordination, showing instead serine and lysine in the equivalent positions, which might be less effective as putative coordination sites.

The identification of bacopasides as novel AQP modulators expands the database of pharmacophore properties of AQP ligands. Bacopasides I and II themselves might not be ideal as drug candidates, exceeding limits of Lipinski's Rule of Five for molecular weight, hydrophobicity, and numbers of hydrogen bond donors and acceptors—although natural products often show biologic activity as exceptions to the rule (Ganesan, 2008). Bacopasides administered *in vivo* are likely to act as metabolic derivatives as well as intact compounds. More work is needed to define *in vivo* metabolites of bacopasides and characterize their effects on aquaporins. Nonetheless, bacopasides could serve as lead compounds for the design of small-molecule blockers of aquaporins.

Our results suggest the trisaccharide moiety is a key component. An intriguing idea would be to design compact membrane-permeable trisaccharides for blocking water flux; addition of key sulfonfyl or other groups could inhibit parallel AQP functions. Endogenous polysaccharide osmolytes in cells might function as natural modulators of aquaporin channels, a concept that has not to our knowledge been considered previously.

Bacopa monnieri extract (also known as brahmi) has been used in Ayurvedic remedies since ancient times to improve memory and treat anxiety and depression (Russo and Borrelli, 2005). Brahmi has been suggested to have beneficial effects on psychological state, cognitive performance, and memory in human subjects and animal models; neuroprotective effects after ischemic brain injury; and anti-inflammatory actions in processes linked to neurodegenerative disorders (Singh and Dhawan, 1982; Sairam et al., 2002; Rehni et al., 2007; Zhou et al., 2007; Saraf et al., 2010; Aguiar and Borowski, 2013; Downey et al., 2013; Liu et al., 2013; Kongkeaw et al., 2014; Williams et al., 2014). A meta-analysis of human clinical studies (generally with *B. monnieri* administered 250–450 mg/day for up to several months) improved mental response time and attention, and had potential benefits on memory (Kongkeaw et al., 2014). No serious adverse events were noted; minor side effects included diarrhea and dry mouth.

Beneficial outcomes ascribed to brahmi could in part involve block of AQP1 channels. AQP1 is expressed abundantly in brain choroid plexus where cerebral spinal fluid is produced (Boassa and Yool, 2005; Johansson et al., 2005) and in proximal kidney to facilitate water reabsorption (Nielsen and Agre, 1995). AQP1 is found in peripheral vasculature endothelia, red blood cells, and other cell types (Nielsen et al., 1993). Block of AQP1 could contribute to the anti-inflammatory benefits of brahmi treatment. Macrophages express AQP1 channels, which are required for interleukin-1 β release and neutrophilic inflammation responses (Raboli et al., 2014). An alcoholic extract of *B. monnieri* decreased tumor necrosis factor- α production in mouse macrophages preincubated for 1 hour, with an IC₅₀ near 1 mg/ml (Williams et al., 2014).

Pharmacologic inhibitors of AQP1 channels could be useful for intervention in many conditions, including slowing metastasis in AQP1-positive cancer subtypes. In a subset of aggressive cancers, AQP1 expression is up-regulated (Saadoun et al., 2002; Moon et al., 2003; Yool et al., 2010; El Hindy et al., 2013). AQP1 channels located at lamellipodial edges have been implicated in enhancing migration and

metastasis (Hu and Verkman, 2006; McCoy and Sontheimer, 2007). Block of the AQP1 ion channel impairs migration in AQP1-expressing HT29 colon cancer cells (Kourghi et al., 2016).

A comprehensive portfolio of selective aquaporin modulators is needed for clinical and basic research. Further exploration of AQP modulators in traditional herbal medicines is merited (Pei et al., 2016). New ligand modulators of aquaporin channel activity could be present in the armamentarium of traditional herbal medicines, but they remain to be discovered.

Acknowledgments

The authors thank John Sandham and the Botanic Gardens of Adelaide for identified samples of the water hyssop *Bacopa monnieri*, and Dr. Agatha Labrinidis and the Adelaide Microscopy core facility for access to equipment, support, and training in live cell imaging.

Authorship Contributions

Participated in research design: Pei, Campbell, Hardingham, Yool.

Conducted experiments: Pei, Kourghi, De Ieso, Campbell, Doward.

Performed data analysis: Pei, Kourghi, De Ieso, Yool.

Wrote or contributed to the writing of the manuscript: Pei, Kourghi, De Ieso, Yool.

References

- Agre P, Preston GM, Smith BL, Jung JS, Raina S, Moon C, Guggino WB, and Nielsen S (1993) Aquaporin CHIP: the archetypal molecular water channel. *Am J Physiol* **265**:F463–F476.
- Aguiar S and Borowski T (2013) Neuropharmacological review of the nootropic herb *Bacopa monnieri*. *Rejuvenation Res* **16**:313–326.
- Anthony TL, Brooks HL, Boassa D, Leonov S, Yanochko GM, Regan JW, and Yool AJ (2000) Cloned human aquaporin-1 is a cyclic GMP-gated ion channel. *Mol Pharmacol* **57**:576–588.
- Boassa D and Yool AJ (2003) Single amino acids in the carboxyl terminal domain of aquaporin-1 contribute to cGMP-dependent ion channel activation. *BMC Physiol* **3**:12.
- Boassa D and Yool AJ (2005) Physiological roles of aquaporins in the choroid plexus. *Curr Top Dev Biol* **67**:181–206.
- Brooks HL, Regan JW, and Yool AJ (2000) Inhibition of aquaporin-1 water permeability by tetraethylammonium: involvement of the loop E pore region. *Mol Pharmacol* **57**:1021–1026.
- Calamita G, Bishai WR, Preston GM, Guggino WB, and Agre P (1995) Molecular cloning and characterization of AqpZ, a water channel from *Escherichia coli*. *J Biol Chem* **270**:29063–29066.
- Campbell EM, Birdsall DN, and Yool AJ (2012) The activity of human aquaporin 1 as a cGMP-gated cation channel is regulated by tyrosine phosphorylation in the carboxyl-terminal domain. *Mol Pharmacol* **81**:97–105.
- Detmers FJ, de Groot BL, Müller EM, Hinton A, Konings IB, Sze M, Flitsch SL, Grubmüller H, and Deen PM (2006) Quaternary ammonium compounds as water channel blockers. Specificity, potency, and site of action. *J Biol Chem* **281**:14207–14214.
- Devuyt O and Yool AJ (2010) Aquaporin-1: new developments and perspectives for peritoneal dialysis. *Perit Dial Int* **30**:135–141.
- Downey LA, Kean J, Nemej F, Lau A, Poll A, Gregory R, Murray M, Rourke J, Patak B, Pase MP, et al. (2013) An acute, double-blind, placebo-controlled crossover study of 320 mg and 640 mg doses of a special extract of *Bacopa monnieri* (CDRI 08) on sustained cognitive performance. *Phytother Res* **27**:1407–1413.
- El Hindy N, Bankfalvi A, Herring A, Adamzik M, Lambertz N, Zhu Y, Siffert W, Sure U, and Sandalcioglu IE (2013) Correlation of aquaporin-1 water channel protein expression with tumor angiogenesis in human astrocytoma. *Anticancer Res* **33**:609–613.
- Esteva-Font C, Jin BJ, Lee S, Phuan PW, Anderson MO, and Verkman AS (2016) Experimental evaluation of proposed small-molecule inhibitors of water channel aquaporin-1. *Mol Pharmacol* **89**:686–693.
- Fu D, Libson A, Miercke LJ, Weitzman C, Nollert P, Krucinski J, and Stroud RM (2000) Structure of a glycerol-conducting channel and the basis for its selectivity. *Science* **290**:481–486.
- Ganesan A (2008) The impact of natural products upon modern drug discovery. *Curr Opin Chem Biol* **12**:306–317.
- Gao J, Wang X, Chang Y, Zhang J, Song Q, Yu H, and Li X (2006) Acetazolamide inhibits osmotic water permeability by interaction with aquaporin-1. *Anal Biochem* **350**:165–170.
- Hu J and Verkman AS (2006) Increased migration and metastatic potential of tumor cells expressing aquaporin water channels. *FASEB J* **20**:1892–1894.
- Huber VJ, Tsujita M, Kwee IL, and Nakada T (2009) Inhibition of aquaporin 4 by antiepileptic drugs. *Bioorg Med Chem* **17**:418–424.
- Huber VJ, Tsujita M, Yamazaki M, Sakimura K, and Nakada T (2007) Identification of arylsulfonamides as aquaporin 4 inhibitors. *Bioorg Med Chem Lett* **17**:1270–1273.
- Johansson PA, Dziegielewska KM, Ek CJ, Habgood MD, Møllgård K, Potter A, Schuliga M, and Saunders NR (2005) Aquaporin-1 in the choroid plexuses of developing mammalian brain. *Cell Tissue Res* **322**:353–364.
- Kongkeaw C, Dilokthornsakul P, Thanarangsarit P, Limpeanchob N, and Norman Scholfield C (2014) Meta-analysis of randomized controlled trials on cognitive effects of *Bacopa monnieri* extract. *J Ethnopharmacol* **151**:528–535.
- Kourghi M, Pei JV, De Ieso ML, Flynn G, and Yool AJ (2016) Bumetanide derivatives AqB007 and AqB011 selectively block the aquaporin-1 ion channel conductance and slow cancer cell migration. *Mol Pharmacol* **89**:133–140.
- Liu X, Yue R, Zhang J, Shan L, Wang R, and Zhang W (2013) Neuroprotective effects of bacopaside I in ischemic brain injury. *Restor Neurol Neurosci* **31**:109–123.
- Martins AP, Ciancetta A, de Almeida A, Marrone A, Re N, Soveral G, and Casini A (2013) Aquaporin inhibition by gold(III) compounds: new insights. *ChemMedChem* **8**:1086–1092.
- McCoy E and Sontheimer H (2007) Expression and function of water channels (aquaporins) in migrating malignant astrocytes. *Glia* **55**:1034–1043.
- Migliati E, Meurice N, DuBois P, Fang JS, Somasekharan S, Beckett E, Flynn G, and Yool AJ (2009) Inhibition of aquaporin-1 and aquaporin-4 water permeability by a derivative of the loop diuretic bumetanide acting at an internal pore-occluding binding site. *Mol Pharmacol* **76**:105–112.
- Moon C, Soria JC, Jang SJ, Lee J, Obaidul Hoque M, Sibony M, Trink B, Chang YS, Sidransky D, and Mao L (2003) Involvement of aquaporins in colorectal carcinogenesis. *Oncogene* **22**:6699–6703.
- Nielsen S and Agre P (1995) The aquaporin family of water channels in kidney. *Kidney Int* **48**:1057–1068.
- Nielsen S, Smith BL, Christensen EI, and Agre P (1993) Distribution of the aquaporin CHIP in secretory and resorptive epithelia and capillary endothelia. *Proc Natl Acad Sci USA* **90**:7275–7279.
- Niemietz CM and Tyerman SD (2002) New potent inhibitors of aquaporins: silver and gold compounds inhibit aquaporins of plant and human origin. *FEBS Lett* **531**:443–447.
- Papadopoulos MC and Verkman AS (2008) Potential utility of aquaporin modulators for therapy of brain disorders. *Prog Brain Res* **170**:589–601.
- Parsels LA, Parsels JD, Tai DC, Coughlin DJ, and Maybaum J (2004) 5-fluoro-2'-deoxyuridine-induced cdc25A accumulation correlates with premature mitotic entry and clonogenic death in human colon cancer cells. *Cancer Res* **64**:6588–6594.
- Pei JV, Burton JL, Kourghi M, De Ieso ML, and Yool AJ (2016) Drug discovery and therapeutic targets for pharmacological modulators of aquaporin channels, in *Aquaporins in Health and Disease: New Molecular Targets For Drug Discovery* (Soveral G, Casini A, and Nielsen S, eds) pp 275–297, CRC Press, Oxfordshire, United Kingdom.
- Preston GM, Jung JS, Guggino WB, and Agre P (1993) The mercury-sensitive residue at cysteine 189 in the CHIP28 water channel. *J Biol Chem* **268**:17–20.
- Raboli V, Wallemme L, Lo Re S, Uwambayinema F, Palmari-Pallag M, Thomassen L, Tyteca D, Octave JN, Marbaix E, Lison D, et al. (2014) Critical role of aquaporins in interleukin 1 β (IL-1 β)-induced inflammation. *J Biol Chem* **289**:13937–13947.
- Rehni AK, Pantlya HS, Shri R, and Singh M (2007) Effect of chlorophyll and aqueous extracts of *Bacopa monnieri* and *Valeriana wallichii* on ischaemia and reperfusion-induced cerebral injury in mice. *Indian J Exp Biol* **45**:764–769.
- Reizer J, Reizer A, and Saier MH, Jr (1993) The MIP family of integral membrane channel proteins: sequence comparisons, evolutionary relationships, reconstructed pathway of evolution, and proposed functional differentiation of the two repeated halves of the proteins. *Crit Rev Biochem Mol Biol* **28**:235–257.
- Russo A and Borrelli F (2005) *Bacopa monnieri*, a reputed nootropic plant: an overview. *Phytomedicine* **12**:305–317.
- Saadoun S, Papadopoulos MC, Davies DC, Bell BA, and Krishna S (2002) Increased aquaporin 1 water channel expression in human brain tumours. *Br J Cancer* **87**:621–623.
- Sairam K, Dorababu M, Goel RK, and Bhattacharya SK (2002) Antidepressant activity of standardized extract of *Bacopa monnieri* in experimental models of depression in rats. *Phytomedicine* **9**:207–211.
- Saparov SM, Kozono D, Rothe U, Agre P, and Pohl P (2001) Water and ion permeation of aquaporin-1 in planar lipid bilayers. Major differences in structural determinants and stoichiometry. *J Biol Chem* **276**:31515–31520.
- Saraf MK, Prabhakar S, and Anand A (2010) Neuroprotective effect of *Bacopa monnieri* on ischemia induced brain injury. *Pharmacol Biochem Behav* **97**:192–197.
- Schindelin J, Arganda-Carreras I, Frise E, Kaynig V, Longair M, Pietzsch T, Preibisch S, Rueden C, Saalfeld S, Schmid B, et al. (2012) Fiji: an open-source platform for biological-image analysis. *Nat Methods* **9**:676–682.
- Seeliger D, Zapater C, Krenc D, Haddoub R, Flitsch S, Beitz E, Cerdà J, and de Groot BL (2013) Discovery of novel human aquaporin-1 blockers. *ACS Chem Biol* **8**:249–256.
- Singh HK and Dhawan BN (1982) Effect of *Bacopa monnieri* Linn. (brahmi) extract on avoidance responses in rat. *J Ethnopharmacol* **5**:205–214.
- Tajkhorshid E, Nollert P, Jensen MO, Miercke LJ, O'Connell J, Stroud RM, and Schulten K (2002) Control of the selectivity of the aquaporin water channel family by global orientational tuning. *Science* **296**:525–530.
- Trott O and Olson AJ (2010) AutoDock Vina: improving the speed and accuracy of docking with a new scoring function, efficient optimization, and multithreading. *J Comput Chem* **31**:455–461.
- Williams R, Münch G, Gyengesi E, and Bennett L (2014) *Bacopa monnieri* (L.) exerts anti-inflammatory effects on cells of the innate immune system in vitro. *Food Funct* **5**:517–520.
- Yang B, Kim JK, and Verkman AS (2006) Comparative efficacy of HgCl₂ with candidate aquaporin-1 inhibitors DMSO, gold, TEA⁺ and acetazolamide. *FEBS Lett* **580**:6679–6684.
- Yool AJ (2007) Functional domains of aquaporin-1: keys to physiology, and targets for drug discovery. *Curr Pharm Des* **13**:3212–3221.
- Yool AJ, Brokl OH, Pannabecker TL, Dantzer WH, and Stamer WD (2002) Tetraethylammonium block of water flux in aquaporin-1 channels expressed in kidney thin limbs of Henle's loop and a kidney-derived cell line. *BMC Physiol* **2**:4.

- Yool AJ, Brown EA, and Flynn GA (2010) Roles for novel pharmacological blockers of aquaporins in the treatment of brain oedema and cancer. *Clin Exp Pharmacol Physiol* **37**:403–409.
- Yool AJ and Campbell EM (2012) Structure, function and translational relevance of aquaporin dual water and ion channels. *Mol Aspects Med* **33**:553–561.
- Yool AJ, Morelle J, Cnops Y, Verbavatz JM, Campbell EM, Beckett EA, Booker GW, Flynn G, and Devuyst O (2013) AqF026 is a pharmacologic agonist of the water channel aquaporin-1. *J Am Soc Nephrol* **24**:1045–1052.
- Yool AJ and Weinstein AM (2002) New roles for old holes: ion channel function in aquaporin-1. *News Physiol Sci* **17**:68–72.
- Yu J, Yool AJ, Schulten K, and Tajkhorshid E (2006) Mechanism of gating and ion conductivity of a possible tetrameric pore in aquaporin-1. *Structure* **14**:1411–1423.
- Zhang W, Zitron E, Hömme M, Kihm L, Morath C, Scherer D, Hegge S, Thomas D, Schmitt CP, Zeier M, et al. (2007) Aquaporin-1 channel function is positively regulated by protein kinase C. *J Biol Chem* **282**:20933–20940.
- Zhou Y, Shen YH, Zhang C, Su J, Liu RH, and Zhang WD (2007) Triterpene saponins from *Bacopa monnieri* and their antidepressant effects in two mice models. *J Nat Prod* **70**:652–655.

Address correspondence to: Dr. Andrea J. Yool, Medical School South level 4, Frome Road, Adelaide SA 5005 Australia. E-mail: andrea.yool@adelaide.edu.au



Contents lists available at ScienceDirect

Insect Biochemistry and Molecular Biology

journal homepage: www.elsevier.com/locate/ibmb

Molecular and functional characterization of multiple aquaporin water channel proteins from the western tarnished plant bug, *Lygus hesperus*

Jeffrey A. Fabrick^{a,*}, Jinxin Pei^b, J. Joe Hull^a, Andrea J. Yool^b^a USDA-ARS, U.S. Arid Land Agricultural Research Center, 21881 North Cardon Lane, Maricopa, AZ 85138, USA^b University of Adelaide, School of Medical Sciences, Frome Rd., Medical School South, Adelaide, SA 5005, Australia

ARTICLE INFO

Article history:

Received 17 September 2013

Received in revised form

27 November 2013

Accepted 1 December 2013

Keywords:

Aquaporin

Major intrinsic protein family

Lygus hesperus

Western tarnished plant bug

Hemiptera

Superaquaporin

S-aquaporin

ABSTRACT

Aquaporins (AQPs) are integral membrane channel proteins that facilitate the bidirectional transfer of water or other small solutes across biological membranes involved in numerous essential physiological processes. In arthropods, AQPs belong to several subfamilies, which contribute to osmoregulation, respiration, cryoprotection, anhydrobiosis, and excretion. We cloned and characterized five novel AQPs from the western tarnished plant bug, *Lygus hesperus*, a polyphagous insect pest of food and fiber crops throughout western North America. The *L. hesperus* AQPs (LhAQP1–5) belong to different phylogenetic subfamilies, have unique transcription profiles and cellular localizations, and all transport water (but not glycerol) when heterologously expressed in *Xenopus laevis* oocytes. Our results demonstrate that multiple AQPs with possible compensatory functions are produced in *L. hesperus* that likely play important roles in maintaining water homeostasis in this important insect pest.

Published by Elsevier Ltd.

1. Introduction

Aquaporins (AQPs) belong to the ancient class of major intrinsic proteins (MIPs), which are integral membrane channel proteins found in all kingdoms of life. These proteins facilitate the bidirectional transfer of water or sometimes other small neutral solutes across biological membranes involved in numerous essential physiological processes (Hachez and Chaumont, 2010; Gomes et al., 2009; King et al., 2004). AQPs are best known for their diverse roles in water transport related to cell water balance regulation [reviewed in Agre et al. (1998); Carbrey and Agre, 2009], but they

also transport a wide range of solutes, including urea and glycerol, hydrogen peroxide, dissolved gasses (CO₂, NO, NH₃), and certain metalloids (Cohen, 2013; Hachez and Chaumont, 2010). Whereas most solutes permeate through the monomeric channel, AQPs usually assemble as tetramers forming a fifth central pore that in some cases functions to conduct ions (Yool and Weinstein, 2002; Yool, 2007).

The functional diversity of AQPs is facilitated by key modifications to their structure. In general, members of the MIP superfamily share a number of structural features, including six helical transmembrane (TM) domains connected by five alternating extracellular/intracellular loops with intercellular amino and carboxyl termini, two canonical Asp-Pro-Ala (NPA) motifs, and the aromatic/arginine (ar/R) selectivity filter (Zardoya, 2005). Together, the canonical amino- and carboxyl-terminal halves form two tandem repeats, each containing a single NPA motif, forming the ‘aquaporin’ or ‘hourglass’ fold (Jung et al., 1994; Murata et al., 2000) and ultimately shaping the selective TM channel. ‘Classical’ or ‘orthodox’ AQPs allow water diffusion through an extremely narrow and electrostatically-selective pore that precludes the permeability of large, hydrophobic, or incorrectly charged solutes (Murata et al., 2000). In another functional class of AQPs known as the aquaglyceroporins, the composition of the ar/R constriction site and the corresponding larger, more hydrophobic three-dimensional shape of the pore enables permeation of additional solutes, such as

Abbreviations: AQP, aquaporin; MIPs, major intrinsic proteins; NPA motif, Asparagine-Proline-Alanine motif; ar/R, aromatic arginine; DRIPs, *Drosophila* intrinsic proteins; BiB, Big Brain protein; RNAi, RNA interference; PRIPs, *Pyrocoelia rufa* integral proteins; LhAQP, *Lygus hesperus* aquaporin; RACE, rapid amplification of cDNA ends; cDNA, complementary DNA; CDS, coding sequence; ORF, open reading frame; RT-PCR, reverse transcriptase polymerase chain reaction; Tni cells, cultured *Trichoplusia ni* cells; EGFP, enhanced green fluorescent protein; cRNA, complementary RNA; TM, transmembrane; RPIPs, *Rhodnius prolixus* integral proteins; DVIPs, *Dermacentor variabilis* integral proteins; LHIPs, *Lygus hesperus* integral proteins; ER, endoplasmic reticulum; EST, expressed sequence tag; SIP, short basic intrinsic proteins.

* Corresponding author. Tel.: +1 520 316 6335; fax: +1 520 316 6330.

E-mail addresses: jeff.fabrick@ars.usda.edu, jeff.fabrick@ars.usda.gov (J. A. Fabrick).

0965-1748/\$ – see front matter Published by Elsevier Ltd.

<http://dx.doi.org/10.1016/j.ibmb.2013.12.002>

polyols (Fu et al., 2000; Hub and de Groot, 2008). Members of a recently identified subfamily known as ‘superaquaporins’ or “S-aquaporins” exhibit low sequence similarity with other AQPs, altered NPA signature motifs, and anomalous subcellular localization (Ishibashi, 2006, 2009; Nozaki et al., 2008; Calvanese et al., 2013).

Whereas vertebrate AQPs have been studied extensively [reviewed in King et al. (2004); Verkman 2008; and Ishibashi et al., 2009], far less attention has been given to invertebrate AQPs. In arthropods, AQPs are involved in regulating the movement of high volume liquid diets, osmoregulation, respiration, cryoprotection and anhydrobiosis [reviewed in Campbell et al. (2008); Spring et al., 2009; and Cohen 2013]. Genome sequencing indicates that insects may contain up to 5–8 genes encoding putative aquaporin-like transcripts (Campbell et al., 2008; Drake et al., 2010), but the complete repertoire from any single species is yet to be fully characterized. Multiple functional AQPs have been found in several insects, including three from *Aedes aegypti* (Duchesne et al., 2003; Drake et al., 2010) and *Bombyx mori* (Kataoka et al., 2009a; Azuma et al., 2012), and two from the oriental fruit moth, *Grapholita molesta* (Kataoka et al., 2009b), the pea aphid, *Acyrtosiphon pisum* (Shakesby et al., 2009; Wallace et al., 2012), the sleeping chironomid, *Polypedilum vanderplanki* (Kikawada et al., 2008), and *Drosophila melanogaster* (DRIP and BiB) (Kaufmann et al., 2005; Yanocho and Yool, 2002). For *A. aegypti*, studies have shown that a water-specific DRIP (AeaAQP) is involved in water movement in Malpighian tubules and tracheoles (Duchesne et al., 2003). RNA interference (RNAi) knockdown further revealed a role in diuresis in Malpighian tubules for three of the six putative AQPs (Drake et al., 2010). Functional AQPs from *B. mori* include, AQP-Bom1 (a water-specific DRIP), AQP-Bom2 (an aquaglyceroporin), and AQP-Bom3 (a water-specific PRIP), all of which play important roles in water reabsorption and recycling within the cryptonephric rectal complex (Kataoka et al., 2009a; Azuma et al., 2012). *G. molesta* has a functional water-specific DRIP (AQP-Gra1) and an aquaglyceroporin (AQP-Gra2) (Kataoka et al., 2009b). In *A. pisum*, ApAQP1 was shown to be a water-specific AQP (Shakesby et al., 2009) whereas ApAQP2 exhibited aquaglyceroporin activities, transporting water and glycerol in *Xenopus* oocytes (Wallace et al., 2012). Two *P. vanderplanki* AQPs (PvAQP1 and PvAQP2) facilitated water permeation, but not transport of glycerol in *Xenopus* oocytes (Kikawada et al., 2008). Among the *D. melanogaster* AQPs characterized are a water-selective AQP called *Drosophila* integral protein or DRIP, which is involved in excretion and osmoregulation (Kaufmann et al., 2005), and the novel AQP known as Big Brain (DmBiB), which does not permeate water, but functions as a cation channel (Yanocho and Yool, 2002). Other arthropods having at least one functionally characterized AQP include: *Cicadella viridis* (La Caherec et al., 1997); *Rhodnius prolixus* (Echevarria et al., 2001); *Anopheles gambiae* (Liu et al., 2011); *Blattella germanica* (Herranz et al., 2011); *Eurosta solidaginis* (Philip et al., 2011); *Bemisia tabaci* (Mathew et al., 2011); *Belgica antarctica* (Goto et al., 2011); *Anomala cuprea* (Nagae et al., 2013); and the ticks, *Dermacentor variabilis* (Holmes et al., 2008), *Rhipicephalus sanguineus* (Ball et al., 2009), and *Ixodes ricinus* (Campbell et al., 2010).

Numerous species within the hemipteran family Miridae are important agricultural pests causing crop damage from feeding with specialized piercing-sucking mouthparts (Wheeler, 2001). One such mirid bug is *Lygus hesperus* Knight (the western tarnished plant bug), a highly polyphagous pest causing economic losses in numerous cropping systems in western North America (Wheeler, 2001). Lygus bugs are “cell rupture” feeders (previously termed “lacerate-and-flush”) that first puncture host tissue and inject saliva containing digestive enzymes (Miles, 1987; Strong and Kruitwagen, 1968; Shackel et al., 2005; Backus et al., 2007). The

pre-digested fluid is then pumped through the food canal for absorption of nutrients primarily within the midgut epithelium of the alimentary tract (Wheeler, 2001; Habibi et al., 2008). Some hemipterans use specialized biochemical processes or gut morphology (e.g. filter chambers) to abate osmotic stress and remove excess dietary fluid (Douglas, 2006; Gullan and Cranston, 2005; Lehane and Billingsley, 1996; Hubert et al., 1989; Mathew et al., 2011). Lygus bugs lack the specialized filter chamber or gastric caecae of sap feeding hemipterans, and instead have a simple, cimicomorph type alimentary tract typical of other mesophyll feeders (Goodchild, 1966; Habibi et al., 2008).

Here, we characterize five AQPs (LhAQP1–5) from *L. hesperus*. Based on sequence conservation and phylogenetics, bioinformatic predictions, cellular and tissue localization, temporal expression, and functional analysis, the LhAQPs belong to different subfamilies but all function as water-specific channel proteins. Localization and transcription profiles for LhAQPs provide clues about the putative roles these functionally redundant AQPs may play in maintaining *L. hesperus* water homeostasis. The combination of standard molecular cloning techniques and the mining of transcriptome data for AQPs provides an unprecedented opportunity to comprehensively identify and characterize AQPs within *L. hesperus*.

2. Materials and methods

2.1. Insects

A laboratory colony of *Lygus hesperus* was maintained at the USDA-ARS U.S. Arid Land Agricultural Research Center in Maricopa, AZ, USA. The colony was fed green beans and artificial diet at 25 °C under 20% humidity and with an L14:D10 photoperiod (Debolt, 1982; Patana, 1982).

2.2. cDNA isolation and 5'-RACE of LhAQPs

Total RNA was extracted from 100 mg of *L. hesperus* adults and 2nd–3rd instar nymphs using TRIzol[®] reagent (Invitrogen-Life Technologies, Carlsbad, CA). cDNA was produced using random hexamer primers and SuperScript III First-strand Synthesis System (Invitrogen-Life Technologies) according to manufacturer's recommendations. PCR primers 1LhAQP5–8LhAQP3 (Table 1) were designed using Primer3Plus (Untergasser et al., 2007) from four putative *Lygus lineolaris* AQPs obtained from a *L. lineolaris* transcriptome sequencing project (O.P. Perera, unpublished). Four partial LhAQPs (named LhAQP1–4) were PCR amplified using ExTaq DNA polymerase premix (Takara-Clontech, Palo Alto, CA) and primer pairs (Table 1). Products were electrophoresed on a 1% agarose gel and visualized using SYBR Safe (Invitrogen-Life Technologies). Bands were gel-purified using Montage DNA Gel Extraction Kit (EMD Millipore, Billerica, MA) and ligated into pCR2.1-TOPO using TOPO TA Cloning Kit (Invitrogen-Life Technologies). Plasmid DNA was propagated in OneShot TOP10 chemically competent *Escherichia coli* and purified using QIAprep Spin Mini-Prep Kit (Qiagen, Valencia, CA). Inserts were sequenced with T7 and M13 Reverse vector primers by the Arizona State University DNA Core Lab (Tempe, AZ).

The 5' and 3' ends of LhAQP1–4s were identified by rapid amplification of cDNA ends (RACE) using the SMARTer RACE cDNA Amplification Kit (Clontech). At least two sense and two antisense primers were designed for each partial LhAQP consensus sequence (Table 1). The primers were used with Universal Primer A (Clontech) in fully nested PCR to amplify 5' and 3' ends (Table 1). PCR products were sub-cloned into pCR2.1-TOPO (Invitrogen-Life Technologies) and sequenced as indicated above.

Table 1

Nucleotide primers used to obtain partial and full-length *Lygus hesperus* aquaporins (LhAQP1–5), rapid amplification of cDNA ends (5'- and 3'-RACE), reverse transcriptase-PCR (RT-PCR) amplification of cDNA, and for sub-cloning into pIB expression vector.

Primer	Primer DNA sequence ^a	Direction	LhAQP	Application
AcF	5'-ATGTGCGACGAGAAGTTG-3'	Sense	–	RT-PCR
AcR1	5'-GTCACGGCCAGCCAAATC-3'	Antisense	–	RT-PCR
1LhTub5	5'-CACCAAGTCGTTTCATGTTGG-3'	Sense	–	RT-PCR
2LhTub3	5'-GTCACCACCTTGCCTCAGGTT-3'	Antisense	–	RT-PCR
1LhAQP5	5'-CAAACCTCTGAGCCTTCCCACA-3'	Sense	3	Partial cloning ^b
2LhAQP3	5'-GTCGAGTCAACACGCTGGT-3'	Antisense	3	Partial cloning
3LhAQP5	5'-GTCGAGTCAACACGCTGGT-3'	Sense	4	Partial cloning
4LhAQP3	5'-CTTTTCCAAGCCGCTTCAT-3'	Antisense	4	Partial cloning
5LhAQP5	5'-TTGGGTACGGAGGATGTGG-3'	Sense	1	Partial cloning
6LhAQP3	5'-TTACAAATCGTAAGAAGTCTCGTC-3'	Antisense	1	Partial cloning
7LhAQP5	5'-GGAAGTGTTTGGAGCAGAGC-3'	Sense	2	Partial cloning
8LhAQP3	5'-GCAGTGTGGTGTAGAAAAGTGG-3'	Antisense	2	Partial cloning
18LhAQP5	5'-TGCCTCTGACTGGATCAGGA-3'	Sense	1	3'-RACE ^c
19LhAQP5	5'-GTTGACAGTGGGACAACCA-3'	Sense	1	3'-RACE
20LhAQP3	5'-GCCTGACCTCAGTGACTCC-3'	Antisense	1	5'-RACE
21LhAQP3	5'-CATCTGAACGACCGAAGCAA-3'	Antisense	1	5'-RACE
22LhAQP5	5'-TGGCCCTCATCTTCTGGTT-3'	Sense	2	3'-RACE
23LhAQP5	5'-CCCCGTGAGAGTCTTGGTC-3'	Sense	2	3'-RACE
24LhAQP3	5'-TGATTGTCTCCATGATTTCG-3'	Antisense	2	5'-RACE
25LhAQP3	5'-TGCCCCAGTACGTAGAATGC-3'	Antisense	2	5'-RACE
34LhAQP3	5'-CTGGCGAGCAGCACATCGGGGTCA-3'	Antisense	2	5'-RACE
35LhAQP3	5'-CACCAACGCCCATGATTGCTCCCATGA-3'	Antisense	2	5'-RACE
36LhAQP5	5'-TGCTGCTCTGCATCGGCTCGCTTC-3'	Sense	2	3'-RACE
37LhAQP5	5'-CCGCGATGTGCTGCTGCCAGGACT-3'	Sense	2	3'-RACE
26LhAQP3	5'-AGCGCCGAAATTTGGGGCAGTCCAG-3'	Antisense	3	5'-RACE
27LhAQP3	5'-CGAGCGACATGTGCCCATGACCAG-3'	Antisense	3	5'-RACE
28LhAQP5	5'-GGTCATGGGGCAGATGTCGCTCGTC-3'	Sense	3	3'-RACE
29LhAQP5	5'-GACCGCCGGTTTCTGCACCACCTCA-3'	Sense	3	3'-RACE
30LhAQP3	5'-GCGGGATTCATGCTGGAACCCGTGGA-3'	Antisense	4	5'-RACE
31LhAQP3	5'-CGGCACCTCCGATGGCGCCAAAGACA-3'	Antisense	4	5'-RACE
32LhAQP5	5'-AAGCGGTGGTGGCCGAAGCATCG-3'	Sense	4	3'-RACE
33LhAQP5	5'-TGGCCCATCGGAGGTGCCGCTATG-3'	Sense	4	3'-RACE
38LhAQP5	5'-ATGATGGGCGCACACAGTTCATC-3'	Sense	1	Cloning CDS ^d
39LhAQP3	5'-TTACAAATCGTAAGAAGTCTGCTCG-3'	Antisense	1	Cloning CDS
40LhAQP5	5'-ATGGTGACCGACTCGGGCGGA-3'	Sense	2A	Cloning CDS
41LhAQP3	5'-CTACGATTGGCCTCCCTGAGGAA-3'	Antisense	2A	Cloning CDS
42LhAQP5	5'-ATGGTACTCCACTCGTTTTGAACAGGGTG-3'	Sense	2B	Cloning CDS
43LhAQP5	5'-ATGGGAGTCAAGACCGGATCCG-3'	Sense	2C	Cloning CDS
44LhAQP5	5'-ATGAACAGTGGGAACAGCGTTTTCTGTG-3'	Sense	2D	Cloning CDS
86LhAQP5	5'-GGATCCATGACGATGAGCGAAT-3'	Sense	2E	Cloning CDS & pIB
45LhAQP5	5'-ATGCTCCGAGATCAAAAGCACG-3'	Sense	3	Cloning CDS
46LhAQP3	5'-TTATATGGTGGCGTCACTTCTTGT-3'	Antisense	3	Cloning CDS
47LhAQP5	5'-ATGCCAGACAAGAGGAGTCAAGTCAA-3'	Sense	4	Cloning CDS
48LhAQP3	5'-TCATGCGTGTCTGTTTTCAITTC-3'	Antisense	4	Cloning CDS
79LhAQP5	5'-ATGGGGGGCATCTTCGG-3'	Sense	5	Cloning CDS
80LhAQP3	5'-TTAGAGATCTTTTTCTTCCCAGGA-3'	Antisense	5	Cloning CDS
61LhAQP5	5'-ATTCGATGCTGTTGGTAGGG-3'	Sense	1	RT-PCR ^e
62LhAQP3	5'-CTGATCCAGTCAGAGGCACA-3'	Antisense	1	RT-PCR
63LhAQP5	5'-GGAAGTGTTTGGAGCAGAGC-3'	Sense	2	RT-PCR
64LhAQP3	5'-TGGCCAGTGTATTTACCAA-3'	Antisense	2	RT-PCR
65LhAQP5	5'-GGTGCTTAGTTTCGCTTTGG-3'	Sense	3	RT-PCR
66LhAQP3	5'-CGGTAGATCACTGCTGAAA-3'	Antisense	3	RT-PCR
67LhAQP5	5'-CGGTAGATCACTGCTGAAA-3'	Sense	4	RT-PCR
68LhAQP5	5'-CCCAGTGGTTATCCCATTTG-3'	Antisense	4	RT-PCR
77LhAQP5	5'-CGACTTACGCCCTTCTTGT-3'	Sense	5	RT-PCR
78LhAQP3	5'-GGAACCGATCCAGTAGACGA-3'	Antisense	5	RT-PCR
81LhAQP5	5'-GGATCCATGGTGACCGACTC-3'	Sense	2A	pIB
82LhAQP3	5'-AGGCCTCGATTGGCTCCCTCG-3'	Antisense	2A	pIB
83LhAQP5	5'-GGATCCATGGTACTCCACTC-3'	Sense	2B	pIB
84LhAQP5	5'-GGATCCATGGGAGTCAAGACCGGAT-3'	Sense	2C	pIB
85LhAQP5	5'-GGATCCATGAACAGTGGGAAC-3'	Sense	2D	pIB
86LhAQP5	5'-GGATCCATGACGATGAGCGAAT-3'	Sense	2E	pIB
73LhAQP5	5'-GGATCCATGCCTCCGAGATCAAAAGC-3'	Sense	3	pIB
74LhAQP3	5'-AGGCCTTATGGTGGCGTCACTTCTTGT-3'	Antisense	3	pIB
75LhAQP5	5'-GGATCCATGCCAGACAAGAGGAGTCA-3'	Sense	4A	pIB
76LhAQP3	5'-AGGCCTTGGTGTCTGTTTTCAITTC-3'	Antisense	4A	pIB
89LhAQP5	5'-GGAGAGAGTCCACTGAGGTACGCATCAAGGTATTA-3'	Sense	4A	pIB
90LhAQP3	5'-TAATACCTGATGCGTACCTCAGTGGAGCTCTCC-3'	Antisense	4A	pIB
87LhAQP5	5'-GGATCCATGGGGGATCTT-3'	Sense	5	pIB
88LhAQP3	5'-AGGCCTGAGATCTTTTTCTTTC-3'	Antisense	5	pIB
LhAQP1 Met3 F	5'-ATGCCACTTCTGAAGAAG-3'	Sense	1	pIB
EGFP-LhAQP1 OE F	5'-gacgagctgtacaagATGATGGGCGACCAC-3'	Sense	1	Domain swap/pIB

(continued on next page)

Table 1 (continued)

Primer	Primer DNA sequence ^a	Direction	LhAQP	Application
EGFP-LhAQP1 OE R	5'-GTGGTCGCCCATCATctgtacagctcgtc-3'	Antisense	1	Domain swap/pIB
BtAQP1N-LhAQP1 F	5'-TAGTTGCTGAGTTCTGGGAAC-3'	Sense	1	Domain swap/pIB
BtAQP1N-LhAQP1 R	5'-GTTCCAGGAATCAGCAACTA-3'	Antisense	1	Domain swap/pIB
LhAQP1N-BtAQP1 F	5'-CGTCGCTGAGTTCTGAGGAC-3'	Sense	1	Domain swap/pIB
LhAQP1N-BtAQP1 R	5'-GTCCCTACGAACTCAGCGACG-3'	Antisense	1	Domain swap/pIB
LhAQP1-EGFP F	5'-GTTCTTACGATTTGatggtgagcaagggcgag-3'	Sense	1	Domain swap/pIB
LhAQP1-EGFP R	5'-ctgcctctgctcaccatCAAATCGTAAGAAC-3'	Antisense	1	Domain swap/pIB
Stul-EGFP F	5'-AGGCCTATGGTGAGCAAG-3'	Sense	–	Domain swap/pIB
EGFP R stop	5'-TACTTGTACAGCTCGTCCATG-3'	Antisense	–	Domain swap/pIB
20BtAQP3	5'-TCAGAAATCATAAGAGCTCTCATC-3'	Antisense	–	Domain swap/pIB

^a Underlined sequence corresponds to restriction enzyme sites (C*GATCC = BamHI, GGTAC*C = KpnI, GAGCT*C = SacI, AGG*CCT = Stul). Sequence in lower case indicates regions within primers corresponding to EGFP used in overlap extension PCR to produce LhAQP1 chimera with EGFP at amino- or carboxyl-terminus. Italicized sequence corresponds to primer regions from BtAQP1 (ABW96354.1) used in overlap extension PCR to produce LhAQP1–BtAQP1 amino-terminal domain swaps.

^b Partial LhAQPs 1–4 were PCR amplified using primer pairs 1LhAQP5 + 2LhAQP3 (LhAQP1), 3LhAQP5 + 4LhAQP3 (LhAQP2), 5LhAQP5 + 6LhAQP3 (LhAQP3), and 7LhAQP5 + 8LhAQP3 (LhAQP4).

^c For 5' and 3' RACE at least two sense and two antisense primers were used to amplify ends of LhAQP1–4 (18LhAQP5 and 19LhAQP5 for 3'-RACE of LhAQP1; 20LhAQP3 and 21LhAQP3 for 5'-RACE of LhAQP1; 22LhAQP5, 23LhAQP5, 36LhAQP5, and 37LhAQP5 for 3'-RACE of LhAQP2; 24LhAQP3, 25LhAQP3, 34LhAQP3, and 35LhAQP3 for 5'-RACE of LhAQP2; 26LhAQP3 and 27LhAQP3 for 5'-RACE of LhAQP3; 28LhAQP5 and 29LhAQP5 for 3'-RACE of LhAQP3; 30LhAQP3 and 31LhAQP3 for 5'-RACE of LhAQP4; 32LhAQP5 and 33LhAQP5 for 3'-RACE of LhAQP4).

^d Full-length coding sequences for LhAQPs were confirmed by PCR amplification from adult *Lygus hesperus* cDNA using primer pairs 38LhAQP5 + 39LhAQP3 (LhAQP1), 40LhAQP5 + 41LhAQP3 (LhAQP2A), 42LhAQP5 + 41LhAQP3 (LhAQP2B), 43LhAQP5 + 41LhAQP3 (LhAQP2C), 44LhAQP5 + 41LhAQP3 (LhAQP2D), 86LhAQP5 + 41LhAQP3 (LhAQP2E), 45LhAQP5 + 46LhAQP3 (LhAQP3), 47LhAQP5 + 48LhAQP3 (LhAQP4), and 79LhAQP3 + 80LhAQP (LhAQP5).

^e For reverse transcriptase-PCR (RT-PCR), LhAQP-specific primers were used to amplify products from within each ORF using primer pairs 61LhAQP5 + 62LhAQP3 (LhAQP1), 63LhAQP5 + 64LhAQP3 (LhAQP2), 65LhAQP5 + 66LhAQP3 (LhAQP3), 67LhAQP5 + 68LhAQP3 (LhAQP4), and 77LhAQP5 + 78LhAQP3 (LhAQP5).

Concurrent with cloning the four putative partial cDNAs (LhAQP1–4), we sequenced and *de novo* assembled a Roche 454 transcriptome from normalized cDNA libraries prepared from 0 to 5 day old post-eclosion *L. hesperus* adults (Hull et al., 2013). In addition to confirming the presence of the LhAQP1–4 transcripts (Table 2), the *L. hesperus* 454 transcriptome also revealed an additional putative full-length aquaporin-like transcript, designated as LhAQP5.

Full-length LhAQP coding sequences (CDS) corresponding to open reading frames (ORFs) were confirmed by PCR amplification from *L. hesperus* adult cDNA using primer pairs (Table 1). All

products corresponding to full-length LhAQP CDS were PCR amplified using ExTaq DNA polymerase (Takara-Clontech), sub-cloned into pCR2.1-TOPO (Invitrogen-Life Technologies), and sequenced as indicated above.

2.3. Bioinformatics and phylogeny

Sequences were analyzed in Vector NTI (Life Technologies) and comparison against the non-redundant public sequence database was made using BLAST search programs (Altschul et al., 1990). Sequence analysis tools of the ExpASY Molecular Biology Server of Swiss Institute of Bioinformatics, including Translate and Compute pI/MW were used to analyze the deduced LhAQP protein sequences. Predictions of intra/extracellular domains and transmembrane helices were made using TMPred (Hofmann and Stoffel, 1993), TMHMM 2.0 (Krogh et al., 2001), Phobius (Käll et al., 2004), RHYTHM (Rose et al., 2009), TOPCONS (Bernsel et al., 2009), HMMTOP (Tusnady and Simon, 2001), and TopPredII (Claros and von Heijne, 1994). Protein subcellular localization was predicted using Wolf PSORT (Horton et al., 2007). Multiple sequence alignments were performed using CLUSTALW (Larkin et al., 2007). Phylogenetic analysis using predicted full-length AQP protein sequences was performed with the unweighted pair group method with arithmetic mean (UPGMA, Sneath and Sokal, 1973), neighbor-joining (Saitou and Nei, 1987), and minimum evolution and maximum parsimony (Saitou and Nei, 1986) methods. Trees were constructed with 10,000 bootstrap replicates using MEGA version 5 (Tamura et al., 2011). Only the UPGMA tree is shown, as all trees were similar. Glycosylation predictions were made using post-translational modification servers found at the Center for Biological Sequence Analysis (<http://www.cbs.dtu.dk/services/>).

2.4. RNA extraction and semi-quantitative reverse transcription PCR

Lygus representing different developmental stages (egg, 1st instar nymph, 2nd–3rd instar nymph, 4th–5th instar nymph, and adult) were collected, weighed, and frozen in liquid nitrogen. Total tissue weight for each stage ranged from 60 to 112 mg. For tissue distribution RT-PCR, heads, legs, accessory glands, testes, ovaries,

Table 2

Aquaporin protein transcripts identified by cDNA cloning and from *de novo*-assembled *Lygus hesperus* and *Lygus lineolaris* transcriptomes.

LhAQP	LhAQP NCBI accession number	Number of <i>L. hesperus</i> AQP isotigs per isogroup ^a	CDS (bp) ^b	ORF (aa) ^c	Number of putative <i>L. lineolaris</i> AQP contigs ^d	CDS (bp) ^e	ORF (aa) ^f
1	KF048092	2	864	287	5	864	287
2A	KF048093	– ^g	789	262	–	–	–
2B	KF048094	–	813	270	–	–	–
2C	KF048095	–	885	294	–	–	–
2D	KF048096	–	846	281	–	–	–
2E	KF048097	9	768	255	2	768	255
3	KF048098	10	804	267	2	804	267
4A	KF048099	1	837	278	–	–	–
4B	KF048100	–	798	265	2	798	265
5	KF048101	5	798	265	–	–	–

^a Total number of contigs comprising LhAQPs obtained from *de novo*-assembled adult *Lygus hesperus* 454 transcriptome (Hull et al., 2013).

^b Number of nucleotides comprising *L. hesperus* AQP coding sequences (CDS) obtained from RACE and PCR cloning.

^c Number of residues from translation of *L. hesperus* AQP CDS using ExpASY Translate tool (<http://web.expasy.org/translate/>).

^d Total number of putative AQP contigs obtained from *de novo*-assembled *Lygus lineolaris* transcriptome sequencing libraries (personal communication from O.P. Perera).

^e Number of nucleotides comprising *L. lineolaris* CDS for AQP transcripts obtained by aligning contigs and generating consensus sequences.

^f Number of residues from translation of *L. lineolaris* AQP CDS using ExpASY Translate tool (<http://web.expasy.org/translate/>).

^g “–” indicates that for cloned AQP cDNAs no contigs/isotigs were found in *de novo*-assembled *Lygus hesperus* or *Lygus lineolaris* transcriptomes.

midguts, and Malpighian tubules were dissected from adults and stored in RNAlater (Ambion-Life Technologies) at -80°C . Tissue samples were homogenized using Kontes pestles (Fisher Scientific, Pittsburg, PA) and total RNA was extracted using TRIzol[®] reagent (Invitrogen-Life Technologies). RNA concentration was determined using a NanoDrop ND1000 spectrophotometer (NanoDrop Technologies/Thermo Scientific, Wilmington, DE). Total RNA was treated with DNA-free[™] DNase I (Ambion-Life Technologies) to remove genomic DNA contamination, if any, carried over during total RNA extraction. Integrity of the total RNA was confirmed on the Agilent 2100 Bioanalyzer using the RNA Nano 6000 LabChip kit (Agilent Technologies, Santa Clara, CA) according to manufacturer's instructions.

Samples were diluted and 1 μg of DNase-treated total RNA was used to prepare cDNA using random decamer primers according to the protocol described in RetroScript cDNA Synthesis Kit (Ambion-Life Technologies). For reverse transcriptase-PCR (RT-PCR), LhAQP-specific primers were used to amplify 503–547-bp products from within each ORF (Table 1). Nucleotide primer sequences for 63LhAQP5 and 64LhAQP3 are conserved in LhAQP2A-E and therefore, end-point RT-PCR products represent transcriptional profiles for LhAQP2 as a group. Likewise, 67LhAQP5 and 68LhAQP3 primer sequences are found in both LhAQP4A and LhAQP4B. The appropriate number of PCR cycles was determined empirically and included 25, 28, and 30 cycles. Actin (AcF + AcR1) and β -tubulin (1LhTub5 + 2LhTub3) were used as amplification controls for stages and tissues, respectively (Hull et al., 2013). Products were electrophoresed on 0.8% agarose gels and visualized using SYBR Safe (Invitrogen-Life Technologies).

2.5. Expression in *Tni* cell culture and fluorescence microscopy

To observe cellular localization, recombinant LhAQPs were expressed using the pIB/V5-His TOPO TA (Invitrogen-Life Technologies) insect cell expression vector in cultured *Trichoplusia ni* (*Tni*) cells (Allele Biotechnology, San Diego, CA). Recombinant proteins were expressed as chimeras with the enhanced green fluorescent protein (EGFP) produced in frame with LhAQPs either at their amino- or carboxyl termini.

A pIB/*Stul*-EGFP reporter cassette was modified from pIB/V5-His TOPO TA (Life Technologies) and used to express chimeric LhAQP2-5-EGFP recombinant proteins in cultured *Tni* cells. Full-length LhAQP2A-E, LhAQP3, LhAQP4A-B, and LhAQP5 coding sequences were first cloned into pCR2.1-TOPO (Invitrogen-Life Technologies) using PCR with KOD DNA polymerase (EMD Millipore) and primers that introduced *Bam*HI and *Stul* restriction sites on the 5' and 3' ends of LhAQPs, respectively [81LhAQP5 + 82LhAQP3 (LhAQP2A), 83LhAQP5 + 82LhAQP3 (LhAQP2B), 84LhAQP5 + 82LhAQP3 (LhAQP2C), 85LhAQP5 + 82LhAQP3 (LhAQP2D), 86LhAQP5 + 82LhAQP3 (LhAQP2E), 73LhAQP5 + 74LhAQP3 (LhAQP3), 75LhAQP5 + 76LhAQP3 (LhAQP4A and 4B), and 87LhAQP5 + 88LhAQP3 (LhAQP5)]. LhAQP/pCR2.1-TOPO plasmids and pIB/*Stul*-EGFP were digested with *Bam*HI-HF and *Stul*, gel-purified using an EZNA gel extraction kit (Omega Bio-Tek, Norcross, GA), and ligated using Mighty Mix DNA ligation kit (Takara-Clontech). Because LhAQP4B is preferentially PCR amplified over LhAQP4A, additional overlap extension PCR steps were needed to make LhAQP4A/pCR2.1-TOPO with the appropriate restriction sites. The first PCR amplified the 5' end of LhAQP4A with a 5' *Bam*HI site but missing 36 bp from LhAQP4B using 75LhAQP5 + 90LhAQP3. The second PCR amplified the 3' end of LhAQP4A including the unique 36 bp and a 3' *Sac*I site using 89LhAQP5 + 76LhAQP3. The final step involved PCR amplification using the two previous reactions as templates with

75LhAQP5 + 76LhAQP3. The resulting PCR product was cloned into pCR2.1-TOPO (Invitrogen-Life Technologies), digested with *Bam*HI and *Stul*, and sub-cloned into pIB/*Stul*-EGFP as described above. High-fidelity KOD DNA polymerase (EMD Millipore) was used for all PCR amplifications. Orientation and correctness of the pCR2.1-TOPO and pIB/*Stul*-EGFP inserts were confirmed by sequencing at the ASU DNA Core Lab. All restriction enzymes were from New England Biolabs (Ipswich, MA).

Because LhAQP1 has endogenous *Bam*HI and *Stul* restriction sites, we used overlap extension PCR to make the EGFP-LhAQP1 pIB expression vector variants. To make LhAQP1-EGFP/pIB (chimeric LhAQP1 with EGFP at carboxyl-terminus), the first PCR reactions (38LhAQP5 + LhAQP1-EGFP R and LhAQP1-EGFP F + EGFP R stop) amplified the coding sequences for LhAQP1 and EGFP, respectively. The final PCR amplification used the two previous reactions as templates with the LhAQP1 gene-specific sense primer 38LhAQP5 and the EGFP-specific antisense primer, EGFP R stop. Similarly, for EGFP-LhAQP1/pIB (chimeric LhAQP1 with EGFP at amino-terminus), the first PCR reactions (*Stul*-EGFP F + EGFP-LhAQP1 OE R and EGFP-LhAQP1 OE F + 39LhAQP3) amplified the coding sequences for EGFP and LhAQP1, which were then used as templates for final PCR using the sense primer *Stul*-EGFP F and the LhAQP1-specific antisense primer, 39LhAQP3. Final products were sub-cloned into pIB/V5-His-TOPO (Invitrogen-Life Technologies) and DNA was sequenced at ASU DNA Core Lab.

An expression vector with a truncated LhAQP1 beginning at base position 28 (corresponding to the third methionine in translated LhAQP1, see Supplemental Fig. 1) and a carboxyl-terminal EGFP was prepared by overlap extension PCR. The first PCRs used LhAQP1 Met3 F + LhAQP1-EGFP R and LhAQP1-EGFP F + EGFP R stop to amplify the CDS corresponding to Met3-truncated LhAQP1 and EGFP, respectively. Products of these reactions were used as templates for final amplification using LhAQP1 Met3 F + EGFP R stop and were sub-cloned in pIB/V5-His-TOPO (Invitrogen-Life Technologies) and sequenced as above.

To compare the cellular localization of LhAQP1 with that of *B. tabaci* aquaporin 1 (BtAQP1) we used EGFP-BtAQP1/pIB plasmid DNA from Mathew et al. (2011) and prepared amino-terminal domain swaps between LhAQP1 and BtAQP1. To make EGFP-BtAQP1N-LhAQP1/pIB (chimeric LhAQP1 tagged at amino-terminus EGFP with 117 bp from 5' of BtAQP1 replacing 207 bp from LhAQP1 5' end), *Stul*-EGFP F + BtAQP1N-LhAQP1 R and BtAQP1N-LhAQP1 F + 39LhAQP3 products were used as templates for overlap extension PCR with *Stul*-EGFP F + 39LhAQP3. For EGFP-LhAQP1N-BtAQP1/pIB (chimeric BtAQP1 tagged at the amino-terminus with EGFP and with 207 bp from the 5' end of LhAQP1 replacing the first 117 bp of BtAQP1), PCR products from *Stul*-EGFP F + LhAQP1N-BtAQP1 R and LhAQP1-BtAQP1 F + 20BtAQP3 were templates for overlap extension PCR with *Stul*-EGFP F + 20BtAQP3. The resulting products from final overlap extension PCR were sub-cloned and sequenced as above.

Transfections and fluorescent imaging were performed according to protocols largely based on those of Hull et al. (2012) and Mathew et al. (2011). *Tni* cells maintained as adherent cultures in serum-free insect culture media (Allele Biotechnology) at 28°C were transfected in 35 mm #1.5 glass bottom dishes (In Vitro Scientific, Sunnyvale, CA) with 2 μg plasmid DNA using Insect GeneJuice transfection reagent (Novagen/EMD Biosciences, Madison, WI) for 5–12 h. Two days post transfection, media was replaced with IPL1-41 insect media (Invitrogen-Life Technologies) and cells were imaged using an Olympus FSX-100 fluorescence microscope with FSX-BSW imaging software (Olympus, Center Valley, PA). Images were processed using IrfanView (<http://www.irfanview.com/>) with gamma correction set at 1.5.

2.6. cRNA synthesis, *Xenopus* oocyte expression and permeability assays

LhAQP ORFs were sub-cloned into a modified *Xenopus laevis* β -globin plasmid expression vector (Anthony et al., 2000), linearized with *Sac*II, and transcribed *in vitro* (T3 mMessage mMachine; Ambion-Life Technologies). *In vitro*-transcribed complementary RNA (cRNA) corresponded to the full-length ORFs (residues 1–287 for LhAQP1, residues 1–262 for LhAQP2A, 1–267 for LhAQP3, 1–278 for LhAQP4A, 1–265 for LhAQP5). cRNA (20 ng μ L⁻¹) was suspended in sterile water prior to injection.

Unfertilized *X. laevis* oocytes were defolliculated with collagenase (type 1A, 1.5 mg mL⁻¹; Sigma, St. Louis, MO) and trypsin inhibitor (15 mg mL⁻¹) in modified OR-2 saline [125 mM NaCl, 3.25 mM KCl, 2.5 mM MgCl₂, and 10 mM 4-(2-Hydroxyethyl) piperazine-1-ethanesulfonic acid (HEPES); pH 7.6] at 18 °C for 1.5 h, washed in modified OR2 saline solution, and maintained in modified ND96 saline (96 mM NaCl, 2 mM KCl, 5 mM MgCl₂, 0.6 mM CaCl₂, 5 mM HEPES, pH 7.6) supplemented with 100 μ g/ml penicillin and 100 U/ml streptomycin, and 10% (V/V) heat-inactivated horse serum. Oocytes were injected with 50 nL of water containing 1 ng of LhAQP cRNA and were incubated for 2 or more days at 18 °C to allow protein expression.

For quantitative swelling assays, oocytes incubated in isotonic modified ND96 saline (without serum or antibiotics) for 1–2 h at room temperature were tested for water permeability by swelling in 50% hypotonic saline (isotonic diluted with an equal volume of water). Glycerol permeability was assayed by measuring swelling rates of oocytes in saline in which NaCl was partially substituted by glycerol [31 mM NaCl, 130 mM glycerol, 2 mM KCl, 5 mM MgCl₂ and 5 mM HEPES]. Swelling rates were quantified by relative increases in oocyte cross-sectional area imaged by video microscopy (charge-coupled device camera; Cohu, San Diego, CA) at 0.5 frames per second for 45 s using NIH ImageJ software. Rates were measured as described previously (Anthony et al., 2000; Boassa and Yool, 2003) using Prism (GraphPad Software Inc., San Diego, CA). Data for oocyte volume (*V*), standardized to the initial volume (*V*₀) as a function of time, were fit by linear regression to determine the swelling rate from the slope value (V/V_0)(s⁻¹ * 10⁵). The University of Adelaide Animal Ethics committee approved all surgical procedures and the procedures followed protocols approved under the Australian Code of Practice for the Care and Use of Animals for Scientific Purposes.

3. Results

3.1. Cloning, topology and homology of LhAQPs

RT-PCR and primer pairs 1LhAQP5 + 2LhAQP3, 3LhAQP5 + 4LhAQP3, 5LhAQP5 + 6LhAQP3, and 7LhAQP5 + 8LhAQP3 (Table 1) amplified four partial LhAQP fragments of 638, 759, 717, and 643 bp, respectively, from *L. hesperus* 2nd–3rd instar nymph and adult cDNA. The cloned fragments were sequenced and BLAST analysis revealed high similarity with the aquaporin family (data not shown). Using the sequences from the partial clones, we identified the 5' and 3' ends by RACE and full-length LhAQP1–4 cDNAs were PCR-amplified, cloned, and sequenced (Supplemental Fig. 1 and Table 2). Coincidental with the process of cloning the full-length LhAQP cDNAs, we completed a *de novo* assembled Roche 454 transcriptome of *L. hesperus* adults (Hull et al., 2013) that independently validated LhAQP1–4 transcripts and revealed an additional putative full-length aquaporin-like transcript, designated LhAQP5.

The 864-bp full-length coding sequence (CDS) of LhAQP1 (KF048092) corresponds to an open reading frame (ORF) encoding

287 amino acids (Supplemental Fig. 1 and Table 2). The predicted isoelectric point (pI) and molecular weight of LhAQP1 is 5.6 and 29.7 kDa, respectively. While no N- or C-glycosylation sites are predicted for LhAQP1, one O-glycosylation site is predicted at Thr19. However, because LhAQP1 has no predicted signal peptide, it is possible the mature protein is not exposed to glycosylation machinery. Like other members of the aquaporin superfamily (Murata et al., 2000), LhAQP1 has two Asn-Pro-Ala (NPA) motifs and residues predicted to comprise the ar/R constriction (Phe100, His224, Ser233, and Arg239) (Supplemental Figs. 1, Fig. 1, and Supplemental Table 1). Seven different TM/topology prediction programs revealed that LhAQP1 likely has six TM-spanning regions with intracellular amino- and carboxyl-termini (Table 3 and Supplemental Table 2), fitting the pattern known for other members of the aquaporin superfamily.

Nested 5'-RACE PCR using primers 24LhAQP3, 25LhAQP3, 34LhAQP3, and 35LhAQP3 revealed sequence variation resulting in different start sites for LhAQP2 (Supplemental Fig. 1, Fig. 2, and Table 2), including LhAQP2A (KF048093, 789-bp CDS encoding 262 amino acids), LhAQP2B (KF048094, 813-bp CDS encoding 270 amino acids), LhAQP2C (KF048095, 885-bp CDS encoding 294 amino acids), LhAQP2D (KF048096, 846-bp CDS encoding 281 amino acids), and LhAQP2E (KF048097, 768-bp CDS encoding 255 amino acids). While all variant LhAQP2s contain the 768-bp CDS that comprise LhAQP2E, RT-PCR and cloning verified that transcripts for all five full-length variant forms are present in *L. hesperus*. Predicted pIs for LhAQP2A–E are 5.1, 5.2, 4.9, 5.6, and 5.4, respectively. Molecular weights predicted by Compute pI/MW ExpASY tool for LhAQP2A–E are 27.9, 28.7, 31.2, 30.0, and 28.8 kDa, respectively. The same two putative N-glycosylation sites (NGSK and NLTG) were predicted in all LhAQP2 translated sequences. Several amino-terminal threonines (Thr3 for LhAQP2A–B, Thr4–5 for LhAQP2C, and Thr2 for LhAQP2E) are predicted to be O-glycosylated. No C-glycosylation sites were predicted for LhAQP2A–E. As for LhAQP1, all LhAQP2s are predicted to lack signal peptide, glycosylation may not occur on those predicted motifs. In contrast with many aquaporins that contain two NPA motifs, the LhAQP2s have one conserved amino-terminal NPA motif and a second motif comprised of Asn-Pro-Val (NPV). The four residues predicted to comprise the ar/R selectivity filter (Phe, Ser, Ala, and Arg) are conserved in all LhAQP2 translated sequences (Supplemental Fig. 1; Fig. 1, and Supplemental Table 1). Analysis of transmembrane topology indicates that LhAQP2A–E likely have six TM helices with intracellular amino and carboxyl termini, although Phobius predicts only five TM helices for all LhAQP2 translated proteins and RHYTHM and TOPCONS predict seven TM helices for LhAQP2C and LhAQP2D, respectively (Table 3 and Supplemental Table 2).

LhAQP3 (KF048098) has an 804-bp full-length CDS containing ORF encoding 267 amino acids (Supplemental Fig. 1 and Table 2). The predicted pI and molecular weight of LhAQP3 is 5.9 and 28.8 kDa, respectively. While no C-mannosylation sites are predicted, two N-glycosylation motifs (20-NLSM-23 and 93-NVTW-96) and three O-glycosylation sites (Thr141, Thr142, and Thr266) are predicted for LhAQP3. LhAQP3 has an Asn-Pro-Cys (NPC) motif at residues 89–91 and an NPA motif at residues 207–209 (Supplemental Figs. 1, Fig. 1, and Supplemental Table 1) with conserved ar/R constriction residues Phe69, Ala195, Gly204, and Arg210 (Supplemental Fig. 1 and Supplemental Table 1). Predicted TM topology for LhAQP3 is consistent with known patterns of AQP-folding, and all seven analyses predicted six TM-spanning regions and intracellular amino and carboxyl termini (Table 3 and Supplemental Table 2).

Two full-length LhAQP4 isoforms were identified by RT-PCR and cloning, with LhAQP4A (KF048099) having CDS of 837 bp encoding 278 amino acids and LhAQP4B (KF048100) having CDS of 798 bp

LhAQP4A	-----MPDKRSRVNTLVGM	14
LhAQP4B	-----MPDKRSRVNTLVGM	14
LhAQP1	-----MMGDHSSIDMPRSEEGVQTEKTPLLHKGS DVPVSKLSKKKKNHADGSKSFLGT	52
LhAQP2B	-----MATPLVLRVTDSSGGMTMSEFTNNDATIKVEEGKDT	36
LhAQP2C	MGVTTGSDVQSLETLGSAEIRVPEMATPLVLRVTDSSGGMTMSEFTNNDATIKVEEGKDT	60
LhAQP2E	-----MTMSEFTNNDATIKVEEGKDT	21
LhAQP2A	-----MVTDSGGMTMSEFTNNDATIKVEEGKDT	28
LhAQP2D	-----MNSGNSVFLASHDRIGRQPRVTDSSGGMTMSEFTNNDATIKVEEGKDT	47
LhAQP3	-----MPPRSKARYTSLLRDDGFTNL	21
LhAQP5	-----MGGIFGLIVSSAYIGLTCLIAWWAR	25
LhAQP4A	NELARAGDLG---KAVVAEALGTLFITYFGIMSCIA---LVPGNLVQISLCLFGFVVMVSV	68
LhAQP4B	NELARAGDLG---KAVVAEALGTLFITYFGIMSCIA---LVPGNLVQISLCLFGFVVMVSV	68
LhAQP1	EDVEKFDVAVG---RALVAEFLGTMLLVVVGCGACVGS D-VAQPTTSLIALAFGFIIASV	108
LhAQP2B	DSNGSKTDVGRYLEVFGAELVGTGVLLCIGCASC IAGDDDKPI TDFHSALTFGFTVSTII	96
LhAQP2C	DSNGSKTDVGRYLEVFGAELVGTGVLLCIGCASC IAGDDDKPI TDFHSALTFGFTVSTII	120
LhAQP2E	DSNGSKTDVGRYLEVFGAELVGTGVLLCIGCASC IAGDDDKPI TDFHSALTFGFTVSAII	81
LhAQP2A	DSNGSKTDVGRYLEVFGAELVGTGVLLCIGCASC IAGDDDKPI TDFHSALTFGFTVSTII	88
LhAQP2D	DSNGSKTDVGRYLEVFGAELVGTGVLLCIGCASC IAGDDDKPI TDFHSALTFGFTVSTII	107
LhAQP3	SMIKVRRLLG----IGLAEMFGVALFLATGCGNLVSTI SNSEPSHINTVLSFALGISSAI	77
LhAQP5	QLADRLQIES----NFKKLLLEGIATWELCATCFELI IVADNYGVSTYALFLFVLT--I	79
. * : : :		
LhAQP4A	QALGHVSGGNLNPVAVTCGLLITGRITIIIRAALYIAAQCLGAIGGAAMAKFFFTPE--DKVG	126
LhAQP4B	QALGHVSGGNLNPVAVTCGLLITGRITIIIRAALYIAAQCLGAIGGAAMAKFFFTPE--DKVG	126
LhAQP1	QMIGHISGAHINPAVTIGLLACGRIGLIMSILYIPFQLAGAVAGAALLQYLVE--LKKD	166
LhAQP2B	CIFGHISAAHLNPAVTVAFYVLGHINVPMLLVYFIAQIMGAIMGVGLVLLTPEG-WIKS	155
LhAQP2C	CIFGHISAAHLNPAVTVAFYVLGHINVPMLLVYFIAQIMGAIMGVGLVLLTPEG-WIKS	179
LhAQP2E	CIFGHISAAHLNPAVTVAFYVLGHINVPMLLVYFIAQIMGAIMGVGLVLLTPEG-WIKS	140
LhAQP2A	CIFGHISAAHLNPAVTVAFYVLGHINVPMLLVYFIAQIMGAIMGVGLVLLTPEG-WIKS	147
LhAQP2D	CIFGHISAAHLNPAVTVAFYVLGHINVPMLLVYFIAQIMGAIMGVGLVLLTPEG-WIKS	166
LhAQP3	IIFAPISGMLNPNLVTLVWGMHMSLVKVFYVTFQVIGAYLGVAFIAAVTPDIEGPP	137
LhAQP5	WWSRNWGDATACPYTHFEDVAEGKKLIGQALVMI LAQLAGGLTYGYSQFLWSLE--VSA	137
. * . . . * : : * *		
LhAQP4A	DLGATLLNPSITPGQVVAIEFMLGFVLFVIFGVIDPNKPDAKIVAPLAIGLTV-AVGHL	185
LhAQP4B	DLGATLLNPSITPGQVVAIEFMLGFVLFVIFGVIDPNKPDAKIVAPLAIGLTV-AVGHL	185
LhAQP1	AIGVVSVGAGLTEGQAFAVEAVITAVLLLVCAVTDPNRSDLANSAPVAIGLAI-ACSHI	225
LhAQP2B	DMCVTQPHDNLTYGQAAGIEFVATMALIFLVCGLSDPRCAARQDSVPLKFAALL-IALS	214
LhAQP2C	DMCVTQPHDNLTYGQAAGIEFVATMALIFLVCGLSDPRCAARQDSVPLKFAALL-IALS	238
LhAQP2E	DMCVTRPHDNLTYGQAAGIEFVATMALIFLVCGLSDPRCAARQDSVPLKFAALL-IALS	199
LhAQP2A	DMCVTQPHDNLTYGQAAGIEFVATMALIFLVCGLSDPRCAARQDSVPLKFAALL-IALS	206
LhAQP2D	DMCVTQPHDNLTYGQAAGIEFVATMALIFLVCGLSDPRCAARQDSVPLKFAALL-IALS	225
LhAQP3	GFCTTHPNPDVTTSQFAVEFFLGFFLSCLCHVLDKRRASQQHGLVFAKFAVLV-VALAL	196
LhAQP5	NHRGRAYEACTADLQVPALIGAVIEGAATCVCRLASRFIAELNPAFGSELDAFIGTSLVV	197
: * . : : . . : : :		
LhAQP4A	SCIDSTGSSMNPARRSLGSVAMIN---KWDNHVWYVWGPCMGGIVAAIILYQFVLSAPPQEY	242
LhAQP4B	SCIDSTGSSMNPARRSLGSVAMIN---KWDNHVWYVWGPCMGGIVAAIILYQFVLSAPPQEY	242
LhAQP1	FAVPLTSGSMNPARRSFGPAAMVG---QWDNQWIYVWVAPLVGAACAGAVYRIIFRPAKDD-	281
LhAQP2B	AVGKYTGASLNPVRS LGPAIWTG---NWNQHVVYVWVSPLSAGIVTPLFYTTTCFLRGQS-	270
LhAQP2C	AVGKYTGASLNPVRS LGPAIWTG---NWNQHVVYVWVSPLSAGIVTPLFYTTTCFLRGQS-	294
LhAQP2E	AVGKYTGASLNPVRS LGPAIWTG---NWNQHVVYVWVSPLSAGIVTPLFYTTTCFLRGQS-	255
LhAQP2A	AVGKYTGASLNPVRS LGPAIWTG---NWNQHVVYVWVSPLSAGIVTPLFYTTTCFLRGQS-	262
LhAQP2D	AVGKYTGASLNPVRS LGPAIWTG---NWNQHVVYVWVSPLSAGIVTPLFYTTTCFLRGQS-	281
LhAQP3	PLGKYEGGSANPARRSLGPALLSG---DWNDQWLYWTAPNFGAAFAAVIYRAFFDAPIFED	253
LhAQP5	AAFNYSGGYFNPAALATSLKLGCDGHATAEQHFFVYWI GSTVGVAVASVFLFKNPEVRAKVS	257
* . ** : . . . : : ** . . . : :		
LhAQP4A	SQVPGESSTEVRKIVLPDESSEMKRLGKGNENSNA	278
LhAQP4B	SQVPG-----ESSTEMKRLGKGNENSNA	265
LhAQP1	-----DSSYDL-----	287
LhAQP2B	-----	
LhAQP2C	-----	
LhAQP2E	-----	
LhAQP2A	-----	
LhAQP2D	-----	
LhAQP3	VDSDGKTR-----EVDATI-----	267
LhAQP5	LLGKEKDL-----	265

Fig. 1. Amino acid sequence alignment of LhAQPs. The deduced amino acid sequences of the LhAQPs were aligned using CLUSTALW. NPA motifs are shown with grey highlight and residues that correspond to the ar/R constriction site (Phe56, His180, Cys189, and Arg195 from *Homo sapiens* AQP1, EAL24446.1) are shown in bold. A predicted mercury-sensitive cysteine (Cys86) from LhAQP3 is shown with white text on black highlight. Identical residues in all sequences are shown as "*" and partial identity or residues with conserved side chains are shown as ":" and ".".

Table 3
Prediction of intra/extracellular and transmembrane topology for *Lygus hesperus* aquaporins 1–5 (LhAQP1–5).

	No. residues	Number of predicted transmembrane helices by topology prediction tools ^a							Consensus position ^b	
		TMpred	TMHMM	Phobius	RHYTHM	TOPCONS	HMMTOP	TopPredII	N-terminus	C-terminus
LhAQP1	287	6	6	6	6	6	6	6	Inside	Inside
LhAQP2A	262	6	6	5	6	6	6	6	Inside	Inside
LhAQP2B	270	6	6	5	6	6	6	6	Inside	Inside
LhAQP2C	294	6	6	5	7	6	6	6	Inside	Inside
LhAQP2D	281	6	6	5	6	7	6	6	Inside	Inside
LhAQP2E	255	6	6	5	6	6	6	6	Inside	Inside
LhAQP3	267	6	6	6	6	6	6	6	Inside	Inside
LhAQP4A	278	6	6	6	6	6	6	6	Inside	Inside
LhAQP4B	265	6	5	6	6	6	6	6	Inside	Inside
LhAQP5	265	6	5	5	6	7	5	6	Outside	Inside

^a Predictions of intra/extracellular domains and transmembrane helices were made using TMpred (Hofmann and Stoffel, 1993), TMHMM 2.0 (Krogh et al., 2001), Phobius (Käll et al., 2004), RHYTHM (Rose et al., 2009), TOPCONS (Bernsel et al., 2009), HMMTOP (Tusnady and Simon, 2001), and TopPredII (Claros and von Heijne, 1994).
^b The amino- and carboxyl-terminal ends of LhAQPs were predicted to be either intracellular or extracellular based on consensus positions from the seven different prediction software programs.

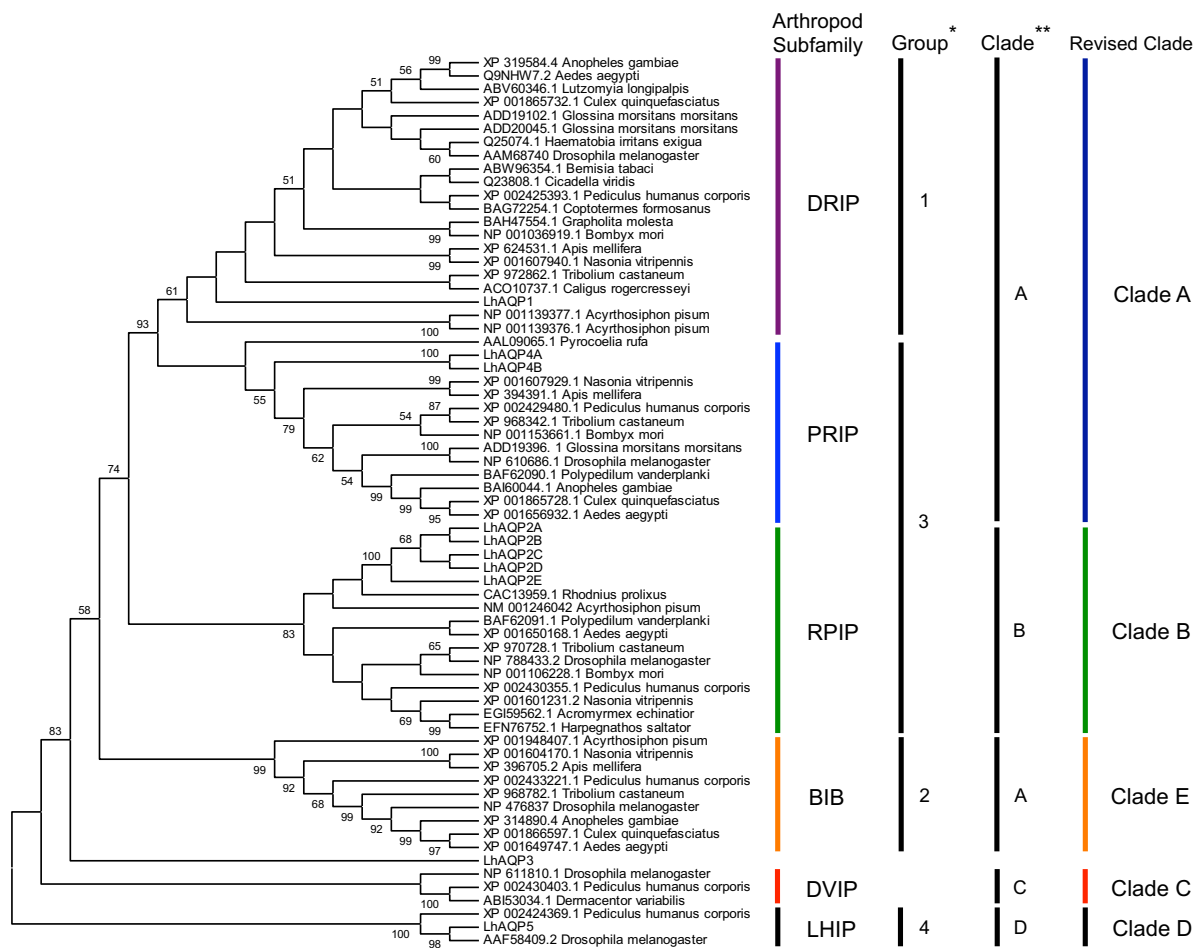


Fig. 2. Phylogenetic analysis and classification of LhAQPs and other arthropod aquaporins. Translated LhAQP sequences were compared with other arthropod aquaporins and the evolutionary history was inferred using the UPGMA method (Sneath and Sokal, 1973) in MEGA5 (Tamura et al., 2011). The bootstrap consensus tree inferred from 10,000 replicates (Felsenstein, 1985) and branches corresponding to partitions reproduced in less than 50% of bootstrap replicates are collapsed. The percentage of replicate trees in which the associated taxa clustered together in the bootstrap test (10,000 replicates) are shown next to the branches. The evolutionary distances were computed using the Poisson correction method (Zuckerkanndl and Pauling, 1965) and are in units of the number of amino acid substitutions per site. The analysis involved 67 amino acid sequences. All positions containing gaps and missing data were eliminated. A total of 147 positions were in the final dataset. Taxonomic name and accession number for each sequence is given. Representatives from six major arthropod subfamilies (DRIPs, PRIPs, RPIPs, BiBs, DVIPs, and LHIPs) are shown. The proposed subfamily names follow the nomenclature proposed by Campbell et al. (2008) and includes *Drosophila* intrinsic proteins DRIPs, *Pyrocoelia rufa* integral proteins PRIPs, *Rhodnius prolixus* integral proteins RPIPs, *Big Brain* BIBs, *Demacenter variabilis* integral proteins DVIPs, and *Lygus hesperus* integral proteins LHIPs. The group and clade (as indicated by superscript "*" and "**") correspond to the four groups (1–4) [by Kambara et al. (2009) and Goto et al. (2011)] or clades (A–D) [by Wallace et al. (2012)], respectively. Revised clades A–E are indicated.

encoding 265 amino acids. The predicted pI and molecular weight of LhAQP4A is 6.3 and 29.1 kDa, respectively, and 6.8 and 27.6 kDa for LhAQP4B. The CDS for LhAQP4A and LhAQP4B are identical except for 39 bp (positions 757–796) that are missing from LhAQP4B. This difference likely results from alternative splicing of an exon encoding 13 amino acids. The LhAQP4B transcript is either more abundant in *L. hesperus* and/or preferentially cloned over LhAQP4A, as 11 of the cloned 47LhAQP5 + 48LhAQP3 PCR products corresponded to LhAQP4B versus none for LhAQP4A. LhAQP4A is, however, present in *L. hesperus*, as transcripts were found by RACE, overlap extension PCR, and 454 transcriptome sequencing. Because LhAQP4A and LhAQP4B only differ after residue 252, both have two conserved NPA motifs at positions 80–82 and 196–198 and ar/R residues Phe60, His184, Ser193 and Arg199 (Supplemental Figs. 1, Fig. 1, and Supplemental Table 1). TM topology analysis indicated the presence of six TM-helices for LhAQP4A and 5–6 helices for LhAQP4B, with only TMHMM showing five and a weak probability score for a sixth putative TM-spanning region corresponding to residues 170–190 in LhAQP4B (Table 3 and Supplemental Table 2).

The 798-bp CDS of LhAQP5 (KF048101) encodes 265 amino acids (Supplemental Fig. 1 and Table 2) with a predicted molecular weight of 28.9 kDa and a pI of 5.6. No C-, N- or O-glycosylation sites are predicted for LhAQP5. While the size of the translated LhAQP5 and presence of two NPA motifs is consistent with other insect AQPs (Campbell et al., 2008), the positioning and sequence conservation of the motifs differ from those seen in previously characterized insect AQPs. Based on alignment with the other LhAQPs, the residues comprising what would be the LhAQP5 amino-terminal NPA motif are instead Cys-Pro-Tyr (Supplemental Figs. 1, Fig. 1, and Supplemental Table 1). An NPA motif sequence is located 89 residues downstream at position 180–182, however, the spatial positioning of this motif is not consistent with the classical two-NPA motif “hour-glass” aquaporin folding pattern (Jung et al., 1994). A second NPA motif, conserved in the carboxyl terminal domain in other aquaporins, is located at position 208–210. Furthermore, other than Phe73, the predicted ar/R constriction residues are not conserved with orthodox AQPs (Val196, Gly205, and Leu211) (Supplemental Figs. 1, Fig. 1, and Supplemental Table 1). TM topology predictions for LhAQP5 varied, but the consensus topology from TmPred, TMHMM, RHYTHM, HMMP, and TopPredII predicted six TM-spanning regions with intracellular amino and carboxyl termini (Table 3 and Supplemental Table 2). Phobius predicted five TM helices and TOPCONS predicted seven TM regions (Table 3 and Supplemental Table 2).

We used CLUSTALW and MEGA 5.1 UPGMA, Maximum Likelihood, Maximum Parsimony, and Neighbor-Joining phylogenetic analysis to compare LhAQPs with other arthropod aquaporins (Fig. 2). Invertebrate aquaporins were previously classified by Campbell et al. (2008) and Mathew et al. (2011) into at least three subfamilies (*Drosophila* intrinsic proteins - DRIPs, Big Brain proteins - BIBs, and *Pyrocoelia rufa* integral proteins - PRIPs). More recently they were grouped into four major clusters [groups 1–4 by Kambara et al. (2009) and Goto et al. (2011)] or clades A–D (Wallace et al., 2012). Sequence alignment and phylogenetic analysis of full-length LhAQP protein sequences with 57 other invertebrate aquaporin sequences retrieved from GenBank showed the existence of at least six distinct families of arthropod AQPs, including DRIPs, PRIPs, *R. prolixus* integral proteins - RPIPs, BIBs, *Dermacentor variabilis* integral proteins - DVIPs, and *Lygus hesperus* integral proteins - LHIPs (Fig. 2). While analysis by Wallace et al. (2012) includes BIBs, DRIPs, and PRIPs within a single clade (e.g., A), analysis here and by others (Kambara et al., 2009; Drake et al., 2010; Goto et al., 2011; Herraiz et al., 2011) indicates that BIBs are sufficiently diverged from DRIPs and PRIPs to warrant classification into a separate clade, which we term clade E using the

nomenclature of Wallace et al. (2012) (Fig. 2). Here, we classify six subfamilies based on the nomenclature of Campbell et al. (2008) that are contained within five clades (A–E). Whereas, clades B, C, and D are identical to those from Wallace et al. (2012), the clade A described here contains both the DRIP and PRIP subfamilies and does not contain the BIBs (clade E). Furthermore, of the four AQP groups from Kambara et al. (2009) and Goto et al. (2011), group 1 corresponds to subfamily DRIP, group 2 corresponds to BIB, group 3 contains both PRIPs and RPIPs, and group 4 corresponds to the new subfamily LHIP (Fig. 2).

Based on phylogenetic analysis, the LhAQP proteins segregated into different subfamilies comprising DRIPs (LhAQP1), PRIPs (LhAQP4A and LhAQP4B), RPIPs (LhAQP2A–E), and LHIPs (LhAQP5). LhAQP3 is unique and appears to fall outside currently classified aquaporin-like sequences (Campbell et al., 2008; Kambara et al., 2009; Goto et al., 2011) and may represent a novel subfamily/clade of AQPs. Furthermore, while a BIB-like protein has been found in the hemipteran *A. pisum*, no *lygus* BIB-like sequence has yet been identified.

LhAQP1 aligned within the DRIP subfamily of clade A and overall shares 42% identity with members of that subfamily. LhAQP1 is most homologous (46% identity) to the *B. mori* (NP_001036919.1), *A. aegypti* (Q9NH7.2), and *Coptotermes formosanus* (BAG72254.1) DRIP-like aquaporins. LhAQP4A and LhAQP4B aligned within the PRIP subfamily, which also belongs to clade A (Fig. 2). LhAQP4B shares 41% identity across the PRIP subfamily and is most closely related with aquaporins from *Tribolium castaneum* (XP_968342.1) (45% identity), *Pediculus humanus corporis* (XP_002429480.1) (45% identity), *Culex quinquefasciatus* (XP_001865728.1) (44% identity), and *B. mori* (NP_001153661.1) (43% identity).

The LhAQP2s aligned within the RPIP aquaporin subfamily or clade B (Fig. 2). LhAQP2E shared an average of 36% identity with other RPIPs, with the most closely related sequences corresponding to aquaporins from *R. prolixus* (CAC13959.1) and *A. pisum* (NM_001246042.2) having 42 and 35% identity, respectively.

LhAQP5 aligns within subfamily LHIP (clade D) and includes other putative aquaporin sequences that lack functional characterization (Fig. 2). LhAQP5 shares 41 and 52% identity with *P. humanus corporis* (XP_002424369.1) and *D. melanogaster* (AAF58409.2), respectively. BLAST analysis (data not shown) reveals that these LHIP subfamily members share significant sequence similarity with vertebrate S-aquaporins 11 and 12, which, although not well characterized, have highly deviated NPA motifs and are thought to function in intracellular trafficking of water (Ishibashi, 2006, 2009).

3.2. Temporal expression and tissue localization

Transcriptional expression patterns of the LhAQPs were investigated using end-point RT-PCR over the life cycle of *L. hesperus*, including eggs, nymphs (1st, 2nd–3rd, 4th–5th instars), and adults. LhAQP1 transcripts are present in all development stages and most highly abundant in eggs (Fig. 3A). LhAQP2 and LhAQP5 transcripts have similar profiles through development, with little or no transcripts evident in eggs, but constitutive expression in all nymphal instars and adults. LhAQP3 and LhAQP4 transcripts are constitutively present in all developmental stages.

End-point RT-PCR using RNA extracted from different adult tissues show that LhAQP transcripts are differentially expressed (Fig. 3B). All five LhAQPs were found in midguts and transcripts for all but LhAQP5 were present in Malpighian tubules. LhAQP1 transcripts were the only LhAQP abundant in ovaries. LhAQP2 and LhAQP3 transcripts were found primarily in midguts and Malpighian tubules. LhAQP4 transcripts were most abundant in male testes and Malpighian tubules. Surprisingly, in addition to midguts,

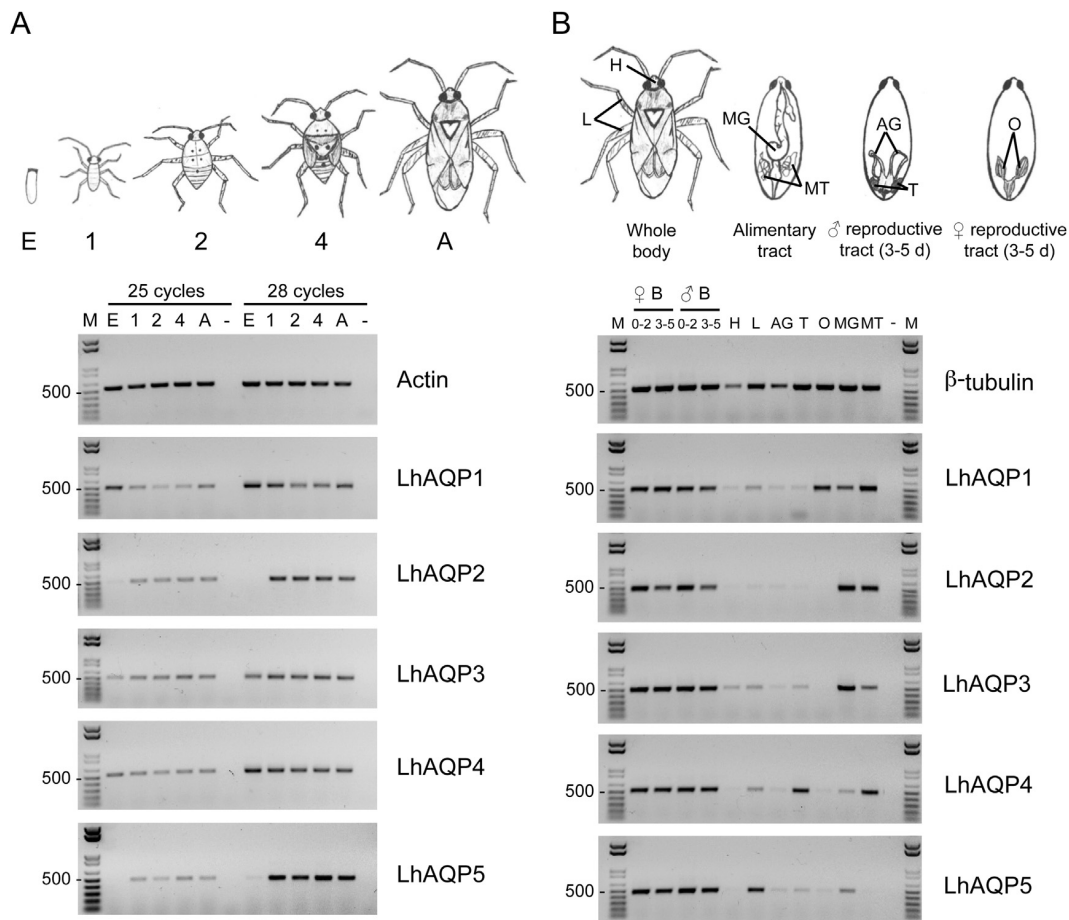


Fig. 3. Transcriptional profiles of LhAQPs through development and in different tissues. (A) Transcriptional expression of all five LhAQPs in *L. hesperus* developmental stages. cDNA was prepared from 1.0 μ g of DNase-treated total RNA from eggs (E), 1st instar nymphs (1), 2nd–3rd instar nymphs (2), 4th–5th instar nymphs (4), and adults (A). The appropriate annealing temperatures and number of RT-PCR cycles was determined empirically with 25 and 28 cycles shown. Actin was amplified as an internal reference gene and “–” designates a no template control. (B) Transcriptional expression profile of all five LhAQPs from dissected *L. hesperus* tissues. cDNA made from female and male whole bodies (0–2 d or 3–5 d old adults), heads (H), legs (L), accessory glands (AG), testis (T), ovaries (O), midguts (MG), and Malpighian tubules (MT) were analyzed by RT-PCR (results with 28 cycles is shown). β -tubulin was used as an amplification control for tissues. Products were electrophoresed on 0.8% agarose gels and visualized using SYBR Safe (Invitrogen). Lane M corresponds to 1 kb Plus DNA Ladder (Invitrogen).

LhAQP5 transcripts were present in leg tissue. Faint bands were also visible in leg tissue for LhAQP1, LhAQP3, and LhAQP4.

3.3. Cellular localization

All arthropod aquaporins characterized to date involve intracellular protein synthesis and subsequent translocation to plasma membranes, where they exhibit their transport function (Campbell et al., 2008; Cohen, 2013). WOLF PSORT (Horton et al., 2007) predictions of subcellular localization of each translated sequence were consistent with presumed functionality; all LhAQPs were predicted to be associated with the plasma membrane (data not shown). However, LhAQP2A, LhAQP2E, LhAQP3, LhAQP4A, LhAQP4B, and LhAQP5 either had potential endoplasmic reticulum (ER) retention signals, or in the case of LhAQP2A, LhAQP2E, and LhAQP3, had PSORTII k-NN scores for ER equal to or above those for the plasma membrane (data not shown).

To examine cellular localization of each LhAQP, chimeric recombinant LhAQP proteins tagged with enhanced green fluorescent protein (EGFP) were produced in cultured Tni cells. First, we made LhAQP/pIB constructs with carboxyl-terminal-tagged EGFP chimeric proteins (Fig. 4A, products #1–11). Examination of

transfected cells by fluorescence microscopy showed that LhAQP2A-EGFP, LhAQP2B-EGFP, LhAQP2C-EGFP, LhAQP2D-EGFP, LhAQP2E-EGFP, LhAQP3-EGFP, and LhAQP4B-EGFP recombinant chimeras were produced and transported primarily to the plasma membrane in Tni cells (Fig. 4B). LhAQP1-EGFP, LhAQP4A-EGFP, and LhAQP5-EGFP were not detectable at the cell surface, but rather were primarily intracellular with distribution patterns consistent with either localization in the Golgi apparatus (Fig. 4B, panel c and panel j for LhAQP1-EGFP and LhAQP4A-EGFP, respectively) or the ER (Fig. 4B, panel l for LhAQP5-EGFP).

Our localization results for LhAQP1-EGFP were unexpected, as other insect DRIP-like aquaporins are associated with the plasma membrane (Le Caherec et al., 1997; Duchesne et al., 2003; Liu et al., 2011; Mathew et al., 2011; Azuma et al., 2012) where they facilitate transport of cellular and extracellular water. A Met3-LhAQP1-EGFP/pIB construct (Fig. 4A, product #11) was made to test whether a truncated LhAQP1 produced using the methionine located at base 27 as the start codon would influence Tni cellular localization. Like LhAQP1-EGFP, Met3-LhAQP1-EGFP was intracellular (Fig. 4C, panel a) and exhibited Golgi-like localization (Kawar and Jarvis, 2001). Furthermore, placement of EGFP at the amino-terminus of LhAQP1 (EGFP-LhAQP1, Fig. 4A, product #12) did not alter the translocation

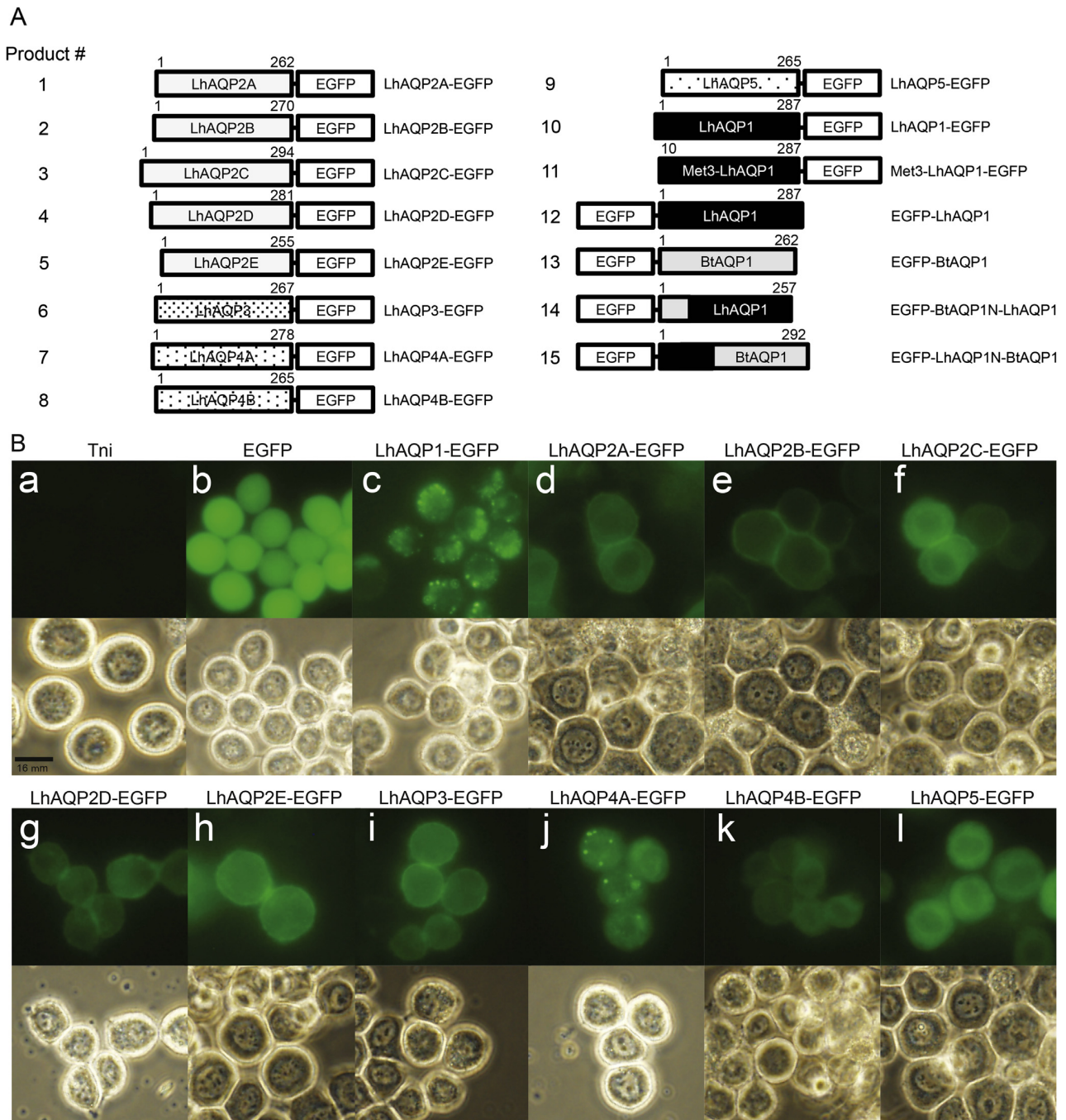


Fig. 4. Cellular localization of LhAQPs heterologously expressed in cultured Tni cells. (A) Schematic diagram of LhAQPs produced as EGFP chimeras in cultured Tni cells. Recombinant LhAQPs were expressed as chimeras with the enhanced green fluorescent protein (EGFP) using the pIB/V5-His TOPO TA (Invitrogen-Life Technologies) insect cell expression vector in Tni cells. Whereas LhAQP2-5 were all produced with EGFP at their carboxyl termini (products #1–9), recombinant LhAQP1 was produced with EGFP either at the carboxyl terminus (Product #10) or at the amino terminus (product #12). Product #11 corresponds to a truncated LhAQP1 beginning at base position 28 (corresponding to third methionine in translated LhAQP1) with EGFP at the amino terminus. Domain swapping was performed between LhAQP1 and *B. tabaci* AQP1 (BtAQP1) from Mathew et al. (2011) with product #13 corresponding to the full-length BtAQP1 chimera with EGFP at the amino terminus. Product #14 corresponds to LhAQP1 with 69 residues from the amino terminus replaced by the first 39 residues from BtAQP1. Product #15 corresponds to a chimeric protein having the first 39 residues of BtAQP1 replaced with 69 residues from the amino terminus of LhAQP1 produced in frame with the final 223 residues from BtAQP1. (B) Expression of recombinant carboxyl-terminal EGFP-labeled LhAQPs in Tni cells. Cells were transfected with 2 µg pIB plasmid DNA corresponding to LhAQP1-5-EGFP (panels c-l) using Insect GeneJuice transfection reagent (Novagen/EMD Biosciences) for 5–12 h with microscopic imaging (top image detecting fluorescence and bottom image is phase contrast) performed two days post transfection. Panel (a) shows untransfected Tni cells and panel (b) shows cells transfected with EGFP/pIB. Panels (c-l) show cells transfected with LhAQP-EGFP/pIB plasmid DNA. All proteins were produced as chimeras with carboxyl-terminal EGFP. (C) Domain swapping of LhAQP1 and BtAQP1 amino termini and expression in Tni cells. Panel (a) corresponds to Met3-LhAQP1 (10 residues truncated from LhAQP1). Panels (b) and (c) show localization of amino-terminal tagged LhAQP1 and BtAQP1, respectively. Panel (d) shows expression of LhAQP1 with the amino terminus of BtAQP1 is at the cell surface, whereas panel (e) shows expression of BtAQP1 with the amino terminus of LhAQP1 is subcellular. All cells were imaged using an Olympus FSX-100 fluorescence microscope with FSX-BSW imaging software (Olympus, Center Valley, PA) and processed using IrfanView with gamma correction set at 1.5.

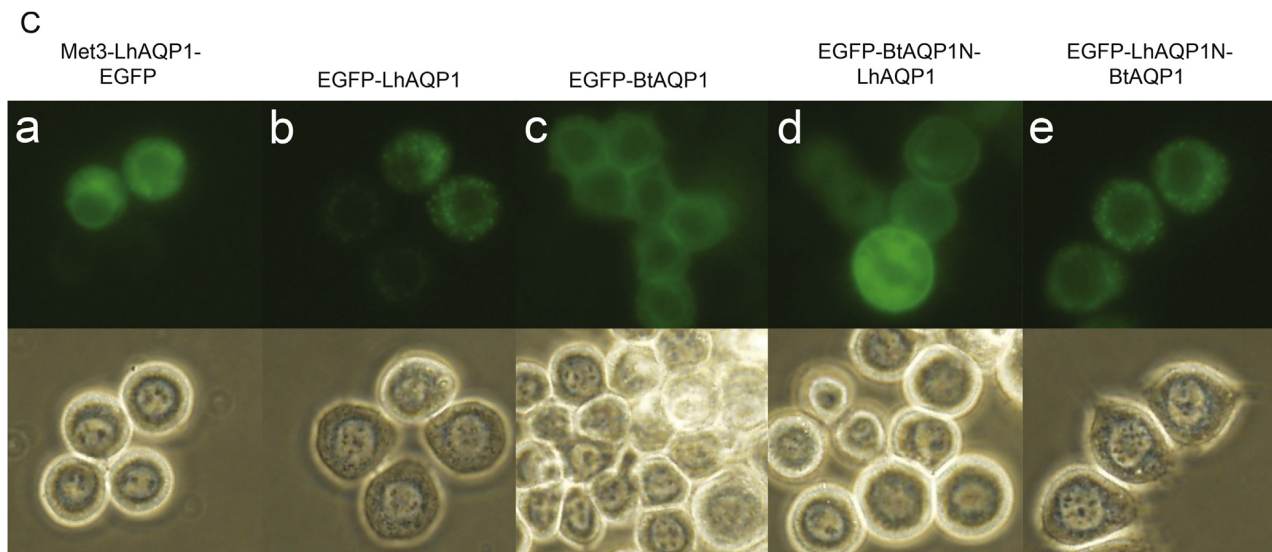


Fig. 4. (continued).

of LhAQP1, indicating the position of EGFP was not responsible for the observed intracellular localization (Fig. 4C, panel b).

To test the influence of the amino terminus of LhAQP1 on cellular localization, we produced EGFP chimeras that switched the first 69 amino acid residues from LhAQP1 with the first 39 residues from the *B. tabaci* aquaporin 1 (BtAQP1) and vice versa. Whereas the addition of the amino terminus of BtAQP1 to LhAQP1 (EGFP-BtAQP1N-LhAQP1) rescued localization to the cellular plasma membrane in Tni (Fig. 4C, panel d), the addition of the LhAQP1 amino terminus to BtAQP1 (EGFP-LhAQP1N-BtAQP1) resulted in impaired translocation, with intracellular fluorescence primarily limited to small punctae reminiscent of the Golgi apparatus (Fig. 4C, panel e). These results indicate that the first 69 residues at the amino terminus of LhAQP1 are responsible for intracellular localization of LhAQP1 in Tni cells.

3.4. Oocyte functional analysis

The functions of LhAQPs in water and glycerol transport were tested using the *Xenopus* oocyte expression system, measuring volume changes indicative of net influx of water or glycerol in hypotonic and isotonic solutions, respectively (Fig. 5A). We observed significantly higher swelling rates ($p < 0.01$) in LhAQP1, 2, 3, 4, and 5-injected oocytes in hypotonic saline (mean \pm SEM 14.4 ± 2.5 for LhAQP1, 14.2 ± 1.2 for LhAQP2A, 27.1 ± 2.6 for LhAQP3, 19.0 ± 1.8 for LhAQP4A, and 13.4 ± 0.6 for LhAQP5 $V/V_0 \times 10^5 \times \text{sec}^{-1}$) compared to water-injected control oocytes ($5.1 \pm 0.5 V/V_0 \times 10^5 \times \text{sec}^{-1}$) (Fig. 5B). Furthermore, none of the LhAQP-injected oocytes showed appreciable transport of glycerol, based on the absence of swelling. Instead, observed negative slopes (Fig. 5A) indicated a slight shrinkage in the glycerol-substituted saline (-3.1 ± 1.3 for LhAQP1, -5.6 ± 2.6 for LhAQP2A, -3.1 ± 1.3 for LhAQP3, -5.8 ± 1.2 for LhAQP4A, and -6.4 ± 1.1 for LhAQP5; $V/V_0 \times 10^5 \times \text{sec}^{-1}$), indicating relative aquaporin impermeability to glycerol.

4. Discussion

Aquaporins are integral membrane proteins belonging to a large family of water channel proteins or MIPs that facilitate transport water and/or other small solutes across cellular membranes (Benga,

2009; Kruse et al., 2006). Because water and solute transport are universal requirements for living cells, these proteins are found in most organisms. The total number of invertebrate AQPs identified in insects is rapidly increasing, with genome sequencing implicating at least 5–8 genes per organism encoding putative AQPs (Campbell et al., 2008; Drake et al., 2010). High-throughput next generation transcriptomic sequencing and *de novo* assembly provides an opportunity to obtain comprehensive “snapshots” of active gene transcripts in organisms without prior genomic support (Hull et al., 2013; Grabherr et al., 2011). Here, we gleaned the transcriptomes of two mirid plant bugs, *L. hesperus* (Hull et al., 2013) and *L. lineolaris* (O.P. Perera, unpublished), to identify expressed sequence tag (EST) sequences encoding putative AQPs.

Arthropods have multiple functional AQPs, and based on other animal systems these proteins likely play diverse physiological roles (Campbell et al., 2008; Gomes et al., 2009). Unfortunately, for most invertebrates comprehensive molecular and functional characterization of AQPs trails their initial identification. For example, *D. melanogaster* has eight putative AQPs, but only two have been assigned functions (Kaufmann et al., 2005; Yanochko and Yool, 2002). *A. aegypti* has six putative AQPs and RNAi knockdown was used to show that three have apparent roles in diuresis in Malpighian tubules (Drake et al., 2010). However, the roles of those transcripts in mosquitoes not exhibiting an obvious phenotype are yet to be defined, and biochemical characterization of all AeAQPs is not complete. This report attempts to identify and characterize a complement of AQPs from the hemipteran pest, *L. hesperus*.

Five full-length LhAQPs that likely represent the primary AQP transcripts from *L. hesperus* were cloned and characterized. We used phylogenetic alignments of LhAQPs with other arthropod representatives to classify at least six subfamilies of arthropod AQPs, including three (DRIPs, PRIPs, and BIBs) previously described by Campbell et al. (2008). Three new subfamilies [named using nomenclature described by Campbell et al. (2008)] include the RPIPs (named for *R. prolixus* integral protein), DVIPs (named for *D. variabilis* integral protein), and LHIPs (named for *L. hesperus* integral protein). Within these phylogenetic subfamilies, three functional classes of AQPs have been characterized for arthropods, including water-specific AQPs, aquaglyceroporins, and monovalent cation channels (BIBs) (Campbell et al., 2008; Echevarria et al.,

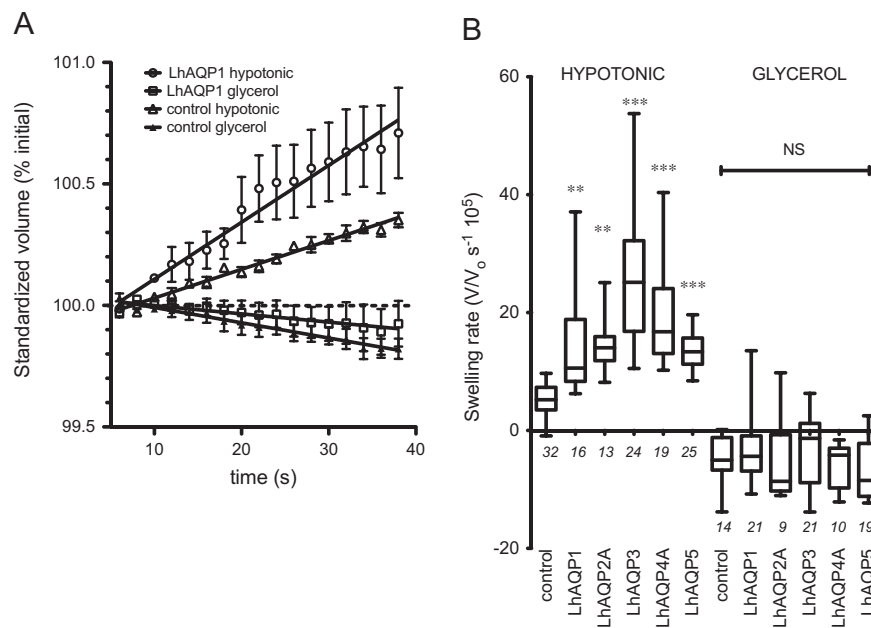


Fig. 5. Osmotic water and glycerol permeability of *Xenopus* oocytes expressing LhAQPs. (A) Representative examples of mean swelling rates (\pm SEM) of control and LhAQP1-expressing oocytes as a function of time after introduction of oocytes into 50% hypotonic saline or isotonic glycerol-substituted saline at time zero. Volumes of the oocytes at each time point (V) are standardized to the initial area at time zero (V_0). (B) Compiled swelling rates (slope values of linear regression fits of V/V_0 versus time) showed significant osmotic water permeability of LhAQP-expressing oocytes (LhAQP1–5) compared with control oocytes (ANOVA and post-hoc Bonferroni tests, with ** indicating $p < 0.01$ and *** $p < 0.001$). No significant glycerol permeability was found using saline in which 130 mM glycerol replaced 65 mM NaCl. Box plots show 25th and 75th quartiles (box), median values (solid horizontal line within box), and error bars span the full range of data points. Sample sizes (n) are shown near the x-axis.

2001; Duchesne et al., 2003; Le Caherec et al., 1996; Shakesby et al., 2009; Mathew et al., 2011; Kataoka et al., 2009a; Wallace et al., 2012; Yanocho and Yool, 2002). An important distinction is that the functional classes do not necessarily correspond with phylogenetic classifications. For example, the RPIP subfamily includes some AQPs that function to transport water and glycerol/urea and hence are aquaglyceroporins (Fig. 2). But, not all members of the RPIP subfamily transport glycerol and are therefore not functional aquaglyceroporins (includes PvaAQP2 in Kikawada et al., 2008; the LhAQP4 isoforms, Fig. 5) [see Supplemental Table 1 for phylogenetic and functional classification of representative invertebrate AQPs].

Phylogenetic analysis assigned the LhAQP proteins to different subfamilies, including DRIPs (LhAQP1), PRIPs (LhAQP4A and LhAQP4B), RPIPs (LhAQP2A–E), and LHIPs (LhAQP5). The arthropod DRIP subfamily includes a number of water-specific AQPs generally promoting fluid homeostasis by moving water through tissues to facilitate excretion and/or maintenance of osmotic potential (Campbell et al., 2008; Mathew et al., 2011). Based on conserved AQP motifs and sequence similarity (Fig. 2), predicted topology (Table 3 and Supplemental Table 2), and formation of water-specific pores in *Xenopus* oocytes (Fig. 5), LhAQP1 is a water-specific AQP from the DRIP subfamily. Two LhAQP4 isoforms belong to the arthropod PRIP subfamily which includes AQPs with diverse physiological functions, such as water recycling in the cryptonephric rectal complex (Azuma et al., 2012), hydration and dehydration responses to environmental stress (Kikawada et al., 2008), and water and nitrogen homeostasis during oogenesis (Herraiz et al., 2011). The LhAQP2 isoforms belong to the RPIP arthropod subfamily, which contains a number of AQPs with putative multi-functional transport channel functions, including the aquaglyceroporins. Members of the RPIP subfamily are important for osmoregulation and *Buchnera* symbiosis in aphids (Wallace et al., 2012), water homeostasis in fat body (Kikawada et al., 2008), urine formation (Echevarria et al., 2001), and water homeostasis/

urea excretion in midgut and Malpighian tubules (Kataoka et al., 2009a). We classify LhAQP5 into a new subfamily of arthropod AQPs called the LHIPs. These proteins share similarity with ‘superaquaporins’ (Morishita et al., 2004) or ‘S-aquaporins’ (Ishibashi, 2006), which are quite diverged from other families of AQPs. These divergences include altered NPA motifs and anomalous subcellular localization (Ishibashi, 2006, 2009; Nozaki et al., 2008; Calvanese et al., 2013). Although LhAQP3 transports water (and not glycerol) in *Xenopus* oocytes, it falls outside currently classified aquaporin-like sequences and may represent an additional unclassified subfamily of water-transporting AQPs (Fig. 2). Contigs encoding a BiB-like protein were not found in our search of the *L. hesperus* or *L. lineolaris* transcriptomes.

Two canonical NPA motifs along with residues that comprise the ar/R constriction site (Sui et al., 2001; Beitz et al., 2006) are critical for determining the selectivity for solutes that transverse the AQP channel. Of the LhAQPs, only LhAQP1 and LhAQP4 have two conserved NPA motifs (Fig. 1 and Supplemental Table 1). Both LhAQP3 and LhAQP5 have substitutions within the first NPA motif (Asn-Pro-Cys for LhAQP3; Cys-Pro-Tyr for LhAQP5), and for LhAQP2 the second NPA motif is Asn-Pro-Val (Fig. 1 and Supplemental Table 1). In human AQPs, four residues (Phe56, His180, Cys189, and Arg195 from AQP1 and Phe77, His201, Ala210, and Arg216 from AQP4) form the narrowest restriction point within the AQP water channel that is only slightly larger than size of a single water molecule (Sui et al., 2001; Beitz et al., 2006; Ho et al., 2009). The corresponding ar/R constriction residues for LhAQPs include Phe/His/Ser/Arg for LhAQP1, Phe/Ser/Ala/Arg for LhAQP2, Phe/Ala/Gly/Arg for LhAQP3, Phe/His/Ser/Arg for LhAQP4, and Phe/Val/Gly/Leu for LhAQP5 (Fig. 1 and Supplemental Table 1). Wallace et al. (2012) reported that insect MIPs (including some aquaglyceroporins) within the RPIP subfamily (clade B from Wallace et al., 2012) have small neutral residues at position H5 that contribute to a wider, more hydrophilic ar/R constriction, which is required for passage of

larger solutes. However, we found that none of the LhAQPs facilitate the transport of glycerol in *Xenopus* oocytes, including LhAQP2, LhAQP3, or LhAQP5, which contain similar ar/R residues to those found in other insect aquaglyceroporins. Therefore, insect AQPs may have diverse functional roles that are not necessarily predicted by sequence conservation. Residues yet to be defined could additionally influence permeation pathways in the AQP channel and participate in defining solute permeabilities.

Levels of LhAQP transcripts differed little during *L. hesperus* development with all five apparently constitutively present in nymphs and adults (Fig. 3A). LhAQP1, 3, and 4 transcripts were detected in eggs (Fig. 3A), indicating a possible role in embryonic development. It is not known whether these LhAQP transcripts were embryonic or maternally derived. LhAQP transcripts are abundant in various adult *L. hesperus* tissues (Fig. 3B), with all LhAQPs present in Malpighian tubules and LhAQP1–4 present in the midgut. These results are consistent with reports of other AQPs associated with fluid absorption and excretion in arthropods (Spring et al., 2009; Le Caherec et al., 1997; Echevarria et al., 2001; Kaufmann et al., 2005; Kataoka et al., 2009a; Liu et al., 2011; Mathew et al., 2011; Azuma et al., 2012). LhAQP1 is the only transcript found in ovaries, and LhAQP4 is abundant in male testes (Fig. 3B). The presence of LhAQPs in reproductive tissues is not unprecedented, as 12 of 13 known mammalian AQPs are expressed in female and male reproductive systems [reviewed in Zhang et al., (2012)]. Vertebrate AQPs have numerous known functions in males, including spermatogenesis, seminal fluid production, and fluid transport in testis and numerous ducts and tubules (Zhang et al., 2012). Vertebrate females have AQPs that function in tubal fluid transport, water homeostasis of the uterus, cervix, placenta, and oviduct, maintenance of amniotic fluid, gamete transport and fertilization, early embryo development, and implantation (Zhang et al., 2012). Arthropod AQPs may also function in reproduction, including those found in ovaries of the tick *D. variabilis* (Holmes et al., 2008), the cockroach *B. germanica* (Herraiz et al., 2011), and the mosquitoes *A. aegypti* (Drake et al., 2010) and *A. gambiae* (Liu et al., 2011). Interestingly, transcripts from all five LhAQPs were detected in leg tissue, which could indicate a possible role in muscle respiration. Indeed, water transport is important in flight muscles during periods of high-energy demand (Wigglesworth, 1965; Wigglesworth and Lee, 1982) and a water-specific AQP identified in *A. aegypti* Malpighian tubules has been shown to be involved in respiration by transporting water through tracheolar cells (Duchesne et al., 2003).

Heterologous expression of LhAQP-EGFP chimeras in Tni cells showed that LhAQP2 (isoforms A–E), LhAQP3, and LhAQP4B are produced and transported to the cell surface (Fig. 4B). Carboxyl-terminal EGFP-tagged LhAQP1, LhAQP4A, and LhAQP5 were likewise produced in Tni cells but did not localize at the plasma membrane. They instead localized primarily to cytosolic punctae (LhAQP1 and LhAQP4A) reminiscent of the Golgi apparatus (Kawar and Jarvis, 2001) or exhibited a diffuse cytosolic distribution with a prominent perinuclear ring (LhAQP5) similar to that described (Thomas et al., 1998) for endoplasmic reticulum localization (Figs. 4B, C). We also performed domain-swapping experiments between LhAQP1 and the *B. tabaci* AQP1 (BtAQP1) previously shown to translocate to the cell surface in cultured insect cells (Mathew et al., 2011). Here, the replacement of the amino-terminus of BtAQP1 with that of LhAQP1 prevented the chimera from reaching the cell surface (Fig. 4C). Furthermore, when the amino terminus of LhAQP1 was replaced with that of BtAQP1, localization to the cellular plasma membrane in Tni was rescued (Fig. 4C). These results indicate that some LhAQPs may either have an intracellular localization or that *L. hesperus* and Tni cells differ such that some proteins are not correctly processed by the Tni intracellular protein trafficking machinery. The latter is likely for LhAQP1. LhAQP5

however, might have subcellular function, as it resembles other supraaquaporins thought to function as intracellular water channels that regulate free and bound water movement across subcellular organelle membranes (Ishikawa et al., 2005; Nozaki et al., 2008; Ishibashi, 2006).

S-aquaporins or supraaquaporins represent a subfamily of AQPs characterized as having relatively poor sequence similarity with other AQPs and atypical NPA motifs (Morishita et al., 2004; Ishibashi, 2006). Here, we report the first functional S-aquaporin (LhAQP5) from an insect. Both plants and animals have S-aquaporins with atypical amino-terminal NPA motifs (HsAQP11, HsAQP12, SIP1.1, SIP1.2, and SIP2.1) (Supplemental Table 1). These AQPs localize on the membrane of intracellular organelles (Ishikawa et al., 2005; Morishita et al., 2005; Itoh et al., 2005) and are thought to participate in the transport of intracellular water through cell organelles, regulation of organelle volume, regulation of intracellular waste products via secretory granules, and maintenance of cellular activities through the distribution of free water (Nozaki et al., 2008). Several S-aquaporins have high lysine content at their carboxyl termini that may act as ER-localization signals (Cosson and Letourneur, 1994), including LhAQP5 with residues 261-KEKD-264 that resemble carboxyl terminal ER retention motifs. Furthermore, Guan et al. (2010) indicates that NPA motifs are important for targeting orthodox AQPs to the plasma membrane and the atypical NPA motifs of the S-aquaporins may aid in their subcellular localization.

Water homeostasis is a critical function for all life. Animals (including insects) have developed both behavioral and physiological adaptations to facilitate osmoregulation and balance internal water equilibrium with water lost to the environment. Terrestrial insects in particular are under continuous osmotic stress and must balance water losses to evaporation through the cuticle, respiratory transpiration, and excretion, and gain water by direct ingestion of fluids, generation of metabolic water, and/or absorption of atmospheric water vapor (Cohen, 2013). Disrupting water balance by targeting the osmoregulatory system including water channel proteins in arthropod pests remains a promising avenue for developing selective and environmentally compatible pest control strategies (Cohen, 2013). However, there are no commercially effective and selective methods yet available that target either water channels or the regulatory pathways controlling water homeostasis in arthropod pests. Furthermore, arthropods have evolved mechanisms by which critical functions (such as embryogenesis, immunity, apoptosis, membrane transport, digestion, metamorphosis, neural-motor function, to name a few) may have redundant or compensatory routes of activity (Masel and Siegal, 2009; Moczek et al., 2011). Indeed, insects produce multiple AQPs with overlapping tissue expression patterns (see Fig. 3B; Drake et al., 2010) and knockdown of individual AQP transcripts by RNAi does not necessarily lead to negative phenotypes (Shakesby et al., 2009; Drake et al., 2010; Herraiz et al., 2011), which is indicative of possible functional redundancy. Yet, the AQPs and the mechanisms by which water homeostasis is maintained remain promising areas of research that may lead to new controls for pests of medical and agricultural importance (Cohen, 2013). Further studies are needed to develop comprehensive models of arthropod AQP function and novel strategies to disrupt osmoregulation.

Acknowledgements

We thank Lolita Mathew, Lynn Forlow-Jech, Sarah Bjorklund, and Eric Hoffmann for technical support, O.P. Perera for providing partial *Lygus lineolaris* aquaporin transcriptome sequences (unpublished) that helped with initial cloning of LhAQPs, and Dale Spurgeon for helpful comments. This is a cooperative investigation

between USDA-ARS and the University of Adelaide. The research described in this manuscript was partially supported by funds from Cotton Inc. Mention of trade names or commercial products in this article is solely for the purpose of providing specific information and does not imply recommendation or endorsement by the U.S. Department of Agriculture. USDA is an equal opportunity provider and employer.

Appendix A. Supplementary data

Supplementary data related to this article can be found at <http://dx.doi.org/10.1016/j.ibmb.2013.12.002>

References

- Agre, P., Bonhivers, M., Borgnia, M.J., 1998. The aquaporins, blueprints for cellular plumbing systems. *J. Biol. Chem.* 273, 14659–14662.
- Altschul, S.F., Gish, W., Miller, W., Myers, E.W., Lipman, D.J., 1990. Basic local alignment search tool. *J. Mol. Biol.* 215, 403–410.
- Anthony, T.L., Brooks, H.L., Boassa, D., Leonov, S., Yanochko, G.M., Regan, J.W., Yool, A.J., 2000. Cloned human aquaporin-1 is a cyclic GMP-gated ion channel. *Mol. Pharmacol.* 57, 576–588.
- Azuma, M., Nagae, T., Maruyama, M., Kataoka, N., Miyake, S., 2012. Two water-specific aquaporins at the apical and basal plasma membranes of insect epithelia: molecular basis for water recycling through the cryptonephric rectal complex of lepidopteran larvae. *J. Insect Physiol.* 58, 523–533.
- Backus, E.A., Cline, A.R., Ellerseick, M.R., Serrano, M.S., 2007. *Lygus hesperus* (Hemiptera: Miridae) feeding on cotton: new methods and parameters for analysis of nonsequential electrical penetration graph data. *Ann. Entomol. Soc. Am.* 100, 296–310.
- Ball, A., Campbell, E.M., Jacob, J., Hoppler, S., Bowman, A.S., 2009. Identification, functional characterization and expression patterns of a water-specific aquaporin in the brown dog tick, *Rhipicephalus sanguineus*. *Insect Biochem. Mol. Biol.* 39, 105–112.
- Beitz, E., Wu, B., Holm, L.M., Schultz, J.E., Zeuthen, T., 2006. Point mutations in the aromatic/arginine region in aquaporin 1 allow passage of urea, glycerol, ammonia, and protons. *Proc. Natl. Acad. Sci. USA* 103, 269–274.
- Benga, G., 2009. Water channel proteins (later called aquaporins) and relatives: past, present, and future. *IUBMB Life* 61, 112–133.
- Bernsel, A., Viklund, H., Hennerdal, A., Elofsson, A., 2009. TOPCONS: consensus prediction of membrane protein topology. *Nucleic Acids Res.* 37, W465–W468.
- Boassa, D., Yool, A.J., 2003. Single amino acids in the carboxyl terminal domain of aquaporin-1 contribute to cGMP-dependent ion channel activation. *BMC Physiol.* 3, 12.
- Calvanese, L., Pellegrini-Calace, M., Oliva, R., 2013. In silico study of human aquaporin AQP11 and AQP12 channels. *Protein Sci.* 22, 455–466.
- Campbell, E.M., Ball, A., Hoppler, S., Bowman, A.S., 2008. Invertebrate aquaporins: a review. *J. Comp. Physiol.* B, 178, 935–955.
- Campbell, E.M., Burdin, M., Hoppler, S., Bowman, A.S., 2010. Role of an aquaporin in the sheep tick *Ixodes ricinus*: assessment as a potential control target. *Int. J. Parasitol.* 40, 15–23.
- Carbrey, J.M., Agre, P., 2009. Discovery of the aquaporins and development of the field. *Handb. Exp. Pharmacol.*, 3–28.
- Claros, M.G., von Heijne, G., 1994. TopPred II: an improved software for membrane protein structure predictions. *Comput. Appl. Biosci.* 10, 685–686.
- Cohen, E., 2013. Chapter one – water homeostasis and osmoregulation as targets in the control of insect pests. In: Cohen, E. (Ed.), *Target Receptors in the Control of Insect Pests: Part I, Advances in Insect Physiology*, vol. 44. Academic Press, pp. 1–61.
- Cosson, P., Letourneur, F., 1994. Coatamer interaction with di-lysine endoplasmic reticulum retention motifs. *Science* 263, 1629–1631.
- Debolt, J.W., 1982. Meridic diet for rearing successive generations of *Lygus hesperus*. *Ann. Entomol. Soc. Am.* 75, 119–122.
- Douglas, A.E., 2006. Phloem-sap feeding by animals: problems and solutions. *J. Exp. Bot.* 57, 747–754.
- Drake, L.L., Boudko, D.Y., Marinotti, O., Carpenter, V.K., Dawe, A.L., Hansen, I.A., 2010. The aquaporin gene family of the yellow fever mosquito, *Aedes aegypti*. *PLoS One* 5, e15578.
- Duchesne, L., Hubert, J.F., Verbavatz, J.M., Thomas, D., Pietrantonio, P.V., 2003. Mosquito (*Aedes aegypti*) aquaporin, present in tracheolar cells, transports water, not glycerol, and forms orthogonal arrays in *Xenopus* oocyte membranes. *Eur. J. Biochem.* 270, 422–429.
- Echevarria, M., Ramirez-Lorca, R., Hernandez, C.S., Gutierrez, A., Mendez-Ferrer, S., Gonzalez, E., Toledo-Aral, J.J., Ilundain, A.A., Whittembury, G., 2001. Identification of a new water channel (Rg-MIP) in the Malpighian tubules of the insect *Rhodnius prolixus*. *Pflug. Arch. Eur. J. Phys.* 442, 27–34.
- Felsenstein, J., 1985. Confidence limits on phylogenies: an approach using the bootstrap. *Evolution* 39, 783–791.
- Fu, D., Libson, A., Miercke, L.J., Weitzman, C., Nollert, P., Krucinski, J., Stroud, R.M., 2000. Structure of a glycerol-conducting channel and the basis for its selectivity. *Science* 290, 481–486.
- Gomes, D., Agasse, A., Thiébaud, P., Delrot, S., Gerós, H., Chaumont, F., 2009. Aquaporins are multifunctional water and solute transporters highly divergent in living organisms. *BBA-Biomemb.* 1788, 1213–1228.
- Goodchild, A.J.P., 1966. Evolution of the alimentary canal in the Hemiptera. *Biol. Rev.* 41, 97–139.
- Goto, S.G., Philip, B.N., Teets, N.M., Kawarasaki, Y., Lee Jr., R.E., Denlinger, D.L., 2011. Functional characterization of an aquaporin in the Antarctic midge *Belgica antarctica*. *J. Insect Physiol.* 57, 1106–1114.
- Grabherr, M.G., Haas, B.J., Yassour, M., Levin, J.Z., Thompson, D.A., Amit, I., Adiconis, X., Fan, L., Raychowdhury, R., Zeng, Q., Chen, Z., Mauceli, E., Hacohen, N., Gnirke, A., Rhind, N., di Palma, F., Birren, B.W., Nusbaum, C., Lindblad-Toh, K., Friedman, N., Regev, A., 2011. Full-length transcriptome assembly from RNA-Seq data without a reference genome. *Nat. Biotech.* 29, 644–652.
- Guan, X.G., Su, W.H., Yi, F., Zhang, D., Hao, F., Zhang, H.G., Liu, Y.J., Feng, X.C., Ma, T.H., 2010. NPA motifs play a key role in plasma membrane targeting of Aquaporin-4. *IUBMB Life* 62, 222–226.
- Gullan, P.J., Cranston, P.S., 2005. *The Insects: an Outline of Entomology*, third ed. Blackwell Publishing Ltd, Massachusetts.
- Habibi, J., Coudron, T.A., Backus, E.A., Brandt, S.L., Wagner, R.M., Wright, M.K., Huesing, J.E., 2008. Morphology and histology of the alimentary canal of *Lygus hesperus* (Heteroptera: Cimicomorpha: Miridae). *Ann. Entomol. Soc. Am.* 101, 159–171.
- Hachez, C., Chaumont, F., 2010. Aquaporins: a family of highly regulated multifunctional channels. *Adv. Exp. Med. Biol.* 679, 1–17.
- Herraz, J., Chauvigne, F., Cerdá, J., Bellas, X., Piulachs, M.-D., 2011. Identification and functional characterization of an ovarian aquaporin from the cockroach *Blattella germanica* L. (Dictyoptera, Blattellidae). *J. Exp. Biol.* 214, 3630–3638.
- Ho, J.D., Yeh, R., Sandstrom, A., Chorny, I., Harries, W.E., Robbins, R.A., Miercke, L.J., Stroud, R.M., 2009. Crystal structure of human aquaporin 4 at 1.8 Å and its mechanism of conductance. *Proc. Natl. Acad. Sci. USA* 106, 7437–7442.
- Hofmann, K., Stoffel, W., 1993. TMbase – a database of membrane spanning proteins segments. *Biol. Chem. Hoppe-Seyler* 374, 166.
- Holmes, S., Li, D., Ceraul, S., Azad, A., 2008. An aquaporin-like protein from the ovaries and gut of American dog tick (Acari: Ixodidae). *J. Med. Entomol.* 45, 68–74.
- Horton, P., Park, K.-J., Obayashi, T., Fujita, N., Harada, H., Adams-Collier, C.J., Nakai, K., 2007. Wolf PSORT: protein localization predictor. *Nucl. Acids Res.* 35, W585–W587.
- Hub, J.S., De Groot, B.L., 2008. Mechanism of selectivity in aquaporins and aquaglyceroporins. *Proc. Natl. Acad. Sci. USA* 105, 1198–1203.
- Hubert, J.F., Thomas, D., Cavalier, A., Gouranton, J., 1989. Structural and biochemical observations on specialized membranes of the filter chamber, a water-shunting complex in sap-sucking homopteran insects. *Biol. Cell* 66, 155–163.
- Hull, J.J., Hoffmann, E.J., Perera, O.P., Snodgrass, G.L., 2012. Identification of the western tarnished plant bug (*Lygus hesperus*) olfactory co-receptor Orco: expression profile and confirmation of atypical membrane topology. *Arch. Insect Biochem. Physiol.* 81, 179–198.
- Hull, J.J., Geib, S., Fabrick, J.A., Brent, C.S., 2013. Sequencing and *de novo* assembly of the western tarnished plant bug (*Lygus hesperus*) transcriptome. *PLoS ONE* 8, e55105.
- Ishibashi, K., 2006. Aquaporin subfamily with unusual NPA boxes. *Biochim. Biophys. Acta* 1758, 989–993.
- Ishibashi, K., 2009. New members of mammalian aquaporins: AQP10–AQP12. *Handb. Exp. Pharmacol.*, 251–262.
- Ishibashi, K., Hara, S., Kondo, S., 2009. Aquaporin water channels in mammals. *Clin. Exp. Nephrol.* 13, 107–117.
- Ishikawa, F., Suga, S., Uemura, T., Sato, M.H., Maeshima, M., 2005. Novel type aquaporin SIPs are mainly localized to the ER membrane and show cell-specific expression in *Arabidopsis thaliana*. *FEBS Lett.* 579, 5814–5820.
- Itoh, T., Rai, T., Kuwahara, M., Ko, S.B., Uchida, S., Sasaki, S., Ishibashi, K., 2005. Identification of a novel aquaporin, AQP12, expressed in pancreatic acinar cells. *Biochem. Biophys. Res. Commun.* 330, 832–838.
- Jung, J.S., Preston, G.M., Smith, B.L., Guggino, W.B., Agre, P., 1994. Molecular structure of the water channel through aquaporin CHIP. The hourglass model. *J. Biol. Chem.* 269, 14648–14654.
- Käll, L., Krogh, A., Sonnhammer, E.L.L., 2004. A combined transmembrane topology and signal peptide prediction method. *J. Mol. Biol.* 338, 1027–1036.
- Kambara, K., Takematsu, Y., Azuma, M., Kobayashi, J., 2009. cDNA cloning of aquaporin gene expressed in the digestive tract of the Formosan subterranean termite, *Coptotermes formosanus shiraki* (Isoptera: Rhinotermitidae). *Appl. Entomol. Zool.* 44, 315–321.
- Kataoka, N., Miyake, S., Azuma, M., 2009a. Aquaporin and aquaglyceroporin in silkworms, differently expressed in the hindgut and midgut of *Bombyx mori*. *Insect Mol. Biol.* 18, 303–314.
- Kataoka, N., Miyake, S., Azuma, M., 2009b. Molecular characterization of aquaporin and aquaglyceroporin in the alimentary canal of *Grapholita molesta* (the oriental fruit moth) – comparison with *Bombyx mori* aquaporins. *J. Insect Biotech. Sericol.* 78, 81–90.
- Kaufmann, N., Mathai, J.C., Hill, W.G., Dow, J.A.T., Zeidel, M.L., Brodsky, J.L., 2005. Developmental expression and biophysical characterization of a *Drosophila melanogaster* aquaporin. *Am. J. Physiol.-Cell Ph.* 289, C397–C407.

- Kawar, Z., Jarvis, D.L., 2001. Biosynthesis and subcellular localization of a lepidopteran insect alpha 1,2-mannosidase. *Insect Biochem. Mol. Biol.* 31, 289–297.
- Kikawada, T., Saito, A., Kanamori, Y., Fujita, M., Snigorska, K., Watanabe, M., Okuda, T., 2008. Dehydration-inducible changes in expression of two aquaporins in the sleeping chironomid, *Polypedium vanderplanki*. *BBA-Biomemb.* 1778, 514–520.
- King, L.S., Kozono, D., Agre, P., 2004. From structure to disease: the evolving tale of aquaporin biology. *Nat. Rev. Mol. Cell. Biol.* 5, 687–698.
- Krogh, A., Larsson, B., von Heijne, G., Sonnhammer, E.L.L., 2001. Predicting transmembrane protein topology with a hidden Markov model: application to complete genomes. *J. Mol. Biol.* 305, 567–580.
- Kruse, E., Uehlein, N., Kaldenhoff, R., 2006. The aquaporins. *Genome Biol.* 7, 206.
- Larkin, M.A., Blackshields, G., Brown, N.P., Chenna, R., McGettigan, P.A., McWilliam, H., Valentin, F., Wallace, I.M., Wilm, A., Lopez, R., Thompson, J.D., Gibson, T.J., Higgins, D.G., 2007. Clustal W and clustal X version 2.0. *Bioinformatics* 23, 2947–2948.
- Le Caherec, F., Deschamps, S., Delamarche, C., Pellerin, I., Bonnet, G., Guillam, M.T., Thomas, D., Gouranton, J., Hubert, J.F., 1996. Molecular cloning and characterization of an insect aquaporin – functional comparison with aquaporin 1. *Eur. J. Biochem.* 241, 707–715.
- Le Caherec, F., Guillam, M.T., Beuron, F., Cavalier, A., Thomas, D., Gouranton, J., Hubert, J.F., 1997. Aquaporin-related proteins in the filter chamber of homopteran insects. *Cell Tiss. Res.* 290, 143–151.
- Lehane, M.J., Billingsley, P.F., 1996. *Biology of the Insect Midgut*, first ed. Chapman and Hall, London.
- Liu, K., Tsujimoto, H., Cha, S.-J., Agre, P., Rasgon, J.L., 2011. Aquaporin water channel AqAQP1 in the malaria vector mosquito *Anopheles gambiae* during blood feeding and humidity adaptation. *Proc. Natl. Acad. Sci. USA* 108, 6062–6066.
- Masel, J., Siegal, M.L., 2009. Robustness: mechanisms and consequences. *Trends Genet.* 25, 395–403.
- Mathew, L.G., Campbell, E.M., Yool, A.J., Fabrick, J.A., 2011. Identification and characterization of functional aquaporin water channel protein from alimentary tract of whitefly, *Bemisia tabaci*. *Insect Biochem. Mol. Biol.* 41, 178–190.
- Miles, P.W., 1987. Plant-sucking bugs can remove the contents of cells without mechanical damage. *Experientia* 43, 937–939.
- Moczek, A.P., Sultan, S., Foster, S., Ledon-Rettig, C., Dworkin, I., Nijhout, H.F., Abouheif, E., Pfennig, D.W., 2011. The role of developmental plasticity in evolutionary innovation. *Proc. Biol. Sci.* 278, 2705–2713.
- Morishita, Y., Matsuzaki, T., Hara-chikuma, M., Andoo, A., Shimono, M., Matsuki, A., Kobayashi, K., Ikeda, M., Yamamoto, T., Verkman, A., Kusano, E., Ookawara, S., Takata, K., Sasaki, S., Ishibashi, K., 2005. Disruption of aquaporin-11 produces polycystic kidneys following vacuolization of the proximal tubule. *Mol. Cell. Biol.* 25, 7770–7779.
- Morishita, Y., Sakube, Y., Sasaki, S., Ishibashi, K., 2004. Molecular mechanisms and drug development in aquaporin water channel diseases: aquaporin superfamily (superaquaporins): expansion of aquaporins restricted to multicellular organisms. *J. Pharmacol. Sci.* 96, 276–279.
- Murata, K., Mitsuoka, K., Hirai, T., Walz, T., Agre, P., Heymann, J.B., Engel, A., Fujiyoshi, Y., 2000. Structural determinants of water permeation through aquaporin-1. *Nature* 407, 599–605.
- Nagae, T., Miyake, S., Kosaki, S., Azuma, M., 2013. Identification and characterisation of functional aquaporin water channel (*Anomala cuprea* DRIP) in a coleopteran insect. *J. Exp. Biol.*
- Nozaki, K., Ishii, D., Ishibashi, K., 2008. Intracellular aquaporins: clues for intracellular water transport? *Pflugers Arch.* 456, 701–707.
- Patana, R., 1982. Disposable diet packet for feeding and oviposition of *Lygus hesperus* (Hemiptera: Miridae). *J. Econ. Entomol.* 75, 668–669.
- Phillip, B.N., Kiss, A.J., Lee Jr., R.E., 2011. The protective role of aquaporins in the freeze-tolerant insect *Eurosta solidaginis*: functional characterization and tissue abundance of EsAQP1. *J. Exp. Biol.* 214, 848–857.
- Rose, A., Lorenzen, S., Goede, A., Gruening, B., Hildebrand, P.W., 2009. RHYTHM—a server to predict the orientation of transmembrane helices in channels and membrane-coils. *Nucleic Acids Res.* 37, W575–W580.
- Saitou, N., Nei, M., 1986. Strategy for resolving the branching order of humans, chimpanzees and gorillas by using DNA-sequence data. *Am. J. Phys. Anthropol.* 69, 260.
- Saitou, N., Nei, M., 1987. The neighbor-joining method — a new method for reconstructing phylogenetic trees. *Mol. Biol. Evol.* 4, 406–425.
- Shackel, K.A., de la Paz Celorio-Mancera, M., Ahmadi, H., Greve, L.C., Teuber, L.R., Backus, E.A., Labavitch, J.M., 2005. Micro-injection of lygus salivary gland proteins to simulate feeding damage in alfalfa and cotton flowers. *Arch. Insect Biochem. Physiol.* 58, 69–83.
- Shakesby, A.J., Wallace, I.S., Isaacs, H.V., Pritchard, J., Roberts, D.M., Douglas, A.E., 2009. A water-specific aquaporin involved in aphid osmoregulation. *Insect Biochem. Mol. Biol.* 39, 1–10.
- Sneath, P.H.A., Sokal, R.R., 1973. *Numerical Taxonomy*. W.H. Freeman and Company, San Francisco, pp. 230–234.
- Spring, J.H., Robichaux, S.R., Hamlin, J.A., 2009. The role of aquaporins in excretion in insects. *J. Exp. Biol.* 212, 358–362.
- Strong, F.E., Kruitwagen, E.C., 1968. Polygalacturonase in the salivary apparatus of *Lygus hesperus* (Hemiptera). *J. Insect Physiol.* 14, 1113–1119.
- Sui, H., Han, B.G., Lee, J.K., Walian, P., Jap, B.K., 2001. Structural basis of water-specific transport through the AQP1 water channel. *Nature* 414, 872–878.
- Tamura, K., Peterson, D., Peterson, N., Stecher, G., Nei, M., Kumar, S., 2011. MEGA5: molecular evolutionary genetics analysis using maximum likelihood, evolutionary distance, and maximum parsimony method. *Mol. Biol. Evol.* 28, 2731–2739.
- Thomas, C.J., Brown, H.L., Hawes, C.R., Lee, B.Y., Min, M.K., King, L.A., Possee, R.D., 1998. Localization of a baculovirus-induced chitinase in the insect cell endoplasmic reticulum. *J. Virol.* 72, 10207–10212.
- Tusnady, G.E., Simon, I., 2001. The HMMTOP transmembrane topology prediction server. *Bioinformatics* 17, 849–850.
- Untergasser, A., Nijveen, H., Rao, X., Bisseling, T., Geurts, R., Leunissen, J.A.M., 2007. Primer3Plus, an enhanced web interface to primer3. *Nucleic Acids Res.* 35, W71–W74.
- Verkman, A.S., 2008. Mammalian aquaporins: diverse physiological roles and potential clinical significance. *Expert Rev. Mol. Med.* 10, e13.
- Wallace, I.S., Shakesby, A.J., Hwang, J.H., Choi, W.G., Martinkova, N., Douglas, A.E., Roberts, D.M., 2012. *Acyrtosiphon pisum* AQP2: a multifunctional insect aquaglyceroporin. *Biochim. Biophys. Acta* 1818, 627–635.
- Wheeler, A.G., 2001. *Biology of the Plant Bugs (Hemiptera: Miridae): Pests, Predators, Opportunists*. Cornell University Press, Ithaca, NY.
- Wigglesworth, V.B., 1965. *Respiration. The Principles of Insect Physiology*. Methuen Ltd, London, UK, pp. 317–368.
- Wigglesworth, V.B., Lee, W.M., 1982. The supply of oxygen to the flight muscles of insects: a theory of tracheole physiology. *Tissue Cell* 14, 501–518.
- Yanochko, G.M., Yool, A.J., 2002. Regulated cationic channel function in *Xenopus* oocytes expressing *Drosophila* big brain. *J. Neurosci.* 22, 2530–2540.
- Yool, A.J., 2007. Aquaporins: multiple roles in the central nervous system. *Neuroscientist* 13, 470–485.
- Yool, A.J., Weinstein, A.M., 2002. New roles for old holes: Ion channel function in aquaporin-1. *News Physiol. Sci.* 17, 68–72.
- Zardoya, R., 2005. Phylogeny and evolution of the major intrinsic protein family. *Biol. Cell.* 97, 397–414.
- Zhang, D., Tan, Y.-J., Qu, F., Sheng, J.-Z., Huang, H.-F., 2012. Functions of water channels in male and female reproductive systems. *Mol. Aspects Med.* 33, 676–690.
- Zuckerandl, E., Pauling, L., 1965. Evolutionary divergence and convergence in proteins. In: Bryson, V., Vogel, H.J. (Eds.), *Evolving Genes and Proteins*. Academic Press, New York, pp. 97–166.

RESEARCH

Open Access



Pharmacological blockade of aquaporin-1 water channel by AqB013 restricts migration and invasiveness of colon cancer cells and prevents endothelial tube formation *in vitro*

Hilary S. Dorward^{1,2}, Alice Du^{1,2}, Maressa A. Bruhn¹, Joseph Wrin¹, Jinxin V. Pei², Andreas Evdokiou³, Timothy J. Price^{4,5}, Andrea J. Yool² and Jennifer E. Hardingham^{1,2,6*}

Abstract

Background: Aquaporins (AQP) are water channel proteins that enable fluid fluxes across cell membranes, important for homeostasis of the tissue environment and for cell migration. AQP1 knockout mouse models of human cancers showed marked inhibition of tumor-induced angiogenesis, and in pre-clinical studies of colon adenocarcinomas, forced over-expression of AQP1 was shown to increase angiogenesis, invasion and metastasis. We have synthesized small molecule antagonists of AQP1. Our hypothesis is that inhibition of AQP1 will reduce migration and invasiveness of colon cancer cells, and the migration and tube-forming capacity of endothelial cells *in vitro*.

Methods: Expression of AQP1 in cell lines was assessed by quantitative (q) PCR, western blot and immunofluorescence, while expression of AQP1 in human colon tumour tissue was assessed by immunohistochemistry. The effect of varying concentrations of the AQP1 inhibitor AqB013 was tested on human colon cancer cell lines expressing high versus low levels of AQP1, using wound closure (migration) assays, matrigel invasion assays, and proliferation assays. The effect of AqB013 on angiogenesis was tested using an endothelial cell tube-formation assay.

Results: HT29 colon cancer cells with high AQP1 levels showed significant inhibition of migration compared to vehicle control of 27.9 % ± 2.6 % ($p < 0.0001$) and 41.2 % ± 2.7 % ($p < 0.0001$) treated with 160 or 320 μM AqB013 respectively, whereas there was no effect on migration of HCT-116 cells with low AQP1 expression. In an invasion assay, HT29 cells treated with 160 μM of AqB013, showed a 60.3 % ± 8.5 % decrease in invasion at 144 hours ($p < 0.0001$) and significantly decreased rate of invasion compared with the vehicle control (F-test, $p = 0.001$). Almost complete inhibition of endothelial tube formation (angiogenesis assay) was achieved at 80 μM AqB013 compared to vehicle control ($p < 0.0001$).

Conclusion: These data provide good evidence for further testing of the inhibitor as a therapeutic agent in colon cancer.

Keywords: Aquaporin 1, Inhibitor, Colon cancer, Migration, Invasion, Angiogenesis

* Correspondence: jennifer.hardingham@adelaide.edu.au

¹Molecular Oncology, Basil Hetzel Institute, The Queen Elizabeth Hospital, Woodville, SA, Australia

²Discipline of Physiology, School of Medicine, University of Adelaide, Adelaide, SA, Australia

Full list of author information is available at the end of the article



Background

Colorectal cancer (CRC) is the third most commonly diagnosed cancer and the third leading cause of death resulting from cancer in the USA [1]. In Australia it is the second most commonly reported cancer diagnosis after prostate cancer, and the second leading cause of death after lung cancer [2]. A major determinant of patient prognosis is the stage at which the cancer is diagnosed, as surgery is considered curative in up to 70 % of early stage cases. Screening programs have helped with early diagnosis and intervention, but for those not participating in such programs some 12-25 % of CRC patients still present with advanced (stage IV) disease [3]. Furthermore, up to 30 % of patients diagnosed with early localised CRC (stage I or II) and up to 50 % with regional spread to lymph nodes or adjacent organs (stage III) eventually relapse with overt metastatic disease following 'curative' surgery [4]. Adjuvant chemotherapy is offered to stage III patients to eradicate potentially existing micro-metastases but the indication for such treatment in stage II disease is less certain where the benefit shown in clinical trials is small in absolute terms and thus the risk of fluorouracil toxicity likely outweighs the benefit [5]. The dilemma is finding a balance between the benefit of therapy, which may be incremental, and risk of harm, and to that end discovery of new therapeutic targets and pharmacological agents is a continuing goal for improving adjuvant cancer therapy.

Aquaporins (AQP) and their role in cancer progression

Mammalian aquaporins are a family of 13 classes of intrinsic membrane proteins that assemble as tetramers (~30 kDa per subunit) and are known for their role in fluid homeostasis and trans-membrane transport of water and other small solutes [6, 7]. Specific classes of AQP channels have been implicated in enhanced migration, angiogenesis and metastasis in a variety of cancer types [8, 9], prompting the suggestion that inhibitors of AQP channels might provide new tools for cancer therapy [8]. The role of AQP1 in tumour migration and angiogenesis was first demonstrated in a murine melanoma tumour model: in AQP1 null mice tumours were smaller with fewer micro-vessels and more extensive necrosis as compared to AQP1 wild type mice, suggesting that AQP1 deletion impaired endothelial cell proliferation and angiogenesis [10]. AQP1 involvement in angiogenesis has been confirmed in other studies: in a murine melanoma tumour model, mice treated with AQP1 short interfering (si) RNA had significantly smaller tumours and lower microvessel and endothelial marker (factor VIII) densities compared to control mice, suggesting AQP1 knockdown impaired tumour growth and angiogenesis [11]. In mice with genetic deletion of AQP1, microvessel density was significantly reduced and also

the number of lung metastases (5 ± 1 /mouse) as compared with AQP1-expressing mice from the same genetic background (31 ± 8 /mouse, $P < 0.005$) [12]. Colon tumour cells over-expressing AQP1 exhibited increased migratory and invasive capacity in wound healing (migration) and transwell invasion assays [13]. Over-expression of AQP1 in tumour cell lines resulted not only in a predicted increase in cell membrane water permeability, but also a 2 to 3-fold accelerated migration rate of the AQP1-expressing tumour cells as compared to control cells *in vitro*. AQP1 over-expression in mice increased the extravasation of tumour cells injected via the tail vein compared to control mice, and increased by 3-fold the number of lung metastases [14].

It is through enhanced water flux mediated by the AQP channels that cells are believed to acquire an enhanced migratory and invasive phenotype [13, 15]. Interestingly, AQP1 has been shown by our group to have dual water channel and gated ion channel functions [16, 17]. The AQP blocker AqB013, a derivative of bumetanide, has been characterised as a dose-dependent inhibitor of osmotic water fluxes mediated by mammalian AQP1 and AQP4 channels analysed in the *Xenopus laevis* expression system. AqB013 was shown to inhibit the AQP1 water channel function when applied extracellularly, and is thought to cross the membrane to occlude the water channel pore from the cytoplasmic side of the AQP1 channel [18]. Work here is the first to test the efficacy of AqB013 in inhibiting migration, invasion and angiogenesis in colon cancer cell line models.

Methods

Cell lines and cell culture

HT29 and HCT-116 colon cancer cell lines (ATCC, Manassas, USA) were cultured in complete medium composed of DMEM (Life Technologies, Carlsbad, CA, USA) supplemented with 1 x glutaMAX™ (Life Technologies), 1 x penicillin-streptomycin solution (Life Technologies) and 10 % foetal bovine serum (FBS). Cultures were maintained in 5 % CO₂ at 37 °C. Their authenticity was confirmed (CellBank Australia, Melbourne, Vic). Human umbilical vein endothelial cells (HUVEC) (PromoCell, Heidelberg, Germany) were cultured in endothelial growth medium (PromoCell) according to the protocol supplied, and maintained in 5 % CO₂ at 37 °C. Cells were confirmed to be negative for mycoplasma using the Universal Mycoplasma Detection kit (ATCC) according to the manufacturer's protocol.

Colon tissue samples

Human colon tumour and matched normal mucosal tissue samples were obtained from 57 patients undergoing surgery for CRC at The Queen Elizabeth Hospital. The protocol was approved by The Queen Elizabeth Hospital

Ethics of Human Research Committee (approval no. 1993059) and informed consent was obtained in all cases.

Expression analysis of AQP1

Quantitative PCR

Cells at 70-80 % confluence were harvested and RNA extracted using the PureLink™ RNA Mini kit (Life Technologies). RNA was extracted from the frozen archived colon tumour and matched normal mucosa samples by pulverizing tissue under liquid nitrogen, and extracting RNA as before. RNA concentration was quantified using the NanoDrop 2000 spectrophotometer (Thermo Scientific, Waltham, MA, USA) and the integrity (RIN score) assessed using the 2100 Bioanalyzer (Agilent Technologies, Santa Clara, CA, USA). RNA (500 ng) was reverse transcribed using the iScript™ cDNA synthesis kit (Bio-rad, Carlsbad, CA, USA). qPCR of AQP1 and the reference gene phosphomannose mutase 1 (PMM1) [19] was performed using multiplex Taqman expression assays (Life Technologies), in triplicate via the CFX96™ Thermal Cycler (Bio-Rad). Each reaction contained 0.75 µL of each TaqMan® Gene Expression Assay (Life Technologies), 2 µL cDNA, 4.0 µL ultrapure water (Fisher Biotec, Wembley, WA, Australia) and 7.5 µL SsoFast™ probes supermix (Bio-rad) in a total volume of 15 µL. Results were calculated according to the $2^{-\Delta\Delta C_t}$ relative quantification method.

Western blot

Cells were lysed with RIPA buffer containing 1 % β-mercaptoethanol, 1 % HALT protease inhibitor 100X solution, 150 U Benzonase (all from Sigma, St Louis, MO, USA) on ice for 10 minutes, homogenized by passing through a 21 gauge needle and centrifuged at 14,000 x g for 15 minutes at 4 °C to pellet the cell debris. As AQP1 can be glycosylated [20], the supernatant was treated with PNGaseF (Promega, Madison, WI, USA) to cleave N-linked oligosaccharides. Protein was quantified (EZQ® assay, Life Technologies) and 50 µg of each sample was resolved by SDS-PAGE on a 12 % Mini-Protean® TGX Stain-Free™ Gels (Bio-Rad) and transferred to PVDF membranes using the Trans-Blot® Turbo™ Transfer Pack and System (Bio-Rad). Membranes were blocked with TBST containing 5 % skim milk for 1 hour and incubated overnight at 4 °C with anti-AQP1 rabbit polyclonal (H-55) (1/500; Santa Cruz Biotechnology Inc, Santa Cruz, CA, USA). Following three washes in TBST, membranes were incubated with goat anti-rabbit IgG HRP secondary antibody (1/2000) and Streptactin-HRP Conjugate (1/10000) (both from Bio-Rad) at room temperature for 1 hour, and washed. Chemiluminescence substrate was applied (Clarity™ Western ECL Blotting Substrate, Bio-Rad) and blots analysed using the

ChemiDoc™ Touch Imaging System (Bio-Rad). Image Lab™ Software (Bio-Rad) was used for relative quantification of bands, normalized to total protein loaded in each lane.

Immunofluorescence

Cells grown on coverslips at 80 % confluence were fixed with 4 % paraformaldehyde and permeabilized with 0.5 % triton X-100. Image-iT® FX Signal Enhancer (Life Technologies) was applied directly to cover slips in accordance with manufacturer's instructions. Cells were stained with a 1/400 dilution of rabbit polyclonal anti-human AQP1 (Abcam®, Cambridge, UK) and for the antibody isotype matched control, a 1/400 dilution of normal rabbit IgG was used (Cell Signaling Technology, Beverly, MA, USA). Cells were then stained with a 1/200 dilution of goat anti rabbit IgG H&L (Alexa Fluor® 568) secondary antibody (orange fluorescence) and the nuclei stained with NucBlue® Fixed Cell Ready Probes™ Reagent (blue fluorescence) (both from Life Technologies). Coverslips were mounted on slides with ProLong® Gold antifade reagent (Life Technologies), and images captured using the Zeiss LSM 700 microscope (Carl Zeiss Microscopy, Jena, Germany).

Immunohistochemistry

Tissue sections (5 µm) were deparaffinised by heating at 55-60 °C for 2 hours, soaking in xylene and hydrating by passing through a graded series of ethanol to water. Antigen retrieval was carried out by microwaving the slides in 10 mM sodium citrate for 20 mins. Endogenous peroxidase was quenched by incubating the slides in Peroxidized I reagent (Biocare Medical, Concord, CA, USA) for 5 min and background staining was blocked by incubation in Background Sniper reagent (Biocare Medical). Slides were stained using a 1:100 dilution of AQP1 monoclonal antibody 10C11 (Abcam, Cambridge, UK) and detected using the MACH 3™ mouse HRP polymer detection system according to the manufacturer's protocol (Biocare Medical). Slides were counterstained in haematoxylin (Sigma-Aldrich, St Louis, MO, USA).

AQP1 inhibitor and vehicle control

AqB013 was dissolved in dimethyl sulfoxide (DMSO) at a 100 mM (stock solution), which was diluted into complete medium to yield the indicated working concentrations for the experiments. DMSO was used as the vehicle control at a dilution equivalent to that in the highest dose of the drug used in the treatments.

Effect of AQP1 inhibition on cell migration (wound healing assay)

HT29 or HCT-116 cells were grown in complete medium (DMEM with 10 % FCS) to 80-90 % confluence

in triplicate wells of a 24-well untreated plastic tissue culture plate, serum starved overnight, then treated with 1 $\mu\text{g}/\text{mL}$ mitomycin C in complete medium to prevent cells from proliferating. Wells were treated with increasing amounts of the inhibitor with vehicle (DMSO) as control. A p10 pipette tip was used to scratch a wound through the cell monolayer and cells were monitored as they migrated across the wound using a Nikon Eclipse microscope (40X magnification) at time 0, 16, 32, 48, 64 and 80 hours: 20 measurements were taken of the wound width at each time point using the NIS-Elements software and averaged. Wound closure was calculated as a percentage relative to the initial wound width.

Spheroid basement membrane extract (BME) invasion assay

Cells were cultured into spheres in an ultra-low attachment plate according to the manufacturer's protocol (Cultrex[®] 3D 96 Well Spheroid BME Cell Invasion Assay, Trevigen[™]), then covered with Invasion Matrix (a proprietary extracellular matrix blend comprised of basement membrane extract, derived from murine EHS sarcoma cells and collagen) together with the inhibitor AqB013 from 0 (untreated) to 160 μM , and with vehicle control. The area of the sphere was measured at each time point to assess invasion into the surrounding matrix, using the NIS-Elements software. The change in sphere area was calculated as a percentage relative to the initial sphere size; percent invasion of the test sphere was subtracted from the percent invasion of the vehicle control to indicate the extent of invasion into the matrix.

Cell proliferation assay

HT29, HCT-116 or HUVEC were grown overnight, then AqB013 was added to triplicate wells from 0 (untreated) up to 320 μM . DMSO was added to triplicate wells as vehicle control. Proliferation was quantified after 48 hours using the Cell Titer 96[®] Aqueous Non-Radioactive cell Proliferation Assay (Promega) and absorbance at 490 nm read on a FLUOstar OPTIMA 96 well microplate reader (BMG Lab Tech, Ortenberg, Germany).

Angiogenesis assay

Human umbilical vein endothelial cells (HUVECs) were seeded at 1×10^4 cells per well in a 96 well plate pre-coated with BME (basement membrane extract: reconstituted protein matrix comprised of laminin, collagen IV, entactin, and heparin sulphate proteoglycan) and incubated in endothelial growth medium (PromoCell, Heidelberg, Germany) containing VEGF according to the Cultrex *In Vitro* Angiogenesis Assay Kit protocol (Trevigen, Gaithersburg, MD, USA). Wells were treated in triplicate with AqB013 from 0 (untreated) to 80 μM

and with vehicle as a control. Cells were stained with Calcein AM dye at 24 hrs and imaged using a Nikon Eclipse fluorescence microscope. Endothelial tube formation was quantified as the number of junctions formed.

Statistical analysis

Statistical analysis was carried out in Graph Pad[®] prism 5. A one-way ANOVA with Tukey's multiple comparisons test was carried out for qRT-PCR results, for proliferation assays and for the angiogenesis assays. For the migration and invasion assays, a two-way ANOVA was performed to determine the significance between the data points of the final time point, also a first order polynomial regression was fitted to the data sets and an F-test used to determine significance ($p < 0.05$). Statistical significance was accepted at $p < 0.05$.

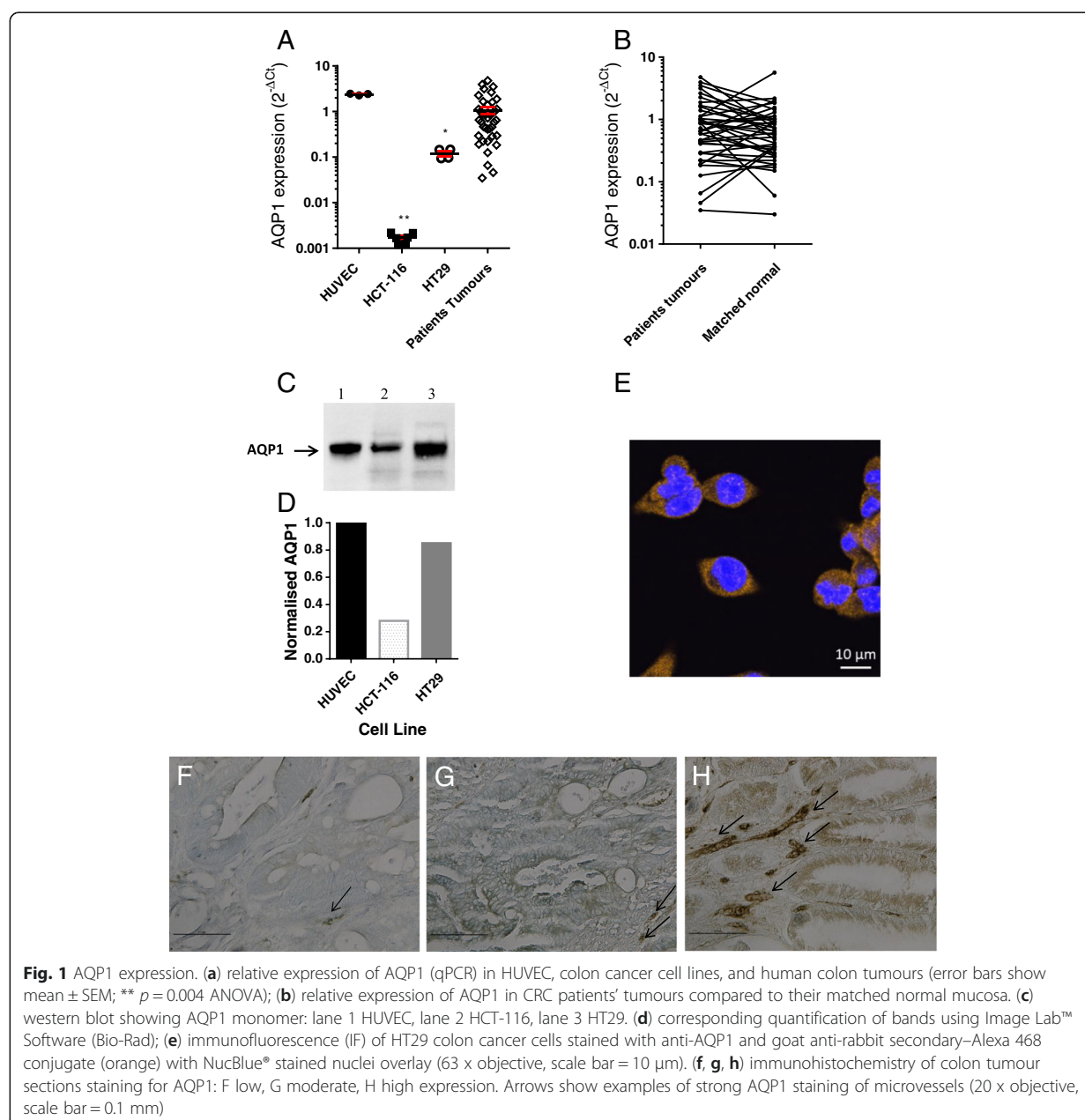
Results

Expression of AQP1

Of the cell lines, the human umbilical vein endothelial cells (HUVEC) showed the highest expression of AQP1, HT29 showed a moderate level of expression, while HCT-116 showed a low level of expression. The range of expression levels was similar to that found in patients' tumour samples (Fig. 1a). Using the $2^{-\Delta\Delta\text{Ct}}$ relative quantification method, AQP1 was over-expressed (by >1.6-fold) in 22/57 (39 %) colon tumours compared to matched normal mucosa (Fig. 1b). Western blot (Fig. 1c) shows bands at approximately 28 KDa and relative quantification confirmed that AQP1 expression in HCT-116 cells was reduced by 67 % compared to HT29 cells, and by 72 % compared to HUVEC (Fig. 1d). Immunofluorescence staining showed both cytoplasmic and membrane AQP1 expression in HT29 cells (Fig. 1e). Immunohistochemistry of colon tumour sections showed that AQP1 is expressed variably in the apical membrane and in the cytoplasm. The range in staining for AQP1 concurs with the range of expression levels in tumour tissue at the mRNA level (Fig. 1a). In malignant crypt epithelial cells the expression of AQP1 varies from low intensity 1+ (Fig. 1f), moderate intensity 2+ (Fig. 1g) and high intensity 3+ (Fig. 1h): Endothelial cells of the micro-vessels show high staining intensity (arrows in Fig. 1 f–h) and reflects the high expression of AQP1 in endothelial cells at the mRNA level (HUVEC Fig. 1a).

Treatment with AqB013 slows migration of colon cancer cells expressing significant amounts of AQP1

At the final time-point HT29 cells treated with 160 μM or 320 μM AqB013 had a significantly reduced wound closure compared to vehicle control of 27.9 % \pm 2.6 % ($p < 0.0001$) and 41.2 % \pm 2.7 % ($p < 0.0001$) respectively (2-way ANOVA with Bonferroni post hoc test) (Fig. 2a).



The dose response curve showed that the IC₅₀ was 132.7 μ M, Hill Slope -2.8. Treatment of HCT-116 cells (low level of AQP1 expression) with AqB013 showed no significant effect on migration (Fig. 2b).

Treatment with AqB013 reduces invasion of colon cancer cells

The area of the spheres was measured as the cells invaded the surrounding matrix. For HT29 spheres treated with 80 μ M or 160 μ M of AqB013, there was a 59.5 % \pm 1.4 % ($p = 0.0003$) or 60.3 % \pm 8.5 % ($p <$

0.0001) decrease in invasion respectively at 144 hours compared to the vehicle control (Fig. 2c). A reduced rate of invasion was also found compared to the vehicle control (F-test, $p = 0.001$). The IC₅₀ was 55.6 μ M, Hill Slope -5.17. Treatment of HCT-116 with AqB013 showed no significant effect on spheroid invasion (Fig. 2d). There was no appreciable cytotoxic effect as there was no effect on proliferation of HCT-116 at concentrations of AqB013 up to 320 μ M, although there was a small decrease in proliferation of HT29 treated at 160 μ M AqB013 (Fig. 2e).

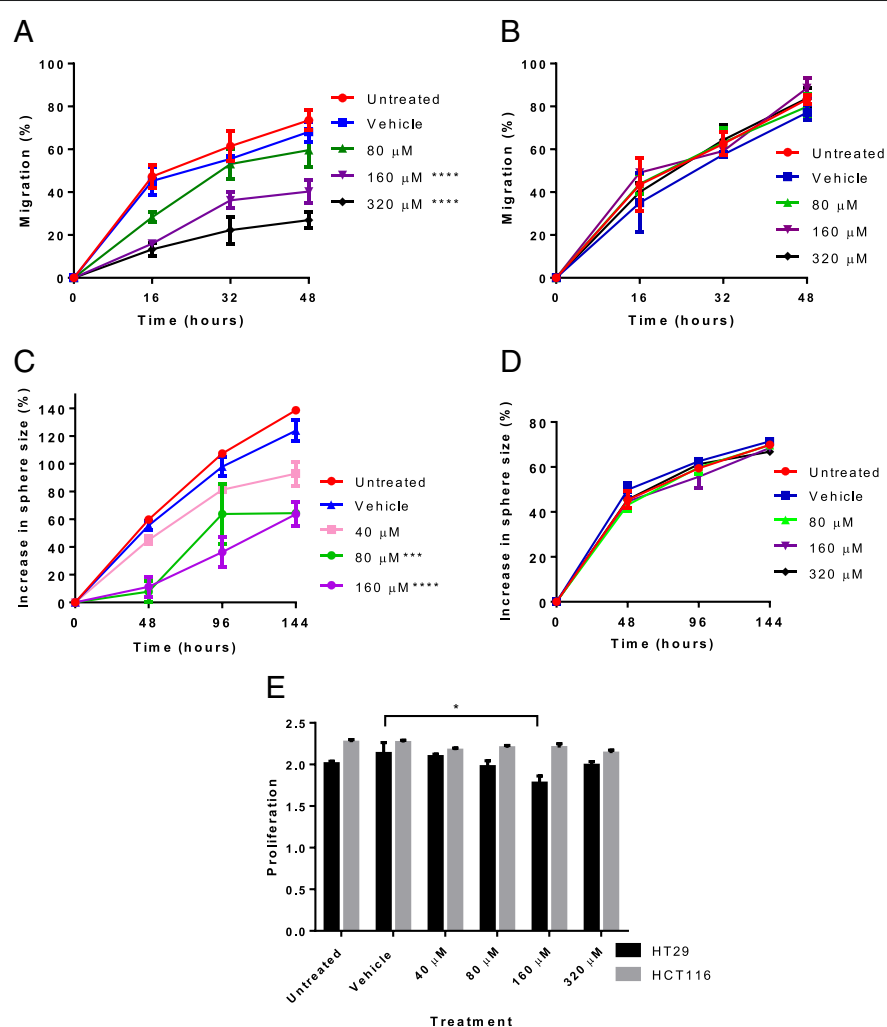


Fig. 2 Migration and invasion. **a**, HT29 cells treated with 160 μ M or 320 μ M AqB013 had a significantly reduced migration compared to vehicle control. **b**, HCT-116 cells treated with up to 320 μ M AqB013 showed no significant effect on wound closure. **c**, the effect of AqB013 on HT29 cell invasion ($n = 3$) measured by an increase in sphere size (%) relative to vehicle control: in spheres treated with 80 μ M or 160 μ M of AqB013 there was a significant decrease in invasion at 144 hours compared with vehicle. **d**, HCT-116 cells treated with up to 320 μ M AqB013 ($n = 3$) showed no significant effect on invasion. ** $p = 0.004$; *** $p < 0.001$ **** $p < 0.0001$. **e**, AqB013 treatment up to 320 μ M had no effect on cell proliferation of HCT-116, at 160 μ M AqB013 HT29 showed 17% reduced proliferation (* $p = 0.03$ ANOVA). Proliferation measured in absorbance units at 490 nm. The error bars show standard error of the mean

Treatment of endothelial cells with AqB013 markedly inhibits tube formation

Compared to vehicle control, treatment of HUVECs with 40 μ M AqB013, showed a 43 % reduction in the number of junctions formed (34.0 ± 3.0 , $p < 0.01$) while treatment with 80 μ M AqB013 resulted in a reduction of 89.5 % (6.3 ± 2.4 , $p < 0.0001$) (Fig. 3a–d). As expected there was no significant difference in the number of junctions formed between untreated and vehicle treated HUVECs (64.3 ± 3.0 versus 60 ± 2.5 respectively) (Fig. 3e). There was no effect on viability or proliferation of HUVEC treated at up to 80 μ M AqB013 (Fig. 3f).

Discussion

Small molecule pharmaceuticals have an established therapeutic use and our team has synthesised an AQP inhibitor, based on bumetanide [21], that blocks AQP1-mediated water flux [18]. Bumetanide is a loop diuretic that has long been used to treat patients with oedema [22]. Furthermore the incidence of clinically significant side-effects of bumetanide therapy is very low compared to that associated with chemotherapy drugs currently given as adjuvant therapy for CRC, making it an attractive alternative to current chemotherapeutics. AQP1 has been implicated in tumour progression in murine

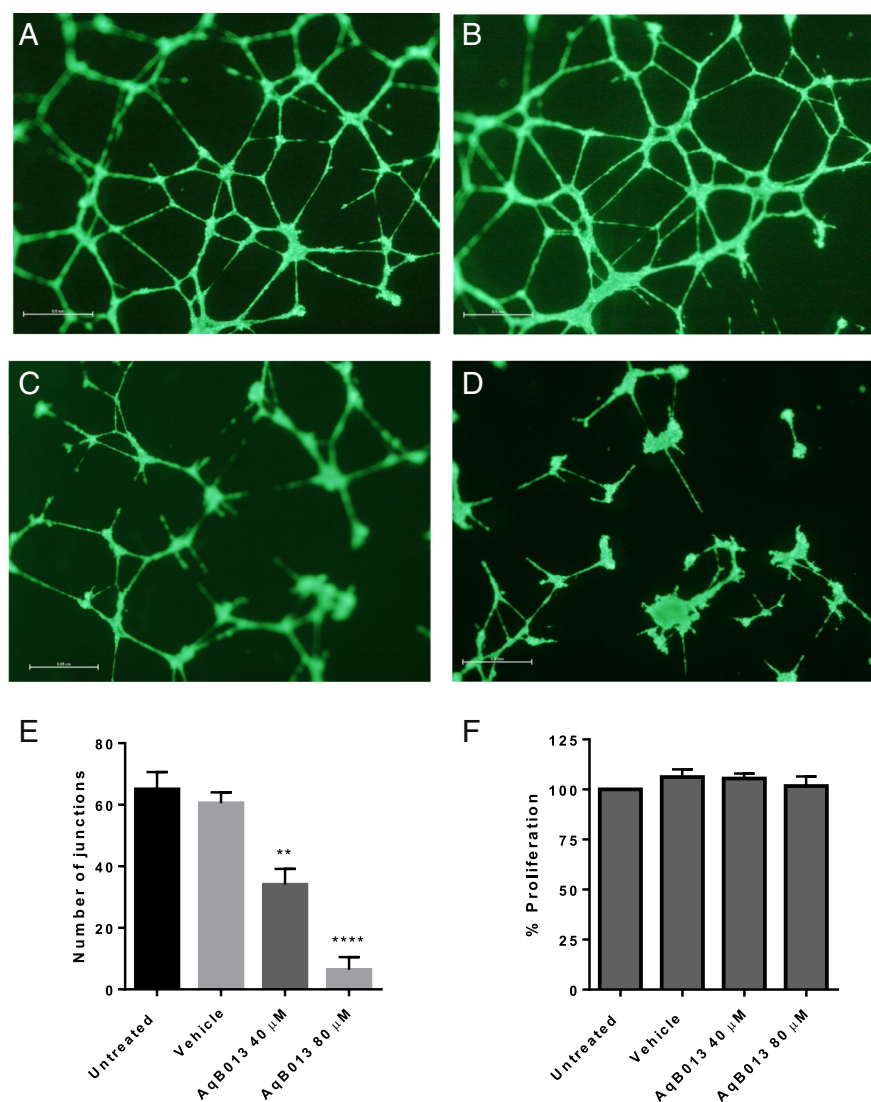


Fig. 3 Angiogenesis assay. HUVEC tube-forming assay measured by the number of junctions: **a**, untreated HUVEC; **b**, vehicle treated HUVEC; **c**, HUVEC treated with 40 μM AqB013; **d**, HUVEC treated with 80 μM AqB013 (40 x magnification, scale bar = 0.5 mm); **e**, graph shows significant inhibition of endothelial tube formation by AqB013 at 40 μM and 80 μM, ** $p < 0.01$, **** $p < 0.0001$ respectively (ANOVA). **f**, AqB013 treatment had no effect on proliferation of HUVECs

models and may thus serve as a potential target for small molecule inhibitors to treat cancer in subgroups expressing AQP1. The *in vitro* testing of drugs is the first step in establishing the efficacy of targeting specific molecules in abrogating the migration and invasion of cancer cells, or in suppressing angiogenesis.

In this study, inhibition of AQP1 by the inhibitor AqB013 was effective in reducing migration (wound closure assay) and invasion (spheroid formation assay) in the high AQP1-expressing HT29 cells, while not affecting migration or invasion in HCT-116 cells that had much lower expression of AQP1. As both untreated and

vehicle-treated HT29 and HCT-116 cells showed similar efficiency of wound closure and invasion, these results suggest that AQP1 was indeed the target of inhibition. In breast cancer cells, AQP5 polarizes to the leading edge of migrating MDA-MB-231 cells, and that knock-down of AQP5 in these cells significantly suppressed cell migration velocity in narrow channels [23]. Similarly, knockdown of AQP5 in MCF7 breast cancer cells resulted in significantly reduced proliferation and migration [24]. However we have shown that the expression of AQP5 in HCT-116 is low (Additional file 1), similar to that of AQP1, suggesting that in these cells an

alternative mechanism of migration is used which would explain why these cells are resistant to the inhibitory effect of AqB013. Migration in HCT-116 cells that express low amounts of AQP1 and AQP5 may be enhanced by expression of the calcium activated chloride channel TMEM16A as it has recently been reported that the high metastatic-potential colon cancer cell lines HCT-116 and SW620 express TMEM16A while primary colon cancer cell lines HCT8 and SW480 cells do not. Knock-down of TMEM16A by short hairpin RNA in SW620 resulted in significantly reduced migration in wound-closure assays [25]. In addition HCT-116 cells have been shown to have high levels of micro RNA 224 which has recently been shown to activate the Wnt- β catenin pathway to promote migration and invasion of HCT-116 cells [26, 27], rendering the cells resistant to the effects of AQP inhibition.

AQP1 has been shown to have dual water channel and gated ion channel functions [16, 28, 29]. The AQP1-mediated cationic conductance has been implicated in influencing rates of net fluid transport in primary cultures of choroid plexus [30], and similarly this mechanism may be responsible for regulating net fluid flux in migrating epithelial and endothelial cells. However work by the Yool group has previously shown that endogenous chloride conductance in *X. laevis* oocytes is not blocked by AqB013. Furthermore in mouse intact gastric antral muscle, the addition of AqB013 did not change the resting membrane potential and had no substantial effect on the rhythmic electrical conduction properties [18]. Taken together these data suggest that the effect of AqB013 on impeding the migration of human colon cancer cells and endothelial cells expressing AQP1 is mediated by blocking the water channel activity of AQP1.

Conclusions

These studies have shown clear links between AQP1 activity and cancer cell migration and invasion, and endothelial cell tube-forming capacity, indicating the importance of characterising suitable AQP1 blockers. This study provides preliminary data showing that the AQP1 inhibitor AqB013 abrogates endothelial tube formation and reduces cancer cell migration and invasion and will be further investigated in an *in vivo* mouse xenotransplant model of human colon cancer. Small molecule pharmaceuticals have an established therapeutic use and as this new drug is a modification of bumetanide, it should be well-tolerated in cancer patients with far fewer side-effects than from currently used chemotherapeutic drugs. Furthermore, in view of the documented role of AQP1 in murine tumour angiogenesis [10, 12], it is envisaged that in metastatic CRC patients, AQP1 inhibitors may have a role combined with anti-

vascular endothelial growth factor (VEGF) therapy, or as an alternative anti-angiogenesis therapy in cases that become resistant to anti-VEGF therapy. The inhibition of AQP1 clinically may slow down the progression of CRC, increasing the window for optimal treatment resulting in better survival outcomes, particularly in early stage cases where micro-metastatic disease is present.

Additional file

Additional file 1: Expression of AQP1 and AQP5. qPCR ($2^{-\Delta C_t}$) results normalised to reference gene PMM1. (PDF 95 kb)

Competing interests

The authors declare that they have no competing interests.

Authors' contributions

JH, AY, AE, TP made substantial contributions to conception and design of the study and to interpretation of data; HD, JH made substantial contributions to acquisition and analysis of data and co-wrote the manuscript. HD, AD carried out the angiogenesis assays; HD, MB and JP carried out the migration assays; HD carried out the invasion and proliferation assays, JW performed the immunohistochemistry. All authors reviewed and approved the manuscript.

Author details

¹Molecular Oncology, Basil Hetzel Institute, The Queen Elizabeth Hospital, Woodville, SA, Australia. ²Discipline of Physiology, School of Medicine, University of Adelaide, Adelaide, SA, Australia. ³Disciplines of Surgery and Orthopedics, School of Medicine, University of Adelaide, Adelaide, SA, Australia. ⁴Medical Oncology, The Queen Elizabeth Hospital, Woodville, SA, Australia. ⁵School of Medicine, University of Adelaide, Adelaide, SA, Australia. ⁶Level 1, Basil Hetzel Institute, The Queen Elizabeth Hospital, 28 Woodville Road, Woodville, SA 5011, Australia.

Received: 28 September 2015 Accepted: 18 February 2016

Published online: 24 February 2016

References

1. Siegel R, DeSantis C, Jemal A. Colorectal cancer statistics, 2014. *CA: Cancer J Clin*. 2014;64(2):104–17.
2. AIHW: Cancer in Australia: an overview 2014. Cancer series no. 90. Cat. no. CAN 88. Canberra AIHW; 2014.
3. Cole SR, Tucker GR, Osborne JM, Byrne SE, Bampton PA, Fraser RJ, Young GP. Shift to earlier stage at diagnosis as a consequence of the National Bowel Cancer Screening Program. *Med J Aust*. 2013;198(6):327–30.
4. Young PE, Womeldorph CM, Johnson EK, Maykel JA, Brucher B, Stojadinovic A, Avital I, Nissan A, Steele SR. Early Detection of Colorectal Cancer Recurrence in Patients Undergoing Surgery with Curative Intent: Current Status and Challenges. *J Cancer*. 2014;5(4):262–71.
5. Gray R, Barnwell J, McConkey C, Hills RK, Williams NS, Kerr DJ. Adjuvant chemotherapy versus observation in patients with colorectal cancer: a randomised study. *Lancet*. 2007;370(9604):2020–9.
6. Agre P, King LS, Yasui M, Guggino WB, Ottersen OP, Fujiyoshi Y, Engel A, Nielsen S. Aquaporin water channels—from atomic structure to clinical medicine. *J Physiol*. 2002;542(Pt 1):3–16.
7. Hachez C, Chaumont F. Aquaporins: a family of highly regulated multifunctional channels. *Adv Exp Med Biol*. 2010;679:1–17.
8. Verkman AS. Aquaporins. *Curr Biol*. 2013;23(2):R52–5.
9. Ribatti D, Ranieri G, Annese T, Nico B. Aquaporins in cancer. *Biochim Biophys Acta*. 2014;1840(5):1550–3.
10. Saadoun S, Papadopoulos MC, Hara-Chikuma M, Verkman A. Impairment of angiogenesis and cell migration by targeted aquaporin-1 gene disruption. *Nature*. 2005;434:786–92.
11. Nicchia G, Stigliano C, Sparaneo A, Rossi A, Frigeri A, Svelto M. Inhibition of aquaporin-1 dependent angiogenesis impairs tumour growth in a mouse model of melanoma. *J Mol Med*. 2013;91(5):613–23.

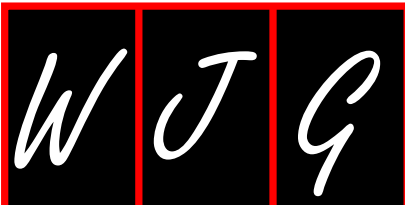
12. Esteva-Font C, Jin B-J, Verkman AS. Aquaporin-1 gene deletion reduces breast tumor growth and lung metastasis in tumor-producing MMTV-PyVT mice. *FASEB J*. 2014;28(3):1446–53.
13. Jiang Y. Aquaporin-1 activity of plasma membrane affects HT20 colon cancer cell migration. *IUBMB Life*. 2009;61(10):1001–9.
14. Hu J, Verkman AS. Increased migration and metastatic potential of tumor cells expressing aquaporin water channels. *FASEB J*. 2006;20(11):1892–4.
15. Papadopoulos MC, Saadoun S, Verkman AS. Aquaporins and cell migration. *Eur J Physiol*. 2008;456(4):693–700.
16. Anthony TL, Brooks HL, Boassa D, Leonov S, Yanochko GM, Regan JW, Yool AJ. Cloned human aquaporin-1 is a cyclic GMP-gated ion channel. *Mol Pharmacol*. 2000;57(3):576–88.
17. Yu J, Yool AJ, Schulten K, Tajkhorshid E. Mechanism of gating and ion conductivity of a possible tetrameric pore in aquaporin-1. *Structure*. 2006;14(9):1411–23.
18. Migliati E, Meurice N, DuBois P, Fang JS, Somasekharan S, Beckett E, Flynn G, Yool AJ. Inhibition of Aquaporin-1 and Aquaporin-4 Water Permeability by a Derivative of the Loop Diuretic Bumetanide Acting at an Internal Pore-occluding Binding Site. *Mol Pharmacol*. 2009;76(1):105–12.
19. Rubie C, Kempf K, Hans J, Su T, Tilton B, Georg T, Brittner B, Ludwig B, Schilling M. Housekeeping gene variability in normal and cancerous colorectal, pancreatic, esophageal, gastric and hepatic tissues. *Mol Cell Probes*. 2005;19(2):101–9.
20. Smith BL, Preston GM, Spring FA, Anstee DJ, Agre P. Human red cell aquaporin CHIP. I. Molecular characterization of ABH and Colton blood group antigens. *J Clin Invest*. 1994;94(3):1043–9.
21. GA Flynn, AJ Yool, ER Migliati, LS Ritter. Aquaporin modulators and methods of using them for the treatment of edema and fluid imbalance. US Patent 7,906,555, 2011.
22. Hutcheon DE, Martinez JC. A Decade of Developments in Diuretic Drug Therapy. *J Clin Pharmacol*. 1986;26(8):567–79.
23. Stroka Kimberly M, Jiang H, Chen S-H, Tong Z, Wirtz D, Sun Sean X, Konstantopoulos K. Water Permeation Drives Tumor Cell Migration in Confined Microenvironments. *Cell*. 2014;157(3):611–23.
24. Jung HJ, Park J-Y, Jeon H-S, Kwon T-H. Aquaporin-5: A Marker Protein for Proliferation and Migration of Human Breast Cancer Cells. *PLoS ONE*. 2011;6(12), e28492.
25. Sui Y, Sun M, Wu F, Yang L, Di W, Zhang G, Zhong L, Ma Z, Zheng J, Fang X et al. Inhibition of TMEM16A Expression Suppresses Growth and Invasion in Human Colorectal Cancer Cells. *PLoS ONE*. 2014;9(12), e115443.
26. Amankwatia EB, Chakravarty P, Carey FA, Weidlich S, Steele RJC, Munro AJ, Wolf CR, Smith G. MicroRNA-224 is associated with colorectal cancer progression and response to 5-fluorouracil-based chemotherapy by KRAS-dependent and -independent mechanisms. *Br J Cancer*. 2015;112(9):1480–90.
27. Li T, Lai Q, Wang S, Cai J, Xiao Z, Deng D, He L, Jiao H, Ye Y, Liang L et al. MicroRNA-224 sustains Wnt/ β -catenin signaling and promotes aggressive phenotype of colorectal cancer. *J Exp Clin Oncol*. 2016;35(1):1–11.
28. Yool AJ. Functional domains of aquaporin-1: keys to physiology, and targets for drug discovery. *Curr Pharm Des*. 2007;13(31):3212–21.
29. Yool AJ, Campbell EM. Structure, function and translational relevance of aquaporin dual water and ion channels. *Mol Aspects Med*. 2012;33(5-6):553–61.
30. Boassa D, Stamer WD, Yool AJ. Ion channel function of aquaporin-1 natively expressed in choroid plexus. *J Neurosci*. 2006;26(30):7811–9.

Submit your next manuscript to BioMed Central
and we will help you at every step:

- We accept pre-submission inquiries
- Our selector tool helps you to find the most relevant journal
- We provide round the clock customer support
- Convenient online submission
- Thorough peer review
- Inclusion in PubMed and all major indexing services
- Maximum visibility for your research

Submit your manuscript at
www.biomedcentral.com/submit





Basic Study

Rhubarb extract partially improves mucosal integrity in chemotherapy-induced intestinal mucositis

Juliana E Bajic, Georgina L Eden, Lorraine S Lampton, Ker Y Cheah, Kerry A Lymn, Jinxin V Pei, Andrea J Yool, Gordon S Howarth

Juliana E Bajic, Jinxin V Pei, Andrea J Yool, Gordon S Howarth, Discipline of Physiology, Faculty of Health Sciences, School of Medicine, The University of Adelaide, Adelaide 5005, Australia

Georgina L Eden, Lorraine S Lampton, Kerry A Lymn, School of Animal and Veterinary Sciences, The University of Adelaide, Roseworthy Campus 5371, Australia

Ker Y Cheah, Gastroenterology Department, Women's and Children's Hospital, North Adelaide 5006, Australia

Kerry A Lymn, 2nd Gastroenterology Department, Women's and Children's Hospital, North Adelaide 5006, Australia

Gordon S Howarth, 2nd School of Animal and Veterinary Sciences, The University of Adelaide, Roseworthy Campus 5371, Australia

Gordon S Howarth, 3rd Gastroenterology Department, Women's and Children's Hospital, North Adelaide 5006, Australia

Gordon S Howarth, 4th Women's and Children's Health Research Institute, Women's and Children's Hospital, North Adelaide 5006, Australia

Author contributions: Eden GL and Lampton LS contributed equally to this work; Yool AJ and Howarth GS designed the research; Bajic JE, Eden GL, Lampton LS, Cheah KY and Lymn KA performed the research; Pei JV and Yool AJ contributed *ex vivo* tools; Eden GL, Lampton LS and Howarth GS analysed the data; Bajic JE, Eden GL and Howarth GS wrote the paper.

Institutional review board statement: This collaborative project was a joint venture between The University of Adelaide, Flinders University, UniSA and the Cancer Council SA. The University of Adelaide is licensed under the Act to acquire and use animals only when approval has been granted by its Animal Ethics Committee (AEC). No animal may be held or used for any purpose until written approval has been obtained from the AEC. The use of animals for teaching, research or experimentation is regulated by State legislation - the South Australian *Animal*

Welfare Act 1985. Internal approval for this study was obtained from the AEC (approval number: S-2010-111).

Institutional animal care and use committee statement: All animal experimentation was approved by the AEC of the University of Adelaide (approval number: S-2010-111) and complied with the National Health and Medical Research Council Code of Practice for Animal Care in Research and Teaching.

Conflict-of-interest statement: The authors wish to acknowledge no conflict of interest.

Data sharing statement: There are no additional data available in relation to this manuscript.

Open-Access: This article is an open-access article which was selected by an in-house editor and fully peer-reviewed by external reviewers. It is distributed in accordance with the Creative Commons Attribution Non Commercial (CC BY-NC 4.0) license, which permits others to distribute, remix, adapt, build upon this work non-commercially, and license their derivative works on different terms, provided the original work is properly cited and the use is non-commercial. See: <http://creativecommons.org/licenses/by-nc/4.0/>

Manuscript source: Invited manuscript

Correspondence to: Juliana E Bajic, BHSc (Hons), Discipline of Physiology, Faculty of Health Sciences, School of Medicine, The University of Adelaide, Frome Road, Adelaide 5005, Australia. juliana.bajic@adelaide.edu.au
Telephone: +61-8- 83137591
Fax: +61-8-83133788

Received: April 11, 2016
Peer-review started: April 13, 2016
First decision: June 20, 2016
Revised: July 7, 2016
Accepted: August 8, 2016
Article in press: August 8, 2016
Published online: October 7, 2016

Abstract

AIM

To investigate the effects of orally gavaged aqueous rhubarb extract (RE) on 5-fluorouracil (5-FU)-induced intestinal mucositis in rats.

METHODS

Female Dark Agouti rats ($n = 8/\text{group}$) were gavaged daily (1 mL) with water, high-dose RE (HDR; 200 mg/kg) or low-dose RE (LDR; 20mg/kg) for eight days. Intestinal mucositis was induced (day 5) with 5-FU (150 mg/kg) *via* intraperitoneal injection. Intestinal tissue samples were collected for myeloperoxidase (MPO) activity and histological examination. *Xenopus* oocytes expressing aquaporin 4 water channels were prepared to examine the effect of aqueous RE on cell volume, indicating a potential mechanism responsible for modulating net fluid absorption and secretion in the gastrointestinal tract. Statistical significance was assumed at $P < 0.05$ by one-way ANOVA.

RESULTS

Bodyweight was significantly reduced in rats administered 5-FU compared to healthy controls ($P < 0.01$). Rats administered 5-FU significantly increased intestinal MPO levels ($\geq 307\%$; $P < 0.001$), compared to healthy controls. However, LDR attenuated this effect in 5-FU treated rats, significantly decreasing ileal MPO activity (by 45%; $P < 0.05$), as compared to 5-FU controls. 5-FU significantly reduced intestinal mucosal thickness (by $\geq 29\%$ $P < 0.001$) as compared to healthy controls. LDR significantly increased ileal mucosal thickness in 5-FU treated rats (19%; $P < 0.05$) relative to 5-FU controls. In *xenopus* oocytes expressing AQP4 water channels, RE selectively blocked water influx into the cell, induced by a decrease in external osmotic pressure. As water efflux was unaltered by the presence of extracellular RE, the directional flow of water across the epithelial barrier, in the presence of extracellular RE, indicated that RE may alleviate water loss across the epithelial barrier and promote intestinal health in chemotherapy-induced intestinal mucositis.

CONCLUSION

In summary, low dose RE improves selected parameters of mucosal integrity and reduces ileal inflammation, manifesting from 5-FU-induced intestinal mucositis.

Key words: Fluorouracil; Inflammation; Mucositis; Rats; Rheum

© **The Author(s) 2016.** Published by Baishideng Publishing Group Inc. All rights reserved.

Core tip: Aqueous rhubarb extract partially improved selected parameters of 5-fluorouracil (5-FU)-induced intestinal mucositis in rats. Exposure to 5-FU decreased bodyweight, yet high-dose rhubarb extract (RE) and low-dose RE (LDR) showed no changes. Myeloperoxidase activity was significantly decreased in rats treated with

LDR and 5-FU when compared to the intestinal mucositis control group. Ileal mucosal thickness was significantly improved (19%) in animals with intestinal mucositis and treated with LDR. In *xenopus* oocytes expressing AQP4 water channels, RE blocked swelling induced by a decrease in external osmotic pressure which indicated that water influx across the epithelial barrier was selectively blocked by RE.

Bajic JE, Eden GL, Lampton LS, Cheah KY, Lynn KA, Pei JV, Yool AJ, Howarth GS. Rhubarb extract partially improves mucosal integrity in chemotherapy-induced intestinal mucositis. *World J Gastroenterol* 2016; 22(37): 8322-8333 Available from: URL: <http://www.wjgnet.com/1007-9327/full/v22/i37/8322.htm> DOI: <http://dx.doi.org/10.3748/wjg.v22.i37.8322>

INTRODUCTION

Traditional herbal medicines have been used for centuries in the maintenance and improvement of health or the treatment of illnesses. Globally, ancient herbal remedies have been created based on theories, beliefs and experiences representing various cultures at different times throughout history^[1]. Consequently, traditional herbal medicines are being investigated increasingly for their potential to treat and reduce the symptoms of a wide variety of diseases and disorders, specifically cancer and its treatment-related side-effects. Many cancer patients seek alternative medicines that will complement their standard-care treatments with the hope that they will improve symptoms associated with either the cancer or their anti-cancer treatments^[2].

Cancer is a life-threatening illness affecting millions of individuals world-wide. In westernized countries approximately 50% of the population will develop cancer before the age of 85^[3]. Chemotherapy forms one of the most common strategies for cancer treatment. Cytotoxic chemotherapy drugs, such as 5-fluorouracil (5-FU), act by inhibiting DNA synthesis of not only malignant cells, but also rapidly dividing cells lining the intestinal mucosa^[4]. An increase in cell apoptosis stimulates the production of reactive oxygen species (ROS) and pro-inflammatory cytokines such as tumour necrosis factor- α (TNF- α), interleukin-1 β (IL-1 β) and IL-4 resulting in further tissue and blood vessel damage^[5,6]. This cascade of events results in a range of debilitating clinical side-effects, from nausea and vomiting to inflammation and ulceration of the gastrointestinal tract; and sepsis may occur if untreated^[7,8]. These painful and life-threatening side-effects collectively form a disorder known as intestinal mucositis which affects approximately 60% of patients undergoing chemotherapy^[9]. Current therapies for intestinal mucositis seek to reduce the severity of symptoms rather than acting as a curative

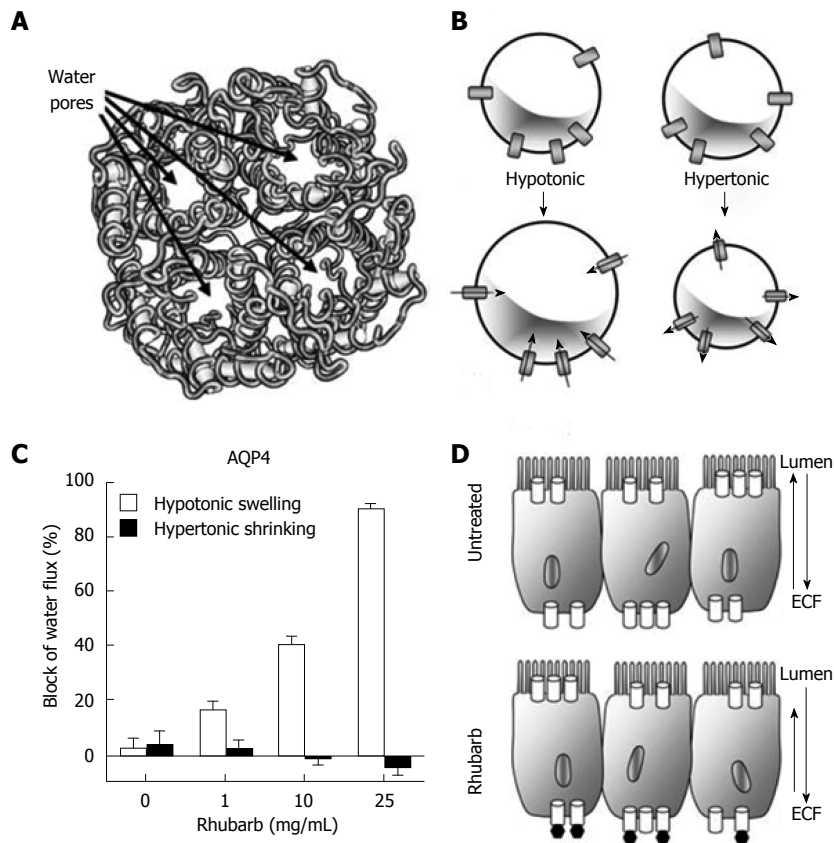


Figure 1 Directional blockade of water flux through an aquaporin-4 channel by reconstituted aqueous rhubarb extract. A: Diagram of a water channel illustrating the intra-subunit water pores in each subunit of the tetramer; B: Illustration of the volume changes induced by osmotic gradients in mammalian AQP4-expressing *Xenopus* oocytes; C: Dose-dependent blockade of swelling but not shrinking responses by rhubarb extract (RE) in AQP4-expressing oocytes; D: Diagram of the hypothesized effect of blockade by extracellular RE at AQP4 channels present in the basolateral side of intestinal barrier epithelial cells, predicted to result in enhanced net fluid absorption.

or preventative measure^[10,11]. Thus, treatments are required with the potential to eliminate or reduce the adverse side-effects of cancer chemotherapy.

Recently, in experimental systems, plant extracts such as grape seed extract (GSE) and Iberogast[®] have been investigated as potential treatments for intestinal mucositis on the basis of their anti-inflammatory and antioxidant constituents^[12-14]. Indeed, plant-sourced molecules and compounds are commonly perceived to be safer therapeutics compared to synthetic compounds^[15]. There are limited studies on the pharmacology of herbal medicines, yet such extracts may offer protection against intestinal mucositis in an experimental setting. The scientific study of further plant-based extracts is therefore warranted.

Rhubarb, *Rheum spp.*, is a herbaceous perennial plant with a long, fleshy stalk, commonly used for cooking and medicine. Dried rhubarb rhizomes were traditionally used in Chinese medicine as a natural remedy for gastrointestinal complications including diarrhoea, constipation and inflammation^[16]. The pharmacological effects have been attributed to the stalk of the plant^[17,18]. Two main active constituents (ethanol-soluble and water soluble) have been

classified in rhubarb stalks. Anthraquinones form the main ethanol-soluble active constituent of rhubarb stalks^[14]. These constituents have exhibited a diarrhoeal effect in mice providing a possible purgative mechanism of action^[18]. In contrast, the aqueous extract of rhubarb has recently demonstrated anti-diarrhoeal properties, believed to be mediated by tannins through regulation of intestinal water secretion and absorption^[18]. Importantly, chemotherapy recipients experiencing intestinal mucositis have altered membrane integrity and impaired water absorption and secretion^[7,19].

Aquaporins (AQPs) are integral membrane proteins responsible for the regulation of water transport across a membrane *via* an osmotic gradient^[20,21]. Aquaporin channels are tetramers with a water pore located in each subunit of the channel (Figure 1A). Water molecules move in single file through aquaporin pores, down osmotic and hydrostatic gradients. As one molecule enters *via* the extracellular region of the channel, another molecule is displaced into the cytoplasm and vice versa^[22]. Currently, 13 mammalian AQPs have been identified (AQP 0-12). AQPs are abundant in tissues reliant on high water permeability

to maintain correct function^[21,23] and are involved in metabolic processes such as kidney, lung, brain and gastrointestinal function^[24-26]. In the human gastrointestinal tract, AQPs 3, 7 and 8 are expressed throughout the mucosal epithelia, and AQP1 is present in endothelial cells of the vasculature. In early stage inflammatory bowel disease, tight junctions and transport systems are impaired, leading to a leaky epithelium. Clinical human biopsies showed that levels of expression of AQPs1 and 3 are reduced in Crohn's Disease and AQPs 7 and 8 are decreased in ulcerative colitis, based on quantitative PCR and immunolabelling assays^[27]. As well, the typical apical localisation of AQP8 in bowel was lost, and the appearance of a faint basolateral signal suggested intestinal epithelial cell polarity was disrupted.

Aquaporin-4 (AQP 4) is believed to provide the principal mechanism for bidirectional water transport across the basolateral membrane of small intestinal enterocytes^[28]. These water channels ensure that efficient water absorption and secretion is maintained, thus allowing for adequate hydration and optimal stool consistency^[29]. Liu *et al.*^[17] demonstrated that the anti-diarrhoeal effect of rhubarb tannins extract occurred *via* the inhibition of AQP 2 and 3 expression *in vitro* and in a mouse model of magnesium sulphate-induced diarrhoea. In addition, the water-soluble polysaccharides of rhubarb have protected the gastrointestinal tract against inflammation resulting from 2,4,6-trinitrobenzene sulfonic acid-induced colitis^[17]. The anti-inflammatory mechanism of action underlying rhubarb extract (RE) remains unclear; however, it is thought that tannins may reduce the production of pro-inflammatory cytokines such as IL-4 and IFN- γ ^[17]. Consequently, RE was explored for its anti-inflammatory potential in intestinal mucositis and its potential to influence water transport across the intestinal mucosa^[17,18].

In the current study, an aqueous fraction of rhubarb was investigated for its potential to reduce intestinal damage induced by the antimetabolite chemotherapy drug, 5-FU in rats. It was hypothesised that RE would decrease the severity of intestinal mucositis by improving histopathological parameters and potentially regulate faecal output *via* water secretion into the intestinal lumen.

MATERIALS AND METHODS

RE preparation

Rhubarb stems (2.5 kg) were sectioned (1 cm) and boiled with absolute ethanol to remove alcohol-soluble components. Once cooled, the liquid was discarded and the residues were further boiled with water. The aqueous rhubarb components were retained for dehydration to obtain a concentrated powder^[17]. Dehydration was conducted by freeze-drying at the South Australian Research and Development Institute, West Beach, South Australia. Four grams of powder

were obtained for every 500 g of fresh rhubarb. Based on fractionation of the extract, the active agent appears to be a water-soluble ethanol-insoluble glycopeptide. Lectin array profiling has indicated that mannose and N-acetylglucosamine are predominant components of the carbohydrate structure. The precise chemical structure and possible presence of more than one isoform with biological activity remains to be determined.

Animal trial, metabolism data and disease Activity index

Six week old female Dark Agouti rats ($n = 32$; 110-150 g) were sourced from the Animal Resources Centre (Western Australia) and Laboratory Animal Services (The University of Adelaide, South Australia). All animal experimentation was approved by the Animal Ethics Committee of the University of Adelaide (S-2010-111). The animal protocol described in this study was designed to minimise pain or discomfort to the animals and complied with the National Health and Medical Research Council Code of Practice for Animal Care in Research and Teaching. Prior to the experimentation period, rats were individually housed in Tecniplast™ (PA, United States) metabolism cages for 48 hours to acclimatise. Rats received *ad libitum* water and 18% Casein diet^[30] and were exposed to a 12 h light-dark cycle in a temperature controlled room (22 °C). After the acclimatisation phase, rats were randomly allocated to four treatment groups ($n = 8$ /group): Water + Saline, Water + 5-FU, Low-Dose Rhubarb (LDR; 20 mg/kg BW) + 5-FU and High-Dose Rhubarb (HDR; 200 mg/kg BW) + 5-FU. Water, HDR and LDR (1 mL) were administered daily *via* orogastric gavage on days 0 to 7. LDR dose for gavage was based on the estimated dose required to block aquaporin water channel activity in the oocyte expression system, and the dose HDR was selected as a 10 fold higher concentration for comparison.

Daily recordings of body weight, feed and water intake and faecal and urine output were conducted. Faecal pellets were collected daily, weighed and placed in a drying oven at 70 °C for 72 h. The percentage weight loss was used as an indication of moisture content in the faecal samples. On day 5, rats were injected with 5-FU (150 mg/kg BW; Hospira Australia Pty Ltd, Melbourne, Victoria) to induce intestinal mucositis. The single high dose of 5-FU used in the current study was determined from previous studies in our laboratory^[31]. Following 5-FU administration, daily disease activity index (DAI) scoring was performed by a blinded researcher based on overall condition, weight loss and stool consistency. Each parameter was scored based on a scale of 0 (normal) to 3 (maximal severity) giving a maximum daily total of 9 for severely affected rats^[32,33].

Blood, organ and tissue collection

Rats were humanely euthanized on day 8 *via* carbon dioxide asphyxiation. Day 8 of the experimental period

represented 3 d post 5-FU exposure and due to the acute nature of 5-FU-induced intestinal mucositis, this was determined to be the optimal day when histological damage in the intestine was most evident. The gastrointestinal tract was removed and emptied, then the lengths of each section [duodenum, jejunum, jejunum-ileum junction (JI), ileum and colon] were recorded and weighed.

Segments (2 cm and 4 cm) of the small intestine tract were collected at approximately 10% (jejunum) and 90% (ileum) of the total small intestine length for histological and biochemical analysis, respectively. Samples for histological analysis were fixed in 10% buffered formalin for 24 h and transferred to 70% ethanol for preservation. Segments for biochemical analysis were weighed and snap-frozen in liquid nitrogen prior to storage at -80°C . The remaining thoracic and abdominal organs (thymus, lungs, heart, spleen, kidneys, liver, stomach and caecum) were weighed and discarded.

Biochemical analysis

Myeloperoxidase (MPO) is an enzyme present in the intracellular granules of neutrophils and provides a quantitative analysis of acute inflammation. The assay was performed with slight modification from Beyer *et al.*^[34]. Segments of the small intestinal tract (jejunum, JI and ileum; 4 cm) were thawed and prepared for MPO assay *via* homogenization in 10 mmol/L phosphate buffer (pH 6.1). Homogenised samples were centrifuged at 13000 rpm for 12 min and the supernatant was discarded. The remaining pellet was resuspended with 0.5% hexadecyltrimethyl ammonium bromide buffer and vortexed prior to a final centrifuge (13000 rpm for 2 min). Supernatant from each sample (50 μL aliquot) was dispensed into a 96-well plate and the MPO reaction was initiated with an *O*-dianisidine dihydrochloride solution (200 μL /well; 4.2 mg *O*-dianisidine dihydrochloride, 12.5 μL hydrogen peroxide (30%) in 2.5 mL potassium phosphate buffer (50 mmol/L, pH 6.1) and 22.5 mL distilled H_2O). A spectrometer (Victor X4 Multilabel Reader, Perkin Elmer, Singapore) measured absorbance (450 nm) at one minute intervals over a 15 min period. The change in absorbance was used to calculate MPO activity within a tissue sample (MPO units/g of intestinal tissue).

Histological analysis

Intestinal samples stored in 70% ethanol were embedded with paraffin wax and cross-sectioned at 4 μm . Histological slides were stained with haematoxylin and eosin for qualitative and quantitative analysis. Qualitative measurements of 40 villus and crypts per intestinal section (jejunum, JI and ileum) were performed blinded using Image ProPlus software for Windows (version 5.1.1; Media Cybernetics, Silver Spring MD, United States) connected to a Nikon

Eclipse 50i light microscope (Nikon Cooperation, Japan) and a ProGres C5 digital camera (Jenoptik, Germany). Intestinal sections were also analysed quantitatively using disease severity scores based on 11 criteria described by Howarth *et al.*^[32]. Each criterion was scored on a scale of 0 (normal) to 3 (severely damaged) for five cross-sections of each intestinal region. The median score for each criterion was calculated and the scores of all criteria were summed to give an overall disease severity score; with a score of 33 indicating maximal tissue damage^[32,33].

Xenopus oocyte preparation

Unfertilized oocytes from *Xenopus laevis* were prepared as described previously^[35,36] and maintained in ND96 saline (96 mmol/L NaCl, 2 mmol/L KCl, 1 mmol/L MgCl_2 , 1.8 mmol/L CaCl_2 , and 5 mmol/L HEPES, pH 7.55) supplemented with 100 $\mu\text{g}/\text{mL}$ penicillin, 100 U/mL streptomycin, and 10% horse serum. Oocytes were injected with 50 nL of water containing 1 ng of rat AQP4 wild-type cRNA and were incubated for 2 or more days at $16\text{--}18^{\circ}\text{C}$ prior to osmotic swelling and shrinking assays in saline without antibiotics or serum. Hypotonic saline (50%) was prepared by diluting isotonic saline with an equal volume of water, whilst 200% hypertonic saline was prepared by doubling the NaCl concentration of the saline. Volume change rates were measured by videomicroscopy at 0.5 frames/s over 30 s using NIH ImageJ software (<http://rsbweb.nih.gov/ij/>), as described previously^[35,36].

Statistical analysis

Statistical analyses were conducted using IBM SPSS Statistics version 19 for Windows (SPSS Inc., Chicago, IL, United States) and GraphPad Prism 6.02 for Windows (GraphPad Software Inc., San Diego, CA, United States). Normality tests were performed on all data sets to determine parametric and non-parametric data. All parametric data (metabolic data, MPO activity and villus height/crypt depth measurements) was analysed using one-way ANOVA with Tukey *post hoc* test. Non-parametric data (DSS and DAI) was analysed using Kruskal-Wallis with Mann Whitney *U post hoc* test. All data were expressed as mean \pm SEM with the exception of disease severity scores which were expressed as medians and range. Values of $P < 0.05$ were considered significant.

RESULTS

Dose-dependent blockade of AQP4 water channel activity by extracellular aqueous RE

Cloned rat AQP 4 water channels expressed in *Xenopus* oocytes were analysed quantitatively for osmotically-driven changes in cell volume in the presence and absence of dried reconstituted aqueous RE. Decreased external osmotic pressure (50% hypotonic saline) induced a volume increase (swelling) that was blocked

Table 1 Total daily food (g) and water (mL) intake, and faecal (g) and urine (mL) output for the trial period prior to the administration of 5-FU (days 1 to 5)

	Water	LDR	HDR
Food intake (g)	51.0 ± 0.7	52.3 ± 2.0	53.8 ± 1.0
Water Intake (mL)	122.5 ± 7.3	129.4 ± 12.0	115.0 ± 7.1
Wet faecal output (g)	6.2 ± 0.3	6.8 ± 0.3	6.6 ± 0.4
Urine output (mL)	79.3 ± 5.6	79.8 ± 6.1	85.8 ± 5.0

Rats were gavaged daily with water, LDR or HDR (1 mL); data expressed as mean (g or mL) ± SEM. LDR: Low-dose RE; HDR: High-dose RE; RE: Rhubarb extract.

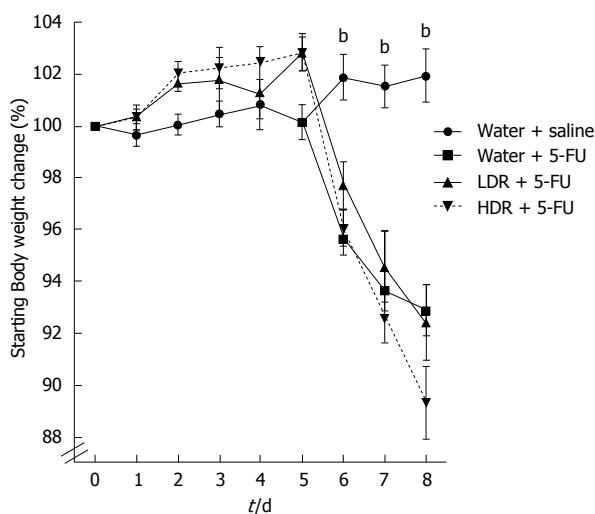


Figure 2 Daily change in starting bodyweight (%) from days 0 to 8 in rats gavaged with water, LDR or HDR and intraperitoneally injected with saline or 5-FU on Day 5. Data are expressed as mean ± SEM. Mean values of 5-FU controls and 5-FU + LDR and 5-FU + HDR were significantly different when vs water + saline controls; ^b*P* < 0.01. LDR: Low-dose RE; HDR: High-dose RE; RE: Rhubarb extract.

by RE (Figure 1B and C). In contrast, the volume decrease (shrinking) induced by 200% hypertonic saline was not significantly altered by RE (Figure 1B and C), indicating that the blocking effect of RE was directional. In the presence of extracellular RE, water influx into the cell mediated by AQP4 was selectively blocked, whereas water efflux was not altered, providing a potentially useful tool for differentially modulating net fluid absorption and secretion in the gastrointestinal tract. The current *ex vivo* study predicted that RE would act on basolateral AQP 4 channels and alleviate water loss across the barrier epithelium (Figure 1D), thereby promoting intestinal health in the experimental setting of chemotherapy-induced intestinal mucositis.

Metabolic data and faecal moisture content

Low dose rhubarb (LDR) and high dose rhubarb (HDR) had no significant effect on metabolic parameters (bodyweight, feed and water intake and faecal and urine output) when compared to controls

Table 2 Total daily food (g) and water (mL) intake, and faecal (g) and urine (mL) output for the trial period after the administration of 5-FU (days 6 to 8)

	Water + saline	Water + 5-FU	LDR + 5-FU	HDR + 5-FU
Food intake (g)	29.1 ± 0.6	11.5 ± 1.6 ^e	7.8 ± 0.6	5.2 ± 1.4 ^d
Water intake (mL)	75.0 ± 4.3	94.4 ± 7.7	107.2 ± 5.1	90.6 ± 12.9
Wet faecal output (g)	3.3 ± 0.2	2.9 ± 0.3	2.1 ± 0.3	1.7 ± 0.3 ^c
Urine output (mL)	47.5 ± 4.7	64.5 ± 6.7	71.0 ± 2.1	70.6 ± 10.4

Rats were gavaged daily with water, LDR or HDR (1 mL) and received an intraperitoneal injection of either saline or 5-FU on day 5. ^c*P* < 0.05, ^d*P* < 0.01 vs water + 5-FU; ^e*P* < 0.001 vs water + saline. All values are expressed as mean [% relative to bodyweight ($\times 10^3$)] ± SEM. LDR: Low-dose RE; HDR: High-dose RE; RE: Rhubarb extract.

prior to administration of 5-FU (Table 1). After 5-FU administration, feed intake was significantly decreased (by 60%; *P* < 0.001) in comparison to healthy controls (Table 2). Furthermore, in 5-FU treated rats administered HDR, feed intake was further reduced by 55% when compared to 5-FU controls (*P* < 0.01). However, normal feed intake was maintained in 5-FU treated rats administered LDR. Although feed intake was significantly reduced in 5-FU controls, there was no reduction in wet faecal output compared to healthy controls. However, in 5-FU treated rats administered HDR, faecal output was reduced by 41% in comparison to 5-FU controls. There were no significant effects on water intake and urine output between control and RE treatment groups (Table 2). Similarly, no significant effects on faecal moisture content were evident among all treatment groups, before or after 5-FU administration (data not shown).

Bodyweight change

A reduction in feed intake was consistent with decreased bodyweight after 5-FU administration (Figure 2). Prior to inducing intestinal mucositis with 5-FU, RE had no significant effect on bodyweight. Treatment with 5-FU resulted in a significant reduction in bodyweight compared to normal controls (*P* < 0.01). However, compared to 5-FU controls, HDR and LDR had no effect on mean bodyweight following 5-FU administration.

DAI score

Administration of 5-FU significantly increased DAI scores in comparison to healthy controls (*P* < 0.01; Figure 3). Days 6 and 8 produced significantly greater DAI scores in 5-FU treated rats administered HDR and LDR, respectively, compared to 5-FU controls; otherwise, RE treatments had no significant effect on symptomatic disease activity.

Visceral gastrointestinal organ weights and lengths

Visceral and gastrointestinal organ weights were expressed as a proportion of bodyweight (Tables 3 and 4). Reductions in relative thymus (by $\geq 35\%$; *P* < 0.001) and relative spleen weight (by $\geq 23\%$; *P*

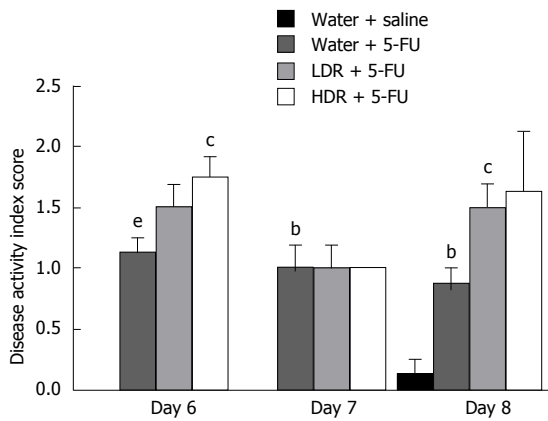


Figure 3 Effects of rhubarb extract and 5-fluorouracil on disease activity scores on days 6 to 8 of the experimental period. Rats received a daily water, HDR or LDR gavage for an 8-d trial period and an intraperitoneal injection of 5-FU or saline on day 5. Disease activity scores were assigned on Days 6 to 8 based on overall condition, weight loss, stool consistency and rectal bleeding. ^b*P* < 0.01, ^a*P* < 0.001 vs water + saline; ^c*P* < 0.05 vs water + 5-FU. LDR: Low-dose RE; HDR: High-dose RE; RE: Rhubarb extract.

Table 3 Visceral organ weights of rats gavaged daily with water, low-dose or high-dose rhubarb extract (1 mL) during an 8-d trial period and administered with an intraperitoneal injection of saline or 5-fluorouracil on day 5

	Water + saline	Water + 5-FU	LDR + 5-FU	HDR + 5-FU
Thymus	14.6 ± 1.3	6.6 ± 0.5 ^e	9.4 ± 0.6	9.5 ± 0.9
Heart	37.5 ± 0.8	39.0 ± 1.0	39.4 ± 0.8	39.1 ± 0.7
Lung	60.0 ± 2.2	63.0 ± 2.5	67.3 ± 4.7	71.9 ± 3.0
Liver	362.9 ± 6.5	362.7 ± 11.0	358.8 ± 7.2	339.7 ± 7.2
Spleen	20.3 ± 0.5	15.6 ± 0.3 ^e	15.2 ± 0.4	14.6 ± 0.5
Kidneys	75.6 ± 5.3	86.5 ± 1.7	88.7 ± 1.1	89.4 ± 2.7
Caecum	39.7 ± 1.1	43.7 ± 2.4	49.2 ± 2.5	47.0 ± 2.1
Stomach	57.3 ± 2.6	55.3 ± 1.1	58.8 ± 0.9	61.9 ± 1.2

^e*P* < 0.001 vs water + saline. All values expressed as mean [% relative to bodyweight ($\times 10^3$)] ± SEM. LDR: Low-dose RE; HDR: High-dose RE; RE: Rhubarb extract.

< 0.001) were apparent in all rats treated with 5-FU when compared to healthy controls (Table 3). In 5-FU treated rats, HDR and LDR had no significant effect on visceral organ weights compared to 5-FU controls.

A significant decrease in the combined jejunum and ileum relative weight (by $\geq 10\%$; *P* < 0.01) was evident in all 5-FU treated rats (Table 4). However, this effect was not present in the duodenum. There was also no effect of HDR or LDR on relative duodenum weight and the combined relative weights of jejunum and ileum in 5-FU treated rats, compared to 5-FU controls. Administration of 5-FU had no effect on relative colon weight in comparison to healthy controls. However, when compared to 5-FU controls, administration of LDR to 5-FU treated rats significantly increased colon weight (29%; *P* < 0.01). Additionally, 5-FU significantly reduced the combined jejunum and ileum length in comparison to healthy controls (Table 5). However,

Table 4 Gastrointestinal organ weights of rats gavaged daily with water, low-dose and high-dose rhubarb extract (1 mL) during an 8-d trial period and administered an intraperitoneal injection of saline or 5-fluorouracil on day 5

	Water + saline	Water + 5-FU	LDR + 5-FU	HDR + 5-FU
Duodenum	0.2 ± 0.0	0.2 ± 0.0	0.2 ± 0.0	0.2 ± 0.0
Jejunum and ileum	2.1 ± 0.1	1.9 ± 0.0 ^b	1.9 ± 0.2	1.9 ± 0.1
Colon	0.5 ± 0.0	0.5 ± 0.0	0.7 ± 0.0 ^d	0.6 ± 0.0

^b*P* < 0.01 vs water + saline; ^d*P* < 0.01 vs water + 5-FU. All values are expressed as mean (% relative to bodyweight) ± SEM. LDR: Low-dose RE; HDR: High-dose RE; RE: Rhubarb extract.

Table 5 Gastrointestinal organ lengths of rats gavaged daily with water, low-dose and high-dose rhubarb extract (1 mL) during an 8-d trial period and administered an intraperitoneal injection of saline or 5-fluorouracil on day 5

	Water + saline	Water + 5-FU	LDR + 5-FU	HDR + 5-FU
Duodenum	5.5 ± 0.2	4.8 ± 0.1	5.1 ± 0.2	4.8 ± 0.2
Jejunum and ileum	71.6 ± 2.3	64.8 ± 0.9 ^a	62.9 ± 1.8	63.5 ± 1.7
Colon	11.1 ± 0.3	10.6 ± 0.4	11.2 ± 0.2	10.8 ± 0.4

^a*P* < 0.05 vs water + saline. All values expressed as mean (cm) ± SEM. LDR: Low-dose RE; HDR: High-dose RE; RE: Rhubarb extract.

this effect was not evident in the duodenum and colon. The administration of HDR and LDR to 5-FU treated rats had no effect on gastrointestinal organ lengths in comparison to 5-FU controls.

Disease severity score

Healthy small intestinal sections achieved median disease severity scores of ≤ 2 . Administration of 5-FU caused significant damage to intestinal structure in the jejunum, JI and ileum; achieving median (range) scores of 21 (18-30), 21 (14-27) and 22 (17-25), respectively, when assessed by semi-quantitative histological scores based on 11 parameters (Figure 4). However, RE had no significant effect on intestinal structure, relative to 5-FU controls.

MPO activity

Increased intestinal MPO activity is a common feature of chemotherapy-induced intestinal mucositis^[31]. When compared to healthy controls, 5-FU resulted in increased MPO activity by 780% in the jejunum and 310% in the JI and ileum (Figure 5). RE had no significant effect on MPO activity within the jejunum and the JI in 5-FU treated rats. However, administration of LDR to 5-FU treated rats resulted in reduced MPO activity by 45% (*P* < 0.05) in the ileum, compared to 5-FU controls.

Villus height, crypt depth and mucosal thickness

The combined measurements of villus height and crypt depth provided an overall indication of mucosal

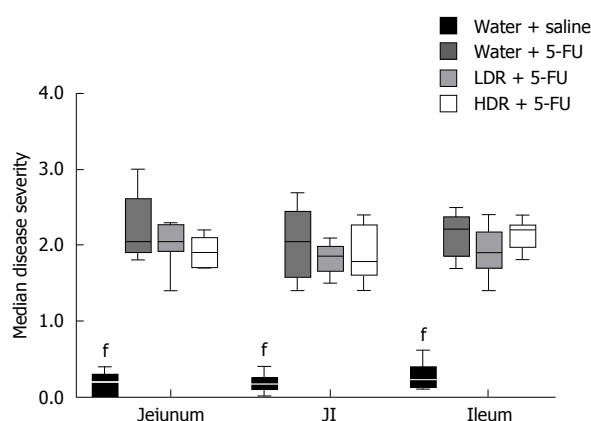


Figure 4 Histological damage assessed by semi-quantitative disease severity score of the jejunum, jejunum-ileum and ileum of rats. Data are expressed as median score (range). Mean values were significantly different vs water + 5-FU ($P < 0.001$). JI: Jejunum-ileum; LDR: Low-dose RE; HDR: High-dose RE; RE: Rhubarb extract.

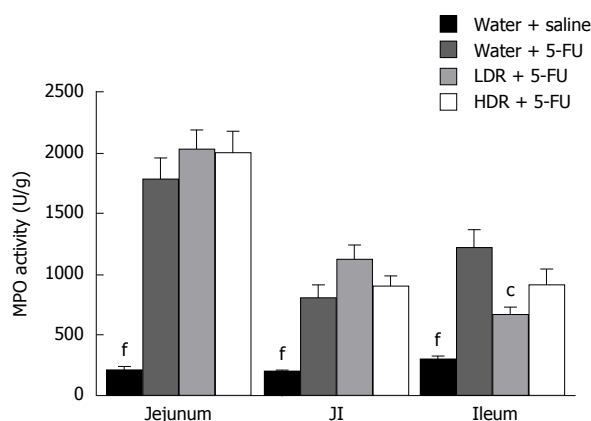


Figure 5 Myeloperoxidase activity present in the jejunum, jejunum-ileum and ileum of rats gavaged with water, low-dose or high-dose rhubarb extract (1 mL) for an 8-d trial period. Rats received an intraperitoneal injection of saline or 5-FU on day 5. Data were expressed as mean [MPO Units (U/g)] \pm SEM. Mean values were significantly different ($P < 0.001$) vs water + 5-FU. $^aP < 0.05$ vs water + 5-FU. JI: Jejunum-ileum; LDR: Low-dose RE; HDR: high-dose RE; RE: Rhubarb extract.

thickness and thus, damage (Figure 6). Administration of 5-FU significantly decreased mucosal thickness by 29% in the jejunum, and 34% in both the JI and ileum when compared to healthy controls. RE had no significant effect on villus height and crypt depth in the jejunum, compared to 5-FU controls. This effect was mirrored in the JI, with the exception of crypt depth which was significantly greater ($P < 0.05$) in 5-FU treated rats receiving HDR. More importantly, administration of LDR to 5-FU treated rats resulted in significantly greater ileal villus heights and crypt depths relative to 5-FU controls; significantly increasing overall ileal mucosal thickness by 19% (Figure 7).

DISCUSSION

Intestinal mucositis remains a debilitating side-

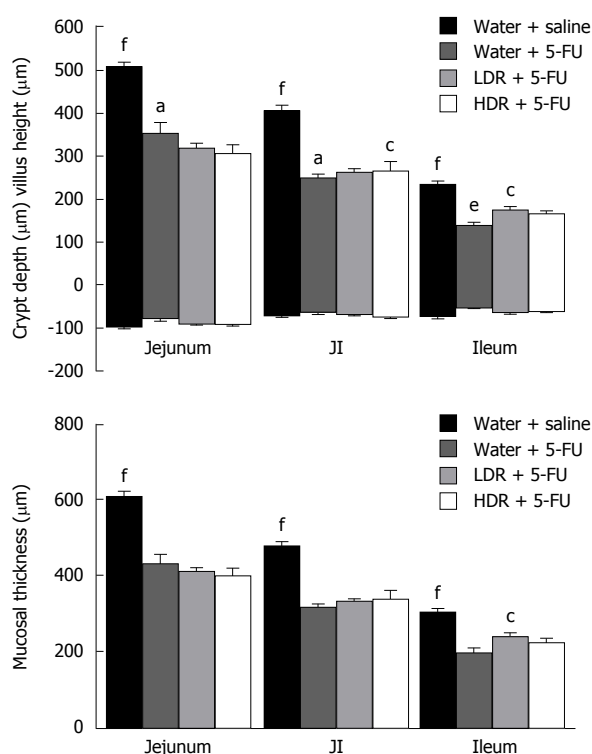


Figure 6 Combination of villus height and crypt depth as a representation of overall mucosal thickness in female Dark Agouti rats. Effects of RE and 5-FU on villus height and crypt depth in female Dark Agouti rats. Rats received a daily water, HDR or LDR gavage for an 8-d trial period and an intraperitoneal injection of 5-FU or saline on Day 5. Mean values were significantly different vs water + 5-FU ($^cP < 0.05$, $^fP < 0.001$). $^aP < 0.05$, $^eP < 0.001$ vs water + saline. JI: Jejunum-ileum; LDR: Low-dose RE; HDR: High-dose RE; RE: Rhubarb extract.

effect of chemotherapy treatment. The current study utilised a rat model of intestinal mucositis to investigate the potential for aqueous RE to protect against damage to the intestinal mucosa and regulate water transport in the intestine. The water-soluble components of rhubarb appeared to target more distal regions of the alimentary tract, partially improving selected parameters of the ileum, such as mucosal thickness and MPO activity associated with the clinical manifestations of 5-FU-induced intestinal mucositis.

Administration of 5-FU significantly decreased feed intake and bodyweight as previously described^[12,31,37]. A reduction in feed intake and bodyweight is observed in cancer patients due to nausea and pain associated with chemotherapy treatment^[38,39]. Interestingly, in the current study, daily administration of HDR to 5-FU treated rats further reduced appetite but maintained bodyweight. It is therefore plausible that the caloric index of HDR may have been contributing to the reduced appetite, yet maintenance of bodyweight in the rats receiving high dose RE.

In the current study, intraperitoneal administration of 5-FU caused significant damage to small intestinal structure, further impacting on intestinal weight and length. Previous studies of experimental intestinal mucositis have noted a correlation between small

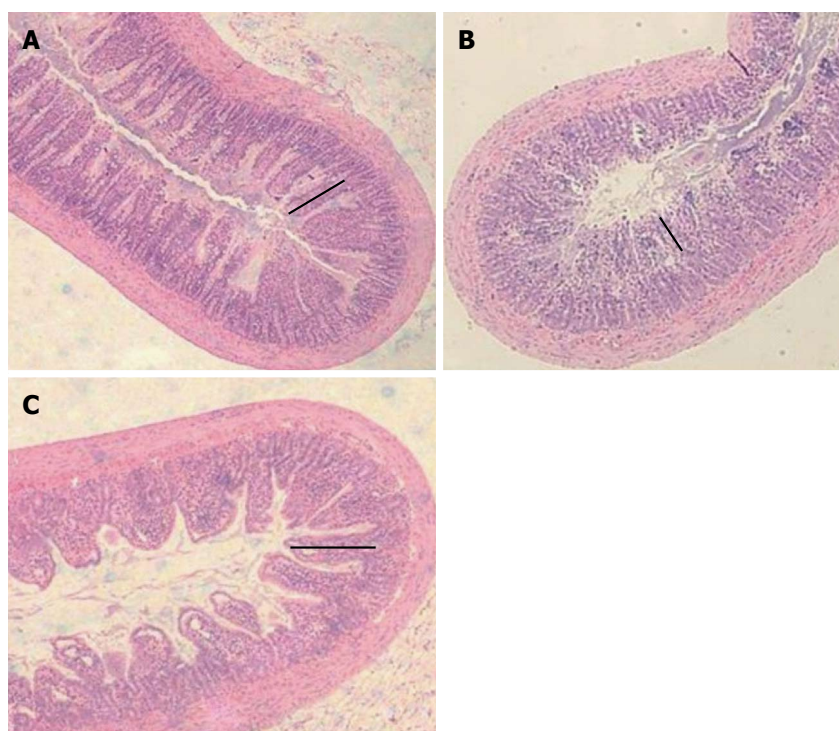


Figure 7 A comparison of the histological structure of ileal sections in a healthy rat (A), after administration of 5-FU (B) and rats treated with LDR + 5-FU (C). Ileum sections of rats from the LDR + 5-FU treatment group (C) exhibited improved mucosal integrity as demonstrated by more defined villi and crypts in comparison to water + 5-FU controls (B). The black line on each diagram represents villus height in each section which was significantly shorter in 5-FU controls. Sections were stained with haematoxylin and eosin and mucosal thickness was analysed by quantitative measurements of villus height and crypt depth. Original photographs were captured at 4 × magnification. LDR: Low-dose rhubarb extract.

intestinal weight and mucosal integrity which was also demonstrated in the current study^[13,31]. Jejunum and ileum weights were significantly decreased in 5-FU treated rats, accompanied by increased villus and crypt damage when compared to healthy controls. Enterocyte apoptosis in 5-FU treated rats was likely responsible for the reduced small intestinal weight. However, RE administered to 5-FU treated rats had no significant effect on intestinal weight, compared to 5-FU controls, which suggested that RE did not enhance cell regeneration after 5-FU toxicity.

Administration of 5-FU may result in exposure of the submucosa to harsh luminal conditions^[6]. As a compensatory mechanism, the muscularis externa contracts to reduce submucosal contact with the luminal environment in an attempt to prevent bacterial translocation. In the current study, the length of the total jejunum and ileum was reduced by 5-FU treatment, as described previously by Mashtoub *et al.*^[31]. However, consistent with previous studies, this effect was not present in the duodenum and colon as 5-FU damage was less severe in these regions of the intestine^[12,13,31].

In the current study, LDR treatment resulted in a significant increase in ileal villus height and crypt depth; possibly representing LDR promoted crypt cell regeneration and hence, increased migration of rejuvenated cells to the villus. Alternatively, LDR may

have exerted an anti-oxidative effect, mediated by the water soluble polysaccharides of rhubarb which may have protected the intestinal mucosa against cell apoptosis; maintaining villus and crypt structure. A reduction in ileal MPO activity by LDR in 5-FU treated rats indicated a decrease in neutrophil activity which further supports the anti-oxidative and anti-inflammatory properties of RE. These results are consistent with previous studies which have exploited plant polysaccharides for their anti-inflammatory and antioxidant properties^[12,40,41]. Cheah *et al.*^[12,14] examined grape seed extract (GSE), a tannin rich by-product of the wine and grape juice industries, in the setting of chemotherapy-induced intestinal mucositis. It was discovered that GSE could partially ameliorate small intestinal inflammation and mucosal damage caused by 5-FU cytotoxicity. Tannins, an active constituent of GSE and possibly RE, possess the ability to prevent the overproduction of ROS or decrease the production of pro-inflammatory cytokines such as IL-4 and IFN- γ ^[12,17]. Further investigations are therefore required to understand the protective and anti-inflammatory mechanism of action of RE in improving acute intestinal inflammation and damage to the mucosa.

A significant improvement in ileal mucosal integrity and inflammation was observed in 5-FU rats treated with LDR, but not HDR. Limited RE studies have been

conducted, therefore the low and high dose range of 20 mg/kg and 200 mg/kg were selected in the current study to determine the effects of RE across a broad dose range. The efficacy of RE in the current study may therefore have been dose-dependent. Prior to this study, the effects of RE on 5-FU-induced mucosal damage and inflammation were unknown and accordingly, the RE optimal concentration remains undefined. The present study suggested that the effectiveness of RE at varying concentrations may follow a normally distributed relationship. Potentially, at high concentrations (≥ 200 mg/kg BW), no significant effects may have been observed due to steric involution of bioactive binding sites. Further studies are therefore required to determine the optimal concentration to attain maximal mucosal protection.

Chemotherapy recipients experiencing intestinal mucositis have altered membrane integrity and impaired water absorption and secretion^[7]. Any molecule of a similar size or shape possesses the capability to attach to the pore vestibule and block the transport of water through AQP channels. Pharmacological blockers of aquaporin fluid fluxes are thought to occlude the pore vestibule and impede the bi-directional transport of water through the channel^[42-44]. In the current study, RE present in the circulatory system may have targeted AQP 4 channels within enterocytes, resulting in a unidirectional blockade, and thereby decreased water secretion into the lumen of the small intestine. This hypothesised theory is further explained in Figure 1D. Wang *et al.*^[29] determined that AQP 4 knockout mice had significantly higher stool moisture content in comparison to wild-type ($P < 0.05$). This suggested that stool consistency was dependent on the functionality of AQP 4 channels. This study also established that AQP 4 channels are scarce within the large intestine. Furthermore, within the large intestine, AQP 4 channels are only present on the initial section of the proximal colon^[29]. Therefore, it is probable that fluid absorption and secretion across AQP 4 channels in the small intestine may have been partly responsible for the moisture content of the faeces in the current study. Further *in vivo* studies should identify the expression levels of AQP 4 and other aquaporins to determine morphological and potential functional changes after 5-FU exposure. Qin *et al.*^[18] demonstrated that aqueous RE improved stool consistency in mice with castor oil and magnesium sulphate-induced diarrhoea. Furthermore, aqueous RE caused constipation when administered to normal mice suggesting that RE may have been acting on AQP 4 channels to alter water absorption in the intestine. Consequently, further studies are required to determine the moisture content of caecal fluid to confirm or refute the hypothesis that RE affects stool consistency. This would allow for comparison of water absorption and secretion in the small intestine, independent of the colon. A reduction in caecal moisture content would suggest that RE was preventing fluid secretion across

small intestinal AQP 4 channels.

In summary, the present study demonstrated that the ancient herbal remedy RE in its aqueous form, at relatively low dose, offers partial protection to the distal intestinal mucosa against tissue damage and inflammation associated with 5-FU-induced intestinal mucositis. Further studies are warranted to identify the anti-inflammatory and antioxidant properties of RE *via* examination of inflammatory cytokines in blood and tissue. This provides preliminary information regarding the potential use of RE as an adjunct to chemotherapy to improve particular histological manifestations of intestinal mucositis. Moreover, the reduced ileal inflammation and improved mucosal thickness suggests further therapeutic potential for other gastrointestinal inflammatory disorders that ultimately affect the more distal regions of the alimentary tract. However, the potential drug-drug interactions of RE and chemotherapy drugs, such as 5-FU should be thoroughly investigated as recent studies have highlighted concern over such interactions^[45]. Future research should also focus on analysing moisture content of caecal fluid to determine whether RE acts as a unidirectional blocker of AQP 4 channels in the small intestine. Finally, further investigation into the active constituents of RE would be beneficial to improve our understanding of its potential utility in bowel disease and its associated mechanism of action.

ACKNOWLEDGMENTS

The authors would like to thank Elizabeth Brown and Joseph Fabian for their assistance with pilot studies. Additionally, the authors would like to thank Shuguan Bi at the University of California Santa Barbara for assistance with lectin array profiling.

COMMENTS

Background

The need to discover effective treatment approaches for chemotherapy-induced intestinal mucositis is growing as cancer incidence continues to increase and thus, the incidence of treatment-related side-effects increases. Traditional medicines are continually being examined for their therapeutic potential in cancer and chemotherapy settings. Accordingly, the aqueous extract of rhubarb (*Rheum Spp.*) was investigated for its potential to improve intestinal integrity and acute inflammation in experimentally-induced intestinal mucositis in rats.

Research frontiers

To our knowledge, this is the first study to identify the therapeutic effect of aqueous rhubarb extract (RE) in experimentally-induced intestinal mucositis.

Innovations and breakthroughs

This is the first study examining the potential for aqueous RE to improve intestinal integrity and acute inflammation in a rat model of 5-FU-induced intestinal mucositis.

Applications

The promising findings presented in the current study indicate that a low dose of aqueous RE improves selected parameters of 5-fluorouracil (5-FU)-induced

intestinal mucositis. Future studies should determine the active factor of the compound so that it can be extracted and further examined for clinical efficacy.

Terminology

5-FU is a widely utilised chemotherapy drug used to treat a range of cancer types from colon to breast cancer. It may be used independently however, is most commonly used in combination with other chemotherapy drugs, such as Methotrexate. RE was obtained from the stalks of the traditional herbal medicine Rheum spp. The low dose of RE (LDR) was based on the estimated dose required to block aquaporin water channel activity in the oocyte expression system, and the high dose (HDR) was selected as a 10 fold higher concentration for comparison. Aquaporins (AQPs) are integral membrane proteins responsible for the regulation of water transport across a membrane via an osmotic gradient. Currently, 13 mammalian AQPs have been identified (AQP 0-12). AQPs are abundant in tissues reliant on high water permeability to maintain correct function and are involved in metabolic processes such as kidney, lung, brain and gastrointestinal function.

Peer-review

This manuscript is well written. The scientific hypothesis and the appropriate tests are well explained and conducted. Results are fairly discussed, notably the question of the need for further experiments investigating an optimal dose.

REFERENCES

- 1 **Wachtel-Galor S**, Benzie IF. Herbal Medicine: An Introduction to Its History, Usage, Regulation, Current Trends, and Research Needs. In: Benzie IFF, Wachtel-Galor S, editors. Herbal Medicine: Biomolecular and Clinical Aspects. Boca Raton FL: Llc., 2011
- 2 **Ashikaga T**, Bosompra K, O'Brien P, Nelson L. Use of complimentary and alternative medicine by breast cancer patients: prevalence, patterns and communication with physicians. *Support Care Cancer* 2002; **10**: 542-548 [PMID: 12324809 DOI: 10.1007/s00520-002-0356-1]
- 3 Australian Institute of Health and Welfare & Australasian Association of Cancer Registries. Cancer in Australia: An overview of 2012. Canberra, 2012
- 4 **Sonis ST**. Mucositis as a biological process: a new hypothesis for the development of chemotherapy-induced stomatotoxicity. *Oral Oncol* 1998; **34**: 39-43 [PMID: 9659518 DOI: 10.1016/S1368-8375(97)00053-5]
- 5 **Soares PM**, Mota JM, Souza EP, Justino PF, Franco AX, Cunha FQ, Ribeiro RA, Souza MH. Inflammatory intestinal damage induced by 5-fluorouracil requires IL-4. *Cytokine* 2013; **61**: 46-49 [PMID: 23107827 DOI: 10.1016/j.cyto.2012.10.003]
- 6 **Sonis ST**, Elting LS, Keefe D, Peterson DE, Schubert M, Hauer-Jensen M, Bekele BN, Raber-Durlacher J, Donnelly JP, Rubenstein EB. Perspectives on cancer therapy-induced mucosal injury: pathogenesis, measurement, epidemiology, and consequences for patients. *Cancer* 2004; **100**: 1995-2025 [PMID: 15108222 DOI: 10.1002/cncr.20162]
- 7 **Gibson RJ**, Keefe DM. Cancer chemotherapy-induced diarrhoea and constipation: mechanisms of damage and prevention strategies. *Support Care Cancer* 2006; **14**: 890-900 [PMID: 16604351 DOI: 10.1007/s00520-006-0040-y]
- 8 **Sakai H**, Sagara A, Matsumoto K, Hasegawa S, Sato K, Nishizaki M, Shoji T, Horie S, Nakagawa T, Tokuyama S, Narita M. 5-Fluorouracil induces diarrhea with changes in the expression of inflammatory cytokines and aquaporins in mouse intestines. *PLoS One* 2013; **8**: e54788 [PMID: 23382968 DOI: 10.1371/journal.pone.0054788]
- 9 **Lalla RV**, Peterson DE. Treatment of mucositis, including new medications. *Cancer J* 2006; **12**: 348-354 [PMID: 17034671]
- 10 **Rubenstein EB**, Peterson DE, Schubert M, Keefe D, McGuire D, Epstein J, Elting LS, Fox PC, Cooksley C, Sonis ST. Clinical practice guidelines for the prevention and treatment of cancer therapy-induced oral and gastrointestinal mucositis. *Cancer* 2004; **100**: 2026-2046 [PMID: 15108223 DOI: 10.1002/cncr.20163]
- 11 **Yazbeck R**, Howarth GS. Complementary medicines: emerging therapies for intestinal mucositis. *Cancer Biol Ther* 2009; **8**: 1629-1631 [PMID: 19633432 DOI: 10.4161/cbt.8.17.9452]
- 12 **Cheah KY**, Howarth GS, Yazbeck R, Wright TH, Whitford EJ, Payne C, Butler RN, Bastian SE. Grape seed extract protects IEC-6 cells from chemotherapy-induced cytotoxicity and improves parameters of small intestinal mucositis in rats with experimentally-induced mucositis. *Cancer Biol Ther* 2009; **8**: 382-390 [PMID: 19305141 DOI: 10.4161/cbt.8.4.7453]
- 13 **Wright TH**, Yazbeck R, Lynn KA, Whitford EJ, Cheah KY, Butler RN, Feinle-Bisset C, Pilichiewicz AN, Mashtoub S, Howarth GS. The herbal extract, Iberogast, improves jejunal integrity in rats with 5-Fluorouracil (5-FU)-induced mucositis. *Cancer Biol Ther* 2009; **8**: 923-929 [PMID: 19276679 DOI: 10.4161/cbt.8.10.8146]
- 14 **Cheah KY**, Howarth GS, Bastian SE. Grape seed extract dose-responsively decreases disease severity in a rat model of mucositis; concomitantly enhancing chemotherapeutic effectiveness in colon cancer cells. *PLoS One* 2014; **9**: e85184 [PMID: 24465501 DOI: 10.1371/journal.pone.0085184]
- 15 **Schepetkin IA**, Quinn MT. Botanical polysaccharides: macrophage immunomodulation and therapeutic potential. *Int Immunopharmacol* 2006; **6**: 317-333 [PMID: 16428067 DOI: 10.1016/j.intimp.2005.10.005]
- 16 **Peigen X**, Liyi H, Liwei W. Ethnopharmacologic study of Chinese rhubarb. *J Ethnopharmacol* 1984; **10**: 275-293 [PMID: 6748707 DOI: 10.1016/0378-8741(84)90016-3]
- 17 **Liu L**, Guo Z, Lv Z, Sun Y, Cao W, Zhang R, Liu Z, Li C, Cao S, Mei Q. The beneficial effect of Rheum tangiticum polysaccharide on protecting against diarrhea, colonic inflammation and ulceration in rats with TNBS-induced colitis: the role of macrophage mannose receptor in inflammation and immune response. *Int Immunopharmacol* 2008; **8**: 1481-1492 [PMID: 18790466 DOI: 10.1016/j.intimp.2008.04.013]
- 18 **Qin Y**, Wang JB, Kong WJ, Zhao YL, Yang HY, Dai CM, Fang F, Zhang L, Li BC, Jin C, Xiao XH. The diarrhoeogenic and antidiarrhoeal bidirectional effects of rhubarb and its potential mechanism. *J Ethnopharmacol* 2011; **133**: 1096-1102 [PMID: 21112382 DOI: 10.1016/j.jep.2010.11.041]
- 19 **Carneiro-Filho BA**, Lima IP, Araujo DH, Cavalcante MC, Carvalho GH, Brito GA, Lima V, Monteiro SM, Santos FN, Ribeiro RA, Lima AA. Intestinal barrier function and secretion in methotrexate-induced rat intestinal mucositis. *Dig Dis Sci* 2004; **49**: 65-72 [PMID: 14992437]
- 20 **Agre P**, King LS, Yasui M, Guggino WB, Ottersen OP, Fujiyoshi Y, Engel A, Nielsen S. Aquaporin water channels--from atomic structure to clinical medicine. *J Physiol* 2002; **542**: 3-16 [PMID: 12096044 DOI: 10.1113/jphysiol.2002.020818]
- 21 **King LS**, Kozono D, Agre P. From structure to disease: the evolving tale of aquaporin biology. *Nat Rev Mol Cell Biol* 2004; **5**: 687-698 [PMID: 15340377 DOI: 10.1038/nrm1469]
- 22 **Cui Y**, Bastien DA. Water transport in human aquaporin-4: molecular dynamics (MD) simulations. *Biochem Biophys Res Commun* 2011; **412**: 654-659 [PMID: 21856282 DOI: 10.1016/j.bbrc.2011.08.019]
- 23 **Ishibashi K**. New members of mammalian aquaporins: AQP10-AQP12. *Handb Exp Pharmacol* 2009; **(190)**: 251-262 [PMID: 19096782 DOI: 10.1007/978-3-540-79885-9_13]
- 24 **Nicchia GP**, Nico B, Camassa LM, Mola MG, Loh N, Dermietzel R, Spray DC, Svelto M, Frigeri A. The role of aquaporin-4 in the blood-brain barrier development and integrity: studies in animal and cell culture models. *Neuroscience* 2004; **129**: 935-945 [PMID: 15561409 DOI: 10.1016/j.neuroscience.2004.07.055]
- 25 **Frigeri A**, Gropper MA, Turck CW, Verkman AS. Immunolocalization of the mercurial-insensitive water channel and glycerol intrinsal protein in epithelial cell plasma membranes. *Proc Natl Acad Sci USA* 1995; **92**: 4328-4331 [PMID: 7538665 DOI: 10.1073/pnas.92.10.4328]
- 26 **Mobasheri A**, Marples D, Young IS, Floyd RV, Moskaluk CA, Frigeri A. Distribution of the AQP4 water channel in normal human tissues: protein and tissue microarrays reveal expression in several new anatomical locations, including the prostate gland and seminal vesicles. *Channels (Austin)* 2007; **1**: 29-38 [PMID:

- 19170255 DOI: 10.4161/chan.3735]
- 27 **Ricanek P**, Lunde LK, Frye SA, Støen M, Nygård S, Morth JP, Rydning A, Vatn MH, Amiry-Moghaddam M, Tønjum T. Reduced expression of aquaporins in human intestinal mucosa in early stage inflammatory bowel disease. *Clin Exp Gastroenterol* 2015; **8**: 49-67 [PMID: 25624769 DOI: 10.2147/ceg.s70119]
- 28 **Koyama Y**, Yamamoto T, Tani T, Nihei K, Kondo D, Funaki H, Yaoita E, Kawasaki K, Sato N, Hatakeyama K, Kihara I. Expression and localization of aquaporins in rat gastrointestinal tract. *Am J Physiol* 1999; **276**: C621-C627 [PMID: 10069989 DOI: 10.1165/ajrcmb.24.3.4367]
- 29 **Wang KS**, Ma T, Filiz F, Verkman AS, Bastidas JA. Colon water transport in transgenic mice lacking aquaporin-4 water channels. *Am J Physiol Gastrointest Liver Physiol* 2000; **279**: G463-G470 [PMID: 10915657]
- 30 **Tomas FM**, Murray AJ, Jones LM. Modification of glucocorticoid-induced changes in myofibrillar protein turnover in rats by protein and energy deficiency as assessed by urinary excretion of Ntau-methylhistidine. *Br J Nutr* 1984; **51**: 323-337 [PMID: 6426502 DOI: 10.1079/BJN19840039]
- 31 **Mashtoub S**, Tran CD, Howarth GS. Emu oil expedites small intestinal repair following 5-fluorouracil-induced mucositis in rats. *Exp Biol Med (Maywood)* 2013; **238**: 1305-1317 [PMID: 24047797 DOI: 10.1177/1535370213493718]
- 32 **Howarth GS**, Francis GL, Cool JC, Xu X, Byard RW, Read LC. Milk growth factors enriched from cheese whey ameliorate intestinal damage by methotrexate when administered orally to rats. *J Nutr* 1996; **126**: 2519-2530 [PMID: 8857513]
- 33 **Murthy SN**, Cooper HS, Shim H, Shah RS, Ibrahim SA, Sedergran DJ. Treatment of dextran sulfate sodium-induced murine colitis by intracolonic cyclosporin. *Dig Dis Sci* 1993; **38**: 1722-1734 [PMID: 8359087 DOI: 10.1007/BF01303184]
- 34 **Beyer AJ**, Smalley DM, Shyr YM, Wood JG, Cheung LY. PAF and CD18 mediate neutrophil infiltration in upper gastrointestinal tract during intra-abdominal sepsis. *Am J Physiol* 1998; **275**: G467-G472 [PMID: 9724257]
- 35 **Campbell EM**, Birdsell DN, Yool AJ. The activity of human aquaporin 1 as a cGMP-gated cation channel is regulated by tyrosine phosphorylation in the carboxyl-terminal domain. *Mol Pharmacol* 2012; **81**: 97-105 [PMID: 22006723 DOI: 10.1124/mol.111.073692]
- 36 **Yool AJ**, Morelle J, Cnops Y, Verbavatz JM, Campbell EM, Beckett EA, Booker GW, Flynn G, Devuyst O. AqF026 is a pharmacologic agonist of the water channel aquaporin-1. *J Am Soc Nephrol* 2013; **24**: 1045-1052 [PMID: 23744886 DOI: 10.1681/ASN.2012080869]
- 37 **Torres DM**, Tooley KL, Butler RN, Smith CL, Geier MS, Howarth GS. Lyprinol only partially improves indicators of small intestinal integrity in a rat model of 5-fluorouracil-induced mucositis. *Cancer Biol Ther* 2008; **7**: 295-302 [PMID: 18059190 DOI: 10.4161/cbt.7.2.5332]
- 38 **Green R**, Horn H, Erickson JM. Eating experiences of children and adolescents with chemotherapy-related nausea and mucositis. *J Pediatr Oncol Nurs* 2010; **27**: 209-216 [PMID: 20562389 DOI: 10.1177/1043454209360779]
- 39 **Smith JL**, Malinauskas BM, Garner KJ, Barber-Heidal K. Factors contributing to weight loss, nutrition-related concerns and advice received by adults undergoing cancer treatment. *Adv Med Sci* 2008; **53**: 198-204 [PMID: 18614435 DOI: 10.2478/v10039-008-0019-7]
- 40 **Cheng CL**, Koo MW. Effects of *Centella asiatica* on ethanol induced gastric mucosal lesions in rats. *Life Sci* 2000; **67**: 2647-2653 [PMID: 11104366 DOI: 10.1016/S0024-3205(00)00848-1]
- 41 **Garrido G**, González D, Lemus Y, García D, Lodeiro L, Quintero G, Delporte C, Núñez-Sellés AJ, Delgado R. In vivo and in vitro anti-inflammatory activity of *Mangifera indica* L. extract (VIMANG). *Pharmacol Res* 2004; **50**: 143-149 [PMID: 15177302 DOI: 10.1016/j.phrs.2003.12.003]
- 42 **Seeliger D**, Zapater C, Krenc D, Haddoub R, Flitsch S, Beitz E, Cerdà J, de Groot BL. Discovery of novel human aquaporin-1 blockers. *ACS Chem Biol* 2013; **8**: 249-256 [PMID: 23113556 DOI: 10.1021/cb300153z]
- 43 **Wacker SJ**, Aponte-Santamaría C, Kjellbom P, Nielsen S, de Groot BL, Rützler M. The identification of novel, high affinity AQP9 inhibitors in an intracellular binding site. *Mol Membr Biol* 2013; **30**: 246-260 [PMID: 23448163 DOI: 10.3109/09687688.2013.773095]
- 44 **Migliati E**, Meurice N, DuBois P, Fang JS, Somasekharan S, Beckett E, Flynn G, Yool AJ. Inhibition of aquaporin-1 and aquaporin-4 water permeability by a derivative of the loop diuretic bumetanide acting at an internal pore-occluding binding site. *Mol Pharmacol* 2009; **76**: 105-112 [PMID: 19403703 DOI: 10.1124/mol.108.053744]
- 45 **Ma L**, Zhao L, Hu H, Qin Y, Bian Y, Jiang H, Zhou H, Yu L, Zeng S. Interaction of five anthraquinones from rhubarb with human organic anion transporter 1 (SLC22A6) and 3 (SLC22A8) and drug-drug interaction in rats. *J Ethnopharmacol* 2014; **153**: 864-871 [PMID: 24685584 DOI: 10.1016/j.jep.2014.03.055]

P- Reviewer: Liew FY, Toucheffu Y S- Editor: Gong ZM
L- Editor: A E- Editor: Wang CH

